Factors determining the development of mammalian sensory neurons and cutaneous innervation *in vivo*

Alana Jane Jackman

A thesis submitted for the degree of

PhD at University College London

Department of Anatomy and Developmental Biology

University College London

June 1997

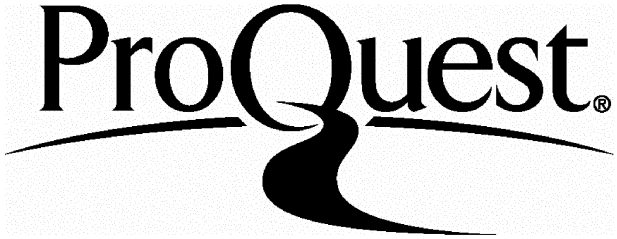

Abstract

The developing innervation of rat hindlimb skin and spinal cord was investigated from E13-E21 using general and phenotype-specific markers. The timing, pattern and density of axon bundles were elucidated using PGP 9.5, GAP 43 and peripherin as pan-neuronal markers, RT97 for A-fibres and CGRP, trkA and IB4 for small A and C-fibres.

RT97 and trkA positive fibres innervated skin at E14, RT97 was also found in the dorsal horn at E14 but no trkA labelling was detected until E18. CGRP expression appears simultaneously in the both targets at E19, suggesting it is expressed subsequent to target innervation. The developmental series implies that large and small diameter fibres innervate the peripheral target together while the central target is innervated by A-fibres prior to C-fibres.

The selectivity of RT97 as an A-fibre label was confirmed by construction of size-frequency histograms at E18. Using *in situ* hybridisation temporal expression of CGRP mRNA was consistent with peptide expression. Quantitative analysis of epidermal innervation shows all subpopulations transiently grow to the skin surface at E17-E18 before retraction of fibres to a sub-epidermal plexus.

Administration of anti-NGF *in utero* results in a selective loss of small diameter DRG cells (Ruit et al, 1992). This treatment was used to examine the consequences upon the remaining DRG subpopulation and the pattern of cutaneous innervation.

DRG counts at E21 showed a cell loss of 43% restricted to the small cell population yet this treatment resulted in total abolition of all epidermal innervation by E21, while sub-epidermal innervation was relatively unchanged. The experimental group showed an

increase in the number and size of larger cells, with a population of cells sized 600-800μm^2.

These results indicate that DRG subpopulations have different developmental patterns of innervation but that anti-NGF treatment renders the epidermis non-permissive to innervation by all fibre types.

Acknowledgements

I would like to acknowledge my supervisor, Maria Fitzgerald for all her guidance during my PhD. I wish to express my thanks for her encouragement and motivation, and for providing the direction in my work.

There are some people I would firstly like to thank in our lab: Jacqueta Middleton, Andrew Allchorne and Penny Ainsworth, not only for technical assistance for their multifaceted skills and wealth of information and advice. I would also like to thank Richard Mannion for preparation of the CGRP probe and for his help in conducting *in situ* hybridisations.

I was fortunate in obtaining assistance outside our lab from Greg Michael at St. Thomas's hospital who carried out isotopic *in situ* hybridisations. I would like to additionally express gratitude to Paul Martin (UCL) for generously sharing his photography and scanning facilities.

During my PhD, all colleagues in the lab were always available and willing to discuss, assist and advice on a great many things, I would like them all to know how much I appreciated their friendship.

Debts are not supposed to be happy things, but those incurred in the preparation of this thesis are all owed to some special friends who showed such generosity, immense kindness and one of the most valuable commodities, time, that I could not have wished for more - although maybe in different circumstances next time. To Simon Beggs, Herve Bester, Jacqueta Middleton, Janie McCluskey and Ana Oliveira - *Go Raibh Maith Agat* (Thank-you).

Finally, the people who have supported me unfailingly and have always been there when I needed them even though far away, my parents, my brother Johnny, and Anthony for all their tolerance and understanding.

Contents

List of Figures

List of Tables

Abbreviation List

Ach	Acetylcholine
AHP	Afterhyperpolarization
BDNF	Brain-Derived-Neurotrophic-Factor
BrdU	Bromodeoxyuridine
CAMs	Cell Adhesion Molecules
CB	B subunit of cholera toxin
CGRP	Calcitonin Gene Related Peptide
ChAT,	Choline Acetyl Transferase
CNS	Central Nervous System
DIG	Digoxygenin
DNES	Diffuse Neuroendocrine System
DREZ	Dorsal Root Entry Zone
DRG	Dorsal Root Ganglion
E	Embryonic
ECMs	Extracellular Matrix Molecule
Eph	Erythropoietin-producing hepatocellular
GAL	Galanin
GAP 43	Growth Associated Protein 43
HF	Hair Follicle
HRP	Horseradish Peroxidase
HTM	High Threshold Mechanoreceptors
ICE	Interleukin-1-β-converting enzyme
IF	Intermediate Filament
IHC	Immunohistochemistry
KB	Kilobase
kDa	Kilodalton

LDCV	Low-Density Carrier Vessicle
LTMR	Low Threshold Mechanoreceptor
LTP	Long-Term Potentiation
NF	Neurofilament
NF-H	High Molecular Weight Neurofilament
NF-L,	Low Molecular Weight Neurofilament
NF-M,	Medium Molecular Weight Neurofilament
NFH-P	Phosphorylated High Molecular Weight Neurofilament
NGF	Nerve Growth Factor
nIF	Neuronal Intermediate Filament
nm	Nanometers
NMJ	Neuromuscular Junction
NSA	Netrin Synergising Activity
NSE,	Neural Specific Enolase
NT-3	Neurotrophin-3
P	Postnatal
PCD	Programmed Cell Death
PDGF	Platelet Derived Growth Factor
PGP	Protein Gene Product
PKC	Protein Kinase C
PNS	Peripheral Nervous System
PPT	Preprotachykinin
PSA	Polysialic Acid
RAGS	Repulsive Axonal Guidance System
RTKs	Receptor Tyrosine Kinase
SA	Slow Adapting
SCG	Superior Cervical Ganglion
SG	Substantia Gelatinosa
SOM	Somatostatin

SP	Substance P
STV	Small Transport Vesicle
TH	Tyrosine Hydroxylase
TM	Transmembrane
TMP	Thiamine monophosphate
TNF	Tumour Necrosis Factor
VIP	Vasoactive Intestinal Peptide

GENERAL INTRODUCTION

1.1 Aim of thesis

The aims of this thesis are to describe the developmental timecourse of rat hindlimb skin innervation by sub-populations of DRG neurons, to examine the developmental interactions between the DRG sub-populations and to investigate the interactions between DRG sensory neurons and target.

A study of central and peripheral axonal projections during development has been undertaken (Mirnics & Koerber, 1995a; 1995b). However, the technique of DiI labelling means that the phenotype of axons cannot be determined. In the present study, a series of general and phenotype-specific markers were used. The morphology, density, and development of stereotypical patterns of axon bundles was examined using immunohistochemical markers for sub-populations of neurons in skin and dorsal horn. Protein Gene Product (PGP) 9.5, Growth Associated Protein (GAP) 43 and peripherin were used as pan-neuronal markers, RT97 as an A-fibre marker and Calcitonin Gene Related Peptide (CGRP), trkA and IB4 for small A and C-fibres.

Specific questions to be considered are whether A-fibres and C-fibres reach their peripheral target at different times and with different developmental patterns. Target innervation in the epidermis was quantified over a specific time period and compared between the identified subpopulations of sensory axons.

In order to characterise developing DRG cells into different subpopulations with confidence, several aspects of DRG cell development were investigated. The light microscope characteristics of DRG cells were examined, to determine if cells at embryonic day (E)18 or E21 could be characterised as large light and small dark. Size-frequency histograms were generated of DRG neurons at embryonic ages E18 and E21.

SP	Substance P
STV	Small Transport Vesicle
TH	Tyrosine Hydroxylase
TM	Transmembrane
TMP	Thiamine monophosphate
TNF	Tumour Necrosis Factor
VIP	Vasoactive Intestinal Peptide

1.2 The development of primary sensory neurons - birth of dorsal root ganglia (DRG) and axon outgrowth

The general processes underlying the first stages of development in the somatosensory system are described in this introduction. There are eight headings under which these parameters are explained, in logical order pertaining to the development of the system. The first four concern the formation of the DRG and the process of axon outgrowth and are discussed below. The last four are described later as part of chapters containing specific information about the background to each of the experiments.

Since this thesis is concerned with the relationship between the DRG subpopulations and the interactions with their target, it is appropriate to outline how these cells are generated and by what process they reach their targets. It is important for the correct functioning of the somatosensory system that primary sensory neurons are specialised to perform different tasks and make appropriate connections to particular peripheral receptor or target tissues. Each DRG neuron innervates two targets, one peripheral and one central, therefore there must be some correlation between them so that in the adult the central pathways/effector cells receive the correct peripheral sensory information with which they are best qualified to process. The targets of the lumbar DRG neuron are the spinal cord and the hindlimb, which consists of both muscular and cutaneous tissue. The function of the DRG is to facilitate the transfer of peripheral sensory information to the central nervous system (CNS), hence its location near the spinal cord. Its role requires that axon outgrowth is accurate to both targets and that specification of different cell types is achieved.

The research in this thesis concerns the interaction between axonal subpopulations and target, hence the nature of the targets and the specific phenotypes of DRG cells will be described in the introduction to the experimental chapters. Upon reaching the target a

period of cell death is observed, after which the stereotypical patterns of connections are established. These aspects are also briefly covered in those experimental chapters.

1) **Gangliogenesis**
2) **Neurogenesis**
3) **Prelude to axonal outgrowth**
4) **Axon outgrowth**

5) **Nature of targets** *see Chapter 4*
6) **Cell death** *see Chapter 7*
7) **Somatotopy** *see Chapter 4*
8) **Characterisation of subpopulations** *see Chapter 3*

1.3 Gangliogenesis

Dorsal root ganglia (DRG) are located in the peripheral nervous system and contain the cell bodies of vertebrate primary somatic sensory neurons. They appear as oval swellings of the dorsal roots. DRGs are derived from the unsegmented neural crest cells. Following somitic dissociation into dermomyotome and sclerotome, neural crest cells migrate into position in the rostral half of the sclerotome where they condense to form a DRG (Verbout, 1985; Teillet et al, 1987; Lallier et al, 1988). The neural crest cells segregate within each ganglion in a distinct topographical arrangement which reflects their original craniocaudal position on the neural primordium (Teillet et al, 1987).

1.4 Neurogenesis

The lumbar DRG cells of the rat are generated in three successive waves corresponding to different subpopulations. The large light cells are born before the small dark cells over the period E11-E15 - approximately midway through gestation, (Lawson et al, 1974; Altman & Bayer, 1984) but recently a third small population born E14-E15 has been reported (Kitao et al, 1996). Further details of this process are found in Chapter 3.

1.5 Prelude to axonal outgrowth: polarity and processes

Once DRG cells are fully differentiated they begin to extend processes or neurites. This is apparent *in vitro* after addition of neurotrophic factors, which results in a radial pattern of short neurites emanating from the DRG. *In vivo* these processes initially grow at the same rate and any one of the minor processes is capable of becoming the axon, but eventually only one accelerates and becomes the axon (Goslin & Banker, 1989). The axon is specialised to transmit information over long distances, i.e. from the cell body to the target, and cell processes gradually acquire the biochemical properties unique to axons.

The first evidence of axonal characteristics is the accumulation of microtubules especially the low molecular weight tau proteins (Black & Baas, 1989). Preceding the onset of axonal outgrowth, all minor processes show GAP 43-like immunoreactivity (see section 4.1). GAP 43 becomes highly concentrated in the axonal growth cone and largely disappears from the other processes, hence it is selectively transported into the neurite that becomes the cell's axon (Sargent, 1989). Axons then become polarised with a positive end where new subunits are added to the growing tip. Additional membrane is added to growth cones to enable advancement towards the target. The main constituents of extension are microtubules, intermediate filaments and neurofilaments (see Chapter 4). Antibodies to these growth cone/axon scaffolding components allow visualisation of the developing axon and it is the principle exploited in this thesis (Chapter 4).

DRG cells are at first bipolar then undergo morphological changes to become pseudounipolar early in development (Takahashi & Ninomiya, 1987). The transition to unipolar cells is caused by the elongation of the cell body cytoplasm. Adult primary sensory neurons are classically described as pseudounipolar, referring to the number of axonal processes (Ranvier, 1875; Ramon y Cajal, 1909). The cell body is located in the DRG, and while one axon originates from the cell body, it divides after a few hundred microns, giving rise to one central axon to the spinal cord and one peripheral axon to the spinal and peripheral nerve. These early reports proposed that a 1:1 ratio existed between the number of fibres in the dorsal root and the number of cells in the DRG. This theory

was challenged with the advent of the electron microscope as it was not possible to obtain this ratio (Coggeshall, 1980; Langford & Coggeshall, 1979; 1980). Initially all studies reported an excess of fibres compared to cells, leading to the conclusion that fibres branch inside the ganglion. Recently, this 1:1 ratio has been obtained using new stereological techniques and indicates that at least the cranial side of the ganglion can be considered pseudounipolar, since the peripheral side of the ganglion is more complex (Tandrup, 1995).

1.6 Axon Outgrowth

During development neurons initiate and extend axonal projections to a specific target. Through this growth process, neurons acquire the distinctive and stereotyped pattern of connections characteristic of the adult nervous system. The complexity of this exercise has been highlighted in recent years by the discovery of many of the underlying molecular mechanisms.

Essentially, there are five stages to this process. The first is the stimulation of neurite outgrowth, under the influence of neurotrophins. Pioneering neurites then navigate through many different tissues in a reproducible and identical pattern to find their way to a specific target. This stage is regulated by interaction of the growth cone with environmental guidance cues: signals from molecules on the surface of other neuronal and non-neuronal cells, and within the extracellular matrix in the pathway of the axon. Simultaneously, target-derived guidance factors then attract the axons while inhibitory factors repulse axons away from inappropriate areas.

These extrinsic factors modulate the cellular mechanisms influencing the rate of extension, orientation and control of the growth cone. Intrinsically, the response of the axon to these external cues has also been investigated, since intracellular machinery integrates the myriad extracellular cues to co-ordinate and direct growth cone navigation. Once at the target site, the neuron must recognise and select a postsynaptic target among the different cell types and establish the correct topographical map. This can be refined after synapse formation by activity-dependent mechanisms. There are several reviews

covering many aspects of this developmental process in detail (Tanaka & Sabry, 1995; Keynes & Cook, 1995; Garrity & Zipursky, 1995; Kennedy & Tessier-Lavigne, 1995), so a brief overview of these stages will be described, focusing on the peripheral and central targets of the lumbar DRG neuron. It is clear however, that the full relationship between each of the stages is not understood although the effect of activity on pathway guidance cues has been examined. Further research is therefore needed to understand the interactions between the various mechanisms controlling neurite outgrowth.

1.6.1 Stimulation of neurite outgrowth

Developing DRG neurons are dependent on neurotrophins for survival after they have reached their target, however, evidence is emerging that they may be dependent, not for survival but for stimulation of outgrowth prior to reaching the peripheral target. *In vitro* this has been apparent because without inclusion of the appropriate neurotrophic factors in the culture media, neurite outgrowth would not occur (See Chapter 7).

1.6.2 Pathway guidance cues

The guidance of migrating cells depends on cues from the local environment. This was initially thought to be mediated through a physical adhesion mechanism but now has been superseded by the discovery that many cues guiding growth cones are not even adhesive in nature and many are in fact inhibitory. The lack of correlation between direction of migration and adhesive strength also contributed to the dismissal of the simple haptotaxis mechanism, where growth cones followed adhesive gradients. It is now realised that the role of cell adhesion is multifaceted utilizing a combination of haptotactic and inhibitory mechanisms. The functional units of cell adhesion are multi-dimensional complexes comprising of three general classes of proteins: cell adhesion molecules and receptors, extracellular matrix proteins and the cytoplasmic plaque/peripheral membrane proteins.

1.6.3 Adhesion Molecules

The cell adhesion molecules (CAMs) have been implicated in axon guidance because of their expression patterns and behaviour *in vitro.* CAMs are cell-surface

macromolecules controlling cell-cell interactions via the regulation of processes such as neural adhesion and migration, neurite outgrowth, axon fasciculation, synaptogenesis and intracellular signalling.

A comprehensive role for these molecules has not yet been defined for two reasons. Firstly, they show paradoxical activity. They can increase cell adhesion and axon fasciculation but are conversely capable of increasing cell motility and neurite outgrowth. Secondly, there is no direct *in vivo* evidence of their actions due to the absence of abnormality associated with gene ablations of the CAMs in mice. Research on individual CAMs and their homologues in different species has provided evidence supportive of their necessity to axonal guidance. The role of individual pathfinding cues has been extensively examined in the zebrafish retinotectal system. Large-scale genetic screening in this vertebrate model revealed mutations relating to over 30 genes. A review of the mutant phenotypes (Karlstrom et al, 1997) shows that individual genes can be mutated to give clear axon-guidance defects, therefore some guidance systems are unique and do not have completely redundant or overlapping functions.

The remaining mutant zebrafish phenotypes show a reduction in the number of axons that arrive at the correct target but not a total elimination of accurate axon guidance. Similarly with drosophila mutants (reviewed in Keynes & Cook, 1995) many growth cones reach their targets but at later stages of development, implying that other cues may ultimately allow errors to be corrected even after loss of contact with pioneer axons. These studies suggest that multiple guidance cues are responsible for the extremely high-fidelity axon guidance *in vivo* and the prevalence of these mutations with partial defects may explain why mouse knockouts show no clearly interpretable axon-guidance defects. The major drawback with the zebrafish mutants is that the nature of the phenotypic aberrations are not yet characterised. It is not known whether the mutations were the result of disruption of the environment or the ability of the growth cone itself to respond to the guidance cues, yielding no significant clues as to how they exert their influence. Closer examination of the earlier invertebrate mutations and the directed mouse mutations reveal how precise defects affect the overall guidance performance.

Do CAMs possess the correct expression patterns and range of interactions to fulfil the criteria of axon guidance molecules? The purpose of CAMs in neurite guidance is not immediately clear, nor is the putative yet paradoxical roles of cell motility and cell adhesion described for these molecules. Clearly neurites must be motile and fasciculated to reach the target but it is vital that they interact with the pathway substrate via a haptotactic mechanism to provide directional cues to the growth cone. On reaching the target area, axons must defasciculate and adhere to the target matrix to transform the growth cone into a synapse. The remainder of this account, will focus on how this may be achieved for different types of neurites by adhesion molecules. Current proposals for achievement of their antagonistic effects are combinations of changes in the expression levels of specific CAMs, their molecular isoforms and also by post-translational modification at different developmental stages.

The CAM family is functionally classified into calcium-dependent and calcium-independent groups. Cadherins are the calcium-dependent group and have a highly conserved cytoplasmic domain that is the site of association with the cytoplasmic plaque proteins. The specific cytoplasmic plaque proteins that bind to cadherins are called catenins. These mediate the interactions between the cadherins, cytoskeletal proteins and signal-transduction pathways to regulate cell adhesion. α-catenin has actin-binding activity and probably serves as the link between Ca^{2+}-dependent CAMs and the cytoskeleton (Rimm et al, 1995). This association is further regulated during development and by phosphorylation to modulate adhesion, proliferation and morphogenesis.

The calcium-independent group of CAMs is largely composed of the immunoglobulin superfamily. These molecules share Ig motifs and fibronectin-III repeats but show multiple isoforms, each with distinct functional effects and expression patterns. Examples of mammalian CAMs from the Ig superfamily include P0, MAG, NCAM (180, 140, 120), L1 and TAG-1. Each of these have chick/drosophila homologues except for the P0 and MAG molecules. Novel non-mammalian CAMs already discovered are NrCAM and neurofascin. The cytoplasmic domains of some Ig family members associate directly with ankyrins. These are a family of spectrin-binding proteins located on the

cytoplasmic surface and facilitate management of cytoskeletal dynamics (Davis & Bennett, 1994).

CAMs bind through homophilic interactions with like molecules on adjacent membranes stimulating activation of several intracellular signalling cascades. Intracellular signalling cascades alter the levels of calcium which is an important second messenger regulating growth cone motility. L1 and cadherin substrates have been shown to directly influence actin and microtubules, but not neurofilaments to produce changes in growth cone morphology of neurites grown *in vitro* (Burden-Gulley & Lemmon, 1996). Heterophilic binding between different CAMs has also been established with L1 and NCAM combining to influence long term potentiation (LTP). In this example, binding occurs between the oligomannosidic carbohydrate on L1 and the Ig domain on NCAM, if binding is abolished by soluble mannosides, LTP is strongly inhibited.

Integrins are a family of heterodimeric proteins composed of α and β subunits that, like CAMs, mediate cell-cell interactions and cell-actin cytoskeleton interactions through the intermediate proteins talin, α-actinin, tensin and vinculin, thus are often described as CAMs. However, they also mediate cell-extracellular matrix adhesive connections and are crucial in linking the CAMs, ECMs and the cytoskeleton. Key intracellular signalling pathways involving integrins are beginning to be identified, including activation of transcription factors and induction of gene expression after binding of CAMs (for review see Lafrenie & Yamada, 1996).

The inclusion of integrins as components in mediating axon guidance means they too must fulfil necessary criteria. A detailed review of the nature of integrin involvement in neural crest-cell migration (Perris, 1997) ascertains that four putative integrin receptor polypeptides are expressed by undifferentiated neural crest (NC)-cells and after *in vitro* and *in vivo* integrin inactivation experiments, some identified subunits show involvement with ECMs. At the same time, results from genetic deletions of single or double subunits dismiss a role for integrins since no overt deficiencies in NC-cell migrations are observed. This finding emphasises the degree of redundancy in yet another mechanism underlying axon guidance and the likelihood that guidance is multifactorial. More pertinent to the

present study, increased integrin expression is connected with the aggregation of NC-cells and is a possible determining factor in the condensation of NC-cells into peripheral nervous ganglia. Subunits α_8 and β_8 have been identified on peripheral sensory neurons (Bossy et al, 1991; Venstrom & Reichardt, 1995; Beauvais et al, 1995) and six heterodimers have been detected in chick/rodent DRG (Song et al, 1992; Sheppard et al, 1994; Tomaselli et al, 1993; Wu & Sontoro, 1994). Perturbation of the α_6 gene alters the formation of skin in mice (Georges-Labousse et al, 1996) and in chick, α_7 is one of the prevalent integrin receptors on neurons and axons in the developing spinal cord (Kil & Bronner-Fraser, 1996).

Expression levels of CAMs that dictate the degree of axon fasciculation are also modified at different stages of outgrowth. During cell motility periods, NCAM and cadherins are downregulated, for example during formation of the mesoblast or on axons at the start of myelination. This downregulation correlates with high motility of myelinating Schwann cells (Edelman & Crossin, 1991). Conversely, outgrowth and fasciculation is promoted by a subgroup of CAMs expressed predominantly on axon pathways in the CNS and PNS during synaptogenesis (Goodman, 1996). Fasciculation is maintained after reaching the target in drosophila overexpressing the NCAM homologue, while in loss of function mutations defasciculation occurs in three CNS pathways prior to reaching the target. Defects of fasciculation are generally dose and stage dependent, with increases in fasciculation leading to subsequent errors in axon pathfinding, yet loss of fasciculation does not appear to prevent growth cones from turning at critical regions and occasionally may facilitate turning during normal development.

Post-translational modifications are a major mediator of CAM function, the best characterised of such is glycosylation. This is regulated by changes in activity of the enzyme that regulates the carbohydrate polysialic acid (PSA). PSA residues are bound by various CAMs, their presence reducing binding rates three-four fold (Boisseau et al, 1991). Binding of PSA to NCAM has been localised to the fourth and fifth Ig-like domains, forming a PSA-acceptor structure (Nelson et al, 1995). The components of the fifth Ig domain are unique to vertebrate NCAM and is consistent with the absence of PSA

binding in *Aplysia* and *Drosophila* NCAM-related molecules. Their effect is to inhibit binding, effectively making axons less sticky and more dynamic and therefore attenuating cellular interactions.

The level of polysialylation of NCAM has been implicated in regulating motor nerve branching and fasciculation, since highest levels of PSA are detected when axons are sorting in the plexus region and branching in the muscle (Landmesser et al, 1990; Tang et al, 1992; 1994). The levels of PSA residues on NCAM have been shown to be developmentally regulated, changing from 30% of mass in embryonic NCAM to only 10% in the adult (Edelman & Crossin 1991). Higher levels during the early period of cell migration, is consistent with less adhesion and greater plasticity, whereas in the retina the developmental shift to PSA-poor forms of NCAM is coincident with increased morphological stability. This regulation is clearly important for neural plasticity, though most of the spinal cord research has focused on the effect of PSA on motoneurons, the detection of PSA during the timeframe of axon defasciculation in the plexus region also infers this may be of importance to sensory neurons. It is also known that PSA enzymatic activity can be regulated both by interaction with the peripheral target and by electrical activity (Bruses et al, 1995).

In fact all of the strategies used by CAMs to affect axon guidance can be modulated by neuronal electrical activity. Levels of the NCAM drosophila homologue, which normally promotes fasciculation, shows decreased presynaptic expression in a hyperactive mutant, with accompanying increases in presynaptic sprouting. Recent *in vitro* models have found an association between CAMs and the defasciculation of mouse DRG nerve terminals (Itoh et al, 1995). Neurite outgrowth is arrested in culture under the influence of action potentials (Fields et al, 1990), consistent with the nerve terminals of DRG neurons defasciculating upon arrival at the sub-epidermis which is coincident with the commencement of low-frequency spontaneous electrical activity (Fitzgerald & Fulton, 1992). Later, terminals refasciculate as neural impulse activity becomes high frequency and phasic in response to sensory stimulation (Fields and Itoh, 1996). In the developmental context, the regulation of CAM expression by

activity-dependent mechanisms would be a powerful mechanism for linking the developing structure of the nervous system to the functional activity of the developing neural network, however the nature of this aspect remains to be established.

1.6.4 Extracellular Matrix Molecules (ECMs)

The extracellular matrix contains an assortment of glycoproteins that have been identified and are known to have important regulatory roles during development (Adams & Watt, 1993). These are now referred to as extracellular matrix molecules (ECMs) and have been designated into three subgroups according to their actions. The first group are permissive molecules that promote cell motility, these include fibronectins, laminins and collagen I, IV and VI. The second group are non-permissive, are mainly absent from the migratory pathway and ineffective on cell motility. These include tenascins (reviewed in Bartsch, 1996), proteoglycans and most collagens. Only one group of ECMs, the aggrecans, belong to the third inhibitory group which are restricted to areas non-permissive to migration and could directly/indirectly impede cell motility.

Cells attach to the ECM directly via components of the collagen-rich interstitial matrix or the basement membrane. The basement membrane is composed of two layers, the basal lamina - immediately adjacent to the cells, and the reticular layer in the underlying connective tissue. The cell binding is mediated by two groups of receptors: syndecans, which are a family of cell surface proteoglycans, and integrins which are discussed above (Gumbiner, 1996).

ECMs provide cues that impose directionality upon the migrating cells as long-range migrations usually occur along basement membranes, so motility can be regulated by the spatio-temporal distribution of ECMs and the response of the cell at definitive time-points. It has been shown that the phenotype and stage of commitment of the cell is important since different cells react differently to the same ECM guidance cue. In addition, certain cell types will only interact with some ECMs.

Apart from roles in migration and motility, the relation of the ECM laminin to the diffusible chemoattractant netrin, raises the possibility that other ECMs may also function as long-range chemotropic factors (Kennedy & Tessier-Lavigne, 1995). This would most

likely occur under particular conditions such as in the embryonic nervous system. Evidence supportive of this theory, is that laminin loosely bound to the interstitial ECM in neonatal peripheral nerve can be released in diffusible form in physiological buffer (Kucherer-Ehret et al, 1990), in contrast to the adult insoluble form in basement membranes. Another novel role for ECM proteins recently reviewed, is in apoptosis (Meredith & Schwartz, 1997). In the absence of appropriate ECM contacts, cells undergo apoptosis/programmed cell death (PCD). Apoptosis is considered to be a default pathway for cells without extracellular signals to prevent it (Raff, 1992).

It would not be surprising if cell adhesion is required for cell survival, since molecules that control cell location should be able to delete cells accidentally localised to an improper environment. The assumption is based on the process of normal morphogenesis, where death of cells lacking proper adhesive contacts occurs. An example of this is the process of cavitation during tube formation, cells in the interior of the cylinder die due to lack of contact with the basement membrane, leaving a hollow tube (Coucouvanis & Martin, 1995). Secretion of matrix-degrading proteases is also an early step in tissue regression and is advantageous to the process since ECMs are cell-type specific and all cell types within the tissue can be affected simultaneously by loss of the ECM (Boudreau et al, 1995). The cellular pathway facilitating this role has been partially established, ECMs signal through integrin receptors which have been shown to regulate a number of components of the death pathway: interleukin-1- β-converting enzyme (ICE), Bcl-2 and P53 (for review see Meredith & Schwartz, 1997). Detailed examination of two ECMs, proteoglycans and laminins, serve to highlight representative non-permissive and permissive roles.

i) Proteoglycans

Proteoglycans belong to the group of non-permissive ECMs and are associated with inhibitory roles. They are the candidate ECM involved in the guidance of sensory neurites innervating the skin. In chick, this guidance is thought to be inhibitory since they are expressed with glycosaminoglycans in the epidermis (Jahoda et al, 1987; Kitamura, 1987) while skin innervation remains sub-epidermal (Martin et al, 1989). DRG axons

avoid chick epidermis *in vitro* but contact the dermis (Verna, 1985; Verna et al, 1986). This avoidance response in neurites can be reproduced *in vitro* by the addition of proteoglycans and glycosaminoglycans (Verna et al, 1989; Snow et al, 1990a) and can be abolished when treated with a glycoprotein synthesis inhibitor (Fichard et al, 1990). Rat skin also contains two populations of galactsaminoglycan-containing proteoglycans whose concentration and ratio changes dramatically from E18 (Habuchi et al, 1986), which coincides with the major period of terminal formation in the epidermis.

The *in vitro* inhibition of neurite growth after contact with proteoglycans also confirmed that proteoglycans fulfilled the criteria of localisation and functional inhibition, for their proposed role as an axon barrier in the roof plate (Snow et al, 1990b). These molecules are also associated with a barrier to axonal growth in the dorsal root entry zone (DREZ) after a critical period corresponding to postnatal days 2-3 in the rat (Pindzola et al, 1993). Proteoglycans in association with tenascin, increase on the CNS side of the DREZ after the critical period when axons cannot enter the spinal cord but are expressed in relatively small amounts prior to the critical period when axons firstly grow into the spinal cord during normal development and secondly, can regenerate. At E18, their expression is restricted to the roof plate but by P2 they spread laterally to the DREZ and into the dorsal columns. This band of expression clearly defines the DREZ and separates the central and peripheral nervous systems.

Proteoglycan expression levels are also increased at the dermal-epidermal junctional zone during the terminal phases of gangliogenesis and their role in the preceding NC-cell migration has been described (Perris, 1997).

The inhibitory reponse to proteoglycans is concentration dependent and can be modified by addition of growth-promoting molecules such as laminin, so the pattern of neurite outgrowth may be regulated by the ratio of growth-promoting to growth-inhibiting molecules (Snow & Letourneau, 1992). An important deciding factor in the type of response may be the combination of integrin receptor on the axon and the composition of the multidomain modular proteoglycan.

ii) Laminins

Laminins are a group of heterotrimers composed of α, β and γ chains (Burgeson et al, 1994). At least seven different heterotrimeric forms of laminin exist (Timpl & Brown, 1994), with five α, three β and two γ chains described. Chains containing the recently discovered α4 and α5 (Iivanainen et al, 1995; Miner et al, 1995) have not yet been characterised. Laminins are localised in the basement membrane separating epithelial cells from underlying stroma and in the basement membrane surrounding fat, muscle and peripheral nerve cells. They are the first ECMs detected in the developing embryo and their primary role is cell-matrix attachment. Additionally, they have potent biological activity on cell growth and migration, tumour growth and metastases, neurite outgrowth and wound repair (reviewed in Malinda & Kleinman, 1996). These different functions may arise from the various chains binding different integrins.

The best characterised and first isolated laminin is referred to as laminin-1, composed of α1β1γ1. Laminin-1 has principal roles in three aspects of neuronal development. It, and other isoforms are located along the migratory paths of NC-cells with the appropriate integrin receptors, and are upregulated at stages preceding gangliogenesis (reviewed in Perris, 1997), while perturbation of laminin or its receptors disrupt migration (Bronner-Fraser, 1986; Bronner-Fraser & Lallier, 1988; Bronner-Fraser, 1993a; 1993b). It is expressed by cells associated with the peripheral nerve and is implicated in Schwann cell migration, differentiation and myelination (Cornbrooks et al, 1983; McGarvey et al, 1984; Hsiao et al, 1993; Anton et al, 1994; Fernandez-Valle et al, 1993). Importantly, it promotes neurite outgrowth from virtually all classes of developing neurons both from the CNS and PNS (Manthorpe et al, 1983; Rogers et al, 1983; Liesi et al, 1984; Unsicker et al, 1985; Engvall et al, 1986). This global effect implies that it is a prime candidate for an *in vivo* guidance molecule, further supported by the widespread distribution of integrin heterodimers responsive to laminin in the CNS and PNS from early developmental stages (Reichardt & Tomaselli, 1991; Bronner-Fraser et al, 1992; Weaver et al, 1995).

The developmental onset and distribution of all ten known laminin chain mRNAs in the pathway and targets of DRG sensory neurons has recently been examined in the mouse (Lentz et al, 1997). At E11.5, α1, α2, α4, β1, γ1 are expressed in the non-neuronal cells surrounding the DRG, and α2, α4, β1, γ1 are found along the peripheral nerve and in the ventral and dorsal roots at all embryonic stages examined. These are downregulated by adulthood except for low levels of γ1. Therefore, laminins may promote peripheral axonal outgrowth and be of importance in maintenance of cells along the mature peripheral nerve. By E13.5, DRG cells express laminin, which becomes progressively more intense as α2, α4, β1 and γ1 chain expression is initiated. Although at P1, DRG neurons are labelled, it is not possible to ascertain at earlier developmental stages whether expression is neuronal. In the limb-bud at E13, β1 and γ1 are widely expressed, α2 and α4 are found in muscle, while α3, α5, β2 and γ2 are restricted to skin. The preferential target distribution of the α laminin chains, suggests a contributory mechanism via which cutaneous and muscle sensory axons identify their target.

In contrast to the above regions, laminins were absent from the grey matter at all ages although they were expressed in discrete regions of the spinal cord, in accordance with previous immunohistochemical data, and in addition were not found in cartilage or along the optic nerve.

Laminins are expressed in the DRG, sensory and motor neuron pathways and differentially in their respective targets. If laminins are responsible for different subsets of neurons distinguishing their target, these axons would have to express appropriate integrins to enable a response to the different laminin isoforms expressed in each of these tissues. For example, muscle afferents should express α2 and/or α4 specific integrins while skin afferents should express integrins responsive to α3 and/or α5. From the information currently available about integrin expression and ligand specificity, Lentz and colleagues, speculate that the α3β1 integrin may be the required receptor for skin afferents, however its localisation is awaited (Lentz et al, 1997), see Chapter 7.

1.6.5 Target-derived guidance cues

Guidance cues emanating from the target are chemotropic in nature. Chemotropism is defined as guidance directed by a gradient of a soluble factor diffusing from a target. This mechanism of axon guidance was previously thought to be chemoattractant only, however, since the early '80s the emergence of chemorepulsive mechanisms has grown more prominent, demonstrating how non-target regions secrete diffusible factors that prevent inappropriate innervation. Chemorepulsion now occupies a position of equal importance with adhesion and chemoattraction in the guidance of developing axons (Dodd & Schuchardt, 1995).

Three identified protein families have become prominent molecules in the search for target-derived guidance cues. These are the netrins, the semaphorins and the Eph-related receptor family and ligands.

i) netrins

The netrins are a small family of secreted proteins capable of guiding cell and growth cone movements *in vivo*. There are two vertebrate members, netrin-1 and netrin-2, whose receptor is DCC, one nematode member, *unc*-6, whose putative receptors are *unc*-5 and *unc*-40. In Drosophila D-netrinA and D-netrinB are the two netrins with the receptor *frazzled*. The netrins appear to be members of a highly structurally-conserved family of axon guidance molecules; further investigations have revealed that they are also conserved in function.

Commissural neurons are born in the dorsal spinal cord and extend axons along a ventral trajectory to their intermediate target, the floorplate, at the ventral midline of the spinal cord. The floorplate has been shown to secrete a long-range chemoattractant (for review see Colamarino & Tessier-Lavigne, 1995a) and additionally has outgrowth-promoting effects (Tessier-Lavigne et al, 1988). It was exploitation of its latter function that led to the identification of netrin-1, but it has subsequently been confirmed as the much sought after floor-plate derived chemoattractant. Netrin-1 (78 kDa) was purified from embryonic chick brains (Serafini et al, 1994) along with another family member netrin-2 (75 kDa), which also promotes commissural outgrowth. Transfection of

the cDNA into COS cells resulted in the release of a diffusible activity, that when co-cultured with a dorsal spinal cord explant, led commissural axons to project towards COS cells expressing either netrin *in vitro* (Kennedy et al, 1994) reproducing their growth pattern towards floor plate explants (Placzek et al, 1990).

Netrin-1 and netrin-2 are differentially distributed in the spinal cord. Netrin-1 is detected in the notocord prior to neural tube closure, then after closure is restricted to the floor plate. Netrin-2 is expressed in the same timeframe and occupies the ventral two-thirds of the spinal cord, exclusive of the floor plate. This suggests a model in which there is a steep gradient of netrin-1 diffusing from the floor plate, superimposed on a lower level of netrin-2 emanating from the ventral cord, which may modulate the netrin-1 gradient by extending it further into the dorsal spinal cord. The commissural neurons would encounter an increasing concentration of netrin protein as they migrate ventrally (Kennedy et al, 1994). At a recent axon guidance meeting (EMBL, Heidelberg, 1996) the cloning of *netrin*-1 and *netrin*-2 genes in the mouse was revealed (Tessier-Lavigne). In contrast to the chick, netrin-2 is not expressed in the spinal cord although netrin-1 expression pattern is compatible to the sum of the two chick genes, it was suggested that in rodents, netrin-1 may additionally perform the functions of chick netrin-2.

Receptors for netrins in Drosophila and C. *elegans* were identified prior to that of the chick netrins. These receptors are evolutionary conserved which helped lead to the characterisation of the chick netrin receptor/s, DCC and neogenin (Keino-Masu et al, 1996). Together DCC and neogenin form a subgroup of the Ig superfamily. DCC was previously cloned as a putative tumour suppressor gene deleted in colorectal cancer. It is expressed in commissural axons and its binding to netrin has been visualised using a specific antibody to netrin. Further confirmation of DCC - netrin interaction was provided by blocking the extracellular domain of DCC *in vitro*, this inhibited netrin-1 and floor plate-evoked outgrowth of commissural axons. Neogenin also binds netrin-1 but is expressed in a complementary pattern to DCC in the chick spinal cord. The authors have suggested it is a passive binding protein that may stabilise the gradient of netrin-1.

In the absence of *in vivo* perturbation data the chemoattractive function of netrin was initially surmised after netrins were determined to be vertebrate homologues of the C*elegans unc*-6 gene and 50% identical (Ishii et al, 1992). The *unc*-6 gene and protein has been well characterised from its distribution, to mutant analysis and putative receptors. These aspects have been the subject of several reviews, but briefly it regulates neuronal outgrowth and cell migration along the dorsoventral axis of the nematode body wall (Kennedy & Tessier-Lavigne, 1995; Keynes & Cook, 1995; 1996; Culotti & Kolodkin, 1996). Drosophila also express two netrins: D-netrinA and D-netrinB in the midline of the developing CNS and mutants show these are required for guidance of commissural neurons and peripheral motor axons (Harris et al, 1996, Mitchell et al, 1996). The chemoattractant functions of netrin have now been confirmed in vertebrate mutants.

The phenotype of null mutants is consistent with the proposed roles of netrin. Homozygotes fail to move their forelimbs independently and are neonate lethal due to defective suckling. The commissural axons deviate from their normal projection towards the floorplate. Analysis of the netrin-1 mutant mice floor plate *in vitro* shows the knockout is unable to promote the outgrowth of commissural axons in a collagen gel assay, indicating that netrin-1 is responsible for this activity of the floor plate (Serafini et al, 1996). Netrin-1 has previously also been attributed with a role rostral to the spinal cord, in attracting cerebellofugal axons to the floor plate (Shirasaki et al, 1995). The mutant confirms this and additionally raises the possibility that netrin-1 is a chemoattractant for migrating cells as well as axonal growth cones.

It is significant that netrin was identified as a putative diffusible factor but in COS cells, more than 80% of netrin protein remains associated with cell surface (Kennedy et al, 1994). The diffusion of the remaining netrin, may be subject to buffering by cell surface or ECM components to establish both soluble and substrate-bound protein gradients (Kennedy & Tessier-Lavigne, 1995). During netrin purification another molecule with separate activity was isolated in the brain extract. This was termed NSA (netrin synergising activity), as it dramatically potentiated the ability of netrins to promote outgrowth but its singular activity and distribution are unknown (Serafini et al, 1994).

The function of the substrate-bound netrin is also unknown but in C. *elegans*, *unc*-6 is expressed as a surface-associated cue on certain pioneer axons where it serves as a labelled pathway to guide follower axons by contact-mediated mechanisms (Wadsworth et al, 1996).

Early information on growth cone navigation focused upon positive influences on growth cone behaviour. Since 1993, evidence has accumulated from disparate sources that growth cone navigation also depends on negative influences. There are now several examples in both vertebrates and invertebrates of inhibitory or repulsive activities and the existence of a family - the semaphorins that mediate this activity (see below) and also a further role for the netrins. Because netrins are associated with chemoattraction, distinctions in the response of a guidance cue must reside at the level of the receptor expressed on subsets of growth cones.

The nematode *unc*-6 mutant revealed that both ventral and dorsal directed migrations were impaired (Hedgecock et al, 1990), and led to the proposal that *unc*-6, and by implication netrin, has dual effects (Culotti, 1994). It is suggested that they may inhibit dorsally migrating cells/axons. Recently, a chemorepellant role for netrins has been established (Colamarino & Tessier-Lavigne, 1995b; Tamada et al, 1995). Motor neurons from the midbrain, hindbrain and spinal cord are deflected from explants of floor plate. Additionally, netrin-1 repels trochlear motor neurons *in vitro* at concentrations similar to those required to attract commissural neurons. The mechanism of this action remains unclear, as it has not been ascertained whether netrins like semaphorins, can initiate growth cone collapse. The matter of chemorepulsion has become somewhat confusing since the announcement of the netrin knockout. It now seems that the dorsal trajectory of trochlear axons is unperturbed in the mutant and their chemorepulsion is maintained in netrin-deficient floor plate explants (Keynes & Cook, 1996; Serafini et al, 1997).

ii) semaphorins/connectin

The protein family particularly associated with chemorepulsive activity is the semaphorins. Seventeen members of the semaphorin family have been identified in grasshopper, Drosophila, chick, mouse and human and it has now been subdivided into four distinct subgroups.

The connection between these independently identified proteins was realised after the cloning of the avian protein collapsin, that induced collapse of sensory growth cones (Luo et al, 1993) in a now classical bioassay developed in the 1980's (Kapfhammer & Raper, 1987). It was quickly ascertained that collapsin was closely related to the grasshopper protein, fasciculin IV (Kolodkin et al, 1992). The possibility that these two proteins represented a larger family was validated after supplementary members of the gene family were identified in Drosophila and human (Kolodkin et al, 1993). This initiated the search for further molecules to arrive at seventeen currently (Puschel et al, 1995; Luo et al, 1995), although the existence of RNA splice variants (Puschel et al, 1995) and human expressed sequence tags (Messersmith et al, 1995) represent additional semaphorins. A further novel group of murine semaphorins with homology to thrombospondin have been identified (Adams et al, 1996; Puschel et al, 1996b).

The semaphorins characteristically share a conserved extracellular "sema" domain of 500 amino acid residues and 16 cysteines, the remainder of the different member sequences are divergent, reflecting the range of functions. Sema I is unique in having a transmembrane domain indicating it has local contact-mediated activity. The remaining semaphorins possess a single Ig domain, are secreted proteins, and therefore diffusible, though the actions of Sema III may be more limited due to its surface association in transfected cells (Luo et al, 1995).

Drosophila Sema II is associated with motoneuron target recognition. In this system, two motoneurons RP1 and RP3 project to muscles 6 and 7. The Sema II mutant, like the connectin molecule below, shows no abnormalities in neuronal connectivity yet ectopic expression in muscles 6 and 7 prevents RP3 from innervating the target (Kolodkin et al, 1993). Similarly, the related molecule fasciculin IV in grasshopper, guides the Ti1

growth cone in the peripheral nervous system by repulsive actions (Kolodkin et al, 1992). Further evidence consistent with repulsive roles for these proteins in other species is reviewed (Keynes & Cook, 1995; Culotti & Kolodkin, 1996).

The best characterised demonstration of semaphorin participation in axonal guidance, is the dorsal-ventral boundary to innervation in the developing vertebrate spinal cord. The ventral spinal cord contains the cell bodies of motoneurons and is the site of termination for proprioceptive muscle afferents. The dorsal spinal cord contains the cell bodies of sensory relay neurons and is the site of termination of cutaneous sensory afferents. The termination sites are clearly demarcated in somatotopically arranged laminae, both muscle and cutaneous afferents enter the spinal cord through the DREZ, yet no theory accounted for the proprioceptive afferents projecting ventrally while the cutaneous afferents remain in the dorsal horn.

In 1993, Fitzgerald and colleagues proposed the existence of an inhibitory substance in the ventral horn that actively repelled sensory cutaneous afferents. They showed that ventral spinal cord tissue can repel the growth of sensory axons *in vitro*.

Sema III (homologue of chick collapsin-1) can cause local collapse in regions of the growth cone *in vitro* (Fan & Raper, 1995). Experiments linking the proposed ventral inhibitory factor and Sema III involved selective *in vitro* outgrowth of either cutaneous sensory or muscle axons, by virtue of their distinct trophic requirements, and distinguishing between their response to ventral spinal cord and Sema III (Messersmith et al, 1995). This established that cutaneous axons (defined by NGF-dependent outgrowth) were deflected by ventral spinal cord and COS cells expressing Sema III, while muscle axons (defined by NT3-dependent outgrowth) were not affected.

Consistent with this result, high expression of Sema III is detected in ventral but not dorsal spinal cord, excluding the floor plate region. (Messersmith et al, 1995; Puschel et al, 1995; Luo et al, 1995). The expression of sema III mRNA in this region of the CNS and in PNS avoided by sensory axons has also been documented (Wright et al, 1995). A comprehensive analysis of seven semaphorin genes in the mouse CNS also concurs with the expression of Sema III/D (Puschel et al, 1996b), and contains extremely important

information relating to the specific function of combined semaphorins, in patterning of spinal cord innervation and is discussed further in Chapter 4.

Peripheral axonal projections are also anticipated to be subject to inhibitory influences. In the chick, lectin binding identified specific areas in the periphery that are inhibitory to growing motor and sensory axons *in vitro* (Tosney & Landmesser, 1985; Davies et al, 1990; Tosney & Oakley, 1990; Oakley & Tosney, 1991). Sema III is one of the molecules proposed to discourage axonal growth in selected areas of the periphery, after its localisation in the dermatome and posterior sclerotome of the rat at E11. Its mRNA is also expressed in mesodermal structures surrounding the axon fascicles with highest levels in the dermamyotome, perinotochordal mesenchyme, pelvic girdle and limb between E12 and E15 (Wright et al, 1995). Important in relation to this thesis, was the finding that sensory axons exiting the DRG were surrounded by Sema III mRNA, that it is temporally and spatially expressed in the limb consistent with the proximo-distal in-growth of axons and that no axonal growth cones penetrate regions of intense Sema III mRNA expression.

Generation of the Sema III mutant recently, has illustrated a population of NGF-sensitive neurons that project ectopically in the ventral spinal cord where sema III is normally expressed (Behar et al, 1996). Defects in other tissues are consistent with previously identified sites of Sema III expression (Wright et al, 1995). The hypertrophy of cardiac tissue and the duplications of cartilaginous and bone structures, suggests Sema III might act as a signal to restrain growth in several developing organs. Analysis of this mutant at each embryonic stage will be required to fully reveal the role of Sema III, especially any innervation defects in the targets of DRG neurons.

The receptors or downstream signalling components for semaphorins have yet to be determined, however, a protein required for collapsin activity has been isolated (Goshima et al, 1995). Collapsin response mediator protein (CRMP-62) expression is confined to the nervous system, with high levels in retina, brain, DRG and spinal cord. It is required for collapsin-induced inward conductance and eliminated growth cone collapse on exposure to collapsin when cultured with DRG cells expressing an antibody to

CRMP-62. It shows homology to the C. *elegan Unc*-33 protein whose knockouts show defective axonal elongation, fasciculation and branching of sensory, motor and interneurons. From the preliminary data it is conceivable that *Unc*-33 and CRMP-62 mediate semaphorin family activity. The fact that CRMP-62 is more widely expressed than collapsin also indicates that it may interact with more than one member of the semaphorin family.

Connectin is a Drosophila protein expressed in muscle during the larval stage that shows repulsive activity. Null mutations cause no obvious phenotype (Nose et al, 1994) but ectopic expression does inhibit specific connections (Nose et al, 1994; Matthes et al, 1995). High levels also prevent motoneuron RP3 from recognising muscles 6 and 7. The nature of semaphorin repulsive activity is diffusible, and the response to connectin is consistent with this, although it functions as a homophilic CAM *in vitro* (Nose et al, 1992). This is another example of different functional responses to the same molecule on either different neurons or surroundings, emphasising that receptor interaction invariably determines the functional response.

iii) The Eph Family

The Eph (Erythropoetin-producing hepatocellular) family of receptors were discovered in 1987 (Hirai et al, 1987), and is the largest subfamily of the fourteen families that comprise the receptor tyrosine kinases (RTKs). They were initially referred to as "orphan receptors" because of the absence of known ligands. Now, fourteen members have been identified in conjunction with eight ligands belonging to another novel family. These molecules are implicated in the development of the vertebrate nervous system.

Receptor molecules contain extracellular regions with Ig-like domains and fibronectin repeats and a cytoplasmic region composed of a single kinase catalytic domain. An important characteristic of the ligands for these receptors is that they are all membrane attached proteins (GPI-linkage/transmembrane domain) and hence require membrane attachment for activity (Davis et al, 1994). Any Eph-ligand interaction is contact-dependent for cell-cell communication and therefore the cellular responses may be

different from those of diffusible signal receptors outlined above. The receptors and ligands can be sub-divided into two groups based on the type of membrane attachment, either GPI-anchored ligands to Eck-type receptors or transmembrane (TM) ligands to Elk-type receptors (Gale et al, 1996)

Their role in axonal guidance has mainly been deduced from examination of the retinotectal system. Posterior tectal membranes were observed to repel temporal axons by collapsing their growth cones. The putative repulsive factor was identified as a ligand for the Eph receptors - RAGS (repulsive axonal guidance signal), (Drescher et al, 1995). This 25 kDa protein possessed the characteristics of GPI-linkage, regionalisation and developmental regulation associated with the repulsive properties of the tectal membrane (Stahl et al, 1990; Bonhoeffer et al, 1995). It was confirmed to repel retinal axons *in vitro* and in a concentration dependent manner. Again in the retinotectal system, the Eph receptor Mek-4 mRNA and its ligand Elf-1 were expressed in graded and complementary patterns in the retina and the tectum (Cheng et al, 1995). These ligands show slightly different distributions and it has been suggested that RAGS has a general repellent function for both temporal and nasal axons whereas the more restricted Elf-1 repels only temporal axons.

Further examples of a guidance role for the Eph family are found in other areas of the nervous system (Keynes & Cook, 1995; Nieto, 1996). In the mouse, the topography of hippocamposeptal projections may be established under the influence of the Eph family. Bsk is an Eph receptor expressed in the hippocampus in a lateral to medial gradient. Its GPI subclass ligands: Elf-1, RAGS and Lerk-3 are expressed in a counter-gradient in the septum. A similar strategy to that of the retinotectal system is proposed where neurons expressing high levels of receptor project to a region with low ligand levels (Nieto, 1996).

An important putative role for this family in the retinotectal system, and if confirmed, for all other sites of Eph expression, is the regulation of preferential branching - a remodelling process. This is extremely significant as the process of establishing the correct topographical map by remodelling after the target is innnervated, is

activity-dependent and stimulated by neurotrophin application. Therefore, the Eph family would be pivotal in linking these identified processes. Preferential branching is stimulated by addition of BDNF, yet is regulated by the inhibitory activity of an unknown GPI-linked membrane bound molecule. The Eph receptor ligands are ideal candidates because of their expression and activity, additionally their receptor expression is not restricted to the growth cone but located along the length of the axon. This would allow them to recognise sites of preferred branching and increases the opportunity for interpretation of graded information (Nieto, 1996).

Elucidation of the cellular reponse generated after ligand-receptor binding is central to determining the extent of their contribution. The primary requirements of ligand-receptor binding and the subsequent phosphorylation of receptors has been established. Generation of a chimeric receptor, consisting of an extracellular Eph component and a cytoplasmic Trk component, highlighted a possible role for the cytoplasmic domain of the TM ligands. Binding of a TM ligand to the chimeric receptor increased the response, suggesting that normal signalling through the Eph receptor could be regulated like the trk receptor (Bambrilla et al, 1995). Furthermore, TM ligands are also substrates for tyrosine kinases activated by platelet derived growth factor (PDGF) (Nieto, 1996). The parallels between Eph binding and trk binding and the link to preferential branching above, is encouraging for the existence of a direct connection between aspects of axon guidance regulation by neurotrophins, possibly mediated by the same intracellular signalling pathways.

2

MATERIALS AND METHODS

2.1 General Methods

2.1.1 Laboratory Animals

All tissue used in this study was obtained from Sprague-Dawley rats of both sexes, ranging in age from embryonic day (E) 13 to postnatal day (P) 10 and adult. Rats were mated and conception confirmed by the observation of a vaginal plug. The morning that the plug was detected was designated as E0 of gestation (full gestation = 21.5 days) and the day of birth as P0.

2.1.2 Tissue Preparation

Pregnant dams were deeply anaesthetized under halothane (4% nitrous oxide/oxygen mixture for induction, 2% for maintaining anaesthesia) and the embryos removed by caesarean section, then the dam was killed by anaesthetic overdose. All embryos up to the age of E18 were immediately decapitated and placed in ice-cold fixative for immersion fixation. Embryos from E18 and animals at all postnatal ages were perfused transcardially with saline until cleared of blood, followed by fixative. The postnatal pups and adults were heavily anaesthetized by intraperitoneal injection of pentobarbitone (Lethobarb); older embryos were first placed on ice. Tissues of interest (hindlimbs, lumbar vertebral column, spinal cord and DRGs) from older embryos and postnatal animals, were dissected out prior to postfixation with the same fixative as used for perfusion.

2.1.3 Fixatives

4% paraformaldehyde (BDH) in 0.1M phosphate buffer (pH 7.4, ice cold) was the fixative of choice for all experiments except Substance P (SP) immunohistochemistry (IHC). Tissue destined for SP IHC was prepared in picric acid fixative: 75mls picric acid (Sigma) in 425mls 4% paraformaldehyde. After postfixation at 4^0C, material was transferred to 20% sucrose in phosphate buffer (stored @ 4^0C) for cryoprotection, except embryos at E13-14. These were first embedded in 5% gelatin and 10% glycerine at 37^0C overnight then returned to fixative for 24 hrs before cyroprotection in sucrose buffer.

2.1.4 Sectioning of Frozen and Wax Prepared Tissue

After postfixation and cryoprotection, tissue was frozen and sectioned on a freezing microtome or cryostat (depending on the thickness required), or processed for wax embedding. Tissue destined for free-floating immunohistochemistry (whole embryos and hindlimbs) was sectioned using a freezing microtome while thin sections of spinal cord prepared for IHC on slides, or *in situ* hybridisation were cut on a cryostat. When IHC was required on DRG sections, the entire lumbar vertebral column was first wax embedded and the DRGs sectioned *in situ*.

Processing Tissue for the Freezing Microtome

Tissue required for free-floating IHC was sectioned using a Leitz 1310 freezing microtome. The fixed tissue was mounted in Tissue Tek/O.C.T compound (Miles Inc.), frozen with CO_2 and cut at 100μms in a transverse plane (see Fig. 2.1). All sections were collected in 0.1M phosphate buffered saline (PBS).

Processing Tissue for the Cryostat

12μm sections of spinal cord were cut using a Bright cryostat, chamber temperature -20^{0}C. The tissue was mounted in tissue tek and frozen onto metal chucks in a liquid nitrogen bath (-80^{0}C). Transverse sections (see Fig. 2.2) were directly collected onto silane-coated slides (BDH), air-dried and stored at 4^{0}C for immunohistochemistry, or placed at -70^{0}C for *in situ* hybridisation as soon as sections were dry.

Wax Embedding and Sectioning

Lumbar vertebral column was removed from fixative and washed twice in PBS for 15 mins. The tissue was dehydrated for no longer than 15-20 mins each in a series of alcohols (30%, 50%, 70%, 90%, 100%, 100%). It was transferred to Histoclear (National Diagnostics) at room temperature, then 50^{0}C each for 20 mins. The embedding procedure consisted of placing the tissue in a 50:50 mixture of histoclear and wax (Fibrowax, BDH) for 30 mins followed by pure wax for 1 hr. Tissue was finally

embedded in blocks of pure wax in plastic weigh boats (BDH) and allowed to solidify quickly over ice. Blocks were stored at 4^0C.

Blocks were mounted onto wooden chucks and sectioned at 6-7μms on a Leitz microtome. Ribbons of wax sections were then floated in a bath of 40^0C distilled water and collected on TESPA (see 2.1.5) coated slides. Slides were air-dried and stored at 4^0C.

Before wax embedded tissue was processed for IHC the slides with tissue sections had to be dewaxed. Slides were first brought to room temperature then placed in xylene (BDH) twice, each for 5-10 mins. These were transferred to 100% ethyl alcohol for 10 mins to remove excess xylene. Slides were then rehydrated for 5 mins each in a series of alcohols (100%, 95%, 70%, 50%, 30%) and brought into distilled water then PBS for immediate use.

2.1.5 TESPA coated slides

Super Premium microscope slides (BDH) were cleaned for 60 mins in a 10% detergent solution, then washed in running tap water for a further 20 mins. Slides were submerged in a mixture of 15mls 37% hydrochloric acid (BDH) and 985mls ethanol for 15 mins. They were washed twice for 2 mins in RNAse-free distilled water (DW). Slides were then baked overnight at 160^0C. The slides were allowed to cool and dipped into 6% Silane (3-Aminopropyl-Triethoxy-Silane, Sigma) in 100% acetone for 10 mins, followed by 5 min washes in acetone, acetone, DW, DW. They were finally air-dried.

2.1.6 Photography and Image Analysis

Photographs

All photographs were taken using an Orthomat E camera unit and Leitz Diaplan microscope.

Camera Lucida Drawings

The pattern and density of nerve fibres in the hindlimb sections and the outline of DRG cells were drawn using a camera lucida. Only neuronal profiles of DRG cells

containing a visible nucleolus were selected to increase the probability of measuring the area of a cross-section near or at the middle of the cell. A section of tissue was placed on a Nikon microscope with an attached Nikon drawing tube. Tracings of the nerves at different magnifications, or cells at x400 were made using Rotring pens and a dia-polarizer filter. The magnification factor was determined by including a scale bar derived from an optical micrometer. The regions of the hindlimb selected for analysis are shown in Fig. 2.3.

2.2 Methods for Chapters 3, 4

2.2.1 Immunohistochemistry Protocol

Free-floating

After collection in 0.1M PBS (Phosphate buffered saline), alternate sections were selected and transferred to multiwelled plates (Nunclon) in PBS. These were washed while agitated for 15 mins. Sections from unperfused animals were preincubated in 0.3% H_2O_2 in PBS for 20-30 mins and then washed in PBS containing 0.1% Triton-X-100 (PBS/TX, at room temperature used for all subsequent washes) for 10 mins. All sections were first incubated with a blocking agent. 20% normal goat serum (NGS, Vector) in PBS/TX was applied for 1 hr with use of antibodies to PGP 9.5, GAP 43, CGRP, RT97 (mouse monoclonal, ascites fluid) and PER. Bovine serum albumin (0.15g BSA, Sigma) in 5mls PBS for 15 mins was used for trkA, IB4 and SP. In addition SP was also blocked with an avidin biotin blocking kit (Vector) for 30 mins.

Primary Antibodies

Antibody	Source
Protein Gene Product 9.5 (PGP)	Ultraclone Ltd
Growth Associated Protein 43 (GAP 43),	Boehringer Mannheim
Biotinylated ISOLECTIN B4 (IB4)	Vector
Calcitonin Gene Related Peptide (CGRP)	Gift from Dr. Iadorola (USA)
RT97	Gift from Dr. J. Wood (UCL)
Peripherin (PER)	Gift from Dr. L. Parysek (USA)
trk A	Gift from Prof L. Reichardt (USA)
Substance P (SP)	Affinity UK

Antiserum was then applied in the following concentrations for 48 hrs at 4^0C:

anti-PGP 9.5:	1:1000	PBS/TX and 2% NGS as diluent.
anti-GAP 43:	1:1000	
anti-CGRP:	1:10 000	
anti-RT97:	1:750	
anti-PER:	1:200	

anti-trkA:	1:2000	PBS/TX as diluent
anti-SP:	1:10 000	
anti-IB4	13µg/ml	

Antiserum was removed and sections washed for 3x20 mins. Biotinylated secondary antibody (Vector) was applied as follows for 1 hr at room temperature.

PGP 9.5	Biotinylated anti-rabbit IgG 1:250.
GAP 43	
PER	Diluent: PBS/TX and 1% NGS

trkA		Biotinylated anti-rabbit IgG 1:250.
		Diluent: PBS/TX
SP		Biotinylated anti-rabbit IgG 1:200.
		Diluent: PBS/TX
RT97	┐	Biotinylated anti-mouse IgG 1:250.
CGRP	┘	Diluent: PBS/TX and 1% NGS

Secondary antibodies were removed and sections washed for 3x20 mins. 30 mins before application, the Vectastain ABC complex was prepared and then applied for 1 hr at room temperature. The standard kit was used for all sections except those with primary antibodies to CGRP, RT97, IB4 and trkA when the Elite kit was utilized. Sections were washed as before and the stain visualised using the chromagen diaminobenzidine (0.05%) in Tris buffer, pH 7.6 plus 0.01% H_2O_2 v/v. After staining, sections were mounted on gelatinised slides, dehydrated, cleared in Histoclear and coverslipped using DPX (BDH).

Sections on slides

Slides with tissue sections (frozen/wax prepared) were treated as above except all washes and diluents were in PBS only to ensure they formed a meniscus when applied. The slides were placed in a humid chamber and 200µls of primary antibody applied to the sections for 24 hrs at 4^0C. Secondary antibody and the ABC complex were each applied for 4 hrs at room temperature.

2.2.2. Counterstaining

Wax embedded sections of DRG were counterstained after IHC to locate the nuclei. The slides were allowed to dry after visualisation of chromagen. Slides were then rehydrated in distilled water and dipped into the Toluidine Blue (0.17g/100mls, 0.1%

borax) counterstain. The intensity of the counterstain was checked under the microscope, then the slides were dehydrated, cleared and coverslipped.

2.2.3 Area Measurements

The camera lucida drawings of DRG outlines were used to generate size-frequency histograms by first retracing the outlines onto a digitizing tablet (Genius Newsketch 1212 pad) then using the TABYLT morphometry program (generously provided by Dr. Jeremy Cook, Dept. Anatomy, UCL) to directly calculate the area of each cell. This data was imported into the Microsoft Excel spreadsheet program and histograms were generated.

2.3 Methods for Chapter 5

2.3.1 Density Analysis

Camera lucida drawings of skin innervation in regions A-D (see Fig. 2.3) immunolabelled in the hindpaw (Chapter 4) were scanned with an AGFA Arcus II flatbed scanner. Digitised images were imported into the program Photoshop 3.0. A new layer (layer-1) was superimposed on the image and the outline of the epidermis traced in a different colour as guide lines. This epidermal outline was then rubbed out from the original drawing.

The outline of the epidermis was selected on the original drawing according to the guide lines in layer 1. The image was then inverted so that the nerve fibres drawn in black were now white on a black background. This step was taken, since some of the nerve fibres would be detected as shades of grey and not absolute black. The histogram function was utilised and the number of absolute black pixels recorded in addition to the total number of pixels for the selection. Values were substituted into a spreadsheet program (Microsoft Excel 4.0). The number of pixels enveloped by the nerve fibres were then calculated by subtracting the number of black (i.e. non-innervation) pixels from the total.

Since density analysis was undertaken at different developmental ages it was important to consider the area of the region under analysis, therefore a calibration value

was calculated from a scale bar on the camera lucida drawing. If the scale bar on the drawing was 100μm, then the number of pixels within a square equivalent to 10000μm^2 was determined. Any region subsequently selected for area analysis was recorded in pixels and automatically converted to μm^2 using the calibration value in the spreadsheet program.

The worksheet in the spreadsheet program was organised as follows to calculate the density of innervation in pixels per μm^2 of tissue:

i) The first column contained a constant derived from our calibration value, i.e. the total number of pixels in a standard area of 10,000μm^2 (Stdpix)

ii) A column representing the total number of pixels in the epidermal area (Totpix)

iii) A column with the total number of background pixels in the epidermal area (BGpix)

To obtain the density of innervation, the computer calculated the number of pixels corresponding to innervation (Innpix), the surface where the measurements were performed (Surface) and finally the density (Dens).

iv) Innpix= Totpix-BGpix

v) Surface= (Totpix x 10,000)/ Stdpix

vi) Dens = Innpix / Surface (in pixels / μm^2).

Stdpix	Totpix	BGpix	**Dens**
Pixels / 10,000 μm^2	Pixels in epidermis	Background pixels in epidermis	**Innpix/Surface**

2.4 Methods for Chapter 6

2.4.1 In Situ Hybridisation

Both isotopic and non-isotopic methods of *in situ* hybridisation were applied to the detection of CGRP mRNA in embryonic spinal cord and DRG. The isotopic detection with S-35 labelled probe was carried out in collaboration with Dr. Greg Michael at UMDS, London. The protocol performed by Dr. Michael is detailed in appendix I and was conducted on embryonic tissue aged E14-E18. Non-isotopic detection with a DIG-labelled CGRP riboprobe was conducted on tissue aged E17 and E18. The probe was prepared by Richard Mannion, UCL and the protocol is detailed in Appendix II.

Hybridisation Protocol

Slides were removed from storage at -70^{0}C, and placed in 4% paraformaldehyde in 0.1M PBS for 10 minutes. After fixation sections were washed in 0.1M PBS three times, acetylated for 10 minutes and permeabilised in 1% triton X-100 (Sigma) for 30 minutes. They were washed again in 0.1M PBS three times and 1ml hybridisation buffer added to each slide and left for 6 hours in a humidified chamber at room temperature.

Sections were then incubated in hybridisation buffer (probe concentration 250-500ng/ml) overnight in a humidified chamber at 45-72^{0}C, and washed in decreasing concentrations of SSC (5x-0.1x) for 1 hour in total. Sections were placed in buffer B1 for 5 minutes then buffer B2 for one hour, before being incubated overnight at 4^{0}C in buffer B2 with anti-digoxygenin alkaline phosphatase-conjugated fab fragments (Boehringer Mannheim; 1:500). After hybridisation with the antibody, they were washed in buffer B1 three times for five minutes, buffer B3 for 5 minutes then the colour reaction product was visualised in buffer B4. The reaction was stopped with TE, sections were washed in de-ionised H_20 and coverslipped using aquamount (BDH).

Solutions

1M phosphate buffer:	0.75M $Na_2HPO_4.7H_2O$ (206.675g/litre)
	0.25 M NaH_2PO_4 (31.975g/litre)
4% paraformaldehyde:	see 2.1.3
3M sodium chloride:	175.71g/litre

Buffers

B1: 0.1M tris pH 7.5, 0.15M NaCl

B2: 5g blocking reagent (Boehringer Mannheim) and 2.5g BSA in 500ml B1. Heat to 60°C then aliquot into 25 ml universals and store at -20°C.

B3: 0.1M tris pH 9.5, 0.1M NaCl, 0.05M $MgCl_2$

B4: 75µg/ml NBT (Boehringer Mannheim), 50µg/ml BCIP, 0.24mg/ml levamisole (Sigma) in buffer B3.

Hybridisation buffer	50% formamide
	5x SSC
	5x Denhardts solution
	250µg/ml baker's yeast RNA
	500µg/ml herring sperm DNA
SSC (1 litre):	175.32g sodium chloride
	88.23g sodium citrate
TE:	10mM tris, Ph 8.0
	1mM EDTA

2.5 Methods for Chapter 7

2.5.1 Anti-NGF Treatment

The protocol for embryonic injections of anti-NGF was modified from Ruit et al, 1992. Briefly, pregnant dams of fifteen days gestation were deeply anaesthetized under halothane (4% nitrous oxide/oxygen mixture for induction, 2% for maintaining

anaesthesia) and a midline surgical incision made. The abdominal wall was opened and the uterine horns exposed. Two embryos from each horn were selected for injection. The 5μl injections of sheep anti-NGF (gift from Professor Clifford Woolf, UCL) were made with a Hamilton syringe with a 30 gauge sterile needle inserted into the rump region of the embryo (Fig. 2.4). The embryo was first visualised through the uterine wall and membranes using a fibre optic light. After the injection was completed the needle was kept in place for some seconds to prevent leakage. The animal was sutured and allowed to recover for three days. At day 18 of gestation the mother was reanaesthetized and a second injection of 10μl was administered and the mother allowed to recover. Finally at E21, the mother was terminally anaesthetized after the injected embryos were harvested and perfused.

2.5.2 Size-frequency Histogram

see 2.2.3

2.5.3 Cell Counts

Counts of DRG cells from control (n=2) and anti-NGF treated (n=3) embryos were conducted on three lumbar DRG from each animal. Counts were conducted using a variation of the physical dissector method (Coggeshall, 1992), referred to as the fractionator technique.

The lumbar vertebral column was transversely and serially sectioned at a thickness of 7μm. Sections throughout each of the three ganglia were identified and the number of sections in each calculated. The total number of sections in each DRG were summed and sequentially numbered, and the new total for the combined ganglia divided by 5 to produce the section separation (k) for the 5 required dissector pairs. For example, if the total number of sections (N) for the three ganglia was 100 (numbered 1-100), then the section separation =20. Section separation dictates that counts would be conducted on every 20th section. A random number (R) generated between 1 and k (e.g. 4) would decide which section the analysis would begin at. Counts are conducted on 5 pairs of sections equally distributed (every 20th) throughout the numbered sections, beginning

with the section number equivalent to the random number. In this example selected pairs would be numbered 4-5, 24-25, 44-45, 64-65, 84-85.

The first section of each pair is referred to as reference section and the second as the look-up section. Up until this stage, this method follows the physical dissector protocol. The fractionator technique departs from the established protocol as the area of the section and volume of the ganglion are not required. Instead, the ganglion section is divided into four approximately equal quadrants. One of the quadrants are randomly selected, and the number of cell "tops" counted. A cell top is defined as a cell that is in the reference section but not the look-up section. The number of tops are recorded (T_1), then the process reversed and the number of tops calculated from the look-up to the reference section (T_2). These tops are averaged (T), multiplied by four (4T) to give the number of cells per whole ganglion section (S) and then multiplied by the total number of sections (N), to provide the number of cells in the three ganglia. The number of cells were finally expressed per lumbar ganglia (G).

Cells per ganglia(G): $(T_1 + T_2)/2 \times 4 = S$

$(S \times N)/3 = G$

2.5.4. Density Analysis

Camera lucida drawings of regions A-D (Fig. 2.3) in the hindpaw from control (n=3) and anti-NGF treated (n=4) embryos were scanned with an AGFA Arcus II flatbed scanner. Digitised images were imported for analysis into the program NIH Image 1.55.

A grid was superimposed on the image so that a comparable analysis frame could be selected for each section. The measuring frame was randomly placed along the section, keeping one edge on the epidermal-dermal border. The random placement of the section ensured that analysis was not biased, in addition the measuring frame was sufficiently large to encompass most of the section.

A threshold level of detection was selected to reveal all innervation and this was maintained for all subsequent analysis. The number of pixels above threshold were calculated and the total number of pixels within the measuring frame recorded. Density

was then expressed as the percentage of pixels above threshold compared to the total number of pixels within the measuring frame.

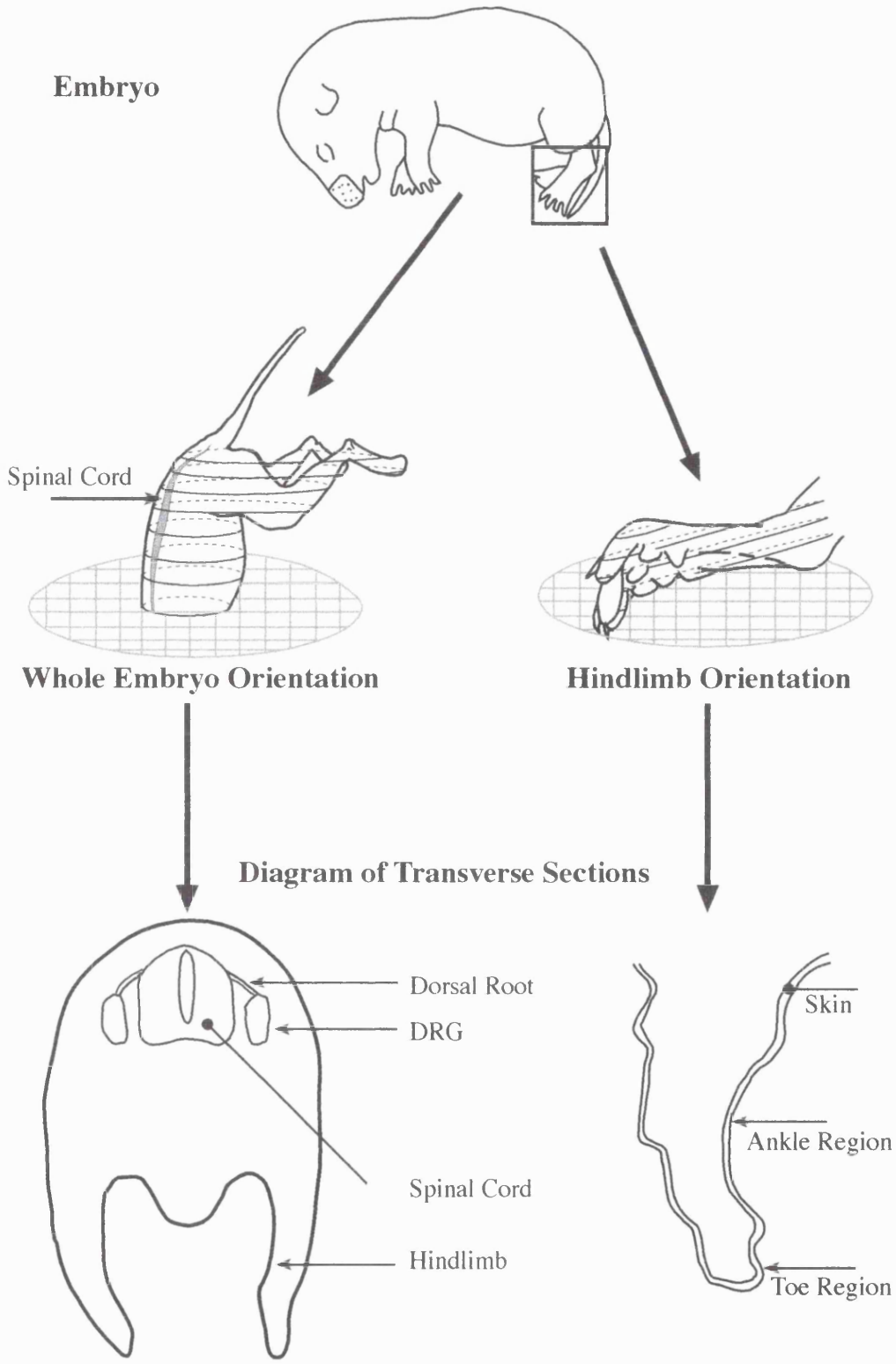

Fig. 2.1: Orientation of Tissue Sectioned on the Freezing Microtome

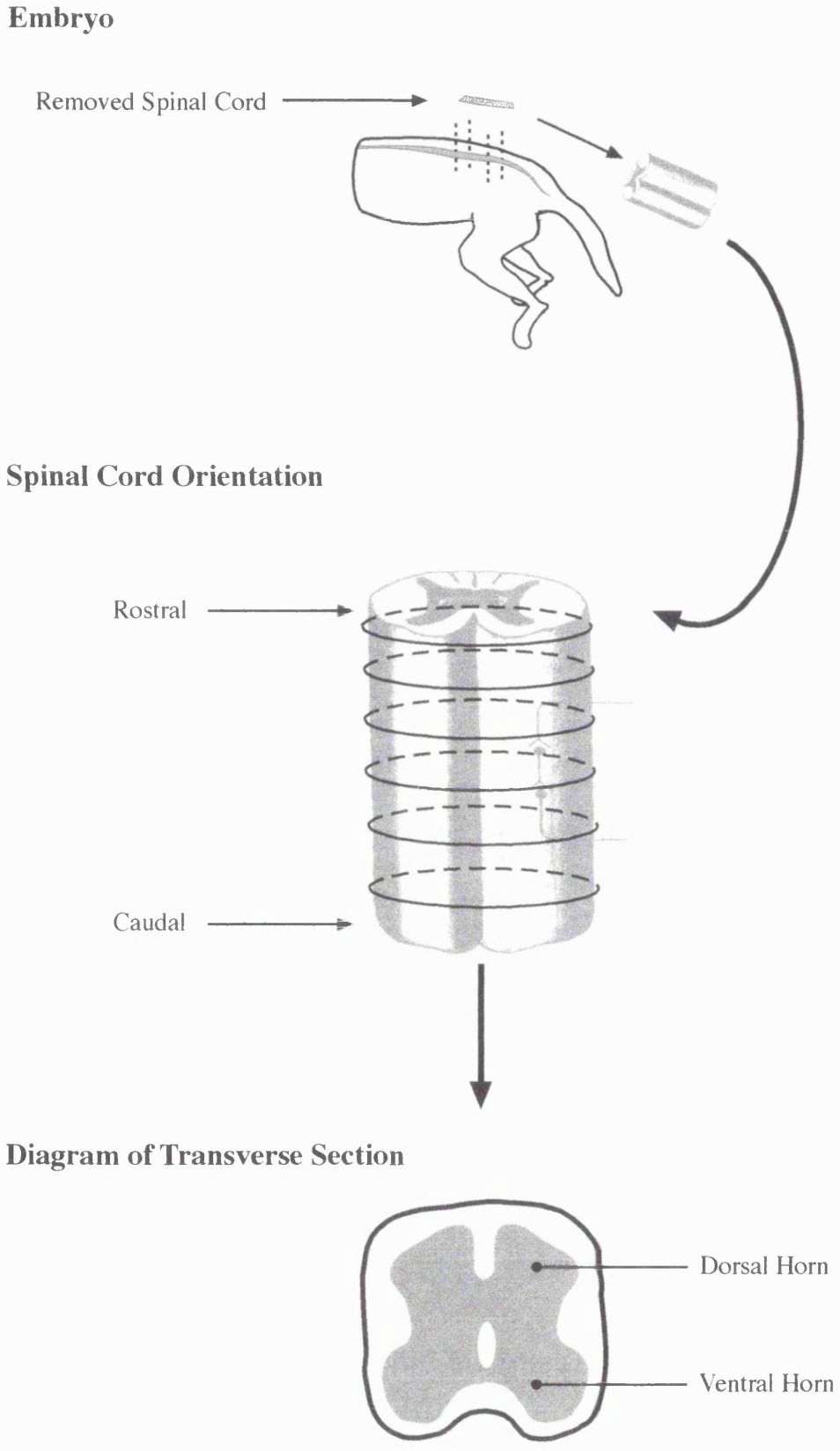

Fig 2.2: Orientation of Tissue Sectioned on a Cryostat

Hindlimb

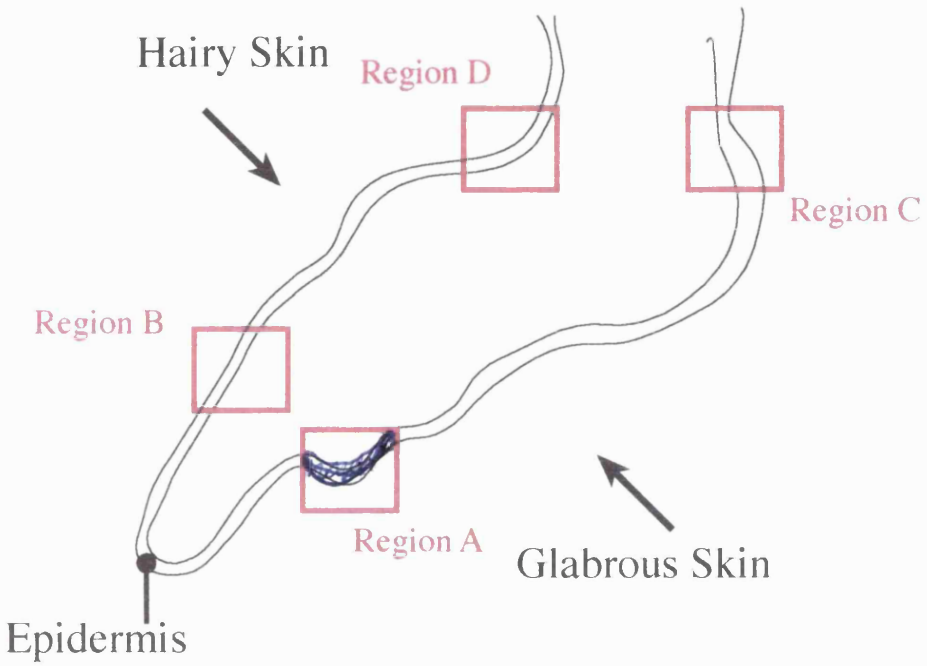

Region	Hindlimb Location
A	First Glabrous Footpad
B	Hairy Skin Opposite Glabrous Footpad
C	Glabrous Skin of the Ankle
D	Hairy Skin of the Ankle

Fig 2.3: The Hindlimb Regions Selected for Innervation Density Analysis

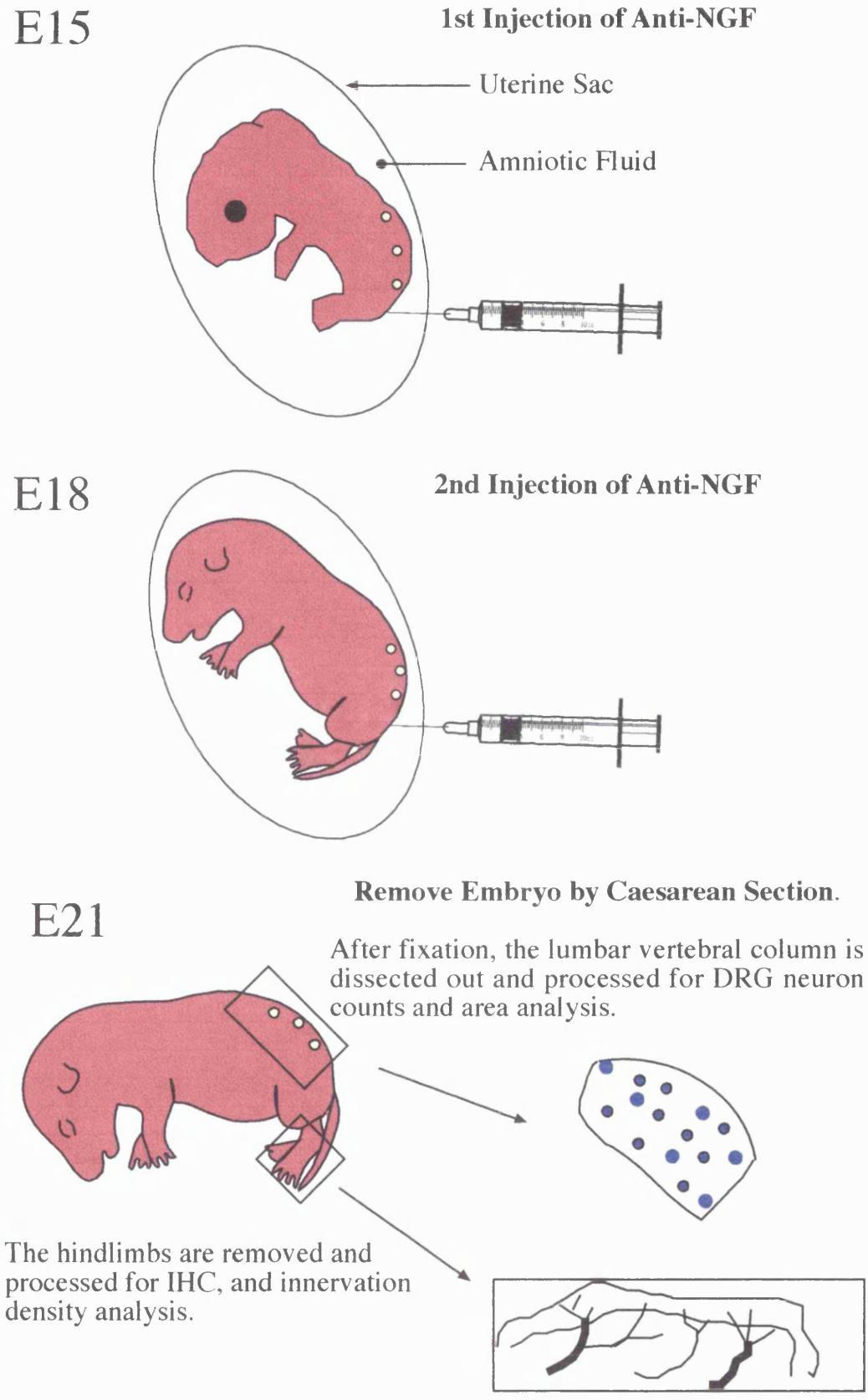

Fig 2.4: Anti-NGF Injection Procedure and Selection of Tissue for Analysis.

3

SIZE-FREQUENCY DISTRIBUTION OF E18 AND E21 DORSAL ROOT GANGLIA (DRG) NEURONS AND DISTRIBUTION OF RT97 IN THE E18 DRG

INTRODUCTION

Classification of adult DRG cells by their cell size and ultrastructural features has led to the definition of two populations, large light and small dark. It is not clear to what extent these two populations can be identified in embryonic life. In this chapter I have described the size and light microscope characteristics of dorsal root ganglion (DRG) cells in the E18 and E21 rat embryo. These morphological characteristics are key indicators of the maturity of cells which previously have not been comprehensively described.

In this chapter I also investigate the distribution of RT97, an antibody against the phosphorylated 200 kDa neurofilament subunit (NFH), in E18 DRG. It's size-frequency distribution in the adult rat DRG is found to closely resemble the normally distributed large light cells (Lawson et al, 1984) but this has not been established in the embryo.

3.1 Growth and Development of DRG Cells

3.1.1 Background

In Chapter 1 the birth and axonal outgrowth of DRG cells was described. Here I concentrate on the fact that DRG cells are not homogenous but differentiate and develop into a heterogeneous population of sensory neurons. These can be classified into subpopulations using various criteria (Willis & Coggeshall, 1991; Lawson, 1992; Snider & Silos-Santiago, 1996):

i) soma size

ii) ultrastructural features

iii) surface and cytoplasmic markers

iv) neurotrophin receptor expression

v) reactivity to growth factors

vi) target field innervation

vii) central termination patterns

viii) physiological characteristics and neurotransmitters

Neuronal phenotypes in the adult have been characterised although they are often a variable and plastic feature after experimental manipulation, or are dependent on the cellular environment (Hokfelt et al, 1994). Many of these criteria may change between the developing and mature animal, and recent developmental studies have discovered differences between the adult and embryonic situation e.g. in chemical phenotype of DRG sensory neurons (Troy et al, 1990a; Bennett et al, 1996b).

The first and most extensively examined criterion upon which cells have been classified, is cell size and ultrastructural features. The outcome of analysis from all of these criteria has resulted in the separation of the DRG population into two broad groups, A-fibres and C-fibres. Based upon the correlation between the soma size, axon size and physiological characterisation, the C-fibres generally emanate from the small DRG cells while A-fibres arise from the large DRG cells (Lawson, 1992). The ratio of unmyelinated to myelinated fibres in dorsal root is 2:1, and since a 1:1 ratio exists between dorsal root fibres and DRG cells it is concluded that C-fibres outnumber A-fibres twofold (Tandrup, 1995).

These aspects have not been fully described in the embryo, yet there is a general assumption that these features exist and can be applied to classify developing cells, without supporting evidence. In view of the developmental differences observed in many of the other classification criteria, in this chapter I have described morphological changes in the size-frequency distribution and light microscopic observations of DRG cells in the E18 and E21 embryo.

The account below details how DRG cells are formed, and how the balance between proliferation, cell death and growth during development contributes to cell size and numbers during this period. Included is an examination of ultrastructural properties of cells which give an indication of their maturity at various stages. The neurotrophin receptor expression, reactivity to growth factors and their effect on target field innervation are described in Chapter 7, while the central termination patterns are covered in Chapter 4. A brief overview of the remaining classification criteria- the physiological characteristics is included here.

3.1.2 Emergence of the DRG cells

Cells from the neural crest migrate ventrally, and at E11 the DNA content of the cells increases considerably before ganglia are recognisable (Sobkowiecz et al, 1973). The ganglia at this stage, however, are merely clusters of cells near the ventral region of the neural crest (Angulo, 1951) and do not appear as discrete entities until E13 (Lawson et al, 1974). Lawson and colleagues, (1974), first detailed the emergence of the rat DRG neurons. This study showed that cell division of neuroblasts takes place until differentiation of cells begins as early as E11. The age at which the neuroblasts terminally differentiate and form neurons, has been referred to as the neuron's birthdate. Birthdates of DRG cells were reported over a four day period, E11-E15, with peak production at E12. Consistent with this, many mitotic figures are observed in the DRG during this period (Lawson et al, 1974; Coggeshall et al, 1994). However these birthdates have been definitively determined by labelling cells at each embryonic age with tritiated thymidine, then autoradiographically examining the DRG in adulthood.

This procedure also allows further insight into the type of cells produced at each age. Lawson classified the tritiated adult DRG cells according to size: large or small, and their ultrastructural appearance: light or dark (see section 3.1.3). Adhering to this criteria, larger light cells with 23% representation, had a maximum frequency of birthdates at E12, with a high rate of cell formation that had mostly stopped by E13. The smaller dark cells with 46% representation had a peak production of cells at E13, and were slower to form, concluding proliferation at E15. This evidence indicated that these two cell types were different from each other, and not merely two stages in the development of an homogenous population. These findings were confirmed by similar studies (Altman & Bayer, 1984; Marti et al, 1987) and another using a slightly different method, whereby injected 5-bromodeoxyuridine (BrdU) was incorporated in the DNA of dividing cells (Kitao et al, 1996).

In the study by Kitao et al (1996) RT97 and IB4 immunohistochemistry was carried out on the BrdU positive cells in adults for classification purposes. The temporal pattern of cell birth was confirmed. RT97 immunoreactive cells which are indicative of

large cells, were born from E11-E14 and IB4 which represented small cells, were born slightly later between E12 and E15 (Kitao et al, 1996). The most striking feature of that study, however, was the isolation of a third population generated from E14-E15. Those cells were both RT97 and IB4 negative, represented 5-10% of the total number of neurons and were described as small (see section 3.1.5).

There is only one report of neurogenesis in adult DRG (Devor & Govrin-Lippmann, 1985), which is consistent with the small increase in the number of cells observed from P15 to the adult (Coggeshall et al, 1994).

3.1.3 Difference between light & dark and large & small DRG cells

An explanation of the ultrastructural and size criteria upon which cells are classified as large light or small dark is discussed here, since this classification criteria is addressed in embryonic rats in the results section of this chapter.

In the adult rat, when DRG cells are examined ultrastructurally or even by the light microscope, they are observed to possess some different cytoplasmic characteristics. It is possible to ascertain which cells are large light or small dark due to differences in the intermediate filament and nissl content of the neurons, and these are sufficient to divide the cells into two populations. The larger light cells have a lighter and more granular but unevenly stained cytoplasm due to clumps of nissl substance, which are aggregations of free ribosomes and rough endoplasmic reticulum. In addition to nissl substance, organelles such as mitochondria are interspersed in lighter regions between microtubules and large numbers of neurofilaments. The smaller dark cells have a dense and evenly stained cytoplasm. This is because organelles are tightly packed with evenly distributed nissl substance and mitochondria. Few neurotubules are present although there are more golgi bodies resulting in a more osmiophilic cytoplasm overall (Yamadori, 1971; Lawson et al, 1974; 1984; Sharp et al, 1982). These observations are similar for the mouse (Lawson & Biscoe, 1979), and chick DRG (Lieberman, 1976).

Further studies have linked the light and dark populations to neuronal cell size. Quantitative analysis of cell size resulted in the discovery of two distinct, but overlapping normal distributions in the mouse (Lawson, 1979) and the rat (Lawson & Harper, 1985).

These distributions were determined to be identical to the two populations defined by cytoplasmic characteristics. In the adult rat, in wax prepared sections, neuronal cross-sectional areas ranged from 100 to 1400μm^2. Two normally distributed populations were described. The first included smaller cells between 100 and 500μm^2 and the second included larger cells, but spanned the entire range of neuronal sizes with a small degree of overlap with the smaller sized distribution. The means of these distributions were 293μm^2 and 877μm^2 respectively. A similar size-frequency histogram was also constructed for cells classified by the appearance of their cytoplasm and these were fitted by normal distributions, with the same range and means as measured cells (Lawson et al, 1984).

3.1.4 Growth of DRG cells

After proliferation, growth of the DRG cell occurs. In the same study where Lawson (1974), detailed the emergence of the DRG cells, the mean cell diameter of cells were charted. A sharp increase in size occurred between E12 and E13 and then another major increase again between E14 and E15. These are dates at which the future large and small cells respectively stop dividing. The larger increase at E15, is just three days after peak production of cells and coincident with the decrease in cell division. Between E15 and E20 there are moderate increases in cell size with another increase in the rate of growth just before birth. However, no increases were observed between P0 and P3, before growth continued until plateauing at P33. Other important features were the establishment of adult cell section:nuclear section diameter ratios and easily distinguishable light and dark cells at P14.

3.1.5 Numbers of DRG cells

DRG cell numbers are subject to change during development depending on the balance between proliferation, growth and cell death. The proliferation and growth of DRG cells have just been described above. The inclusion of cell death into the equation puts those into context however some inconsistencies with recent literature are apparent.

Cell death in the rat DRG begins at E15, this peaks between E17 and E19 and decreases towards birth (Coggeshall et al, 1994). Cell numbers increase steadily until

birth, reaching approximately 20000 neurons, so proliferation must continue during this period to overcome cell death. In Coggeshall's study, the numbers of dividing/proliferating and dying neurons in addition to total cell numbers, were counted from plastic sections throughout embryonic and postnatal stages. In contrast to previous studies (Lawson et al, 1974; Altman & Bayer; 1984; Marti et al, 1987; Kitao et al, 1996), proliferating cells were observed after E15, peaking at E18-E19. This accounts for the continual rise in total cell numbers while cell death is also being observed. Although, Lawson (1974) did record some lighter thymidine incorporation until E19, but decided it may be due to DNA synthesis outside of the S phase of the cell cycle, and did not attribute these cells to any particular population.

This finding of continued proliferation, however, is consistent with the growth pattern suggested by Lawson (1974) since cells are either in a phase of proliferation or growth. In that study, the greatest cell size increases were at E15, when proliferation is at stable levels, growth then slowed from E15 to E19 when Coggeshall (1994) describes peak proliferation. Growth increased again just before birth when numbers of dividing neurons drop abruptly, but cell size did not increase again from then until P3 when the last neuronal divisions are observed. This is also the age when Coggeshall described the appearance of the cells and found that the nissl substance in the ganglion cell cytoplasm was discernible, allowing more cells to be classified as light or dark.

3.1.6 Cell death and subpopulations

Cell death is thought to occur due to competition for limited supplies of target-derived growth factors (Davies & Lumsden, 1984; Oppenheim, 1989; Ruit et al, 1992) so that eventually neuronal numbers are matched to the size of the target. The bulk of DRG cell death occurs prenatally while cell numbers are increasing, between E17 and E19 as described above. However, just after birth when the highest number of DRG neurons are recorded, there is 16% cell death, reducing neurons to approximately 17500. This second wave of cell death occurs between P0 and P3. Explanations for the timing of these two events relates to the onset of target innervation and has led to the proposal that

the two phases of DRG cell death represent the death of the two populations, large light and small dark (Coggeshall et al, 1994).

The essence of this argument is that the large light neurons die prenatally, before the small dark neurons which die postnatally. This hypothesis is derived from several pieces of supporting evidence. From above, we know that the large light neurons are born before the small dark neurons. In addition, DRG neurons have both central and peripheral targets. The central targets are reached by large diameter fibres at E15, when cell death is first detected. The peripheral targets are still being innervated until late gestation when peak cell death occurs, so it is unlikely that these axons have the opportunity to compete for trophic factors and activate the cell death program in their neuronal somas. Hence the prenatal cell death is probably not attributable to competition for trophic factors in peripheral targets, leaving the central target among other possible sources (see Coggeshall, et al 1994). However, the spinal cord is not a good source of nerve growth factor (NGF) which is an essential and selective growth factor for small DRG cells, whose axons do not even reach this target until just before birth. This implies that prenatal cell death arises from large DRG cells only competing for a trophic factor in the spinal cord.

The second instance of cell death is correlated with postnatal peripheral innervation. Peripheral innervation is complete at this time and the arrival of axons has been shown to stimulate NGF synthesis (Davies et al, 1987). The presence of NGF, upon which developing small DRG cells are dependent, could lead to competition for this factor and target dependent cell death of this population. This hypothesis has yet to be verified by counts and size measurements of selectively labelled populations.

3.1.7 Physiological characteristics

i) Membrane properties and conduction velocity

Physiological evidence that sensory neurons are differentiated at birth is derived from examination of the somatic spike. There are some general similarities of all neurons in the rat DRG that are evident at E19 (Mirnics et al, 1993) and at P0 (Fulton, 1987)

where they are characterised by a relatively broad spike with an inflection of the falling phase and a long afterhyperpolarisation (AFP). Despite this, differences exist which can be correlated with their future phenotypes.

Prospective C-fibres possess axons with a relatively slow conduction velocity, their spikes tend to be broader, with a longer AFP and are resistant to blockade with TTX. Meanwhile prospective A-fibres conduct more rapidly, have narrower somatic spikes that are distinguished by a faster rising and falling phase. They are also partially sensitive to TTX.

Development of A-fibres continues postnatally with the onset of myelination and increased axonal conduction velocity (Koerber & Mendell, 1992). In fact, mechanical nociceptors and cells with unmyelinated neurons in the mature animal, resemble relatively immature neurons. Therefore cells that are born later in development (small dark cells) appear to achieve their adult spike characteristics before the cells born earlier (large light cells), suggesting that the spike phenotype is specified early in development. Further evidence that physiological development occurs in the inverse order of birth is derived from the sensory receptor properties.

Fibres classified as slowly or rapidly adapting are identified at E17, but firing frequencies are lower than in the adult (Fitzgerald, 1987c). By E18, mechanoreceptors insensitive to thermal stimulation are detected, these persist postnatally but after the initial two weeks mature into mechanoreceptors with typical adult attributes. At birth, the low threshold mechanoreceptors are more immature than nociceptors, this probably reflects the lack of myelination in the low threshold afferents which prevents higher frequency conduction required for the development of mature receptor properties. However C-fibre maturation is not complete until after the first postnatal week since they can only elicit impulse activity in the dorsal horn after P8 (Fitzgerald, 1985b), and neurogenic extravasation due to SP release does not occur until P10 (Fitzgerald & Gibson, 1984). These late developments are likely to be due to the delayed maturation of the neurons within the substantia gelatinosa (Altman & Bayer, 1984) in view of the appropriate anatomical development of central connections at birth (Fitzgerald & Swett, 1983; Snider,

1992; Mirnics & Koerber, 1995b) and the availability of peptide transmitters (Marti et al, 1987).

The different membrane properties among primary sensory neurons are due to different ionic conductances operating, and developmental changes probably reflect the incorporation of a new set of channel type into the membrane.

ii) Receptor properties

The peripheral receptors are themselves subject to classification into three groups. The first are specialised end organs (Merkel cell touch receptor), the second are free nerve endings that have no structural specifications but are functionally distinct (unmyelinated nociceptors) and finally specialised terminal patterns (axon surrounding an hair follicle). Each tissue has a unique combination of receptors. Aβ-fibres innervate low threshold mechanoreceptors (LTMR) and hair follicle (HF) endings, Aδ project to d-hair follicles and nociceptors while C-fibres innervate polymodal nociceptors.

3.2 RT97 - A Selective Marker of Large Light DRG Cells

3.2.1 Background

RT97 is a monoclonal antibody against a neurofilament subunit and is used as a selective marker of DRG cells. It's size-frequency distribution in the adult rat DRG was determined and found to closely resemble that of the large light population of cells with myelinated axons (Lawson et al, 1984). RT97 can therefore be used as a selective label for this population of neurons in the adult rat DRG. However since this analysis has not been conducted in embryonic DRG, it is not known if the same selective labelling occurs during development. The absence of this information has become notable as other markers of the DRG cell population like trk A, IB4 (Bennett et al, 1996b) and peripherin (Troy et al, 1990a), have been found to show different expression patterns and ranges during development in comparison to the adult. In experiments detailed in Chapter 4, I used this antibody to describe the embryonic development of RT97 positive peripheral axons and proposed that these corresponded to the developing large A-fibres. To be

certain of this, however, it was necessary to investigate the size distribution of RT97 in the embryonic DRG to ensure it was labelling the same population as in the adult. E18 was chosen as the earliest age when size frequency analysis could be accurately and confidently completed, as at this age maturation of the two sizes of DRG sub-populations has begun.

3.2.2 Identification and structure

RT97 antibody is raised against the phosphorylated form of the 200 kDa neurofilament subunit NFH; subsequently also referred to as NFH-P in this thesis. It was discovered in 1982 by Wood and Anderton by raising an antibody against an extract of rat brain. The proof that RT97 does in fact only label the phosphorylated form of NFH came after treatment to dephosphorylate DRG tissue. Normally, non-phosphorylated NFH shows low level staining in the DRG while RT97 is intense in large cells. After dephosphorylation, intense staining is found in the large neurons with NFH but the RT97 label decreases. It was concluded that NFH in large neurons is phosphorylated and that small neurons contain little NFH regardless of phosphorylation state (Perry et al, 1991).

3.2.3 DRG Expression

In the DRG RT97 expression is expressed almost exclusively in the large cells of rat DRG (Lawson et al, 1984; Goldstein et al, 1991). Phosphorylated NF's are found in the DRG of all species examined but their distribution differs between species (Klosen et al, 1994). Lawson and colleagues examined the distribution of this NFH-P in the adult rat DRG and found the shape of the size-frequency histogram was the same as that of the large light DRG cell population, therefore linking NF content to cell type (Lawson et al, 1984). The RT97+ve population overlaps with some small diameter dark cells, but does not cover the entire range of neuron sizes within the DRG. In agreement with this, RT97+ve cells were found not to contain tyrosine hydroxylase (TH), substance P (SP) or somatostatin (SOM) (Lawson et al, 1984), markers characteristic of the small dark population but can be found in cells of peptide-containing size (Price, 1985).

The closeness of the RT97 distribution to the normally distributed large light cells suggested that this antibody could be used as a much needed selective label for this population of neurons in rat DRGs. In the adult approximately 40% of DRG neurons express RT97 (Lawson et al, 1984; Robertson et al, 1991; Kitao et al, 1996) but this data has not been obtained for younger animals. In contrast, 96% of human DRG cells express RT97 therefore it cannot be used as a discriminatory marker for the two types of human primary sensory neurons (Suburo et al, 1992; Vega et al, 1994). However, one study in human DRG showed that even though all cells do express NFH/RT97, a definite subpopulation is more intensely stained (Holford et al, 1994).

The non-phosphoylated 200kDa NF labels all rat perikarya, which in motoneurons and dorsal horn neurons is in globular form, indicating it is in a pre-filamentous stage (Perry & Lawson, 1993). In addition to the DRG, the trigeminal and jugular region of the vagal ganglia show comparable cellular labelling but the nodose region of vagal ganglia only have very fine fibres, while the superior cervical ganglion (SCG) containing sympathetic neurons lack RT97-IR (Lawson et al, 1984).

3.2.4 CNS Expression

Nerve fibres throughout the spinal cord produce an overall dense staining pattern with RT97 but it is not found in any spinal cord somata. However there is a significant amount of non-phosphorylated, globular NFH in all neuronal perikarya. Motoneuronal perikarya and processes are immunoreactive for NFL, NFM and NFH but not RT97. Only the NFL sub-unit is filamentous (Perry & Lawson, 1993). The absence of RT97 in the motoneurons confirms other studies (Lawson et al, 1984; Lee et al, 1987; Mansour et al, 1989). However, there may be some partly phosphorylated NFH in the motoneurons since a polyclonal antibody that detects both phosphorylated and non-phosphorylated forms of NFH shows labelling while nothing is recognised with the antibody to non-phosphorylated NFH. This evidence in addition to the information about filamentous NFL, suggests NF structure in the motoneurons consists of a NFL backbone with poorly phosphorylated sidearms.

In contrast the dorsal horn shows NFH labelling only (Lawson et al, 1984; Perry & Lawson, 1993). This suggests that the NF structure in the dorsal horn departs from the triplet of subunits reported in primary sensory neurons. This triplet is incapable of homopolymeric assembly *in vivo* (Ching & Liem, 1993) but NFH is able to form short filament-like structures on its own (Gardner et al, 1984). NFM expression in the spinal cord has been the subject of some debate as it was initially thought to be absent (Dahl et al, 1981; 1983; Lawson et al, 1984), however subsequent IHC studies (Dahl et al, 1988) and *in situ* hybridisation studies (Muma et al, 1990) have located it in motoneuron cell bodies. All fibres in the white matter and nerve tracts were reactive to NFL, NFM, NFH and RT97 (NFH-P) (Perry & Lawson, 1993).

3.2.5 Peripheral Expression

RT97 is present in non-neuronal tissues but is confined to nerve fibres and within the PNS is confined to neurons of neural crest origin as defined by Weston (1970). This proposes that all RT97 positive cells have a common origin despite staining in the nodose ganglion which is possibly of placodal origin (Le Douarin, 1980). A possible explanation for this discrepancy is incomplete separation of placodal and neural crest-derived neurons during development since there are no clear anatomical boundaries between the nodose and jugular regions of the vagal ganglia in the adult (Lawson et al, 1984). In addition to large diameter DRG cells, RT97 has been found in large diameter fibres and end structures of skin. It has been detected in the endings served by the large myelinated fibres, namely Meissner-corpuscles, merkel discs, hair follicle receptors, pacinian and free nerve endings. No labelling was found in unmyelinated endings, intraepidermal fibres or sympathetic fibres (Sann et al, 1995).

3.2.6 Physiology

Lawson had previously described large light neurons as having a NF rich cytoplasm and myelinated fibres (Lawson et al, 1974). To discover more about the fibres that emanate from RT97+ve somata, an electrophysiological study was undertaken in the rat (Lawson & Waddell, 1991). Intracellular recordings from DRG were made *in vitro*

followed by dye injection and immunohistochemistry. The peripheral nerve or dorsal root were electrically stimulated and conduction velocity measured between that site and the cell body. It was found that neurons with A-fibre conduction velocity (CV) have RT97+ve somata, reinforcing the evidence for the presence this NF subunit in A-fibres and cells. More specifically, all Aδ fibres and Aα/β fibres were RT97+ve. In addition RT97+ve fibres showed a maximum CV of 31m/s in 6-8 week old rats, where the greatest CVs measured 40-50m/s (Lawson et al, 1993). These findings linked NF content, state of myelination and conduction velocity. The data associating A-fibres and RT97 is further supported because RT97 innervation in the skin is unaffected by capsaicin, which selectively destroys small unmyelinated fibres (Sann et al, 1995).

3.2.7 Co-localisation

RT97 is co-localised with peptide-containing DRG cells. 6% of RT97+ve cells are SP+ve but none of these are Aα/β cells. 28% of RT97+ve are CGRP+ve, 38% of these are Aδ with 17% Aα/β cells (McCarthy & Lawson, 1989; 1990). It is also co-localised with the cell membrane ganglioside receptor, GM1. This was visualised using the binding sub-unit of cholera toxin (CB) and suggested 82% of the RT97 population were also CB positive (Robertson & Grant, 1989).

RESULTS

3.3 The Size-Frequency Distribution of E18 and E21 Dorsal Root Ganglia (DRG) Neurons

3.3.1 Aim

The morphological characteristics of embryonic DRG have not been fully investigated. One possibility for the scarcity of information is the difficulty in obtaining basic measurements, for the simple reason that cells are immature, and hence do not display many of the criteria that are used to classify older tissues.

Here the morphological characteristics of DRG cells at E18 and E21 were studied. These specific times were used to compare with experimental work conducted in Chapter 7. It was apparent that descriptions of embryonic material were disparate and incomplete.

3.3.2 Information about experimental protocol

At E18, three lumbar ganglia each from three animals were processed together and examined. The area of cells were measured in three sections from each ganglion, ensuring more than 800 cells from individual ganglia were determined. This data was combined and is presented in Fig. 3.2A, where n=2213 cells. At E21, ganglia from control animals were processed together with experimental material from Chapter 7, but this meant that not all controls were processed simultaneously and hence cannot be pooled. Histograms from all E21 animals (n=7), were compared and their overall distribution patterns were consistent. However to exclude any variation due to embedding procedures only data from two animals is included in this chapter. Three ganglia from each embryo were analysed and the data consolidated and presented in Fig 3.2B, where n= 1951. Only one adult L5 DRG was included in this study for comparative purposes.

In order to construct a size-frequency histogram, profiles of all counterstained cells with a clear nucleolus were drawn using a camera lucida drawing tube at a magnification x400.

3.3.3 Description of cells at E18

On first examination these cells are tightly packed together and seem to be a relatively homogenous population in terms of size and appearance (Fig. 3.1A; B). Some larger cells are conspicuous but the majority of the population visibly appear to be of similar size. The cells are quite round with a large nucleus that is also round and positioned centrally. As detailed in the introduction (3.1.3), cells are usually described by their ultrastructure in addition to size characteristics. Although it is not possible to resolve individual organelles in this light microscope study, the proportions of these are reflected by the colour of the cytoplasm and nucleoplasm in the cells. The majority of cells are of similar colour with a dark homogenous coloured cytoplasm but have a clearly paler nucleus that contain multiple nucleoli. The few larger cells that are observed also have dark cytoplasms.

At E18, therefore, it is possible to visually examine the DRG cells and assign a proportion of them to large or small categories, however, cells could only infrequently be distinguished as light or dark.

3.3.4 Description of cells at E21

The most striking feature that has changed from E18 is the spacing between the cells (Fig. 3.1C; D). Cells are now more widely spaced and although many are of similar size, there is a substantial number that can be clearly distinguished as large or small. The size difference between the largest and smallest cells observed is approximately a magnitude of 2.5. These cells are still round except for some of the larger cells which appear to have elongated, and they retain a round nucleus but fewer multiple nucleoli. The colour of the cells appears to be unchanged, with little evidence of the emergence of a light and dark population. One example of possible classification on this basis are the cells in Fig. 3.1C.

At E21, therefore, many cells could be allocated to large or small categories on the basis of visual examination, however only a minority of cells exhibited differences that could be attributed as light or dark.

3.3.5 Description of cells in the adult

All sections from an adult L5 DRG were examined and regular gaps noted between the cells. There is a clear distinction between the large and small cells. The large cells are positioned among smaller cells and are typically up to three to five times larger. Cell shape is more variable, although nuclei are still centrally located but contain only one nucleolus. The nucleus is also much smaller in comparison to the total cell. Cells can also easily be discriminated by their staining properties. Lighter cells are large, but have a paler nucleus and on higher magnification have a granular cytoplasm. Dark cells are small, have a similar coloured nucleus as the light cells but their cytoplasm is not granular. In many of the small cells the nucleus is not obvious - maybe because the cell has not been sectioned through its centre, whereas the larger cells have a larger nucleus which upon sectioning will appear in more sections.

These cells are easily distinguished by size and colour, with large cells appearing lighter than the smaller darkly stained cells.

3.3.6 Size-Frequency Histograms of E18 and E21 DRG Cells

The size-frequency histogram of E18 DRG cells (Fig 3.2A) shows that cross-sectional areas range from 45μm^2 to 585μm^2. The areas are not distributed normally about the mean value but have a long tail towards the upper end of the distribution. This tail representing larger areas starts from 360μm^2. There is a peak in the distribution between 195-210μm^2. The distribution does not appear to consist of two separate populations at this stage, a feature which is observed in the adult (see Fig. 3.3A, adapted from Lawson et al, 1984 for comparison). The statistical parameters of this distribution are given in Table 3.1.

The E21 size-frequency histogram (Fig 3.2B) ranges from 30μm^2 to 570μm^2. This shows that there has been little change in the size range of the whole distribution from E18. The size of the largest values and the number of larger cells appears to be unchanged while there is an increase in the number of small cells (see below).

The E21 distribution however, is more mature than at E18 because there is some evidence of two separate populations but it is also abnormally distributed with a long tail

of cells above 270μm^2. The peak frequency of the distribution at E21 is found in a smaller size range (120-135μm^2) than at E18. This is probably a feature of the population separation. By visual inspection a curve can be used to delineate the emerging subpopulations (see dotted line on Fig. 3.2B). There may be two populations but largely overlapping (see discussion). The intersection of these curves is found at 180μm^2, this divides the population into 67% small cells and 23% large cells. If the same cell size is used to separate the E18 population it is divided 49%:51%, confirming the lack of separation. The statistical parameters are given in Table 3.1

Table 3.1: Parameters of the E18 and E21 Size-frequency Distributions

Population	Mean (μm^2)	SD	SE	Mode	Median
E18	206.24	79.71	1.69	195-210	201.05
E21	160.25	81.35	1.84	120-135	142.83

From Table 3.1 it can be seen that the mean size of cells has decreased from E18 to E21, due to the large number of cells in the small diameter range. The distributions however are not normally distributed about the mean, so other more informative parameters have been included in the analysis. The median is also smaller in the E21 population. The modal value is lower in the older distribution and this is anticipated at this stage of development.

3.4 RT97 Distribution in the E18 Dorsal Root Ganglia

3.4.1 Aim

E18 was chosen as the earliest age when size-frequency analysis of RT97 positive DRG cells could be adequately completed due to the size maturation of the two DRG sub-populations. Lower lumbar DRG from three E18 embryos were used in this study. Sections were obtained from three DRG levels for each embryo, all treated

immunohistochemically. Expression and size-frequency data was obtained from three sections per ganglia. Analysis of adult DRG was carried out in parallel for comparison.

3.4.2 Localisation and appearance of immunopositive cells

The results of immunohistochemistry on the lower lumbar E18 DRG (Fig. 3.4) demonstrates that immunopositive cells are largely confined to the ventral and ventro-medial regions of the DRG. Cells are often found clustered and mostly away from the margins/edge of the DRG. These were categorised as clearly positive or negative for RT97 with few instances of indeterminate staining. Examination of immunopositive cells at higher magnification (Fig. 3.4B) reveals that staining is concentrated and evenly distributed in the cytoplasm with no nuclear staining above background levels.

In the adult L5 DRG, no clear pattern of localisation of RT97 positive cells can be observed within the DRG but, as at E18, positive cells mostly appear away from the edge of the DRG (Fig. 3.4C). At higher magnification (Fig. 3.4D, E) the size ratio of positive to negative cells is clearly evident, with RT97 mostly present only in the larger cells. The major departure from observations in the embryo is the variation in staining intensity. There is a gradient of reaction product between the cells resulting in some with high density cytoplasmic labelling while others display staining in the perinuclear cap, the majority contain a more intermediate level of reaction product. This makes positive identification more difficult resulting in a small population of unclassified cells, this has also observed by other workers (Woolf, personal communication).

3.4.3 Identification of nucleolar profiles for size-frequency analysis

In order to construct a size-frequency histogram, profiles of all counterstained cells with a clear nucleolus were drawn using a camera lucida drawing tube at a magnification x400. RT97 positive cells were identified and the cross-sectional area of all cells was determined. Examples of counterstained ganglion sections are found in Fig. 3.5. After counterstaining the immunopositive cells are more easily detected from background levels, and using higher magnification (Fig. 3.5E, F), cells with a clearly identifiable nucleolar profile were identified and included in size-frequency analysis.

3.4.4 The size-frequency histogram reveals the existence of two distinct cell populations with respect to RT97-IR at E18

The size-frequency histogram (Fig. 3.6) displays the distribution of RT97 positive and negative neurons (n=2213 cells) and clearly illustrates that RT97-IR neurons represent a distinct subpopulation within the DRG at E18. The histogram shows that RT97 positive cells have cross-sectional areas ranging from 120μm^2 to 435μm^2, these include the large neurons but exclude the smallest neurons in the ganglia. In contrast RT97 negative neurons have a broader distribution ranging from the smallest at 30μm^2 to 540μm^2, covering the entire range of neuronal sizes in the DRG. There is an overlapping population between 120μm^2 and 400μm^2. In effect this means that the RT97 positive population, although distinct, overlaps with the RT97 negative population with respect to neuronal area.

For comparative purposes a histogram of the adult DRG RT97 distribution (Fig. 3.3B) has been included (adapted from Lawson et al, 1984). In Lawson's study, RT97 also represented a distinct subpopulation, however in that study although there was an overlap region of 250μm^2-1000μm^2, the RT97 negative population did not exceed 1000μm^2 leaving a population of neurons sized between 1000-2000μm^2 that were exclusively RT97 positive.

The representation at E18 is somewhat more complicated due to the fact that at E18 two separate, normally distributed populations have not yet developed (see section 3.1). Both populations and the RT97 positive population especially, has a long tail of medium-large sized cells approaching the upper end of the distribution. Although the positive population is overlaps in size with the negative population, closer examination of the parameters of these populations confirms they are separate (see Table 3.2).

Table 3.2: Parameters of RT97 Positive and Negative Populations

Population	Mean (μm^2)	SD	SE	Mode	Median
RT97+ve	248.57	62.43	2.80	195-210	241.43
RT97-ve	193.92	79.93	1.93	200.225	183.14

As described above, the range of the RT97 positive population is more restricted than the RT97 negative population with no cell less than 120μm^2 in size. From Table 3.2 it can be seen that the mean size of the positive population is larger than the negative population even though from the histogram many large cells are observed in the negative population. Since the populations are abnormally distributed, the mean alone is not sufficient to describe them, hence the median which is also larger in the positive population is more informative. However the modal value for both is in the 200-225μm^2 size range, probably reflecting the stage of development of the DRG cells. More information can be deduced by examining the percentage of cells that are larger than the modal size. This calculation indicates that 80% of the positive population is larger than the modal size compared to 45% of negative cells.

3.4.5 RT97 expression in the E18 DRG is 50% less than in the adult DRG

Quantification of the number of RT97 positive profiles in the embryonic DRG revealed that the level of expression is approximately 50% less than the adult DRG (see Table 3.3). The mean number of positively labelled profiles was expressed as a percentage of the total profiles in sections counted. The expression value of 22.5% at E18 was surprisingly low compared to previous reports in the literature for adults (3.2.3). To ensure this result was not due to differences in counting criteria or the labelling procedure, counts were conducted on one adult DRG to compare with the literature. The result of 40% in the adult was extremely close to published values (included in Table 3.3) hence there was unlikely to be any error in this technique.

Table 3.3: Expression of RT97 in E18 and Adult DRG

AGE	DRG (n)	No. +ve Profiles	No. -ve Profiles	Mean % Labelled	Range of %
E18	9	499	1714	22.5	20.2-23.7
Adult	1	44	110	40	40
Adult (1)	-	-	-	40	33-42
Adult (2)	1	-	-	40	35-41
Adult (3)	8	-	-	40	37-49
1=Lawson et al, 1984; 2=Kitao et al, 1996; 3=Robertson et al, 1991					

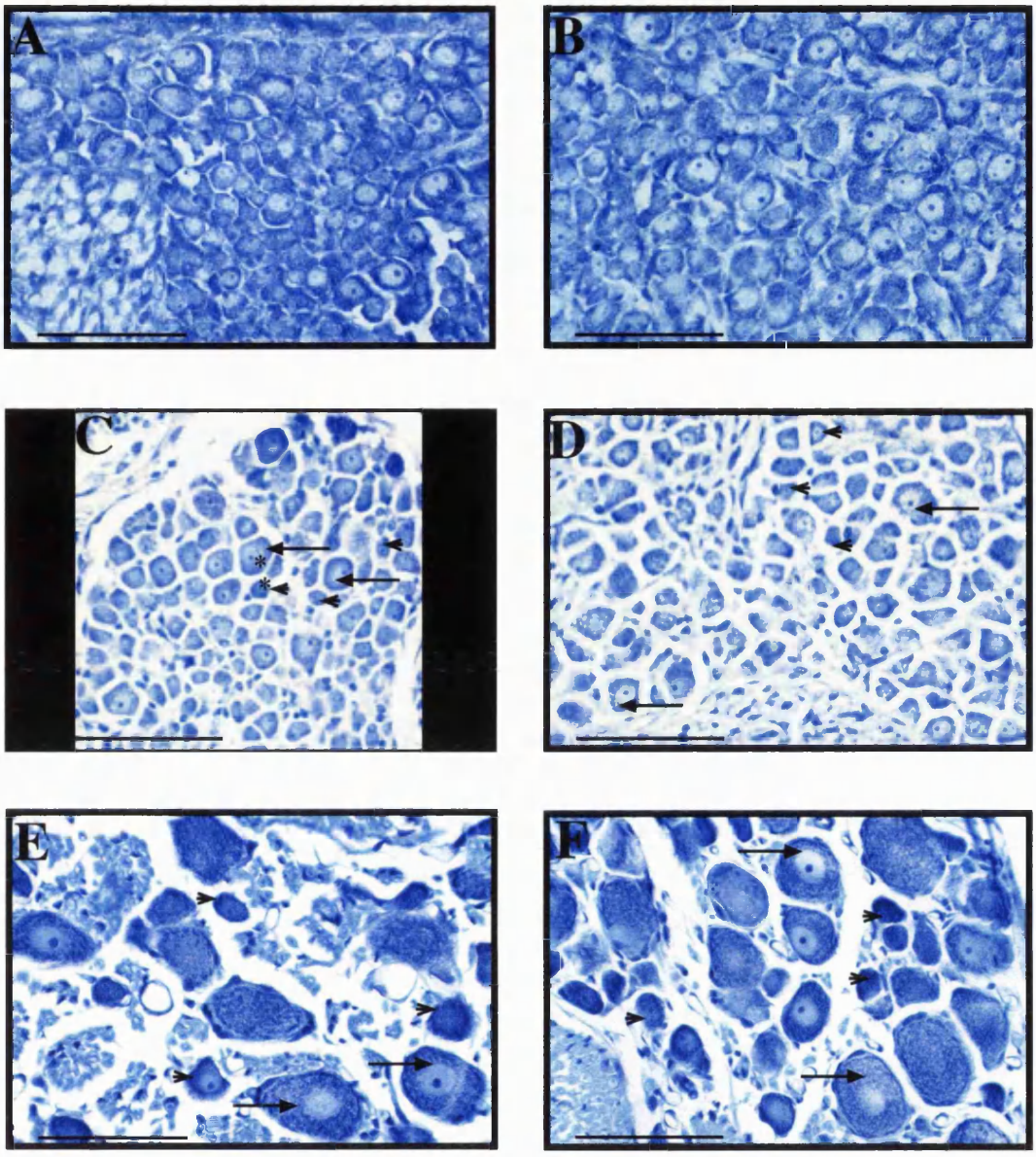

Fig. 3.1: E18, E21 and adult DRG counterstained with Toluidine Blue.

A and B are E18 DRG; C and D are E21 DRG; E and F are adult DRG. These are all at a magnification of x400. In A and B there is little visible difference in the size of cells compared to E21 and adult, where larger cells are denoted by an arrow and smaller cells by an arrowhead. In addition, cells from E18 and E21 cannot be easily classified as large light or small dark but examples of light and dark are denoted by an asterisk in C. This classification is more apparent in the adult sections where the small cells have a darkly staining cytoplasm compared to the cytoplasm of larger cells that have a lighter and more heterogenous appearance. Scale bar = 100μm.

A

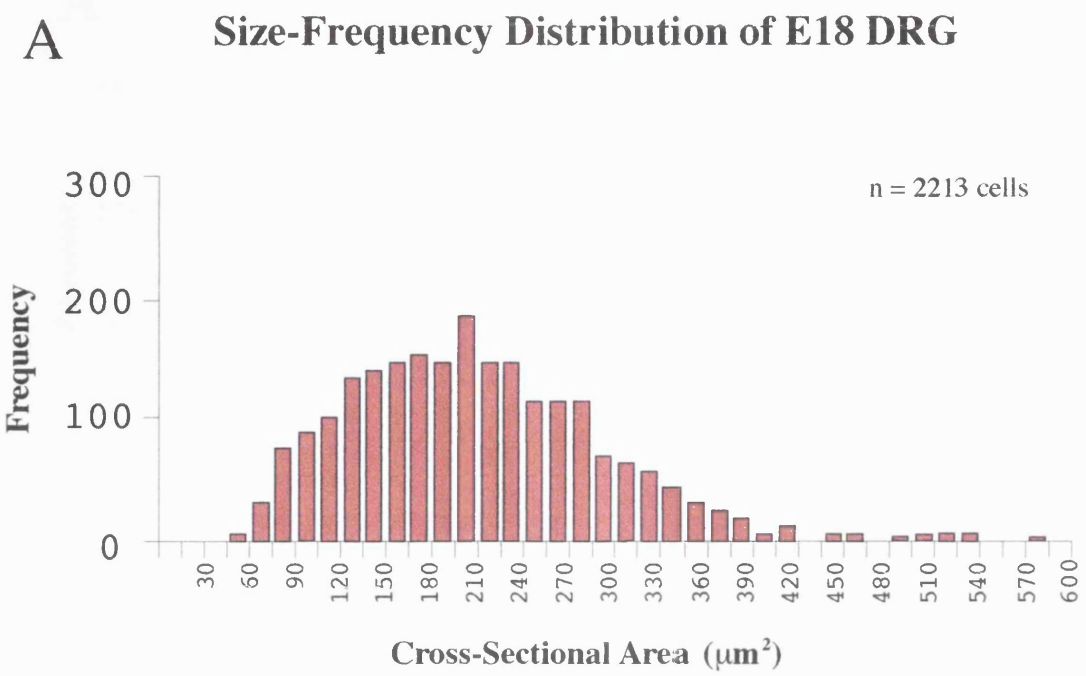

B

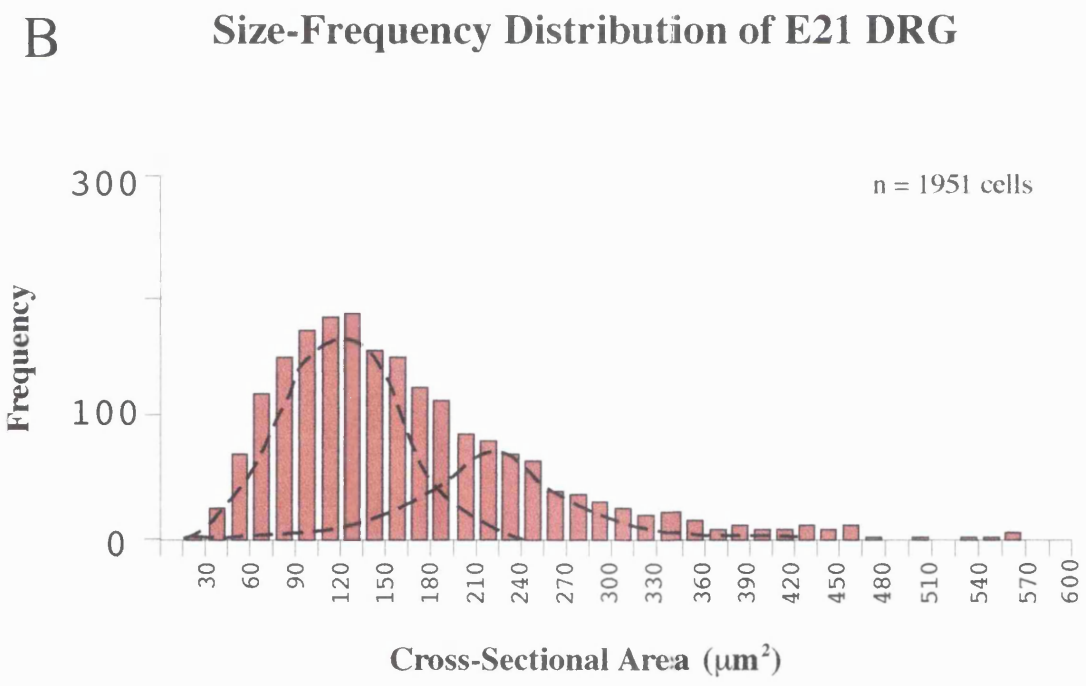

Fig. 3.2: Size-Frequency Distributions of E18 & E21 DRG

These size-frequency histograms show the cross-sectional area of cells within the E18 & E21 DRG. Most of the population appears to be normally distributed, however at both ages there are some larger-sized cells which skew the upper end of the distributions. At E21, some population separation may be emerging, and is shown by the dotted line.

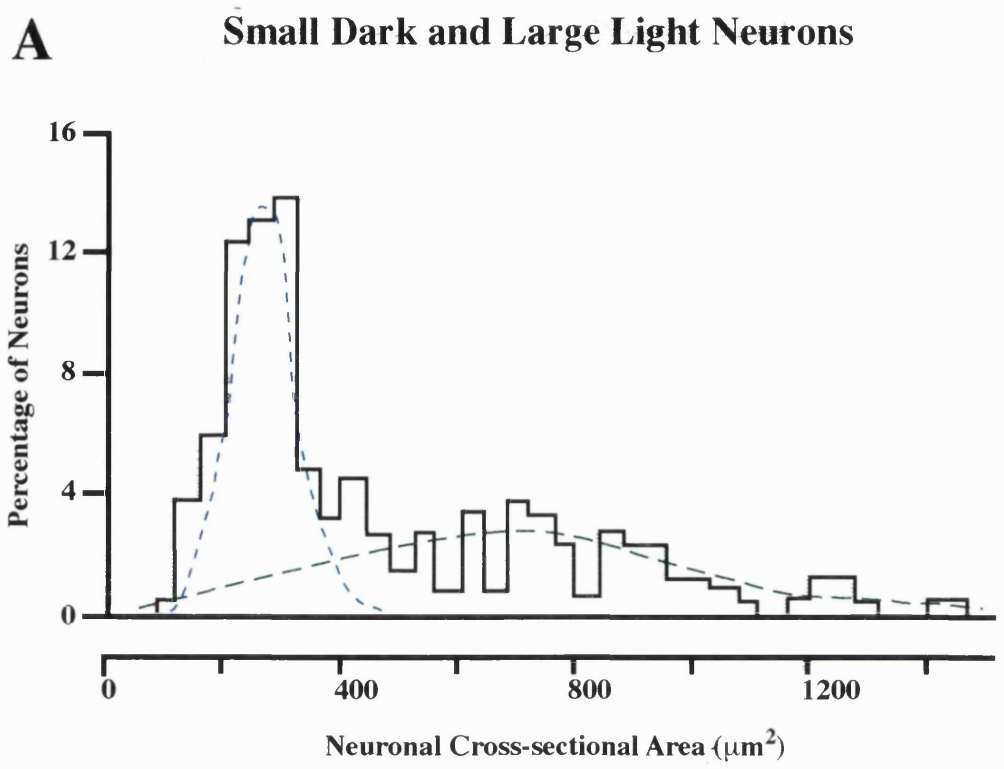

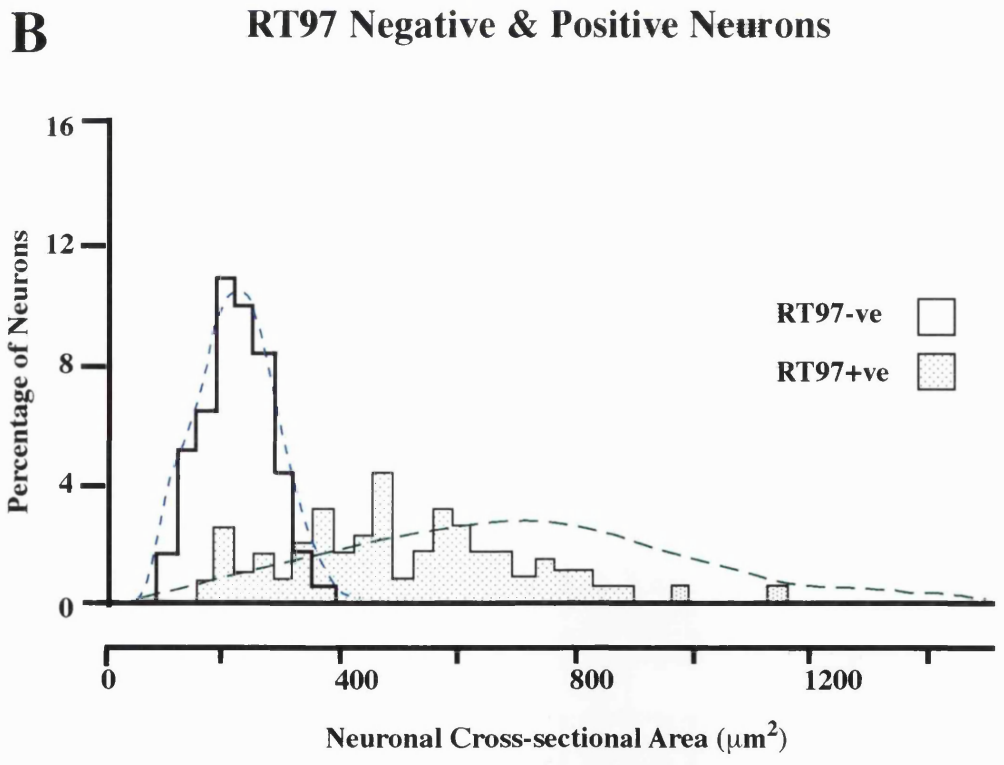

Fig. 3.3: Size-Frequency and RT97 Distribution in Adult DRG

Fig. A shows the cross-sectional areas of adult DRG cells, revealing the bimodal distribution of small cells (blue dotted line) and large cells (green dotted line). Fig. B shows the distribution of RT97 within the adult DRG. The small cell population are mostly negative, while all larger cells are RT97 postive.
(Figures A and B are adapted from Lawson et al, 1984.)

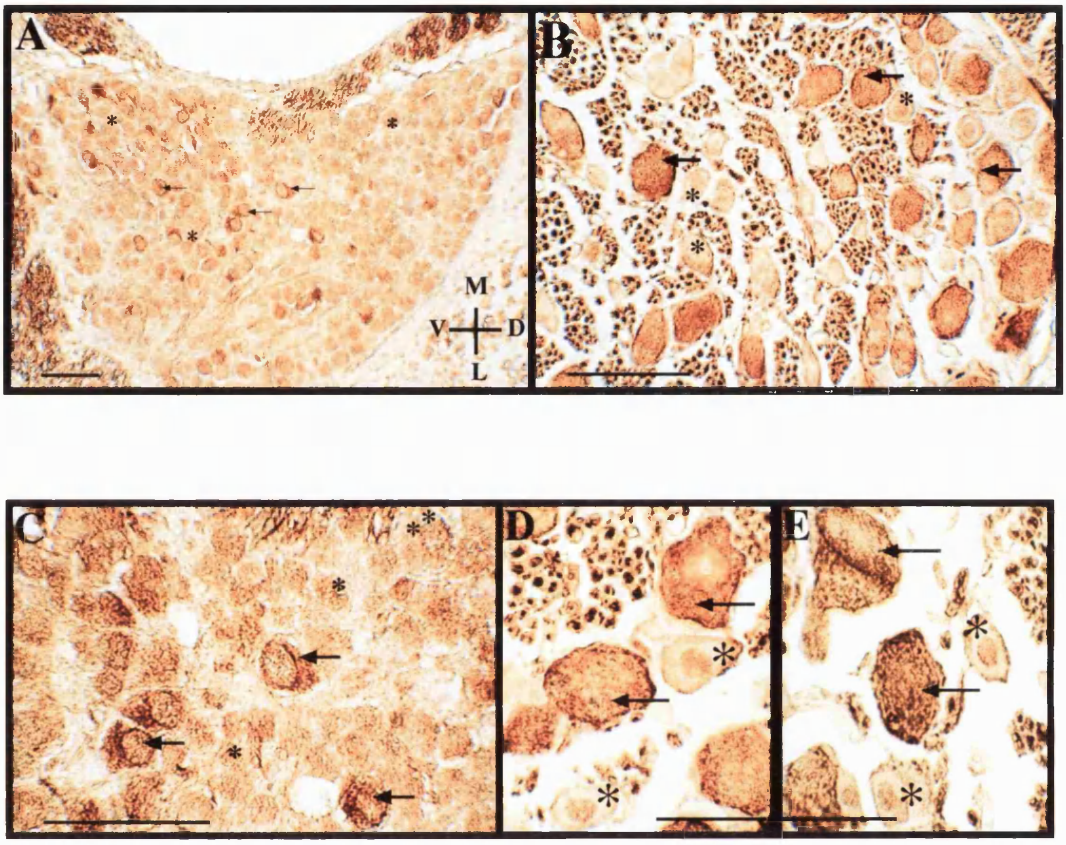

Fig. 3.4: RT97 Immunohistochemistry on E18 and adult DRG

A and B are low power photos of E18 and adult DRG respectively, these show the distribution of immunopositive cells within the DRG. C is a high power photo of E18 DRG; D and E are high power photos of adult DRG. In A, the orientation of the DRG in relation to the spinal cord is indicated by the compass directions where M= medial, L=lateral, D=dorsal and V=ventral. Examples of RT97 immunopositive cells are shown with an arrow and the immunonegative cells with an asterisk. In C, the cell denoted by the double asterisk represents a large RT97 negative cell. Scale bar=100μm.

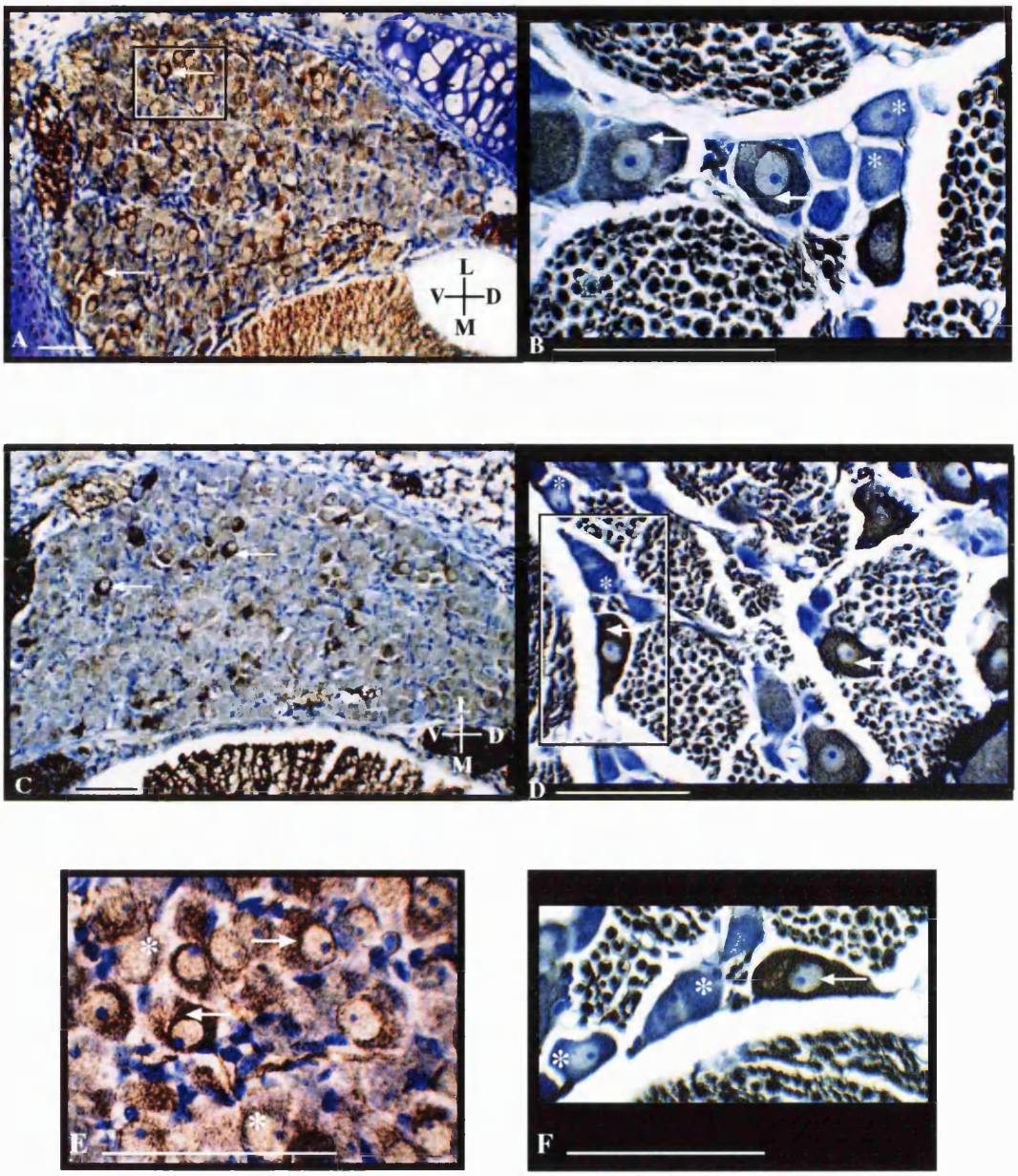

Fig. 3.5: RT97 Immunohistochemistry on E18 and adult DRG counterstained with Toluidine Blue.

A and C are low power photos of E18 DRG, showing the distribution of immunopositive cells within the DRG. B and D are low power photos of adult DRG. E and F are high power views of the inset regions marked in A and D respectively and are examples of cells used for size-frequency analysis. RT97 immunopositive cells are shown with arrows and immunonegative cells with an asterisk. In A and C the orientation of the DRG in relation to the spinal cord is indicated by the compass directions where M= medial, L=lateral, D=dorsal and V=ventral. Scale bar = 100μm.

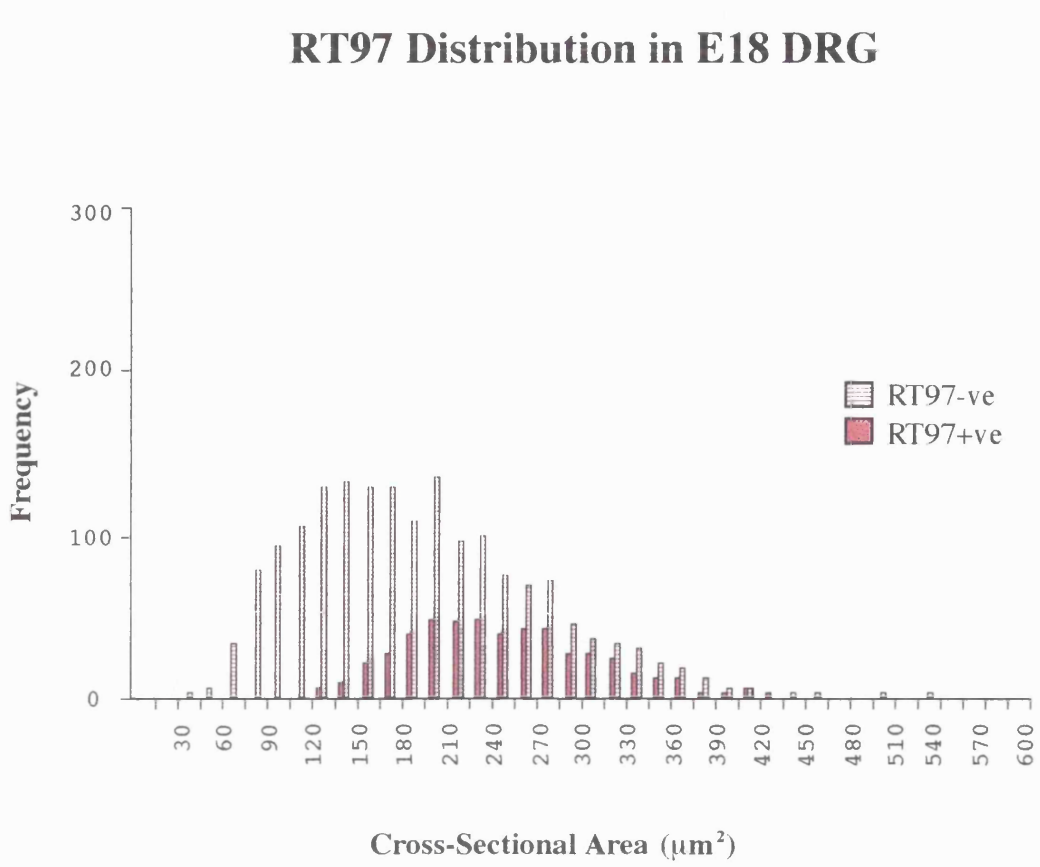

Fig. 3.6: RT97 Antibody Distribution in E18 DRG

This size-frequency histogram shows the cross-sectional area of RT97 positive and negative cells within the E18 DRG. Both populations overlap, but the RT97 positive cells are found in the larger cells.

3.5 Size-frequency Distribution in the Dorsal Root Ganglia (DRG)

In this section I have described the size-frequency histogram of cells from E18 and E21 DRG and determined whether cells at this age can be classified on the basis of their size and morphological characteristics, as examined under the light microscope. This study shows that even by E21, few cells could be classified as light or dark although by inspection under light microscope it is possible to see large cells.

3.5.1 What are the characteristics of E18 DRG cells?

At this age there are many cells closely packed together in the embryonic ganglia. Despite ongoing cell death, cell proliferation ensures that the total number of cells in DRG continues to increase until birth (Coggeshall et al, 1994). Therefore the close packing appears to reflect overall lack of extracellular space at this stage rather than excess cell numbers.

Cell size at E18 is fairly homogenous and it is difficult to discern large from small cells in wax embedded sections. This is to be expected as little growth of cells is reported between E15 and E20, until there is a spate of growth just before birth (Lawson et al, 1974).

The lack of contrast between cells as defined by large light and small dark may be due to two appreciable factors. The first is the necessity of NF accumulation as defined by RT97 for classification purposes. This aspect was investigated in section 3.4 and for discussion of the link between expression of RT97 and classification of cells as large light see section 3.6.5.

The appearance of small dark cells may also depend on the accumulation of peptide-synthesising machinery by small cells. Small cells require more peptide synthesis for putative neurotransmitters that need constant replenishment, whereas large cells utilise non-peptide transmitters retrieved from the synapse or recycled by enzymes (Hökfelt et

al, 1975a; 1975b; Kai-Kai et al, 1986). In support of this, my investigations into the expression of immunoreactivity to the peptides CGRP and SP (Chapter 4) show that no SP is detected in the DRG and CGRP is only detected in a few cells of low intensity at E17. These increase in intensity and number at E18, which also concurs with my *in situ* hybridisation analysis of CGRP mRNA (Chapter 6).

Multiple nucleoli were observed in the E18 DRG cells and to a lesser extent in the E21 DRG, this feature had dissipated by adulthood. There are few reports of multiple nucleoli in the literature as it is generally accepted that each DRG cell contains only one nucleolus, however a study by Hulsebosch and colleagues (1986), revealed that up to 50% of cells in rats aged P0-P14 contained more than one nucleolus. This may have been a slight overestimate due to the counting method but they maintain that even in the adult approximately 20% of DRG cells have multiple nucleoli. This is contrary to the finding in mice, where only 5% of cells are observed to have greater than one nucleolus irrespective of age (Lawson et al 1979).

3.5.2 What are the characteristics of E21 DRG cells?

The cells of the E21 DRG are more widely spaced than at E18, although the actual total cell number has increased from E18 (Coggeshall et al, 1994). There is, however, slightly greater size separation of cells at E21. This finding is consistent with the study of cell growth during the embryo (Lawson et al, 1974) where a large increase in the rate of growth was reported just before birth. There is still a lack of differentiation between cells as dark or light, despite the initiation of peptide expression, implying that NF accumulation may be the important factor.

3.5.3 Are the size-frequency histograms at E18 and E21 similar to those of mature DRG cells?

Histograms at both E18 and E21 depict an immature population of cells due to their size. The distributions are not representative of two separate populations of cells, as in the adult. The shape of the two embryonic distributions are similar as they are abnormally distributed about the mean and are skewed at the upper end of the distribution.

By E21 there is greater size separation and the emergence of two subpopulations. The curves fitted to the E21 size-frequency histogram (Fig. 3.2B) were only applied visually and based on the patterns produced in the adult (Lawson et al, 1984; Fig. 3.3a). At this age however, there may be many more possible "fits" as a clear bimodal population is not evident. The smallest cells recorded are slightly bigger than at E18 but there is no apparent change in the size of the larger cells. The reason why cells at the upper end of the distribution do not appear to have enlarged from E18 to E21 may be due to the smaller sample size at E21 in this study. However, it appears that the proportion of cells changes from E18 when there is 49% small : 51% large, to 67% small : 23% large at E21. This implies that most growth is occurring in the later born small cell population.

There is a possibility that fewer large cells are genuinely present and that these have not increased in size from E18. Selective cell death of the large cells has been proposed to occur during this particular developmental stage (Coggeshall et al, 1994), so the ratio of small to large cells would be greater than in the adult when cell death has also occurred in the small cell population. This period of cell death is concomitant with slow growth of DRG cells, as defined by an increase in the total mean cell diameter (Lawson et al, 1974) and proliferation (Coggeshall et al, 1994). Neither of these studies address which population is undergoing these processes. Until this information is available it is not implausible that the large cells are simultaneously undergoing death and proliferation and hence are not in growth mode.

The other significant difference between these distributions is the size range of the modal frequency. At E18, the modal size is 195-210μm^2 compared to 120-135μm^2 at E21. The modal size at E18 is also closer to its median value in the middle of the distribution. The closeness of the modal and median values at E18 may be a reflection of the largely unseparated distribution which contains an equal proportion of large cells that have not reached full growth capacity, and small cells that do not yet encompass the third population described by Kitao and colleagues (1996). These are cells that are generated between E14 and E15, and both RT97 and IB4 negative. By E21 however, the third

population may be more strongly featured and probably as a direct result of cell death in the larger population, the proportion of cells found in this range changes.

3.5.4 Summary

The results of this study suggest that at E18 and E21 the DRG cell populations are still immature as defined by their morphological characteristics. The classification of cells as large light or small dark is not feasible prior to birth although a size distinction is evident in the E21 population. The size-frequency distributions are not yet bimodal or normally distributed.

3.6 RT97 Distribution in the E18 Dorsal Root Ganglia

In this section I have described the size-frequency distribution and expression of RT97 in the lumbar E18 DRG. The aim was to determine if the reported characteristics of RT97 in the adult were the same in the developing system. My study shows that RT97 can be used in the embryo to sub-divide/classify the DRG into two populations and provides evidence for a distinctive RT97 positive population from an early stage, but there are significant differences from the adult.

3.6.1 Why is it necessary to investigate histochemical characteristics during development if they have already been described in the adult?

This study was conducted because of several recent reports in the literature that characteristics of basic histochemical markers may differ from development to adult. Characteristics such as the specificity, size distribution and expression levels are those which have attracted attention. Examples of these histochemical markers are peripherin, trk A and IB4.

Peripherin is an intermediate filament and in the adult is reported to label small diameter DRG neurons (Portier et al, 1984; Parysek & Goldman, 1988; Ferri et al, 1990; Goldstein et al, 1991). However, a later study examining the ontogeny of peripherin expression in the mouse DRG found that approximately 99% of cells expressed peripherin at E17 (Troy et al, 1990a). This finding meant that peripherin could not be

relied upon as a selective marker of the small diameter population in the embryo. Similarly, a discrepancy exists between the percentage of cells expressing trkA and IB4 during embryonic, postnatal and adult stages.

TrkA is the high affinity NGF receptor and its protein and message is present in 40-50% of mainly small to medium sized adult DRG cells (Verge et al, 1992; Mu et al, 1993; McMahon et al, 1994; Wright & Snider, 1995; Molliver et al, 1995; Averill et al, 1995; Bennett et al, 1996b). Yet in the embryo, 70-90% of cells are found to be NGF dependent (Johnson et al, 1980; Goedert et al, 1984; Ruit et al, 1992; Crowley et al, 1994; Smeyne et al, 1994), and in addition trkA protein is found in 71% of cells at P0 (Bennett et al, 1996b). This cytochemical marker is postnatally downregulated while the IB4 lectin is apparently upregulated postnatally. At P0 only 9% of DRG cells are accounted for by IB4-IR, this figure rises to between 40% (Bennett et al, 1996b) and 67% (Silverman & Kruger, 1990; Plenderleith et al, 1992; Molliver et al, 1995) in the adult.

These studies detail major postnatal shifts in the chemical phenotype of some DRG neurons. This indicates that we can no longer simply assume that characteristics described in the adult are established early in development.

3.6.2 Location of RT97 positive cells within the DRG

The RT97-IR cells were largely confined to the ventral and ventro-medial regions of the E18 DRG, a pattern not observed in the adult. It may reflect a spatial organisation in the birth and maturation of DRG cells, the early RT97 positive large cells being grouped together ventrally. Alternatively, the specificity of RT97 localisation in the embryo may be analogous to the developmental somatotopy observed in the DRG.

Somatotopy is the topographical organisation of cells/axons in one region that is represented in the same spatial relationship in another location (see Chapter 1). The DRG has both central and peripheral terminations; anatomical studies have demonstrated that the central projections of the DRG are somatotopically organised in the dorsal horn (Molander & Grant, 1985; 1986; Swett & Woolf, 1985) and that these are basically correct from the outset (Smith, 1983; Fitzgerald, 1987; Smith & Frank, 1988). However, the relationship

between the DRG and the periphery is not as clear. During embryonic development, there is a rostro-caudal organisation in the DRG and dorsal roots derived from the distribution pattern of peripheral nerves, in addition, the location of sensory neurons from a particular nerve is restricted to the rostral or caudal half of a DRG (Wessels et al, 1990). This topographical relationship is not evident in the adult, consistent with previous studies suggesting that the pattern gets disrupted with growth and myelination (Molander & Grant, 1985; 1986). There is no relationship between the position of cell bodies in the DRG and the position of target muscle (Honig, 1982; Molander & Grant, 1985).

The possibility that cytochemical markers also display characteristic locations within the DRG during development suggests some physiological significance and would depend on organisation of DRG cells according to classification criteria e.g. size, since this is one of the characteristics that define chemical content of cells. Large cells are reportedly concentrated in the ventrolateral part of the ganglion whereas small cells are concentrated in the dorsomedial region of the chick DRG (Hamburger & Levi-Montalcini, 1949). Finding RT97 positive cells in the ventromedial region is at least consistent on the dorso-ventral axis, however, since not all large cells are labelled with this antibody at this time it may explain the absence in the lateral portion and their presence in the medial portion of the DRG. Although, observations in the rat DRG suggest that small and large ganglion cells are randomly scattered throughout the ganglion from the outset (Altman & Bayer, 1982). No such preferred distribution was observed for the peptides SP and SOM in the adult, but a concentration of FRAP cells were found in the dorsal portion of adult DRG sections to the practical exclusion in the ventral part (Price, 1985).

3.6.3 Is there a relationship between RT97-IR and cell size in the embryo?

The size-frequency histogram shows that RT97 positive cells represent a distinct group within the DRG at E18. The positive cells range in size from 120μm^2 to 435μm^2, with no cell below 120μm^2. The smallest neurons in the ganglia are excluded from the RT97-IR population, however, the fact that negative neurons also appear to be among the largest in the ganglia poses a problem in comparison to the previous description of RT97's distribution. In Lawson's study of the adult DRG (Lawson et al, 1984), RT97

was located in the large light cells, mostly at the upper end of the distribution. RT97 was not detected in the smallest cells and although there was an overlap between the negative and positive groups, a range of large-sized cells were exclusively RT97-IR. Here the RT97 positive population, although distinct, overlaps more extensively with the RT97 negative population with respect to neuronal area. The reason for the increased overlap may simply be due to the previous definition of RT97 staining. It has been described as a marker for the large light population (Lawson et al, 1984). However, the large light population itself has a very broad distribution which overlaps substantially with the peptide-containing size range, and another important anomaly is the heterogeneity of staining in the adult.

The description of the large light population is limited by the finding that there are also size sub-categories according to the different arrangement and abundance of neurofilament content. The large A cells have been sub-classified into A_1, A_2 and A_3 (Andres, 1961; Jacobs et al, 1975; Duce & Keen, 1977; Rambourg et al, 1983). These classifications could correlate directly with the heterogeneous RT97 immunostaining since intensity of positive cells ranged from weak to strong, resulting in some unclassifiable cells. They could be relevant in explaining the existence of large RT97 negative cells if the most lightly stained cells are the unclassifiable cells, however, these do not fall into the large size range and no relationship has been established between intensity and cell size after microdensitometric analysis (Lawson et al, 1984). Nonetheless, at E18 when these sub-categories are inapplicable, I find that RT97 positive cells are all intensely stained and negative cells are clearly lacking in reaction product, with the resultant scarcity of unclassified cells.

RT97 immunoreactivity can be described other than by comparison to the large light population. If RT97 positive neurons are described by their size range and the parameters of a normal distribution, it is still be possible to identify them as a discrete sub-population. Table 3.1 contains data describing these parameters. Both the mean and the median were larger in the RT97 positive population. Furthermore, 80% of the positive

population in comparison to 45% of the negative population had cells larger than the modal size.

Analysis of the percentage RT97 expression at all these intermediary ages would resolve whether or not more of the larger cells become RT97 positive or whether expression is switched from smaller to larger cells (see 3.6.4). However, regardless of which assumption is correct, the fact remains that even in the adult, there are some large cells that remain RT97 negative.

The RT97 negative cells in the adult are often larger than 35μm in diameter and these large negative cells may simply lack neurofilaments, although it appears that they are just deficient in the heavier subunit, as large RT97-negative DRG cells reacted positively to NFL (Price, 1985).

In conclusion, the results from my study of RT97 size-distribution in the E18 embryo show that while RT97 positive cells do not include all large neurons, any positive neuron is in the large cell population and can therefore be used as a marker to identify a population of large neurons and fibres in the embryo.

3.6.4 Number of cells expressing RT97 in the embryo and the adult

At E18, 22.5% of DRG cells express RT97 in contrast to 40% in the adult. The data on adult expression analysed in this study is entirely consistent with previous reports (Lawson et al, 1984; Robertson et al, 1991; Kitao et al, 1996). This expression data can be used to resolve some of the problems outlined above in interpreting the discrepancy between the embryonic and adult size-frequency histograms. Since approximately 50% fewer cells appear to express RT97 at E18 than seen in the adult, it is likely that RT97 expression does not shift from smaller to larger cells, but that expression is increased selectively in large cells sometime between E18 and the adult. There are four possibilities to consider; the first two are labelling procedures and artefacts of growth. The latter two - increased expression and cell death - are stronger possibilities, although, this study does not illuminate the reason for the apparent upregulation.

The first possibility is that the low expression could be the result of the antibody used. A monoclonal antibody was used which rules out the variability in affinity for

epitopes that is sometimes found with a polyclonal, even though adult and embryonic tissue were processed simultaneously. Additionally, if protein expression was low this specific antibody may not be sensitive enough, but staining was very intense and this is unlikely to be a problem. Another area of uncertainty is whether the transport rate is greater than synthesis attributing the apparent upregulation to an artefact of growth. NF protein could be transported out of cells faster than it is produced in the soma. Matters of detecting expression patterns and transport could both be solved by examination of the mRNA, which has been achieved successfully with neuropeptides and neurotrophins.

Until expression in the embryo is confirmed using *in situ* hybridisation, rapid transport of NF from the cell body remains credible as an explanation for the number of large, RT97 negative cells at E18. The large cells of the DRG are born first (Lawson, 1974; Altman & Bayer, 1984; Kitao et al, 1996) and are presumably the first to send out axons, therefore they might require NF before smaller axons whose development lags behind, and these consequently could initiate transport from the soma at this early stage. This is also unlikely, as an understanding of the development of NFs (see section 4.8) suggests that the first phase of axon growth is neurite elongation, with limited NF involvement that increases only after synaptogenesis. Immature axons contain NFL and NFM only; NFH appearance is delayed, with it's phosphorylation following after entry into the axon. Levels of NFs increase during transport resulting in mature axons containing all three subunits (Glicksman et al, 1987; Nixon et al, 1987; Oblinger, 1987). This implies that rather than being transported out, this high molecular weight subunit is absent, although RT97 was found in cells at this stage. The fact that the cells are physically smaller and cannot accommodate much neurofilament does not apply because cells as small as 120μm^2 displayed labelling.

Stronger possibilities relate to changes dependent on cues from the development of the sensory system. At some stage between E18 and the adult, more of these large neurons express phosphorylated NFH. This is either because of increased expression in the larger neurons, or a change in the proportion of large to small neurons or a combination of both these processes.

Increased expression alone is likely to occur early in the postnatal period, since the largest increase in NFs occurs during the second growth phase of axons referred to as radial growth. This is concomitant with myelination which firstly only occurs in larger neurons and secondly is a postnatal event (Hoffman et al, 1985; 1987). More conclusive is the finding that the most significant change in neurofilament expression during this period is the large upregulation of NFH mRNA that occurs around P2 (Goldstein et al, 1996). This increase may be sufficient to increase expression of RT97 to 40% of all adult DRG neurons, however, the proportion of RT97 positive cells may increase from E18 but the actual numbers remain the same if the numbers of DRG neurons themselves change.

This would depend on cell death of RT97 negative neurons during this period (see section 3.1.6). The peak of prenatal cell death occurs between E17 and E19 and this has been proposed to be confined to the larger neurons, although there is no direct evidence for this. The second phase of cell death which is much smaller, occurs between P0 and P3 and may be restricted to small cells (Coggeshall et al, 1994). Hence if NFH increases in the early postnatal period, and the largely RT97 negative small cells die, the percentage of RT97 expressing cells would increase quickly postnatally.

Therefore a combination of factors is proposed to explain increased expression of RT97 in the mature animal.

3.6.5 Link between the inability to classify E18 cells as "large light" and "small dark" and the number of large RT97 negative neurons

As described in section 3.1.3, the classification of cells as large light and small dark is based on microscopic observations of the cytoplasm content. Even in the late embryonic stages E18 and E21 (section 3.1), this classification is not feasible due to the smaller cell sizes overall and incomplete bimodal size separation. However, the fact that one of the major criteria for this classification is the presence and abundance of neurofilament makes this less surprising. My data demonstrates that 50% fewer cells are expressing the phosphorylated heavy NF sub-unit at E18 than in the adult, and that there are many large cells with an apparent paucity of NF as defined by RT97. It is only in the adult or possibly the early postnatal animal, where practically all large cells express RT97,

that these cells represent 40% of the total population and the large light or small dark classification can be applied.

3.6.6 Summary

The principle finding of the present investigation is that RT97 positive cells are a distinct group from an early stage enabling RT97 to be used as a marker for the large cell population in the E18 embryo. It is only expressed in 22.5% of the cells compared to 40% in the adult. These results illustrate that, although RT97 size selectivity is established early in development, its expression increases postnatally. In addition, I suggest that the increasing presence of RT97 (phosphorylated heavy NF subunit) in DRG cells, may lead to the appearance of morphological characteristics typical of large light cells in the DRG.

4

THE DEVELOPMENT OF SUBPOPULATIONS OF CUTANEOUS SENSORY NEURONS IN THE DRG, AND THE DEVELOPMENTAL PATTERN OF INNERVATION OF HINDLIMB AND SPINAL CORD IN EMBRYONIC RAT

INTRODUCTION

The dorsal root ganglia (DRG) in the adult rat contains a heterogeneous population of sensory neurons that vary widely in their physiological and cytological properties. Classifications of DRG neurons are traditionally based on their cytological and ultrastructural features. Alternative classification schemes have attempted to correlate carbohydrate surface antigens, specific neuropeptide content, cell size and physiological properties (see Jessel & Dodd, 1986). The reason that such intense efforts have been made to describe the neuronal populations is to discover the selective properties of each of the subpopulations. Functionally this distinction is important as the two main groups A-fibres and C-fibres convey very different information about sensory surroundings.

It is equally important to identify the different subpopulations during development and to ascertain how these develop in relation to each other. The aim of this study is to compare the development of the lumbar sensory neuron subpopulations by anatomical methods on reaching their targets - the hindlimb and spinal cord.

i) Central target

Central processing of sensory information from the periphery has two priorities. The first is to specify the characteristics of the stimulus in terms of the sensory modality, and the second to inform of stimulus position. The type of relationship with the periphery is characterised by two superimposed patterns in the dorsal horn, and is referred to as somatotopy (also see below).

Termination patterns of afferents are important because of their relevance to function - the site of the terminal synapse determines which second order neurons can receive fast monosynaptic input. The following account describes the anatomy of the dorsal horn and its laminar structure (see Willis & Coggeshall, 1991).

Once in the spinal cord, dorsal root fibres bifurcate to give one rostral and one caudal branch. These give off collaterals which penetrate the grey matter and traverse different laminae. The grey matter of the spinal cord is divided into ten layers or laminae based on their neuronal cytoarchitecture. This classification is also important because

neurons in different laminae are also functionally distinct and have different patterns of projections. Different classes of primary afferent fibres of different sensory modalities each terminate in a specific lamina.

Laminae I-VI correspond to the dorsal horn, lamina VII is equivalent to the intermediate zone while laminae VIII and IX constitute the ventral horn. Projections to laminae of the dorsal horn are concentrated upon in this thesis as they receive sensory input from the periphery. Lamina I is the most superficial region of the dorsal horn and receives projections from thinly myelinated Aδ fibres and unmyelinated C fibres. Lamina II, also referred to as the substantia gelatinosa, receives afferent information from non-myelinated or nociceptive C and Aδ fibres, while laminae III and IV receive information from Aβ fibres. The laminar organisation of the spinal cord is evident from E18 in the rat embryo.

ii) Peripheral target

Although discrete laminar boundaries are not evident in the skin, innervation is similarly restricted to regions. Some axons terminate at structures in the dermis while only unmyelinated fibres project into the epidermis. The development of these patterns are examined in Chapter 5 where it is found that innervation of the epidermis changes in three aspects as development proceeds; density, innervation levels and terminal position. The other major aspect of peripheral innervation is the establishment of dermatomes.

Sensory axon fibres from each DRG project to the periphery and innnervate a discrete skin zone called a dermatome (Brown et al, 1992; Scott, 1992). Each dorsal root possesses a dermatome that envelopes a large area of skin and that is distinct from the area innervated by an individual peripheral nerve, which is referred to as an innervation field. Cutaneous innervation fields join to form one continuous field, the dermatome. Dermatomes exist in series along the body surface from the most rostral to the most caudal dorsal roots with dermatomes from each DRG overlapping extensively. This overlap means that each point on the skin is innervated by sensory axons from two or three spinal nerves, however peripheral innervation fields of individual cutaneous axons

do not exhibit the same degree of overlap and provide the discriminatory resolution of the system.

In the chick embryo, axons from each DRG grow directly to their target skin along a defined set of pathways and the axons establish their dermatome precisely at its characteristic location, so skin innervation also resembles the adult innervation pattern from the outset (Scott, 1982). Innervation of skin in the rat is thought to occur ahead of muscle (Reynolds et al, 1991), this is interesting because evidence in chick suggests that sensory fibres follow the pathways of developing limb bud motor axons (Scott, 1986; Landmesser & Honig, 1986).

Sensory innervation of cutaneous tissue is investigated in this chapter to determine if, like the spinal cord, the skin is innervated in successive waves corresponding to different functional phenotypes. Sympathetic innervation is not investigated in this thesis as it only develops perinatally. It is restricted to the hypodermis as birth, then progresses to dermal vessels and piloerector muscles at the end of the first postnatal week in the rat (Schotzinger & Landis, 1990). The adult pattern of sympathetic innervation is not present until the third postnatal week (Reynolds and Fitzgerald, 1995).

iii) Somatotopy

Two superimposed patterns in the dorsal horn are the basis for the specificity of the relationship with the peripheral nervous system.

The first pattern consists of fibres that innervate different receptor types and have characteristic branching patterns in the spinal cord with respect to the 3D spatial occupation. Each point on the periphery (peripheral receptive field), is represented at a particular site along the mediolateral and rostrocaudal extent of the dorsal horn. Afferents that innervate contiguous skin areas have terminals that occupy contiguous regions of spinal cord in the horizontal plane and each cutaneous nerve has its own terminal area within the dorsal horn with little or no overlap between adjacent nerve territories (Koerber & Brown, 1980; Molander & Grant, 1985; 1986; Swett & Woolf, 1985; Woolf & Fitzgerald, 1986; Lamotte et al, 1989; Rivero-Melian, 1993).

The second pattern arises from the correlation between the modality of the peripheral receptor and the laminar location of central terminal arborization in the dorsoventral plane (Shortland et al, 1989; Sugiura et al, 1986). The laminae in the dorsal horn consists of well-defined boundaries and the phenotype of afferents that terminate in each are described above.

These patterns are established early in development and all studies on the laminar termination of different subpopulations suggest these are appropriate from the outset (see Chapter 4 discussion). In addition, at postnatal day (P)0 and P4, cutaneous afferents investigated with B-HRP and DiI show that innervation is somatotopically arranged from earliest stages although there is some overlap at birth which decreases over the first two postnatal weeks (Beggs & Fitzgerald, personal communication).

Sections of hindlimb, DRG and spinal cord from embryonic ages E13-E21 were examined using immunohistochemistry with a series of general neuronal markers and some labels selective for the A-fibre and C-fibre populations. Antibodies to GAP 43, PGP 9.5, peripherin, RT97, SP, CGRP, trkA and IB4 were utilised. An overview of most of the markers used in this study are contained in the introduction to this chapter while RT97 has been described in Chapter 3 and the peptides CGRP and SP are described in Chapter 6.

4.1 Growth Associated Protein (GAP 43)

4.1.1 Background

One of the genes selectively expressed during axonal growth is a gene encoding an acidic membrane protein called growth associated protein 43 (GAP 43), also denoted B50. This protein is a class II beta tubulin that associates with golgi membranes shortly after synthesis. It is rapidly transported (see 4.1.2) from the cell body to the growth cones and nerve terminals where it accumulates (Aigner & Caroni, 1993) and can be used to distinguish axonal from dendritic processes because it is selectively incorporated into the

distal axonal membrane after the establishment of cellular polarity (Goslin et al, 1988; Van Lookeran Campagne et al, 1993). GAP 43 has been shown to be a prominent protein component of growth cone membranes including the filopodial extensions, and this has been confirmed by immunolocalisation showing that it is most heavily concentrated in growth cones with low levels in the cell body (Skene & Willard, 1981; Merri et al, 1986; Skene et al, 1986; Benowitz & Routtenberg, 1987).

4.1.2 Properties & transport

GAP 43 is synthesised as a soluble protein with a highly conserved amino acid sequence. Its secondary structure is an elongated kinked coil with a molecular weight of 43-57 kDA as defined by mobility on a SDS-polyacrylamide gel, however its true size is 23.6 kDA (Benowitz & Routtenberg, 1997). It is a hydrophilic protein post-translationally associated with the cytoskeleton and membranes, mediated by the co-valent attachment of a fatty acid. A structural model has been constructed showing the protein extending away from cytoplasmic surfaces of the neuronal growth cone and synaptic membranes, due to the hydrophilic nature of the protein. This demonstrates how it is in a position to interact with cytoplasmic/cytoskeletal proteins while simultaneously being reversibly attached to the membrane (see Skene, 1989 for a review).

After synthesis, GAP 43 is conveyed by fast anterograde transport at a rate of 400mm/day, via the trans-golgi network from the cell body to the distal extremities. The network consists of two carriers, the large dense cored vesicle (LDCV) and small transport vesicle (STV). GAP 43 is located in mostly uniform sized vesicles of approximately 50nm. It is associated with synaptophysin in the STV's that travel directly to the growth cone and nerve terminals. GAP 43 alone is found in the LDCV's and is targeted to the axolemma for local membrane fusion (see Verkade et al, 1996a for detail).

4.1.3 Control of expression

Regulation of GAP 43 expression exists at the level of mRNA stability and not the transcription rate. NGF regulates the expression levels of GAP 43 in PC12 cells by stabilising the half-life of the mRNA. Degradation of mRNA occurs rapidly in PC12

cells, where $t_{1/2}$=5-8 hrs. NGF increases the half-life five-fold, allowing a high level of accumulation and subsequent translation (Benowitz & Routtenberg, 1997).

4.1.4 Developmental expression

GAP 43 expression continues throughout the period of axon elongation and synaptogenesis in all developing and regenerating systems. This feature allows it to be used as a selective immunohistochemical marker during active growth and terminal formation and mRNA is still expressed well into postnatal life when the protein has decreased (Chong et al, 1994).

Fitzgerald and colleagues, 1991, provided a detailed account of development in the somato-sensory system of the rat using this marker, although previous studies had also described the high levels of GAP 43 present during development of the rodent brain particularly associated with areas of active growth and synaptogenesis (Jacobson et al, 1986; Snipes et al, 1987; McGuire et al, 1988; Dani et al, 1991). The first detected expression of GAP 43 was in the motoneuron pool of the rat spinal cord at E11. A second phase of growth was described from E15-E19. The most significant event was the growth of numerous fine-diameter collaterals from the dorsal root into the dorsal grey matter in a ventrolateral direction. By E19 there is a general network of fibres in the grey matter with a concentration in the substantia gelatinosa (SG), including immunopositive cells. Early in the postnatal period the SG retains its fine network of fibres but loses its cellular staining at P2. Expression in the white matter also fades postnatally with the only new growth being the late appearance of the corticospinal tracts (Fitzgerald et al, 1991).

In the periphery, between E12 and E13 axons wait in the plexus region at the base of the limb bud, then form peripheral nerves on entering the limb at E14. The first branches are cutaneous, penetrating the proximal epidermis at E15. The innervation continues in a proximo-distal direction reaching the toes by E19. After birth, the overall intensity of staining decreases towards the second week, including the withdrawal of the epidermal plexus to a sub-epidermal position (Reynolds et al, 1991).

In the human, GAP 43 was detected in the brain as early as 4 gestational weeks with labelling in the rostral neural tube. The expression matched that of tyrosine

hydroxylase (TH) very precisely, indicating that GAP 43 was contained in monoaminergic neurons but was not found in cholinergic or GABAergic neurons (Milosevic et al, 1995).

4.1.5 Non-neuronal expression

In addition to neurons, the protein is also expressed at restricted developmental stages in Schwann cells, astrocytes and oligodendrocytes (Vitkovic et al, 1988; da Cunha & Vitkovic, 1990; Deloulme et al, 1990; Curtis et al, 1991; 1992; Woolf et al, 1992b). After axotomy, Schwann cells migrate from the neuromuscular junction to denervated muscle and extend GAP 43 processes until axonal reinnervation occurs (Woolf et al, 1992b).

4.1.6 Adult expression

Most sensory neurons decrease their GAP 43 levels as they mature and this downregulation during development coincides with the activity-sensitive elimination of collaterals (Neve & Baer, 1989) and establishment of an adult pattern of connectivity (Aigner & Caroni, 1993). GAP 43 displays low levels in the adult (Barry et al, 1993) except for the brain (Woolf, 1990). More recently, using novel antibodies, significant staining has been observed in the grey matter of the adult spinal cord (Curtis et al, 1993; Naciemento et al, 1993; Ching et al, 1994; Wotherspoon & Priestly, 1995). Previously, the only time significant levels of GAP 43 mRNA were observed in the adult is during regeneration after nerve injury.

During regeneration studies, when lumbar motoneurons were axotomised (Linda et al, 1992; Chong et al, 1992; Booth & Brown, 1993) and compared to controls, GAP 43 in the naive animal was only localised to motoneurons and in the first study, to lamina X. To clarify the origin of the grey matter immunoreactivity, Michael & Priestly, 1995 examined the rat thoracic spinal cord. They found constitutive mRNA expression in the central autonomic nucleus of lamina X and the intermediolateral cell column, indicating GAP 43 presence in the preganglionic sympathetic neurons. This is consistent with representation in the sympathetic ganglia (Schmidt et al, 1991; Hou & Dahlstrom, 1995).

In fact, GAP 43 is constitutively expressed at high levels throughout the autonomic nervous system in addition to the sympathetics, as it has also been reported in preganglionic cranial parasympathetics (Strack et al, 1988), and postganglionic sympathetic (Stewart et al, 1992). This was presumably missed in previous studies confined to lumbar regions, as these excluded autonomic cell groups. Furthermore, the reaction of autonomic neurons to injury has not been ascertained.

4.1.7 Plasticity

Injury to peripheral nerves results in rapid upregulation of GAP 43 expression in the DRG and spinal cord (Van der Zee, 1989; Chong et al, 1992). It is also enriched in axonal sprouts distal to the site of injury (Verhaagen et al, 1996; Tetzlaff et al, 1989) and also in axons proximal to the crush (Verkade et al, 1995). In the rat DRG, induction of GAP 43 mRNA begins 1-2 days after sciatic nerve injury, however, GAP 43 expression is not fully elevated until axon elongation is well under way, hence the induction of GAP 43 appears to be a secondary consequence of axon outgrowth (Skene, 1989). Woolf and colleagues (1990), showed that axotomy triggered GAP 43 production was present in regenerating peripheral nerves. High levels of GAP 43 protein also appear in newly developed growth cones in the dorsal horn after axotomy (Coggeshall et al, 1991) but GAP 43 mRNA is not detected after central dorsal root injury (Chong et al 1992; 1994). As a consequence of this elevation, it was suggested that the increase of GAP 43 in the CNS may contribute to inappropriate synaptic reorganisation of afferent terminals after peripheral injury (Woolf et al 1992a), and the failure of dorsal root section to elevate GAP 43 expression in the DRG or spinal cord may contribute to the poor regenerative response initiated by such lesions (Chong et al, 1994).

4.1.8 Function

i) Role in development and plasticity

In 1989, Skene proposed a GAP Hypothesis to explain the strong correlation between axon growth, elevated GAP 43 synthesis and its presence in growth cones. This suggested that nerve growth is controlled in part, by expression of sub-classes of GAPs

which would play specific and important roles in neurite outgrowth. The first sub-group, including actin and tubulin isoforms, correlate with the actual process of long-distance axonal elongation, essentially the backbone for axon formation. The second group encompassing GAP 43, represent a general role in neurite outgrowth competence. The latter group are down-regulated during development in tandem with the end of growth of terminal arbors, their reintroduction after injury providing the regeneration competence in the adult (Schreyer & Skene, 1991; Doster et al, 1991; Tetzlaff et al, 1991). Woolf and colleagues (1990), also suggested that GAP 43 influences neurite elongation and synaptic formation. Evidence firmly establishing GAP 43 as the intrinsic presynaptic determinant of neurite outgrowth competence and plasticity arose from the following *in vivo* and *in vitro* gene manipulation studies.

In vitro experiments that depleted the level of GAP 43 using anti-sense oligonucleotides, reinforced its role in neurite outgrowth and also morphology. GAP 43-depleted DRG chick neurons extend longer, thinner and less branched neurites with strikingly smaller growth cones. However, the growth response was different depending on the substrate used, suggesting substrate involvement in the potentiation of growth cone responses to external signals. This would affect process formation and guidance (Aigner & Caroni, 1993), but not actual outgrowth as PC12 cells with decreased GAP 43 expression can still extend neurites (Baetge & Hammang, 1991). In non-neuronal cells, GAP 43 expression induces formation of filopodia (Zuber et al, 1989; Strithmatter et al, 1994a) and neurite outgrowth is augmented in GAP 43 expressing PC12 cells, after NGF or cAMP treatment (Yanker et al, 1990; Morton & Buss, 1992). The *in vitro* depletion and overexpression of GAP 43, led to the conclusion that it promotes neurite adhesion and persistent growth cone spreading and branching.

Consistent with these findings, the *in vivo* depletion of GAP 43 in mice resulted in defective neuronal pathfinding during early development (Strithmatter et al, 1995). The transgenic mice were neonatal lethal despite a grossly normal CNS and neurite outgrowth. This study implied that the role of GAP 43 was in amplification of signals from the growth cone, and is only required at certain decision points. However, compensatory

mechanisms by structurally similar proteins such as neurogranin or CAP 23 may have contributed to the apparently normal neuronal architecture (Benowitz & Routtenberg, 1997).

In vivo over-expression in adult transgenic mice led to spontaneous sprouting in the neuromuscular junction and the terminal field of hippocampal mossy fibres. After nerve lesion in these animals, sprouting and terminal arborisation was potentiated (Aigner et al, 1995). In absence of additional trophic factors, GAP 43 itself enables neurons to form axon terminals and therefore is an intrinsic determinant of the growth state. However, in another transgenic GAP 43 mutant, unable to be phosphorylated by protein kinase C (PKC), sprout-promoting activity was diminished (Aigner et al, 1995). These *in vitro* and *in vivo* gene manipulations reveal the role of GAP 43 in the regulation of neurite outgrowth, essential to axonal navigation, synapse formation, plasticity and regeneration, and highlights the role of phosphorylation. Nonetheless, the actual effects of GAP 43 on the growth cones and synaptic terminals is unknown.

ii) Reaction with the terminal membrane

Insoluble GAP 43 in growth cones is associated with the cytoskeletal proteins actin, α-actinin, talin and fodrin (Meiri & Gordon-Weeks, 1990; Moss et al, 1990). These proteins determine shape, motility and pathway guidance and are located on the cytoplasmic face of the plasma membrane at the pre-synaptic terminal. In addition, changes in cell shape after transfection of exogenous GAP 43 are associated with the formation of F-actin, with which GAP 43 is co-localised (Widner & Caroni, 1993).

iii) Intracellular and extracellular messengers

GAP 43 appears to interact extensively with several intracellular messenger systems. It is involved in the control of inositol triphosphate hydroylsis and is a major PKC substrate of developing axons (Skene et al, 1986). PKC phosphorylates the serine 41 site in exon 2 of GAP 43 (Coggins & Zweiss, 1989; Chapman et al, 1991). Extracellular signals also regulate its phosphorylation state (Meiri et al, 1988; Dekker et al, 1989), possibly by modulating the activation and response of G proteins to the

extracellular signals (Igarashi et al, 1993). This is also reported to determine the level of signalling molecules at the nerve terminal (Jolles et al, 1980).

iv) Calmodulin buffer

GAP 43 is a unique calmodulin-binding protein in low calcium concentrations (Andreason et al, 1983). Calmodulin binds to an amino acid "IQ domain" just before the PKC phosphorylation site on exon 2. Its affinity for GAP 43 is calcium independent, but it only binds in low calcium concentrations to unphosphorylated GAP 43, as binding is blocked by PKC-mediated phosphorylation of GAP 43. Once calmodulin is bound however, PKC cannot phosphorylate the Ser 41 site (Shea et al, 1995). Calmodulin is released though, when GAP 43 is phosphorylated by a second messenger, e.g. high calcium concentrations and therefore GAP 43 acts as a calmodulin buffer (Alexander et al, 1987; 1988; Chao et al, 1996).

v) Link between phosphorylation and calmodulin

Bound calmodulin prevents PKC phosphorylation of GAP 43 in response to transient increases in calcium concentration. Further increases in calcium concentration or second messengers, allow PKC to be come superactiviated and phosphorylate the Ser 41 site of GAP 43. At this stage calmodulin cannot reassociate; GAP 43 remains activated and interacts with the cytoskeleton. The free calmodulin is then available to activate other proteins, whose activation leads to GAP 43 dephosphorylation in a feedback loop, and calmodulin reassociation. Ser 41 can be dephosphorylated by either a calcium-independent phosphatase associated with the membrane (Han et al, 1992), or by a soluble calcium and calmodulin dependent phosphatase called calcineurin (Liu & Storm, 1989). The link between these is reviewed in Benowitz & Routtenberg, 1997, but briefly, removal of the dephosphorylating agent (calcineurin) increases neurite outgrowth. Calcineurin is inhibited by immunophilins - proteins which control the actions of immunosuppressants. Calcineurin removal may be mediated by these as it is known that an immunosuppressant enhances GAP 43 phosphorylation and augments axonal

outgrowth, providing further evidence for the crucial role of phosphorylation in GAP 43 outgrowth.

vi) Role of calmodulin binding

Calmodulin is distributed throughout the axoplasm of myelinated axons of the sciatic nerve and is preferentially localised near microtubules (Mata & Fink, 1988). It can activate various enzymes and bind to many proteins depending on local calcium concentrations. Its association with GAP 43 may be to concentrate it at specific sites and regulate the availability of both proteins (Verkade et al, 1996a). Calmodulin binding can be inhibited using antibodies to GAP 43 (Hens et al, 1995). In addition, a mutant that mimics GAP 43 phosphorylation but prevents calmodulin binding, does not possess the same range of neurite-promoting activity, therefore implying that both phosphorylation and calmodulin binding of GAP 43 are necessary for this activity (Aigner et al, 1995). This sequestering of calmodulin by GAP 43 and its potential to control calcium mobilisation, suggests GAP 43 may play a critical role in modulating intracellular signalling by calcium and hence the physiological activity of the neuron.

vii) Relationship with monoamines

More recently, evidence of a physiological relationship between GAP 43 and monoamines has been revealed. Firstly, co-localisation data shows that in the brain stem GAP 43 mRNA overlaps with tyrosine hydroxylase (TH) mRNA (Bendotti et al, 1991) and with serotonin in serotoninergic neurons of the rat spinal cord (Ching et al, 1994). Secondly, release of noradrenaline into the synaptic cleft was prevented after intracellular injections of antibodies to GAP 43, suggesting that it may play a role in exocytosis (Dekker et al, 1989; Hens et al, 1995). Together with the co-localisation data, this implies that GAP 43 could modify monoamine release, possibly through protein kinase C activation.

viii) Long Term Potentiation (LTP)

GAP 43 undergoes a persistent change in phosphorylation during LTP, indicating that the protein plays a role in mediating experience-dependent plasticity. It is thought that

a retrograde signal from the post-synaptic activated NMDA receptor initiates GAP 43 phosphorylation on the pre-synaptic terminal. The change of phosphorylation state induced by the trans-synaptic signal, may allow GAP 43 interaction with the cytoskeleton to produce the characteristic structural changes associated with LTP and neurotransmitter release to potentiate the postsynaptic activity (for review see Benowitz & Routtenberg, 1997).

4.2 Protein Gene Product (PGP) 9.5

4.2.1 Identification and structure

There are 30-50000 protein gene products (PGP's) encoded for by the human genome. PGP 9.5 is a neuron specific cytoplasmic marker discovered by Jackson and Thompson in 1981, then isolated together with Doran in 1983 by high resolution 2-D mapping of soluble proteins from different human organs. Its name is derived from its mobility - 9.5 cm on a polyacrylamide gel.

It has a primary protein structure and is a general cytoplasmic marker for all efferent and afferent nerve fibres, both sensory and autonomic, in addition to neuroendocrine cells. It is a major component of cytoplasm in a wide range of species and occurs in the cell from perikaryon to fine terminals (Gulbenkian et al, 1987). PGP 9.5 in the brain represents the major protein component of neuronal cytoplasm.

PGP 9.5 was determined to be a total marker for identified neuronal structures in the skin focusing on the discovery that nerve endings terminate in the basal layer as well as superficial layers (Wang et al, 1990). It is a particularly good marker because it gives a more complete demonstration of intra-epidermal nerve endings compared to silver impregnated nerves which can only be traced as far as the superficial layers of human epidermis (Novotny & Gommert-Novotny, 1988). A notable finding revealing the importance of PGP 9.5, concentrated on the Meissners Corpuscle using confocal microscopy. Using the silver impregnation technique, branches of afferent nerve fibres displayed thin regions with mitochondrial-rich varicose elements not greater than 5-6μm in diameter. In contrast after examination with PGP 9.5, flattened and discoidal

expansions with a diameter up to 30μm were identified. PGP 9.5 labels the proteinacious component of axoplasm revealing the complete architecture of neural components, reflecting images closer to reality.

This was not the first comparative consideration of PGP 9.5 qualities as a neuronal marker. Karanth and colleagues, (1991) concluded that PGP 9.5 was qualitatively and quantitatively superior for visualisation of cutaneous nerves in comparison to the other markers (NF, NSE, TH, ChAT, Synaptophysin) used in the same study. Its specificity and clarity during development is comparable to that in adult tissue.

4.2.2 Developmental expression

PGP 9.5 is first observed in the rat at E11.5. Cells become positive as soon as they are recognisably neuronal from their morphology or position. Before this, the mitotic ventricular zone, neural tube neuroblasts and migrating neural crest cells are all negative. The first immunoreactivity is located in the DRG and the primary motoneurons at E11.5. By E12 axons from the DRG have reached the spinal cord at the Bundle of His, which becomes more dense until E15. From E11.5 until E13 the positive cells in the DRG are restricted to the ventrolateral region with few immunoreactive cells in the boundary cap, possibly the putative "B" cells (Kent & Clarke, 1991). There is a slight discrepancy in the description of PGP 9.5-IR cells as solely post-mitotic since there are many positive cells in the DRG at E12. This is a stage before the peak generation of cells according to Lawson (1974) hence, it is possible that some of those cells are pre-mitotic.

In the human, PGP 9.5 is first identified in the sub-epidermal plexus at 6 weeks gestation. Initially the IR-nerves are thick and club-shaped and distributed in the superficial dermis. Beaded adult-like fibres are more numerous at 10-12 weeks that extend from this plexus to penetrate the epidermis (Terenghi et al, 1993).

4.2.3 Adult expression

In the mature rat skin, PGP 9.5 is reported in the epidermis, dermis, around sweat glands, blood vessels, hair follicles and arrector pilorum (Karanth et al, 1991). Individual

fibres and nerve fascicles of both a varicose and smooth nature have been described. Likewise in the human, PGP 9.5 is detected in the same sites as identified above in addition to Meissners Corpuscles and Merkel cells. The number and intensity of IR-fibres was greater than neural specific enolase (NSE), NF, CGRP, VIP and NPY (Dalsgaard et al, 1989). Thompson and colleagues, 1983 found PGP 9.5-IR in central and peripheral nerves, retina and the diffuse neuroendocrine system (DNES) with faint traces in the kidney, large intestine, prostate and testis.

4.2.4 Plasticity

The complete disappearance of PGP 9.5 labelling was observed in skin flaps within a few days after denervation (Karanth et al, 1990; Manek et al, 1993), however eight weeks after graft repair PGP 9.5 was seen in a few fibres of denervated foot pads in guinea pig nerve (Santamaria et al, 1994). PGP 9.5 is lost from areas containing thin fibres such as the epidermis and sweat glands but faint staining remains in the dermal nerve trunks even thirteen weeks under a chronic denervation state (Navarro et al, 1997). The residual PGP 9.5 is thought to reside in vacated endoneurial tubes where the myelin protein, P0 is found (Navarro et al, 1995).

After a nerve crush injury, PGP 9.5 labelling is not lost but the Meissners corpuscle endings are abnormal and fibres do not penetrate as far into the epidermis (Navarro et al, 1997).

4.2.5 Function

PGP 9.5 is a carboxy-terminal hydrolase for ubiquitin, a tissue-specific isoenzyme used in post-translational targeting of cell proteins and the likely basis for its specificity (Wilkinson et al, 1989). PGP 9.5 is detected from the birthdate of neurons and increases in intensity into adulthood. It does not appear to be associated with structural proteins, for example neurofilaments, hence its early appearance suggested it may play an important role in neuronal metabolism.

4.2.6 Co-localisation

PGP 9.5 co-localises with another cytoplasmic component, NSE. NSE labels sensory and autonomic fibres but like NF does label all sensory axons. They both stain Merkel cells and nerve cells confirming their neuro-ectodermal origin (Bjorkland et al, 1988). Some PGP 9.5+ve sensory fibres are CGRP+ve while some PGP 9.5+ve autonomic fibres are VIP, CGRP and NPY+ve (Dalsgaard et al, 1989).

4.3 Peripherin

4.3.1 Identification and structure

Peripherin is a 56-57 kDa protein initially identified in neuroblastoma and rat PC12 cells (Portier et al, 1982; 1983a; 1983b; Parysek & Goldman, 1987; 1988; Leonard et al, 1988). Evidence suggested it was a member of the intermediate filament (IF) family (Portier et al, 1984b) but not until it was sequenced, was it finally established it as a type III IF sub-unit (Leonard et al, 1988; Parysek et al, 1988; Thomson & Ziff 1989). One expressed form of peripherin in mice has an additional 32 residues, however the ability of this variant to assemble with other IF proteins and other peripherin splice variants is unknown (Landon et al, 1989).

Peripherin, like the other type III IFs, shares a common 310 amino acid α–helical rod domain containing a hydrophobic heptad repeat essential for assembly. Flanking this central conserved rod are the globular head and tail segments (Lee, 1996). Although it is neuronal specific, it shares more homology with desmin and vimentin than any of the neurofilaments (NFs) (Leonard et al, 1988). Until recently little was known about assembly properties but due to homology to other type III IFs, it was predicted that they would self-assemble. Using mutant peripherin sequences transfected in SW13 cells (a cell line without any detectable IFs) to define regions essential for assembly initiation proved successful. Peripherin, in addition to α-internexin are neuron specific IFs capable of homopolymerisation, which is dependent on the amino-terminal sequence (Cui et al, 1995; Ho et al, 1995).

4.3.2 Expression

In 1983, Portier and colleagues reported the presence of the novel cytoskeletal protein in the peripheral nervous system (PNS), but absent from brain homogenates, indicating its potential as a specific marker for peripheral neurons. The nerve systems and neuronal types reported to express the protein or message are sympathetic, parasympathetic, dorsal root ganglion (DRG) neurons, enteric, neuroblastoma, PC12 cells, ventral horn motoneurons, cranial nerve motor nuclei, brain stem nuclei, cranial nerve roots, corticospinal tract, olfactory epithelium and retinal ganglion cells (Portier et al, 1984b; Leonard et al, 1987; 1988; Parysek et al, 1988; Parysek & Goldman 1988; Aletta et al, 1989).

During development of the rat, peripherin is detected in ventral horn motoneurons, cranial ganglia, olfactory epithelium, retina and optic nerve in addition to the PNS (Escurat et al, 1988). Northern blots of peripherin indicate expression as early as E10, when a few differentiated neurons are present (Parysek et al, 1988). In the mouse, peripherin appears in the ventral part of the spinal cord at E10 and in 10% of DRG cells. At E14 and E17 practically 100% of DRG neurons express peripherin, when in the spinal cord, dorsal columns, fibres from ascending tracts, primary afferents and the lateral motoneuron pool are all labelled. By adulthood, small DRG neurons only are labelled; the spinal cord labelling is restricted to the dorsal and ventral roots and dorsal columns with little present in the ventro-lateral motoneuron cell bodies (Troy et al, 1990a).

Similarly for the rat, peripherin is detected in the neuroepithelium at 34 somites and in the DRG and medially located motoneurons by E12. Levels are generally low in the spinal cord, but in the DRG increase until E18 with stable levels by E20 (Escurat et al, 1990). Recently, an *in situ* hybridisation study has provided results consistent with the downregulation of peripherin from embryonic levels in the rat. At E15-16 all neurons are peripherin positive, by E20 two distinct populations are identifiable and peripherin-IR is more intense and defined in the smaller neurons (Goldstein et al, 1996). This distinction begins to emerge in late embryonic stages coinciding with the timeframe in which most peripheral and central axons have innervated their targets and completed synapse

formation (Altman & Bayer, 1984; Snider et al, 1992), suggesting that the signal responsible for inducing this phenotype is derived from contact with target tissues.

An alternative cause of the downregulation is the link between neurotrophins and induction of phenotypic specificity. Peripherin is homogeneously expressed at E15, a period when there is heterogeneous expression of the trk receptor (Mu et al, 1993) but by E20 axons have presumably established dependency on a specific neurotrophic factor since the receptors are expressed in restricted subpopulations when phenotypic segregation occurs. There is also some evidence supporting neurotrophin exposure in the target determining peptide levels and composition (see Chapter 6). Therefore it is presumed that the target also influences IF expression (Horgan et al, 1990; Marwich et al, 1986). Axotomy experiments also show that the target is important for regulating the expression of IF in the DRG (see below 4.3.4). At P2 the DRG attained adult levels of peripherin expression (Goldstein et al, 1996).

The expression of protein complemented the message expression however contrary to the early reports of Portier et al, 1983; 1984b, peripherin was localised to certain CNS neurons (Leonard et al, 1988; Parysek et al, 1988). Peripherin is found in populations of neurons from a different lineage, with different functions, its common feature the presence in the PNS and axons outside of the central neural axis. (Parysek & Goldman 1988; Escurat et al, 1990; Gorham et al, 1990; Troy et al, 1990; Goldstein et al, 1991). It is expressed concomitantly with axonal growth during development and is the only type III IF found exclusively in motor, sensory and sympathetic neurons (Portier et al, 1993).

In the adult DRG, peripherin is preferentially localised to small diameter neurons however a small population show co-expression with NFL (Parysek & Goldman 1988; Parysek et al, 1988; Ferri et al, 1990; Goldstein et al, 1991). These patterns are well established by P2 according to Goldstein and colleagues, 1996. There is some disagreement, however, about the number of the peripherin-IR cells but not the size distribution of this population (10-40μm diameter). Ferri and colleagues, 1990 describe 66% of neurons as peripherin positive complementary to the 25% distribution for NF

proteins, with 8% co-expression in the size range 20-50μm diameter. In agreement with these figures, 68% of DRG neurons were classified as peripherin-IR (Molliver et al, 1995). In contrast, Goldstein describes 20% less peripherin positive neurons, approximately 46%. In addition, they describe the peripherin positive population at P2 which does not exceed 15μm while NFs have a wider range to 20μm (Goldstein et al, 1996).

Peripherin is more abundant in small cells but is not absent from large cells in the adult. *In situ* hybridisation studies reveal the presence of peripherin mRNA in both large and small cells of the rat (Parysek et al, 1988), in mice also, peripherin is detectable in large cells (Troy et al, 1990b). During rat development peripherin is co-localised with NFL, indicating that it is in some larger cells (Escurat et al, 1990), however in the mature animal, peripherin-IR mostly disappears from large cells. The mRNA may be present in large cells but the protein remains at levels presently beyond detection. This has now been confirmed by Goldstein and colleagues (1996), who show that 80% of peripherin negative cells express peripherin mRNA. Reasons for this are only speculative but translational regulation can be dismissed because the ability of large cells to upregulate peripherin mRNA and protein after injury proves it can be translated. Equally unlikely, are modifications to mask the epitope. Most reasonable is that it is translated but rapidly transported, this is supported by the localisation of peripherin to large-calibre axons of the dorsal root (Molliver & Snider, 1994).

4.3.3 Co-expression

In the adult, peripherin does co-exist with the NFL subunit but only in 6-8% of cells whereas it is predominantly found with neuropeptides. 40% of peripherin positive cells co-localise with SP and 100% co-localise with CGRP in the adult, although it is only substantial in 60%. At P2, the SP co-localisation has reached the mature pattern whereas CGRP is barely detectable in the peripherin positive population, whilst the 20% found in peripherin negative neurons is comparable to the adult (Goldstein, et al, 1991; 1996). SP and CGRP themselves co-exist in a sub-population of capsaicin sensitive neurons,

neurons that are also largely peripherin positive (Ferri et al, 1990). In the chick DRG, 50% of cells express peripherin and are completely co-localised with ovalbumin (Williams et al, 1993). The function of this protein is unknown, but its restriction to the small-medium sized neurons, and co-localisation with peripherin suggests it may have a similar function to peripherin.

4.3.4 Plasticity

Neonatal capsaicin-treated rats examined in adulthood showed a 50% decrease in the number of neurons selectively immunostained for peripherin, as expected for a marker of small diameter neurons exposed to capsaicin. However, there was an increase in the number of cells co-expressing both peripherin and NF, more pronounced than the compensatory total increase in NF-protein expressing neurons (Ferri et al, 1990). The size of neurons were also affected with a mean increase in the diameter of the peripherin and NF co-expressing population, suggesting that a number of normally NF-only neurons, now also express peripherin. Peripherin mRNA also appears in large cells after axotomy (Oblinger et al, 1989; Wong & Oblinger, 1990),

Levels of peripherin mRNA in motoneurons double just four days after sciatic nerve crush. Between 4-7 days after crush, peripherin-IR also increases significantly and these increases are sustained for 6 weeks post-injury. The increase in peripherin expression parallels increases in the DRG of actin and β-tubulin after axotomy (Hoffman et al, 1987; Tetzlaff et al, 1988), moreover no changes in NFM were observed. By 8 weeks post-axotomy the mRNA and protein levels return to control levels (Troy et al, 1990).

4.3.5 Function

Thompson & Ziff, 1989 proposed that peripherin may interact with the plasma membrane since its amino and carboxy terminal ends have properties of charge and hydrophobicity in addition to regions of homology in common with the other IFs, vimentin and desmin. These have already been shown to interact with the nuclear envelope protein lamin B (Georgatos & Bloebel, 1987; Georgatos et al, 1987),

suggesting they form a cytoplasmic scaffolding connecting the plasma membrane with the nuclear membrane (Steinart & Roop, 1988). *In vitro*, peripherin can directly interact with the type V lamin B, indirect evidence also suggests this is possible *in vivo* though the function of this is unclear if lamins are on the inside of the nuclear envelope while peripherin is on the outside (Djabali et al, 1991). The common feature of peripherin expression is its location in the periphery, so the concept of a role in recognition of axonal pathways though the intermediary of membrane proteins is not inconceivable (Escurat et al, 1990).

Peripherin mRNA has been found in both the peripheral and central nervous system neurons that specifically possess long axons, this feature led Leonard et al (1988) to postulate that peripherin may stabilise long axons, in association with microtubules and neurofilaments. Proof of an association between peripherin and NFs came from double-label immunofluoresence studies and immunoelectron microscopy of nerve filaments. These studies showed that peripherin and NF subunit proteins were found co-polymerised in the same filament, although there are also peripherin unique and NF unique filaments (Parysek et al, 1991).

Peripherin synthesis appears to be necessary for regeneration in the adult (Portier et al, 1993). Its synthesis increases in the DRG (Oblinger et al, 1990), and motoneurons (Troy et al, 1990b) after axotomy and during the elongation phase, but decreases when radial growth starts. Because large neurons do not constituitively express peripherin yet show increased mRNA after injury (Oblinger et al, 1989), either constitutive or inducible peripherin is necessary for axon elongation in DRG neurons (Chadan et al, 1994).

The effect of injury on adult neurons often reveals much about their role, as can be deduced from the plasticity experiments outlined above. The possible function of peripherin was determined by observing the different reactions of NFs and peripherin to injury and therefore the different roles they probably play. It was suggested that peripherin provides the stability for axonal outgrowth while NFs restore the axonal calibre and form (Ferri et al, 1990; Troy et al, 1990). The fact that peripherin, unlike NFs,

increase after axotomy in a response that appears to recapitulate development, suggests a facilitatory role in axonal growth both after injury and during development.

Peripherin mRNA levels are greater in late embryonic and early postnatal brain than in the adult (Oblinger et al, 1988c). Small cells do not upregulate peripherin after axotomy (Oblinger et al, 1988b), yet they regenerate. Evidence of small fibre regeneration is twofold. Firstly, during peripheral regenerative growth, only unmyelinated axons stain for GAP 43 (Hall et al, 1992), implying that only small neurons regenerate. Secondly, there is a significant increase in the number of unmyelinated dorsal root axons after spinal hemisection or rhizotomy (Hulsebosch & Coggeshall, 1981; 1983a; 1983b). Therefore the level of peripherin expression in these small cells is sufficient to facilitate regeneration, whereas in larger axons, levels are initially sub-optimal for growth (Wong & Oblinger, 1990).

The elevation of peripherin levels after injury is a direct result of activation of injury-responsive elements contained within the peripherin transgene. This element (9.8 KB genomic segment) has been identified and is a requirement for basal expression in cells that show an injury response. Comparison of this element to other sequences activated in neural stress and injury, revealed a correspondence to the heat-shock proteins. It is yet to be determined whether the peripherin injury response could be abolished by removal of the heat-shock proteins (Belecky-Adams et al, 1993).

In vitro DRG cultures also help elucidate the rolė of peripherin. In culture 100% of P2 neurons express peripherin with only 5% expressing NFL in contrast to the *in vivo* state of 46%, see above (Goldstein et al, 1991). These authors believe that this phenotype is the result of population selection. This could be true since the culture media contained NGF, known to selectively maintain small diameter neurons (Goedart et al, 1984), which at this age *in vivo* already predominantly express peripherin. When cultures in the same media are conducted at E15, very different results emerge. Peripherin and NFL show 100% co-localisation and fail to differentiate into two separate phenotypes, therefore an additional signal to NGF is required. In the same series of experiments, heart and muscle extract were added to the media, these increased the proportion of NFL, but like NGF,

were not sufficient to distinguish between the populations. Considering its possible role in axon outgrowth and the sequence of expression of several IFs (see 4.6.6), it is more likely that the high expression is a preliminary to axon outgrowth.

4.3.6 Regulation

Genomic information about peripherin has led to identification of regulatory sequences that define its specificity and its regulation by neurotrophic factors. *In vitro* and *in vivo* transgenic animal experiments during mouse embryogenesis have revealed that full peripherin regulation is the result of co-operation between intragenic and 5` upstream sequences. These are thought to control the complex and dynamic expression pattern. The temporal and nervous system specific expression is controlled by 5' sequences linked to a reporter gene but the complete cell-type specific expression is only achieved by incorporating intragenic sequences (Belecky-Adams et al, 1993; Duprey & Paulin, 1995).

In 1989, on cloning the rat peripherin gene Thompson & Ziff demonstrated the complete amino-acid sequence including an extended N-terminus region, previously not identified by the Portier group. This region confers unique properties to each IF and indicated the potential for phosphorylation. Aletta et al (1989) then showed that peripherin could be phosphorylated and that phosphorylation could be enhanced in PC12 cells by treatment with NGF, kinase A and C activators and by depolarisation. From the earliest work on peripherin, investigators knew that the protein was inducible by NGF treatment (Portier et al, 1984a; Parysek & Goldman, 1987), since the rat sequence revealed that the peripherin promoter contains sequences homologous to regions of other NGF-regulated promoters. These could be the sequences which function in the transcriptional induction of peripherin by NGF. Those findings raised the possibility that its functional properties could be regulated by environmental signals (Greene, 1989) but the mechanism by which the NGF signal activates the gene is still unknown.

4.4 TrkA

4.4.1 Identification and structure

The Trk family of tyrosine kinases are functional receptors for specific neurotrophins (see sections 4.19; 4.23v). TrkA is the high affinity NGF receptor and was the first of the tyrosine kinase family to be identified (Chao, 1992; Lindsay et al, 1994). It spans the cell membrane and possesses an extracellular and intracellular domain. The extracellular domain has an NGF binding site while the intracellular domain shows tyrosine kinase activity.

The cells expressing trkA have been characterised, indicating that most have small cell bodies and many have cutaneous afferents (Verge et al, 1992; Carroll et al, 1992; Mu et al, 1993; McMahon et al, 1994; Wright & Snider, 1995).

4.4.2 Expression

TrkA protein and message is present in 40-50% of mainly small to medium sized adult DRG cells, ranging from 200-1800μm^2 - with the majority under 800 μm^2 (Verge et al, 1992; Mu et al, 1993; McMahon et al, 1994; Wright & Snider, 1995; Molliver et al, 1995; Averill et al, 1995; Bennett et al, 1996b). These cells project to lamina I and IIo of the dorsal horn (Averill et al, 1995; Molliver et al, 1995). TrkA is heterogeneously expressed in afferents innervating different peripheral targets. Both mRNA and peptide show higher levels in visceral than skin afferents (McMahon et al, 1994; Bennett et al, 1996a).

In the embryo, 70-90% of cells are found to be NGF dependent (Johnson et al, 1980; Goedert et al, 1984; Ruit et al, 1992; Crowley et al, 1994; Smeyne et al, 1994), and in addition trkA protein is found in 71% of DRG cells at P0 (Bennett et al, 1996b). Levels of trkA are downregulated postnatally to reach adult levels at P14.

4.4.3 Co-expression

Most trkA positive cells are labelled by BSI. TrkA is also co-localised with CGRP (92%) (Verge et al, 1989; Crowley et al, 1994; Averill et al, 1995; Silos-Santiago et al,

1995) and peripherin (Molliver et al, 1995). 18% of trkA cells also express the large cells marker RT97 (Averill et al, 1995). TrkA expressing neurons however, are not extensively co-expressed the PKCδ isoform, BSI-B4, LA4 (6%) or α-Internexin (3%), suggesting that trkA positive and negative neurons express different complements of cell surface glyco-conjugates (Averill et al, 1995; Molliver et al, 1995).

4.5 I-B4

4.5.1 Identification and structure

Isolectin B4 (I-B4) is the B-subunit of the plant lectin *Griffonia simplicifolia* agglutinin I, also called *Bandeiraea simplicifolia* (GSA/BSI-1). It is thought to recognise the terminal α-D-galactose epitope of a membrane associated glyco-conjugate, and binds to the soma and central terminals of a sub-population of unmyelinated primary sensory neurons (Plenderleith et al, 1992). The α-D-galactose residue is a lactoseries carbohydrate (Dodd & Jessel, 1985) and along with the other membrane associated carbohydrate - the globoseries carbohydrates (Dodd et al, 1984) encompass the two classes of surface antigens that have been identified in separate populations of DRG neurons.

IB4 is a tetrameric plant lectin with a molecular weight of 155 kD and is composed of two subunits, A and B. Lectins are isolated from a wide variety of natural sources and are highly specific carbohydrates, binding glycoproteins of non-immune origin. The carbohydrates which serve as receptors or binding sites for the lectin are virtually ubiquitous in all biological, including neuronal, membranes. The specificity of lectins means that glyco-conjugates can be distinguished by botanical lectins on the basis of their different carbohydrate moieties (Streit et al, 1985; 1986), even with identical sugar compositions but different residues or anomeric structures (α and β), (Liener et al, 1986).

The globoseries carbohydrates are found in laminae I, III and IV of the spinal cord where low-threshold myelinated afferents terminate and hence form a distinct group from the lactoseries antigens described below (Jessel et al, 1990).

4.5.2 Expression

IB4 lectin binding is first observed in the central processes of small diameter primary sensory neurons as they enter the dorsal horn of the rat spinal cord at E18/E19 (Plenderleith et al, 1992). In the DRG, IB4 expression increases from 9% at P0 to 40% at P14 (Bennett et al, 1996b). However, IB4 has not been reported in the periphery during development. There is also no data available on the degree of co-expression with other DRG markers except for the transient postnatal co-expression with trkA at P3 and P7 (Bennett et al, 1996b).

In the adult, GSA-IB4 labels terminals in the outer SG of the spinal cord with some labelling in the marginal zone. It also differentially stains a large number of thin axons in testicular and corneal whole-mounts (Silverman & Kruger, 1988b). Further staining is located in the small-calibre smooth contour axons of the mystacial pad, in addition to non-neuronal labelling of the vascular lining, surface of follicular cells, sweat glands and some cells of the sebaceous gland and duct (Rice, 1993).

In the adult DRG there are conflicting reports of the degree of expression. Some of this may be due to the type of antibody used and the criteria for deciding positivity. IB4 is only one subunit of the lectin but many studies use GSA-BSI which is a mixture of five isolectins. In one study, 75% of small neurons in the DRG were labelled. The lectin was mostly co-localised with FRAP (90%) with some CGRP co-localisation (10%). This result is not entirely consistent with the innervation pattern in the SG, as FRAP is usually found in the inner SG while CGRP is located in outer SG (Silverman & Kruger, 1988b).

Confirmation of the small degree of CGRP and I-B4 co-localisation was found in peripheral tissues where these markers labelled virtually separate sets of afferents (Ambalavanar & Morris, 1992). The differential labelling pattern in the spinal cord between IB4 and peptidergic CGRP, indicates that the lectin labels a different population. This assumption is reinforced by findings that although the lectin binds to a sub-population of unmyelinated axons in the rat and cat, these are almost exclusively neurons that innervate the skin (Plenderleith et al, 1992; Plenderleith & Snow, 1993). However, labelling is also produced after injection of tracer into the sciatic and saphenous

nerves. This allows visualisation of synaptic terminals in LII of the dorsal horn, derived from cutaneous C-fibres (Kitchener et al, 1993). This study is also significant because no retrograde labelling of motoneurons occurs establishing I-B4 as a unique marker for sensory neurons. Only one report indicates that I-B4 is also located in lamina I, although the most dense labelling was found in inner lamina II (Wang et al, 1994).

In another study using I-B4 conjugated to HRP, a full analysis of co-localisation and size-distribution within the DRG was undertaken (Wang et al, 1994). 51% of the DRG neurons bound and transported I-B4, but strong labelling was only found in 32% of cells. 35% expression has also been reported in the adult DRG (Bennett et al, 1996). Those strongly labelled cells had areas ranging 150-950μm^2, compared to more weakly stained cells that were found in cells as large as 1450μm^2. 85% of those IB4+ve cells were FRAP+ve, in agreement with Silverman & Kruger (1988b). 17% of cells co-localised with SP, 9% with SOM and only 3% with RT97. In addition, they determined that approximately 100% of the SOM and FRAP populations were within the I-B4 population. However, there was a discrepancy in the extent of CGRP co-localisation between the Silverman and Kruger (1988a) and Wang (1994) studies. Wang (1994) found 59% of I-B4 neurons were also CGRP+ve in contrast to the former study which reported 10%. The larger overlap is a more predictable representation considering the overlap in lamina II outer of the SG. However, in the adult very few cells express both trkA and IB4 (Bennett et al, 1996a), yet trkA and CGRP show almost parallel expression patterns (Bennett et al, 1996b). This implies that there should be little overlap between IB4 and CGRP.

4.5.3 Plasticity

Capsaicin treatment or a dorsal rhizotomy results in downregulation of binding in the spinal cord which is consistent with synaptic staining of a primary afferent origin (Ambalavanar et al, 1993). Injection of IB4 into the sciatic nerve after axotomy, reveals transport as far as neuronal cell bodies in the DRG, however, it appears that C-fibres are unable to maintain transganglionic transport after injury therefore abolishing transport to

their central terminals in LII (Kitchener et al, 1994). In animals where the trkA gene has been disrupted the population of IB4 neurons are lost (Silos-Santiago et al, 1995).

4.5.4 Function

The physiological and functional significance of GSA binding sites are unknown. Involvement with nociception is mainly deduced from its localisation, principally at regions where unmyelinated afferents terminate; and its co-localisation with substances which have already been functionally associated with nociception. Nonetheless, the stratified distribution of FRAP and I-B4 to LII inner and II outer respectively led Silverman and Kruger (1990), to hypothesise the existence of two functionally independent C-fibre nociceptor systems.

Cell surface determinants such as this lectin have also been implicated in interactions with second order neurons of the superficial dorsal horn and with target finding in development (Plenderleith et al, 1992). It has been proposed that the glyco-conjugates expressed on subsets of DRG neurons may provide a basis for specific guidance of developing neurites by virtue of glyco-conjugate-mediated adhesive interactions (Dodd & Jessel, 1985; 1986).

4.6 Intermediate Filaments (IF)

Intermediate Filament (IF) proteins are major components in the cytoplasm of most eukaryotic cells and have roles in cell architecture, stability and differentiation. They have a characteristic diameter of 8-10nm which is intermediate between the other major structural components in large diameter myelinated axons, actin filaments (6nm) and microtubules (24nm).

4.6.1 Classification

The IF family is sub-divided into 5 types on the basis of their amino acid sequence, gene structure and cell expression.

Type	Mammalian Protein	Invertebrate Homologue	Tissue Specificity
I	Keratins: Acidic *CP49; Filensin*		Cytoplasmic Proteins
II	Keratins: Basic *CP49; Filensin*		
III	Vimentin Desmin GFAP Peripherin	XIF3	
IV	Neurofilaments: *NF-L; NF-M; NF-H* Nestin α-Internexin	XNIF; Gefeltin; Xefeltin	Nuclear Proteins
V	Lamins		

4.6.2 Structure & Identification

Only the type III and type IV IFs are found in mammalian neuronal cells. Complete sequence information is available for 6 members of the neuronal IF (nIF) family. These are the 3 neurofilament sub-units (NFL, NFM, NFH), α-internexin, peripherin and nestin. They all share a characteristic ~310 amino acid α-helical rod domain, containing a hydrophobic heptad repeat essential for assembly. Flanking this central conserved rod are the globular head and tail segments (Lee, 1996).

4.6.3 Importance of specific IFs to neuronal development

The following sections will concentrate on neurofilaments because of their abundance and expression patterns in developing and mature neurons. The other major IF of interest is the type III IF, peripherin, which along with the phosphorylated form of the NFH subunit have already been described in sections 3.2 and 4.3. This account will

describe in detail the function and properties of NFs as an example of a typical nIF and will briefly describe the remaining IFs.

i) α-Internexin

This was first purified from rat optic nerve and spinal cord (Pachter & Liem, 1985). Initially it was considered to be a NF-associated, IF-like protein, but on sequencing was revealed to be a type IV IF (Fliegner et al, 1990; Chien & Liem, 1994). It has special self-assembly properties *in vitro* (Kaplan et al, 1990) which is a feature of its structure, a hybrid of NFL and NFM.

During development, α-internexin is expressed by all DRG neurons and their processes during embryonic development (Troy et al, 1990; Kaplan et al, 1990). In the mature CNS, α-internexin distribution is similar to that of NFL and peripherin, found in laminae I and III-IV (Molliver et al, 1995). It is abundantly expressed in smaller axons, whereas larger neurons primarily express NF subunits (Kaplan et al, 1990; Fliegner et al, 1994) and is expressed in 34% of thoracic DRG, co-localising mostly with peripherin (Molliver et al, 1995). α-internexin is also unique in being the only marker protein in the DRG that co-localises with the protein kinase C (PKC)δ isoform (Molliver et al, 1995), which has been visualised in afferents in the superficial dorsal horn (Garcia et al, 1993). These findings highlight the discrepancy between the expression in the DRG and spinal cord, where staining of axons with this and other IF proteins appears to be inversely correlated with cell body staining.

ii) Nestin

This is only expressed (transiently in neurons) in multipotent neuroectodermal cells prior to terminal differentiation (Lendahl et al, 1990; Zimmerman et al, 1994). This makes it an excellent marker in early development.

iii) Invertebrate Homologues

Homologues to the mammalian IFs NFM, peripherin and α-internexin have been found in *X.laevis* (Sharpe, 1988; Sharpe et al, 1989; Charnas et al, 1992; Zhao & Szaro, 1997). There are also novel IFs that do not have mammalian homologues. The type III IF

protein, Plastin, is found in the goldfish during optic nerve regeneration (Glasgow et al, 1990) and Tannabin, a 1744-amino acid nIF-like protein is localised in a subset of axons and growth cones of *X.laevis* (Hemmati-Brivanlou et al, 1992). These invertebrate IFs are mainly low molecular weight and their mammalian equivalents are only expressed transiently during development.

4.6.4 Neurofilaments (NF)

NFs were the first type of neuronal IF to be identified due to their abundance in fully differentiated mammalian neurons (Hoffman & Lasek, 1975), where they outnumber microtubules 5-10 fold. They are unique among IFs in possessing side arms (Hirokara et al, 1984) that extend from the filament backbone and their most distinctive feature is the carboxy-terminal tail domains.

Neurofilaments have three subunits: NFL, NFM, and NFH. These are named according to their molecular weight 68, 155 and 200kDa. They are all stable at a neutral pH and physiological ionic strength and hence were easily purified to determine their relative molar amounts: 5:2:1 (Schlaepfer & Freeman, 1978; Liem et al, 1978; 1979).

4.6.5 Function

NFs had previously been confined to a structural role, however, information about the involvement of NFs in the different stages of axon growth together with genetic approaches have shown that NFs have additional roles. They are an essential determinant of radial growth and accordingly, conduction velocity within axons, and may also be involved in regeneration.

The first phase of axon growth is neurite elongation which has limited NF involvement. However, after synaptogenesis, NF expression elevates and myelination begins in parallel with the second growth phase. The second phase consists of fully elongated axons increasing in diameter ten-fold, and is referred to as radial growth. Early evidence showed a linear relationship between NF number and cross-sectional area during normal radial growth, suggesting that NFs are intrinsic determinants of radial growth and

that a mechanism of axon expansion or contraction exists to maintain a constant density of NFs (Friede & Samorajski, 1970; Hoffman et al, 1985; 1987).

The advent of transgenic models has confirmed the importance of the NF-radial growth relationship, but has refuted the proposed constant density mechanism. A recessive mutation in the NFL gene of a quail resulted in loss of NFs. This led to inhibition of normal radial growth and a consequent decrease in axonal conduction velocity. The prevention of radial growth reduces the normal axon calibre, which is the primary determinant of the velocity of nerve impulse propagation along axons. If NFs are overexpressed, the number and density increase, but radial growth in the sciatic nerve is still prevented (Monteiro et al, 1990).

Radial growth can be also be affected by altering the expression of one NF component while overall retaining the same filament number. This means that a constant number or density of NFs are not essential requirements for control of radial growth, but the relationship between sub-units. The use of transgenic mice to alter the subunit composition has revealed that increasing individual subunits inhibits radial growth. Increasing the NFM or NFH subunits reduces growth even more severely (Xu et al, 1996). The reason for the powerful influence of one subunit compared to another is because of their stochiometry. When NFM is increased, reduced NFH is the predictable outcome of competition for co-assembly with limited NFL, however, filament spacing is unaffected (Wong et al, 1995). In another experimental paradigm, NFM overexpression leads to 50% decreases in phosphorylated NFH with increased filament packing, supporting a role for phosphorylated NFH mediating filament spacing.

These studies are conflicting, but the role of phosphorylated NFH is consistent with observations in myelin-deficient trembler mice showing NFs in a less phosphorylated state and more closely packed (de Waugh et al, 1992). The complete absence of NFs ensures there is no framework for axon expansion, the overexpression of one sub-unit alone disturbs the balance required for assembly. The loss of phosphorylated NFH (NFH-P) specifically allows filaments to pack more tightly, decreasing axon calibre, hence it is NFH-P which is essential for mediating radial growth.

Phosphorylation induces extension of NFH and NFM carboxy-terminal domains away from the NF backbone, this could increase the distance between NFs, therefore making them more effective as space-occupying structural supports. (Nixon & Sihag, 1991). Recent *in vitro* experiments determined that NFs maintain the characteristic shape of the axon against the structural demands of the elongation process (Lin & Szaro, 1995). The trembler mutant suggests the presence of myelin encourages phosphorylation, which is required by NFH for radial growth, this may explain why immediately after the initiation of myelination, the second growth phase occurs.

The greater capacity for growth and regeneration in invertebrates and goldfish after injury is correlated with nIF composition (Quitschke & Schechter, 1984; 1986a). In the mammal, several changes take place after injury in the IF composition of the axonal cytoskeleton. Immediately after axotomy, levels of NFL mRNA (Hoffman et al, 1987; 1988; Wong & Oblinger, 1987; Goldstein et al, 1988; Oblinger et al, 1989a), NFL and NFM protein decrease in the DRG, alongside a decrease in axonal calibre (Oblinger & Lasek, 1988; (Greenburg & Lasek, 1988). NFH is downregulated more slowly than the other NFs (Wong & Oblinger, 1990). Peripherin synthesis begins in the DRG neurons, and is found in axons 14 days post axotomy (Oblinger et al, 1989b). Six to eight weeks afterwards, when neurite outgrowth is complete, tubulin mRNA decreases while NFs increase, concomitant with restoration of axonal calibre (Hoffman et al, 1984; Muma et al, 1990).

The initial decrease in neurofilament expression during axonal regeneration recapitulates one aspect of development, with the axon initially displaying a NF-poor cytoskeleton (Wong & Oblinger, 1990). Nevertheless, if the sequence of regeneration reverts exactly to that of development, it would be expected that NFH decreases more than NFL, NFM. Therefore, adult neurons do not completely repeat the ontogenetic pattern of NF expression.

4.6.6 Spatio-Temporal Neuronal Expression

The restricted expression pattern of NFs observed in the adult is achieved following a precise temporal sequence during development. Although this pattern may be

slightly different in different species, even invertebrates show progressive maturation of neurons with successive changes in IF subunit composition (Zhao & Szaro, 1997). Mechanisms described below co-ordinate the gradual replacement of one type of IF system with another during neuronal development.

The earliest IFs associated with mammalian neuronal development, are nestin and vimentin, these are highly expressed in neuroectoderm cells which have the potential to develop into both neurons and glia. Nestin is downregulated during the cell migration from the ventricular to marginal zone then vimentin expression is initiated; the switch from vimentin after postmitotic differentiation is followed by the induction of other nIFs (Lendahl et al, 1990; Tapscott et al, 1981; Cochard & Paulin, 1984; Yachnis et al, 1993).

NFL and NFM appear soon after the terminal mitotic division of neuroblasts in spinal motoneurons but in most other neurons these proteins follow the appearance of α-internexin (Kaplan et al, 1990; Fliegner et al, 1994). The onset of NF expression after α-internexin, is detectable in large motor and sensory neurons during neurite elongation, although expression of the NFH subunit is generally undetectable while neurons are still migrating and extending neurites. Both NFH mRNA (Julien et al, 1988; Oblinger et al, 1989c) and protein (Shaw & Weber, 1982; Willard & Simon, 1983; Pachter & Liem, 1984) accumulate later than NFL and NFH. All NFs increase rapidly during synapse formation and initiation of myelination during the postnatal period (Carden et al, 1987; Schlaepfer & Bruce, 1990).

Peripherin appears later than NFL (Escurat et al, 1990; Gorham et al, 1990) and is transiently expressed in all DRG neurons during embryonic stages. It disappears except for expression in small DRG neurons (Troy et al, 1990), as NF accumulation in the larger neurons is accompanied by marked decreases in both α-internexin and peripherin (Escurat et al, 1990; Gorham et al, 1990; Fliegner et al, 1994).

4.6.7 Overlapping Expression

The expression of different types of nIFs is neither mutually exclusive nor completely overlapping. NF sub-units co-exist with α-internexin in the CNS (Fliegner et al, 1994) and with peripherin in the PNS (Goldstein et al, 1991). Distinct groups are also

demonstrable, with the largest neurons in the sensory and autonomic ganglia expressing NFs and the smallest neurons expressing peripherin, medium-sized neurons express both (Goldstein et al, 1991). This pattern has also been reported for NFs and α-internexin in the same neurons (Vickers et al, 1992).

4.6.8 Non-neuronal expression

NFM and NFL are also expressed in immature Schwann cells (Kelly et al, 1992; Robertson et al, 1992). NFH in T lymphocytes (Murphy et al, 1993) and embryonic heart muscles, which also expresses peripherin (Belecky-Adams et al, 1993).

4.6.9 Assembly

NFL can form an individual short smooth-walled filament, *in vitro* (Glicksman & Willard, 1985) but NFM, NFH or combinations of these two cannot form filaments (Geisler & Weber, 1981; Liem & Hutchinson, 1982; Gardner et al, 1984; Hisanaga & Hirokawa, 1988; 1990; Hisanga et al, 1990, Heins et al, 1993).

Immuno-electronmicroscopy has suggested that all three NF subunits are integral components of filaments (Balin & Lee, 1991; Balin et al, 1991) however, NFs lacking NFH have been reported (Shaw et al, 1981; Debus et al, 1982). *In vitro* and transgenic models revealed that assembly requires NFL associated with stochiometric amounts of NFM or NFH (Lee at al, 1993; Cohlberg et al, 1995). This establishes that NFM and NFH directly participate in the assembly and organisation of NFs, and that *in vivo,* NFs are obligate heteropolymers. Developing axons contain only NFL and NFM, but in mature axons NFs possess all three subunits. The appearance of NFH subunits are delayed, but they may incorporate into pre-existing immature filaments as the axon matures, since NFH in mature axons undergo dynamic exchange with unassembled pools of NFH in neuronal compartments. (Nixon & Sihag, 1991).

The spatial relationship of the three NFs was determined in the DRG. NF68 forms the backbone of the filament with NF155 present alongside contiguously, whereas the NF200 subunit was more peripheral, repeating sequentially along the filament at 100nm intervals (Sharp et al, 1982).

4.6.10 Control of expression

The level of NF expression can be stabilised by post-translational modifications. It has been shown that NGF can induce NF expression in PC12 cells (Lindenbaum et al, 1988; Ikenaka et al, 1990), however, this effect is restricted to subunits NFL and NFM. The resultant increase in expression is maintained due to an NGF-dependent increase in the half-life of the mRNA. This stabilisation is also observed in postnatal cultured DRG neurons (Schwartz et al, 1994). Increasing the NFL mRNA level by overexpressing the transgenes 3-5 fold, produces less than a 50% increase in the protein in the CNS (Beaudet et al, 1993), therefore mRNA production without stabilisation is not sufficient to maintain increases in the protein levels.

The developmental appearance of subunits, the effect of NGF and the response to injury all indicate that NFH expression may be differentially regulated from the other two NF subunits.

4.6.11 Post-translational Modifications

NF proteins contain large numbers of phosphate groups on their carboxy-terminal tail region and these have been considered as the mechanism by which they cross-link and stabilise the axonal cytoskeleton (Julien & Mushynski, 1983; Carden et al, 1985). Recently, attention has been drawn to the amino-terminal head domain after it was recognised that NFs can be phosphorylated at this end.

Lee et al, 1993 have shown that the head and rod regions but not the tail of NFs, are essential for assembly. The head domains of other IFs like vimentin and lamins when phosphorylated, cause disassembly of filaments or assembly inhibition. The phosphorylation sites in the amino-terminal head domain of NF have been identified (Sihag & Nixon, 1990; 1991) and these, by analogy to the other IFs may be responsible for filament assembly.

The link between phosphorylation and polymerisation of filaments implies that polymerisation may be reversible depending on the phosphorylation state. The relevance of this for post-mitotic neurons may rest with control of assembly during development. The amino-terminal sites in NFL are active immediately following synthesis in neurons,

but some activity is removed within 12hrs, possibly indicating that phosphorylation may block premature assembly prior to transport into neurites. This would permit time for integration of other subunits until the stochiometry of the triplet proteins is achieved (Nixon & Sihag, 1991). It is known that each NF can exist in more than one state of phosphorylation (Thorey & Seifert, 1989), and that different phosphorylated isoforms exist in different types of neurons. The significance of these phosphorylation types is that some neuron sites can dephosphorylate rapidly and rephosphorylate extensively, hence exert fine control of assembly and disassembly.

NFL and NFM isolated from rat spinal cord are also post-translationally glycosylated in the domain essential for *in vivo* NF assembly (Dong et al, 1993), further supporting the role of post-translational modifications in NF assembly.

4.6.12 Axonal Transport

Traditional measurements of nIFs movement through axons provided evidence for slow axonal transport at a rate varying between 0.25-3 mm/day. The velocity is dependent on the group of neurons, age of animal and location along the nerve. Motoneuron transport is faster than retinal ganglion cell transport (Lasek et al, 1993), whereas within the same group NFs move more rapidly in immature axons (Hoffman & Lasek, 1980; Hoffman et al, 1983; Willard & Simon, 1983; McQuarrie et al, 1989) and at the proximal end versus distal end of axons (Watson et al, 1989).

Recent analysis of transport mechanisms has revealed there are two pools of NFs in axons, one moving at the slow rate and the other virtually stationary (Nixon & Logvinenko, 1986; Lasek et al, 1992). This changes the view of NFs as static elements and suggests that NFs are highly dynamic with transported units constantly exchanging with the existing stationary network. The overall transport rate therefore, may not reflect the speed of individual transported components as Lasek and colleagues observed some subunits travelling at 72-144mm/day over a short distance. They suggested that NFs could be transported in discrete steps alternating between short fast moving strides and relatively long pauses (Lasek et al, 1993). However, these studies have not elucidated the form in which the NFs are transported. The Lasek model proposed that NF subunits were

transported as filaments (Lasek, 1986; Lasek et al, 1992). Examination of fluorescently tagged NFL in cultured DRG neurons recovered after zonal photobleaching, suggests that oligomers are the transported form (Okabe et al, 1993), possibly the homo/heterotetramers are assembly intermediates (Cohlberg et al, 1995).

The reason why axonal transport slows as the animal matures, may be correlated with the increase in expression of NFs, particularly NFH (Willard & Simon, 1983). Transgenic mice overexpressing human NFH display cell body accumulations mediated by slower NF transport into axons (Collard et al, 1995). The phosphorylation of NFH follows entry of NFs into the axon and continues to increase during transport (Glicksman et al, 1987; Nixon et al, 1987; Oblinger, 1987), this is thought to favour dissociation from the axonal transport machinery. This is desirable as maintaining the NF network, which represents 10% of the axonal proteins, would be a huge burden for the synthetic capacity of the neuron and therefore by slowing transport via formation of a relatively stationary population of slowly turned-over NFs, the neuron can maintain the network with a much smaller supply of newly synthesised NF (Nixon & Logvinenko, 1986).

RESULTS

4.7 Aim

The starting point for my investigation into the developmental timecourse of the innervation of the rat hindlimb begins at E13 when it has been reported that a plexus of nerves is found at the base of the limbud (Mirnics & Koerber, 1995a; Reynolds et al 1991). The investigation stopped at E21, just before birth because by that time the innervation has reached the most distal part of the limb. At each stage peripheral innervation was compared to events in the spinal cord and DRG. The innervation of the hindlimb and spinal cord was investigated using a number of selective immunohistochemical markers of DRG neurons. Examination of an embryo using one marker to chart development reveals much about the developmental path of neurons of that particular phenotype, however, their selectivity means an individual marker will not always capture the full extent of innervation. It is for this reason that I describe a timecourse of innervation using some general markers and a series of selective ones.

4.8 Information about selected markers

Innervation has been investigated here using GAP 43, PGP 9.5, peripherin, RT97, SP, CGRP, IB4 and trkA immunostaining (see Chapter 3, 4.1-4.6 and Chapter 6 for more information).

Growth associated protein 43 (GAP 43) is important as it shows us the location of newly forming axons. Looking at one developmental stage does not however reveal the full extent of innervation that is already present, since it is downregulated after terminal formation. It is more informative when used in conjunction with the general neuronal marker Protein gene product 9.5 (PGP 9.5), to distinguish where new growth is appearing in relation to existing innervation.

The presence of labelling within certain regions of the spinal cord gives us some indication whether its origin is sensory or motor, but to determine which sub-populations contribute to a particular region in the periphery requires more specific and characterised

markers. Peripherin is an intermediate filament found only in small diameter neurons of the adult. During development its labelling is more extensive (Troy et al, 1990) as can be seen from examination of the spinal cord regions. RT97 is a neurofilament and sub-group of the IF family. In the introduction I described how this family has a spatio-temporal expression, resulting in switching from one expression pattern to another with inherent transience. This marker is one of the last of the family to be expressed and is maintained into adulthood where it is found in larger diameter neurons. It was chosen to determine whether larger diameter axons are among the first to innervate targets. The markers of small diameter axons however, display a more restricted pattern at these ages. Characteristic markers of small diameter neurons are substance P (SP), calcitonin gene related peptide (CGRP), IB4 and trkA.

4.9 Information about experimental protocol

The complex morphology of nerve endings, variability of immunohistochemical characterisation and peripheral axon terminals in any given tissue section, means that descriptions and interpretations are based on results that were qualitatively obvious as assessed across several sections from similar locations in several specimens at each age.

For antibody labelling described at each age and region, alternate sections from each tissue block/embryo were stained from n=3+ embryos on at least two separate occasions. In addition embryos were also harvested from two different litters.

Presentation of results

The results of this study are presented in three parts. The first part describes the development of subpopulations within the DRG. The second part describes the innervation of the peripheral target - the hindlimb, and concentrates on the cutaneous innervation in the late foetal stages E17-E20. The final part examines the development of innervation to the central target - the spinal cord.

In each section, the results from different neuronal markers are described together, to give an account of innervation inclusive of all subpopulations at each age. The figures however, are grouped according to the neuronal marker. Hence, from the text,

innervation is viewed from the perspective of a developemntal timecourse while in the figures, the development of specific labelling is emphasised. It is for this reason that specific figures are not referred to in the text. At the end of each section a summary table provides a comparitive overview of the developing innervation with each of the neuronal markers.

4.10 DRG : Description of Innervation

E13 & E14

At E13, there is no GAP 43 staining observed in the lumbar DRG itself until expression begins in a small number of cells at E14. The immunoreactivity is weak in intensity and is diffuse compared to the dorsal root. PGP 9.5 concurs well with the picture provided with GAP 43 as it is only expressed by a few cells at E13. Labelled neuronal cell bodies when present, are clearly visible and widely distributed within the DRG. Dorsal and ventral roots are also detectable. By E14 more cells are labelled and with increased intensity.

Faint diffuse peripherin immunostaining is detectable at E13 with a few strongly labelled punctate cells scattered throughout the DRG. At E14, the DRG and dorsal roots are both staining very intensely. RT97 at E14, has both intensely stained cells and fibres, but is not expressed at E13. Neither the peptides, SP and CGRP, nor the lectin IB4 were immunoreactive at this stage. The remaining small diameter cell marker, trkA, displays a few faintly immunopositive cells at E13 with staining mostly composed of fibres. By E14 cellular staining increases within the DRG.

E15 & E16

Some GAP 43 fibres are visible in the DRG, these are more heavily stained near the dorsal root which is now tightly fasiculated. However there are few cells evident at these ages. PGP 9.5 labels all cells but there is a sub-population of very intensely stained cells. Darkly labelled cells are numerous with peripherin at E15 and E16. Meanwhile the RT97 labelling changes so that, whilst there are still many immunopositive fibres, individual faintly labelled cells are now discernible. Small cell markers are still not

detectable except for trkA, whose immunoreactive cells are weakly labelled at E15 and more strongly labelled, but of a similar proportion of cells, at E16.

E17 & E18

At E17 the DRG is only faintly and diffusely stained with GAP 43, this label continues to decrease at E18. The PGP 9.5 labelled DRG, contains many strongly stained positive cells in contrast to GAP 43 - whose immunoreactivity is apparently downregulated. Peripherin labelling also shows some unique features. The cells remain intensely stained, however, it is easier to discern individual cells at E17 and further still at E18, than at earlier stages. The number of immunolabelled cells appears to decrease but not their intensity.

RT97 staining changes little between E17 and E18. The intensity of the fibre labelling in the DRG has decreased from levels at E16, but strongly positive cell bodies are still clearly identifiable. These are sparsely distributed possibly indicating they are a restricted sub-population. Of the small cell markers, there is still no labelling with SP however, the first labelling with CGRP and IB4 is detected. At E17 a few faint CGRP-IR cell bodies are observed distributed throughout the DRG which by E18 have increased in number and intensity. At E18, there were a number of IB4 positive cells scattered throughout the DRG, these were quite clear with surface labelling only, visualised as a ring around the cell. TrkA appears to be labelling slightly fewer cells but there is little change in its intensity until E18 when this increases.

E19, E20 & E21

GAP 43 immunoreactivity has completely diminished by these late embryonic stages but most neurons are still heavily labelled with PGP 9.5. Peripherin also labels the majority of cells, where at higher magnification individual cells are observed to contain reaction product in the cytoplasm only. Close examination of individual RT97 positive cells, quite distinct now from the fibres, show that the label is cytoplasmic and strengthens the impression formed between E17 and E18 that these represent a

subpopulation of DRG cells. A notable number of these cells are positioned on the ventral and lateral edges of the DRG.

CGRP also labels a sub-population of cells very intensely, these are distributed throughout the DRG but concentrated in the ventro-medial portion. TrkA labelling has also altered slightly, many cells are still labelled but a group of very densely stained cells have emerged at E19. By E20, fewer cells are labelled and those positive cells are darkly stained, enabling the identification of these cells as a distinct subpopulation throughout the DRG. On closer examination the staining is restricted to the cytoplasm only.

4.11 Developmental Summary of Immunolabelling in the DRG

- The earliest markers expressed in the DRG of this study are GAP 43, PGP 9.5, peripherin and trkA at E13
- By E14, the selective A-fibre marker RT97 is also expressed
- Expression of the peptide CGRP does not appear until E17
- The small cell marker IB4 begins to be expressed at E18
- SP expression is not observed in this study by E21
- The full complement of markers with the exception of SP are expressed by E18, when most of the peripheral targets have been innervated
- The overall trend for these markers is to increase expression in the DRG and while some become more restricted (peripherin & trkA) they are still strongly represented
- GAP 43 is steadily downregulated, until no longer detectable at E19

Table 4.1 overleaf, shows the onset and intensity of immunolabelling at each developmental age.

Table 4.1: Onset and Intensity of Immunolabelling in the DRG at each Developmental Age

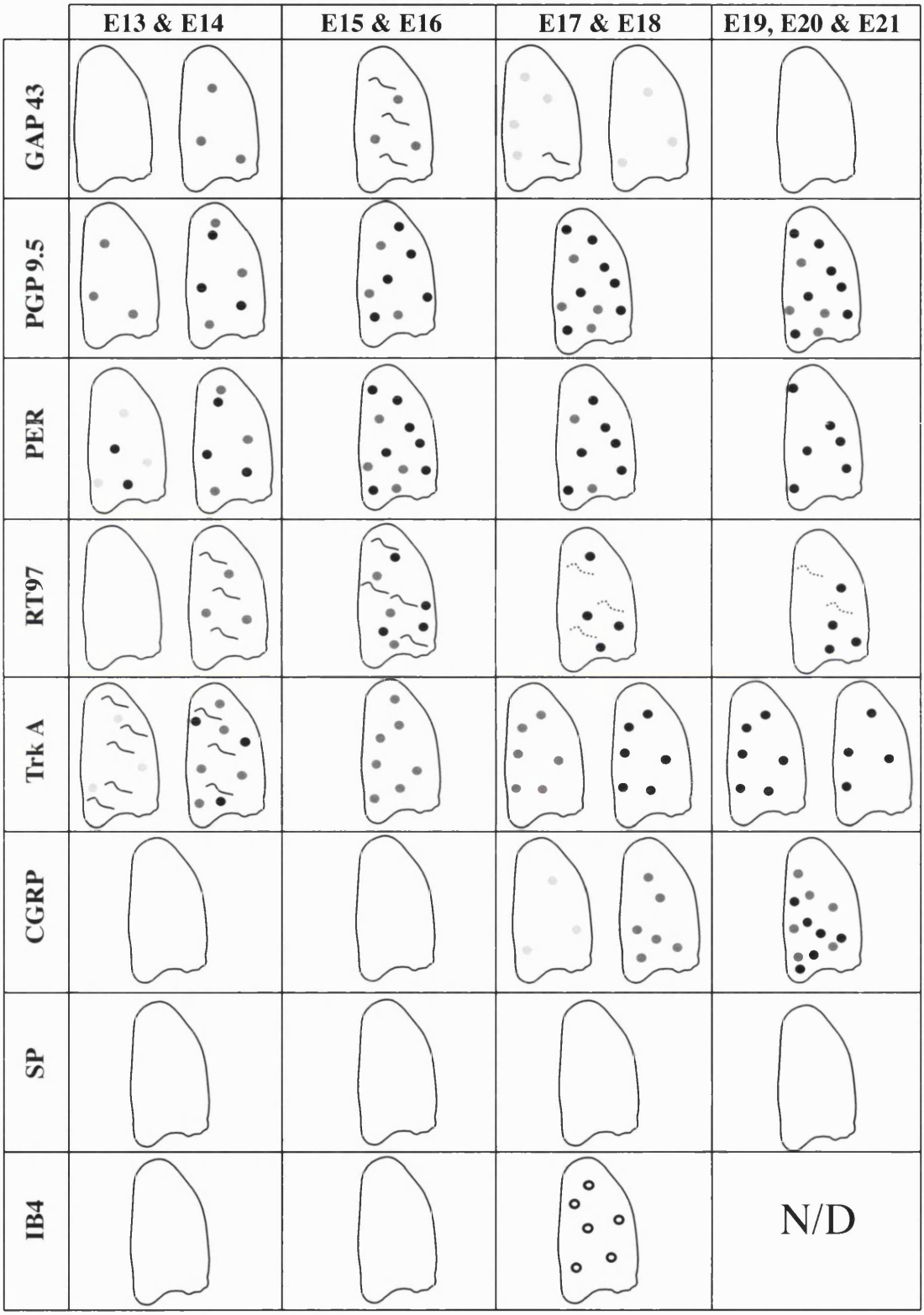

Key to intensity: Low Medium High Surface label Fibre

4.12 Periphery: Description of Innervation

The aim of this section was to use the same antibody markers as above to map subpopulations of peripheral nerves and their terminals in the hindlimb from E13, paying particular attention to the cutaneous innervation and any differences exhibited between the markers. E13 was chosen as the starting point for this spatio-temporal analysis as a plexus of densely bundled spinal nerves reaches the base of the hindlimb by E12 (Wessels et al, 1990; Reynolds et al, 1991; Mirnics & Koerber, 1995a) and grows further into the limb at E13.

The results are described as above, in age groups for the whole series of markers. While results from E13-E16 describe the whole limb, for those from E17 onwards, an overview of innervation at low magnification is followed by a description of specific regions at higher magnification. These regions are described and illustrated in the methods (Fig 2.3), but briefly these are: A and B the first glabrous pad and the hairy skin immediately opposite and one glabrous and one hairy site in the ankle region denoted C and D respectively.

E13 & E14

At E13 only one major GAP 43-IR nerve is seen entering the proximal hindlimb. This is located on the medial part of the leg, is loosely bundled and runs horizontal and perpendicular to the epidermis, actually growing towards the skin. Rapid growth occurs in the next 24 hours where this medially located bundle advances up to half the length of the leg. At its distal end, a thinner fascicle extends further down the leg; there are also a few short fibres directed medially from it. Proximally this bundle has many fibres and becomes more tightly fasiculated with one distinct fascicle guided to the epidermal edge. There is a second small bundle observed on the lateral side of the leg that reaches as far distally as the major medial bundle, but as yet nothing is directed towards muscle.

PGP 9.5 staining is absent from the E13 hindlimb and the pattern at E14 completely resembles that for GAP 43 except that on the lateral side there are some isolated fibres at the edge of the epidermis in the proximal region.

Peripherin is similar in having one major branch of the spinal nerve enter the hindlimb. It shows slightly more development at E13 since it immediately gives rise to a perpendicularly directed fascicle that reaches and penetrates the epidermis. The most important difference with this marker is that the initial bundle is located in a more central position, this branches to form a network but does not terminate over the muscle region. It is also noteworthy that peripherin labelled cell bodies are in the ventral horn at this stage, implying that immunolabelling over muscle may also be derived from motor axons. A long thin fascicle then continues down the centre and medial aspect of the leg, approximately a third of its distance to branch and turn towards, but not penetrate the epidermis. The next day at E14, the major nerve bundle has not advanced much further distally but has developed in the proximal region with many branches easily detectable. The tips of these finest branches terminate in bulbous swellings. In addition, some finer axonal branches proximally terminate over presumptive muscle.

RT97 labelling is not observed in the hindlimb at E13, but at E14 shows a pattern more closely resembling GAP 43 and PGP 9.5. One major bundle enters the hindlimb but splits into a medial and lateral branch immediately. The medial branch is more oblique than perpendicular but reaches the epidermis directly. The lateral branch can extend distally 1/3 - 1/2 way down the leg and subdivide further. The point where both the lateral and medial branches first contact the epidermis is approximately the same distance down the limb. The muscle area is free from labelling.

Neither of the peptides SP and CGRP, nor the lectin IB4 showed any labelling at these ages. TrkA, though present, shows a more restricted pattern than the other markers. At E13 a very fine fascicle is observed in the proximal hindlimb. It extends further than GAP 43 or PGP 9.5 fibres but on the lateral side is not as close to the skin surface; distally this bundle branches into many fine axons although is still absent from the epidermis. By E14 the lateral fascicle has not grown further down the leg but has turned obliquely towards, but does not penetrate the epidermis. In addition, there is now a fine bundle in the centre of the leg.

E15 &E16

GAP 43 staining reaches 3/4 the length of the leg but is more advanced medially. Two large bundles are now in the centre of the leg. The medial and most proximal of these has branched over presumptive muscle and has many fine fibres with visible growth cones at higher magnification. Laterally many evenly spaced fibres extend perpendicularly into the epidermis. Some fibres also travel parallel through the skin and at the distal most end radiate into many fine fibres. E16 innervation extends further medially but is still not in the toe region. The distal-most innervation consists of long fibres coursing through the skin, directly parallel to the surface. Proximally in the lateral part of the leg, fibres are evenly spaced and perpendicular to the surface. These reach directly into the epidermis, many end in swellings. Medially, these fibres appear similar but not as closely spaced. Also on the medial side is a large bundle situated midway down the central leg which branches many times over the muscle region, sending out a network of fine fibres.

PGP 9.5 innervation has not developed much since E14 with no muscular labelling. At E16, the skin innervation is similar except that perpendicular branches on the medial side of the leg are closer than on the lateral side. In addition, there is no branching over muscle although there is a long bundle present in this region. Peripherin labelling also has not increased in the muscle region by E15. On the lateral aspect however, a large fibre branches perpendicular to the surface at regular intervals, finer branches develop between these proximally but not distally. Medially, there is no evidence of this development but innervation has reached more distal extremities. By E16, the medial innervation still extends further distally, although proximally innervation has developed to the same extent as the lateral side. The muscle region receives many branches proximally and is comparable to GAP 43 distally.

RT97 is very similar at E15, except that innervation is still only 1/2 way down the leg and most branching occurs in the medial bundle. By E16 there are few differences from GAP 43 labelling except that innervation in the muscle region is halfway down the leg and proximally the medial perpendicular branches are close together but not connected.

TrkA labelling has not extended any further distally than at E14, but proximally and medially protrudes perpendicularly into the epidermis. Fibres are still very fine and loosely fasciculated. By E16, the main nerve bundle has travelled 3/4 the way down the leg and extends equidistant lateral branches towards skin. These penetrate and then branch in the epidermis, between them are fine singular perpendicular fibres. In the area of the first glabrous pad there are also some faint fibres in the dermal area. The lateral aspect of the leg and hairy skin of the foot are innervated to a lesser extent.

E17 & E18

A low magnification view of GAP 43 innervation shows it has reached the tips of the toes. There are much thinner fibres in the muscle region but these do not branch as extensively as E16. The proximal skin is characterised by repeating patterns in glabrous and hairy skin. Glabrous skin has closely spaced perpendicular fibres compared to hairy skin where a long thin fibre runs along the dermal-epidermal border yielding short branches perpendicularly, both laterally towards the epidermis and medially towards the muscle.

Higher magnification of the regions reveal that there are several differences between hairy and glabrous skin even within a specific region such as the ankle or the foot-pad:

A: Very large fibres enter the foot-pad and supply several perpendicular branches to encompass it fully. These subdivide, but send relatively thick and clumpy ended axons into the skin. They do not reach the edge of the epidermis in all cases. At this stage there are few finer axons visible.

B: A single large parent fibre runs along this hairy skin, yielding a few well spaced perpendicular fibres, these and the parent branch send out a localised radial pattern of fine axons with small growth cones.

C: A single fibre runs along the dermal-epidermal border giving rise to perpendicular branches at regular intervals. These are quite thick and reach the edge of the skin before ending in large swollen tips. However, in between those are a fine mesh of fibres which originate from both the perpendicular fibres and the original branch parallel to the skin

surface. Fibres below dermal level clearly end in growth cones.

D: As described at low magnification, some larger fibres actually course through the skin parallel to the surface, these branch both medially towards muscle and laterally to the skin surface. The majority of the finer axons observed in skin are derived from those lateral perpendicular branches. They are more widely spaced than in glabrous skin and do not reach the edge of the epidermis. The finer fibres are also only in a medial-lateral plane and do not intermix proximal-distally.

By E18 at low magnification, GAP 43 staining is restricted distally to the skin. More fibres, however, are present in the middle of the leg in the proximal region. At this resolution the innervation appears similar to E17. Closer examination reveals the same differences between hairy and glabrous skin.

A: The dermal-epidermal border is much more clearly demarcated. The larger fibres in this region have now yielded finer branches which protrude up into the epidermis. These innervated regions of epidermis are frequent and equally spaced.

B: Larger perpendicular bundles enter the skin and supply a wider area of epidermis. The fine axons continue to spread in a medial-lateral direction with only a few very fine axons radiating in a proximal-distal direction. These fibres do not reach the edge of the epidermis.

C: This proximal glabrous area has developed noticeably upon examination at higher magnification. The thick fibres with clumpy endings have sprouted many fine axons directed proximal-distally. Some of these are at the very edge of the epidermis going directly lateral towards the surface, however, many of the others are on-course to join the proximal-distal fibres from an adjoining parent branch. The labelling of the fine axon mesh has intensified and is located between these parent branches. Deeper layers have also developed, and the growth cone regions observed at E17 have elongated and spread proximal-distal.

D: The initial perpendicular branches have grown towards the edge of the surface and given rise to a second tier of finer branches, these do grow towards each other proximal-distally but do not directly grow towards the edge, nor do they reach it. Growth cones are still visible on these and at even higher magnification there are a few short beaded axons ending intraepidermally.

A low magnification view of E17 PGP 9.5 labelling is similar to that observed with GAP 43. At high magnification the regions are described below.

A: Different to GAP 43 because the thick fibres observed are parallel to the skin surface in the dermal-epidermal border, with no evidence of perpendicular branches in the epidermis.

B: The branches in the skin actually run parallel and close to the surface. Some finer and faint branching is detected these primary perpendicular branches.

C: This region also has quite thick processes in the skin, these enter obliquely and display finer branches that make a network between them. These end close to the surface in growth cones.

D: Again slightly different from GAP 43 and RT97 because there is a branch running proximal-distal close to the surface, however, similarly the perpendicular branches are well spaced.

An overview of E18 PGP 9.5 labelling still shows little innervation located in the muscle region.

A: This marker is still different to GAP 43 as it shows fibres with finer endings, these are close to but not in the epidermis.

B: This region is comparable to GAP 43 as the fine branches from the parent bundle are located along the dermal-epidermal border. Although they are still away from the skin surface.

C: Similar pattern to E17 except that the skin branches seem more torturous, also showing absence of the fine mesh found with GAP 43.

D: PGP 9.5 labelling is most developed in this region. As with GAP 43 labelling, the first perpendicular branches subdivide into very fine axons, but with PGP 9.5 they originate from the part nearest the epidermis. These grow back towards the dermis. The skin itself has grown so innervating fibres are further from the surface than before.

An overview of peripherin labelling at low magnification is similar to the description given above for GAP 43 and PGP 9.5. Subtle differences are noted with closer examination of the E17 foot at higher magnification.

A: Same pattern as GAP 43 but the perpendicular branches have divided and generate finer axons that radiate medially and laterally from original branch and therefore do not reach the epidermal edge.

B: Similar to GAP 43

C: Similar to GAP 43 except the perpendicular fibres are not as thick and do not end in growth cones.

D: Although comparable to GAP 43, it appears that a large fibre does not course through the skin in a proximal-distal direction but a nerve bundle from the dermis yields large perpendicular branches which retain their thickness until their end. They produce a relatively thinner branch proximal-distally which connects with the branch from the adjacent perpendicular fibre. However, like GAP 43, the very fine network observed does not meet in the proximal-distal direction.

By E18 peripherin staining is still as intense throughout the foot compared to GAP 43 labelling which is dissipating.

A: Few changes from E17 except that branches off the perpendicular fibre have grown towards each other.

B: Same pattern as E17 but in glabrous skin there is growth of finer fibres towards each other.

C: The pattern has simplified noticeably from the previous 24 hrs, the finer fibres from E17 have grown thicker and are linked to the adjacent perpendicular fibre in a regular configuration, however, the remaining surrounding area is free of innervating fibres.

D: As with the glabrous skin in this proximal region, the innervation pattern is simplified, although in contrast to the glabrous skin there are still very fine axons radiating from the main perpendicular fibres.

RT97 innervation is very similar to the descriptions above at both ages except that at E17 it has still not reached the toes.

A: Similar to peripherin because the perpendicular branches into the epidermis are much

finer than with GAP 43. These do not have clumpy endings but subdivide into yet thinner axons ending in small growth cones. These do not reach the edge of epidermis.

B: Similar to GAP 43 except for the absence of the fine radial pattern.

C: Thin fibres protrude into the epidermis, however the very fine mesh observed with GAP 43 is not visible although there are branches from both the thin perpendicular fibres and the parent bundle located along dermal-epidermal border.

D: Two large branches project perpendicularly into skin, these also emit finer branches in the lateral-medial orientation and not proximo-distally.

At E18 RT97 labelling most closely resembles that of PGP 9.5 but the toe region is not innervated to same extent.

A: Much more of the pad is innervated from the parent branch which is destined for the most distal extremity. The sub-branches enter the epidermis indirectly and are slightly torturous, these do not reach the skin surface but some end in growth cones. Only a few sparsely distributed fine fibres.

B: Unlike GAP 43 there is a simple pattern with a few equally spaced finer branches.

C: Also displays a simple pattern but the parent bundle parallel to the skin surface gives regular perpendicular branches, a few of which send out finer proximal-distal axons.

D: There are no fine fibres like GAP 43 labelling. The innervation seems pruned even from E17. Little interaction between fibres in the proximal-distal orientation.

TrkA labelling at low magnification shows axons that are loosely fasciculated and extend as far as the toes.

A: All fibres in the pad are thin and wavy. They follow the same pattern as other markers, but only penetrate a short depth into the epidermis.

B: The parent bundle branches into perpendicular fibres which reach directly into the epidermis near the surface, but no further subdivision is detected.

C: More development in this region as perpendicular fibres divide into finer axons, these are directed parallel to the surface in a proximal-distal direction and are regularly spaced.

D: Widely spaced fibres enter the dermis in an oblique manner, these terminate some distance

form the surface before branching in both proximal and distal directions close to epidermal edge.

Labelling with CGRP at E17 is restricted to only a few DRG cells therefore peripheral labelling was not anticipated, however, axonal labelling was detected in two animals at this age but was confined to the muscle region. Heavier innervation was observed at E18 but still not in the skin.

E19, E20 & E21

At low magnification E19 GAP 43 labelling shows a more extensive network in the toe region. Distally the muscle region is also developing.

A: Only the larger fibres are intensely stained. Even at higher magnification only a few growth cones are visible. No labelling is detected in the epidermis

B: Similar as before with finer endings present in the epidermis but still not as a direct result of branching from the parent bundle but from widely spaced perpendicular fibres.

C: Subdermal innervation is arranged in two tiers where fibres produce a criss-cross pattern across muscle. In skin, the major branches are further apart, however between these is much sprouting of thin axons to form an adjoining network. Only few fibres project into the epidermis.

D: A similar degree of pattern development occurs in the hairy skin. Innervation still does not reach the edge but is more widely spaced than before.

By E20, nerves from muscle nearest the hairy skin form a criss-cross network that adjoins the skin innervation. In the toe region there is further anastamosis of nerves, which is most developed at the distal-most extremity. In addition, the pattern of innervation in muscle has matured and appears to have synapsed.

A: There is a new wave of fine short branches from the perpendicular fibres, these extend deeply into the epidermis.

B: The epidermis is free of labelling although there are clear fibres situated along the

epidermal-dermal border.

C: The parent bundles are much fainter and even the perpendicular fibres have decreased in intensity suggesting possible downregulation.

D: Similar to the hairy skin opposite the first glabrous pad as there is clearly no epidermal innervation but fibres are still quite intense and the finer branches form a network.

Labelling is finally detected in the muscle region of the foot with PGP 9.5 at E20.

A: Quite a different innervation pattern from GAP 43 and RT97. The large bundles through the pad have branched into the skin, these have subdivided further and grown towards each other to envelope the area. Nothing is detected in the epidermis but this may also be due to its growth. There are also some beaded fibres in the dermal region. These may be blood vessels or peptidergic fibres.

B: One major fibre enters the dermis perpendicularly. This generates finer branches particularly at its tip but these are faint and travel parallel to surface.

C: The parent bundle is situated in the deep dermis parallel to the skin surface, it produces regular spaced perpendicular fibres directed towards the epidermis, but just at dermal-epidermal junction these subdivide and only these finest axons lie inside the epidermis.

D: Nothing detected in the epidermis, although the perpendicular fibres have branched at their tip to reveal axons in both proximal and distal directions which meet along dermal-epidermal border.

Peripherin labelling at E19 has increased particularly in glabrous skin and in the muscle region where many fine branches are now discernible. In addition there are more large nerve bundles throughout the foot, especially near the hairy skin.

A: Many of the branches from the parent bundle entering the pad region have subdivided along the dermal-epidermal border while the branches previously reaching perpendicularly into the skin have also branched two or three times. These latter fibres are very fine and project into the epidermis but due to the growth of the skin do not reach its edge.

B: A number of changes are detected in this area since E18. From the description at low magnification, additional bundles were observed in the foot. These project close to the skin

and yield a few short branches which are directed laterally towards the surface but only just penetrate the epidermis which has increased in thickness.

C: This is comparable to GAP 43 as there is much development of a network of fibres sub-dermally. The pattern in the skin remains simple as at E18 but these fibres now terminate along the sub-epidermal border.

D: Little change from E18 except that a large bundle is present and the fibres no longer project into the epidermis.

Low magnification analysis of E20 peripherin labelled feet reveal no changes in the pattern from E19

A: The development of a second wave of perpendicular branches from the parent bundle at E19 has now led to fine branches which terminate close to the dermal-epidermal border while the first emerged fine fibres have elongated and project into the epidermis in an overlapping pattern.

B: The innervation in this area is now all sub-epidermal and the fibres observed along the dermal-epidermal border are much coarser.

C: The only change from E19 is that all the perpendicular fibres are joined by fibres running proximal-distal in the dermis.

D: The pattern is similar to E19 except that there are more fibres in a proximal-distal orientation and these are slightly torturous.

E19 RT97 labelled feet clearly show that innervation is diminishing in the epidermis.

A: The skin has grown considerably therefore innervating fibres do not extend as deeply into the epidermis as previously. Any fibres in the epidermis however, are quite fine. These enter perpendicularly and along their length give frequent branches either side in a proximal-distal direction.

B: There are few fibres that are faint and wispy.

C: The fibres are short, perpendicular and unbranched in the dermis.

D Much development has occurred in the dermis but in the epidermis larger fibres stay aligned along the dermal-epidermal border with only a few short axons protruding into the epidermis.

E19 TrkA

A: Many more fibres are present in the skin, these are very fine and seem to have branches in a radial pattern originating from the perpendicular tree. There are also many more fibres coursing throughout the foot pad itself.

B: Short thin fibres are observed at the dermal-epidermal border only.

C: Increased branching occurs sub-dermally but innervation is absent from the epidermis now.

D: A network is formed sub-epidermally similar to the GAP 43 labelling pattern, this extends into the epidermis at close regular intervals.

E19 is when CGRP labelling is first detected in the skin of all foot regions. At low magnification innervation is also seen to extend to the toes. Very strong labelling is detected in the epidermis both proximally in the ankle region and in the toes distally.

A: A large bundle enters the foot pad. It has a beaded appearance throughout. This splits into branches towards the skin which sub-divide en route. These go directly into the epidermis splitting again just on the dermal-epidermal junction but do not branch when in the epidermis. They penetrate less than 1/3 the width of the epidermis.

B: Similar to other markers the large bundle is parallel yet below the dermis. Once in the skin the perpendicular fibres bifurcate and each fork turns towards each other as if wrapping around another structure.

C: Comparable to GAP 43 the nerve fibres form a plexus sub-dermally. Regularly spaced perpendicular branches from this plexus separate in the epidermis and turn towards each other. The axons are still fine and beaded.

D: Innervation is most developed in the muscle region with an occasional fibre in the epidermis.

4.13 Developmental Summary of Immunolabelling in the Periphery

- The first immunopositive fibres in the hindlimb are GAP 43, peripherin and trkA
- By E14, PGP 9.5 and RT97 positive fibres are also present in the hindlimb
- The first target to be innervated appears to be the skin, which is followed by innervation of muscle
- The exception to this is peripherin positive fibres, which from the outset simultaneously reaches the skin and muscle
- Innervation reaches the distal-most part of the hindlimb by E17
- CGRP is observed in the muscle region at E17 but is not detected in the skin until E19 when it is found in all regions simultaneously
- At late embryonic stages, labelling previously observed in the epidermis no longer penetrates to the surface of the skin
- The presence of RT97 and trkA immunopositive fibres suggests that both large and small diameter fibres innervate the peripheral target together
- The relatively late appearance of peptidergic fibres suggests that either these peptide-expressing fibres grow to their target later or that expression of peptides are switched on in existing small diameter fibres after a specific signal.

Table 4.2 overleaf, shows the onset and intensity of immunolabelling in the hindlimb at each developmental age.

Table 4.2: Onset and Extent of Immunolabelled Fibres in the Hindlimb at each Developmental Age

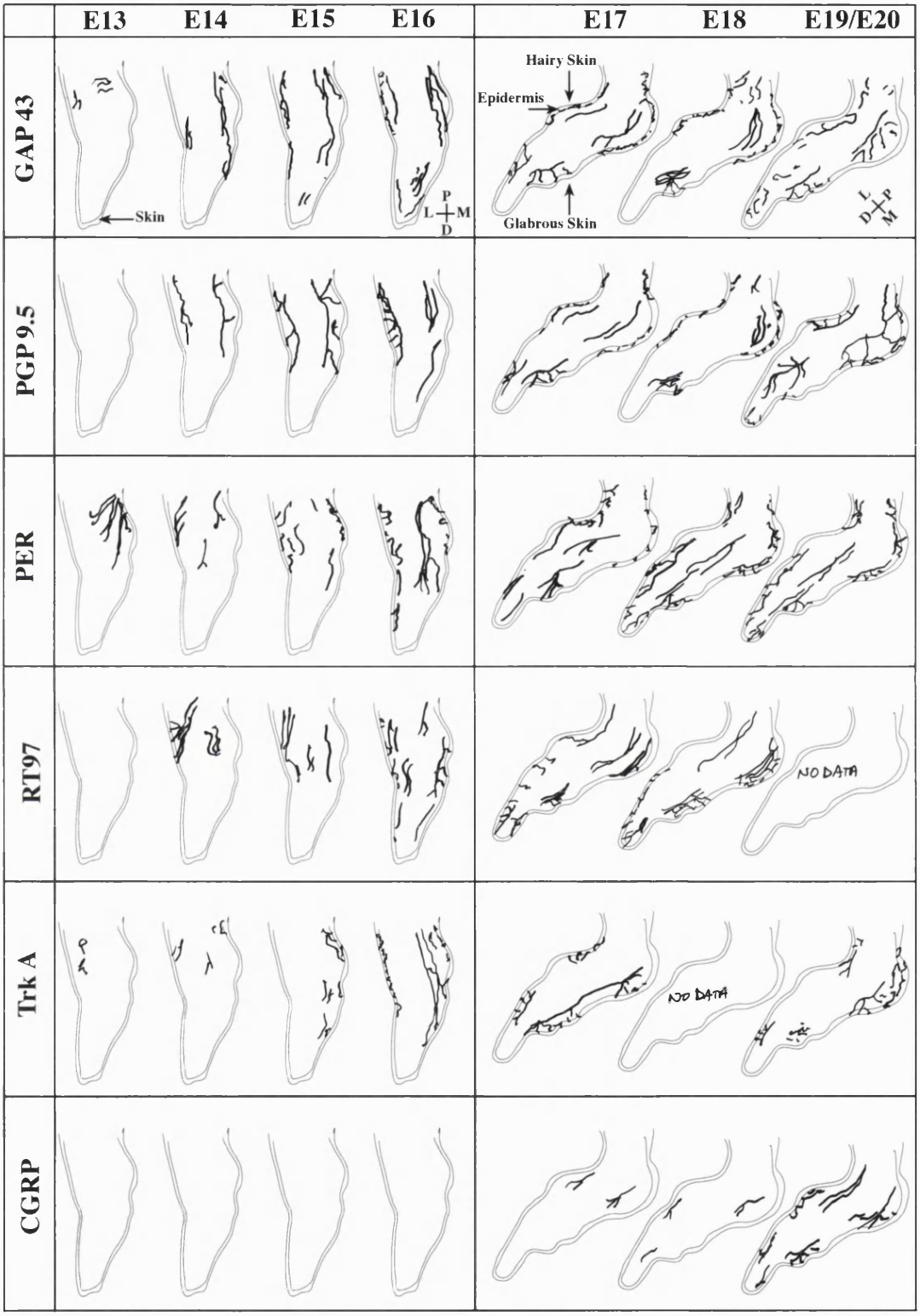

L= Lateral; M= Medial; P= Proximal; D= Distal

4.14 Spinal Cord : Description of innervation

E13 & E14

At the earliest stage examined there is complete absence of GAP 43 in the spinal cord except for the developing Bundle of His, although staining is visible in the white matter. The Bundle of His is the consolidation of dorsal root fibres that have grown towards the spinal cord but not yet penetrated it, during this period before they enter the spinal grey matter they travel up and down the spinal cord. 24 hours later the Bundle of His is more intensely stained and extends medially with one or two axons moving down the lateral side of the cord. The dorsal roots are quite discernible but loosely bundled, as are the ventral roots. The most significant growth at E14 is the faint but intricate tangle of axons in the ventral horn. This is mainly restricted to the most lateral portion, with some medially adjacent to the developing ventral columns. Some faint fibres are observed crossing the ventral commissure.

PGP 9.5 results are similar to those with GAP 43, showing no axonal staining in the grey matter at E13. The ventral spinal cord does display some diffuse cellular stain which on the lateral edges extends more dorsally. By E14, there are few differences except that some ipsilateral projection neurons have extended a few short axons medially.

Peripherin at E13 shows much clearer development of ventral columns including fibres transversing the spinal cord. These appear to be ipsilateral projection neurons. The ventral grey matter is also more clearly defined with axonal labelling in the lateral portion only. At E14, the Bundle of His has developed medially leading with individual axons. Importantly, a single axon also descends ventrally from the most lateral and ventral part of the Bundle of His. Ventrally, the lateral staining has intensified and spread dorsally with the appearance of a few strongly staining cell bodies and faint fibres just ventral and lateral to the central canal. The main finding using this marker compared to GAP 43 or PGP 9.5, is the presence of cell bodies in the ventral horn at E14.

At E13, RT97 labelling is restricted to the Bundle of His, which is much smaller than observed with the above markers, and punctate staining where the lateral and ventral

columns will form. However, a large number of changes are seen within 24 hrs. By E14, The dorsal roots are closely bundled to meet the Bundle of His which appears in a more rostral position. A very significant finding is the appearance of RT97-IR fibres in the dorsal horn of the spinal cord grey matter. Fibres enter and travel ventrally remaining close to the lateral wall. This is before innervation is observed in this location with any marker other than the few peripherin positive fibres. RT97 is also a unique marker at this developmental stage due to the intensity of individual fibres, although no cell bodies are detected.

No labelling in the dorsal horn was obtained with SP nor with CGRP at E13. CGRP, a peptide normally found in adult small diameter DRG neurons, is also found in motoneurons and it is present in the lateral ventral horn at E14. This is the only region in which CGRP is detectable. At higher magnification, this labelling is distinguishable in cell bodies. Using trkA however, no labelling is found in the spinal cord. The dorsal roots are numerous and heavily labelled but loosely bundled to the extent that practically all fibres are individually discernible. These form the Bundle of His at the edge of the spinal cord which is positioned slightly more laterally into the connective tissue. By E14 little has changed, the cord is still absent of any innervation, change is limited to tighter fasciculation of the dorsal roots and Bundle of His.

E15 & E16

At E15, there is clear growth of dorsal root collaterals into the grey matter of the dorsal horn. GAP 43 labelling shows the Bundle of His has moved further medially to form the dorsal columns. The most lateral aspect of these give rise to afferents that project in a ventrolateral arc towards the lateral columns - these correspond to future Aβ fibres. In the ventral horn there are some faintly labelled fibres that are situated at the most ventral aspect, and in addition, some fibres cross the ventral commissure. The ventral roots are still loosely fasciculated. By E16, the dorsal columns have approached the midline but do not meet. The lateral column is well formed but staining is less intense in the region of the dorso-lateral funiculus. At higher magnification of the dorsal horn, the afferents emanating from the most lateral part of the dorsal column are observed to sweep round

and terminate near the dorso-lateral funiculus in the lateral grey matter. Fibres are also observed at the top of the central canal which extend ventrally either side of it. The ventral horn labelling is unchanged apart from a decrease in intensity at the ventral commissure.

PGP 9.5 labelling at E15 is mostly unchanged but there is some faint evidence of one or two axons projecting from the dorsal column into the grey matter ventro-laterally towards the lateral grey matter, corresponding to future 1a fibres. A similar picture is found at E16 except that cellular staining increases in the dorsal horn.

Peripherin at E15 shows axonal labelling in the dorsal horn, but this displays a different pattern and is derived from a different location than seen with GAP 43. The afferents invade the dorsal horn from the medial part of the dorsal column. These arc medially, then ventrally into the mid-dorsal horn. Associated with these afferents is some cellular staining, mostly in the superficial dorsal horn. At the same time axons also invade the grey matter from the lateral walls of the spinal cord, these are short and very fine and follow a torturous path with some ending in bulbous swellings. These may be presumptive ipsilateral projection neurons. In the ventral horn, the pool of axonal staining is situated in a more medial position than at E14 but the cellular label is unchanged. By E16 the dorsal horn labelling retains the same pattern but extends deeper into the dorsal horn. The ventral motor pools are less intensely labelled.

RT97-IR afferents in the E15 dorsal horn have changed their expression pattern considerably since E14 and now more closely resemble the pattern of GAP 43. The ventro-laterally orientated afferents meet another numerous group of axons originating from the lateral cord that project towards the ventricular zone. The ventrally directed axons could be presumptive Aß afferents, but they have not as yet turned laterally. The white matter is also labelled strongly and delineates the spinal cord, enclosing the highly complex tangle of axons in the ventral horn. This network of fibres is located mostly in the lateral and ventral region. Fibres are also identified horizontally crossing the ventral commissure. By E16, collaterals in the dorsal horn now originate from the medial dorsal horn, some follow the pattern of the previous afferents but a few continue ventrally. The projections towards the ventricular zone have advanced medially and dorsally. The other

anomalous observation is some stray axons moving ventrally from the medial edge of each dorsal column. Meanwhile in the ventral horn, axons feed into the ventral commissure and cross to the contralateral side.

There is still no CGRP labelling in the dorsal horn while immunopositive cells appear more dorsally in the ventral horn. TrkA labelling is still absent from the grey matter at E16. The dorsal columns are darkly staining but lighten towards the medial edges.

E17 & E18

A low power overview of the GAP 43 labelled spinal cord shows that the dorsal columns have expanded further medially so that they practically merge. The white matter has established collaterals in the grey matter from the lateral column and to a greater extent the ventral column. The ventral commissure is no longer labelled. On closer examination the dorsal horn contains many fine-diameter longer collaterals that emanate from a more medial aspect of the dorsal columns. These travel in a ventrolateral arc to the dorso-lateral funiculus, which is more faintly labelled than the rest of the lateral column. There are long collaterals that emerge from the most medial aspect of the dorsal columns then grow towards the ventral horn. The dorsal horn is also characterised by many clumps of staining, these are largest medially but more discrete and numerous in the superficial and lateral aspect. There is little evidence of labelling in the ventral horn.

A day later at E18, the dorsal columns have enlarged and moved ventrally to form the dorsal horns proper. The dorsal-lateral funiculus is as fully stained as the rest of the lateral column and there is increased invasion of the grey matter from the lateral columns, and is extensive from the ventral columns. In the dorsal horn, ventrally directed collaterals originating from the medial dorsal columns are not as evident. Afferents to the lateral dorsal column grow deeper than at E17 and there is increased clumps of staining in the superficial dorsal horn.

PGP 9.5 is not as revealing over these 48 hrs as the GAP 43 marker. The differences observed are primarily in the dorsal horn. The dorsal columns are not as expansive although they have merged at E17 and formed dorsal horns at E18. The spinal

grey consists of a general network of fibres but clearly directed lateral or ventral collaterals are not observed. Intrusion of white matter collaterals to the grey matter only begins from the ventral column at E18. However one unique feature at E17 was the presence of some fibres dorsal to the central canal which had disappeared by E18 and alsosome cellular labelling extending ventrally from the most dorsal part of the ventral horn.

Peripherin labelling also shows some unique features. As with the other markers, the dorsal columns have merged but at E18 these have not moved as far ventrally. Also, continuing the pattern set at E15 with this antibody, the dorsal horn collaterals have still not materialised in the most lateral aspect, which is inconsistent with all other labels that begin growth in a lateral to medial progression. At E17 afferents arising from the medial dorsal column grow ventrally straight to the motoneuron pool and have reached the deepest laminae. There are no laterally orientated fibres. Slightly medial to these fibres are some shorter collaterals also aimed ventrally. By E18, these have grown deeper into the dorsal horn and appear to move laterally whilst the very long axons destined for the motor pool are no longer detectable in the deeper laminae. The disappearance of collaterals bound for the motor pool coincides with decreased cellular staining in this region at E18. Previously at E17, there was a transient appearance of numerous very intensely labelled cell bodies with short fibres below them, directed ventrally. Their appearance was during the period when the dorsal horn axons were directed towards this target. However at E18, these cell bodies have diminished in intensity and number and retracted ventrally, in conjunction with the presence of the fibres between the motor pool and the ventral root. Another curious feature is the lack of labelling in the white matter. The only part where labelling occurs at E17 and E18 is at the ventral root exit zone.

RT97 staining changes little between E17 and E18 but exceptions to the above descriptions exist. The pattern of labelling in the dorsal horn resembles peripherin as the lateral dorsal horn is devoid of afferents, this empty area has increased in size since first observed at E16, however, unlike peripherin this area was occupied by RT97 collaterals at an earlier stage of in-growth. Also at E17, similar to GAP 43, there are many clumps of

staining in the lateral superficial dorsal horn. Collaterals leaving the medial dorsal horn have a trajectory which leads them ventrally, then laterally to the lateral column. More projections cross the intermediate grey matter and are directed medially and dorsally towards the central canal. By E18 the axons emanating from the medial dorsal horn diverge into two separate populations. Both initially move ventrally then the first population turns laterally in the region of the dorsal-lateral funiculus. The second continues projecting ventrally towards the motor pool. This pattern is complicated considerably by the arrival of axons from the white matter and from projections crossing the intermediate grey matter from the most lateral aspect of the deep dorsal horn. These project towards the central canal and on a few occasions appear to cross-over to the contra-lateral side. In the ventral horn there is still a large population of afferents that have ramified extensively throughout this area. The most notable feature in this region is a small intensely stained group of medially positioned fibres that project ventrally and join the ventral commisure to cross ventromedially through the grey matter.

Of the small fibre markers, there is still no labelling with SP at E17 and CGRP spinal cord labelling is restricted to the motoneuron cell bodies. These cells are very dense and positioned in the dorsal region of the ventral horn and have moved ventrally at E18. Also at E18, some fine SP fibres with a beaded appearance originate from the medial dorsal columns, these sweep in a ventro-lateral arc to the lateral columns. The heaviest labelling which also appears to be cellular is situated near the midline in the deeper dorsal horn.

The first labelling of the superficial dorsal horn corresponding to future nociceptive fibres is observed between E17 and E18. At E17, trkA labelling of the dorsal columns has increased since E16 and the first in-growth of trkA afferents to the spinal grey matter occurs. Fine diameter afferents enter from the lateral dorsal columns and reach lamina I and II. Within 24 hrs these axons have increased in number and extended deeper but are still confined to superficial dorsal horn, while shorter axons are observed originating from the medial dorsal columns. The lectin IB4 at E18 shows axons originating from the full

extent of the dorsal columns, protruding ventrally into the superficial dorsal horn. These are fine but numerous, producing a network of fibres.

E19, E20 & E21

Individual paths of axons are difficult to define in the E19 GAP 43 labelled spinal cord. More noticeable is the large clumped staining in the deep medial dorsal horn. Labelled fibres are found spanning the intermediate grey matter, these cross to the contralateral side. Dense new labelling is also found in the superficial and lateral dorsal horn. There is general background staining in all of the ventral horn. At E20, labelling across the intermediate grey matter is intensified, this may be due to invasion of the white matter that crosses contralaterally. In addition, the dorsal horn is now heavily labelled by a network of fibres, this is more distinct and especially dense in the superficial dorsal horn. Only a few clumps of staining remain, these are positioned immediately lateral to the central canal.

PGP 9.5 produces overall staining of the spinal cord which makes it difficult to identify individual axons since staining is mostly cellular. At E19 however, there is clearly much heavier labelling in the superficial dorsal horn.

The changes at E19 with peripherin are restricted to the dorsal horn where three distinct groups of labelling are detected. The most striking of these are the collaterals arising from the medial dorsal columns as described at E17. They have not reached the ventral horn since E18 but still persist, projecting ventrally in the dorsal horn. The second group also arise from the medial dorsal columns but these project ventro-laterally, terminating at the dorso-lateral funiculus and the tangle of axons occupying the superficial dorsal horn. The final group are first detected at this age and consist of short collaterals restricted to laminae I and II and the lateral part of the dorsal horn, a location where no previous labelling with peripherin was identified. There are also some faint fibres corresponding to those of GAP 43 crossing through the intermediate grey to the contralateral side.

Few changes are observed with RT97 except that fibres in the intermediate grey matter are less intensely stained.

CGRP labelling shows many changes at E19. A small number of afferents enter the grey matter of the lateral dorsal horn. These project ventrally and are restricted to the lateral region. Another group of fibres arise just medial to the first group, these move further medially before turning ventrally. There are also one or two faintly stained axons that appear from the medial dorsal column and extend a short distance ventro-medially. These have a beaded appearance with axons from both sides meeting dorsal to the central canal. In the ventral horn there are a few darkly stained cells bilaterally in the ventro-medial portion.

SP cellular labelling at E19 has moved laterally from its location at E18, and is now located deep in the mid-dorsal horn. TrkA labelling also develops further at this age. The superficial laminae of the dorsal horn is completely covered by a dense network of fibre and cellular labelling. There are a few lightly stained afferents leaving the medial dorsal column that move ventrally and medially extending to lamina II.

4.15 Developmental Summary of Immunolabelling in the Spinal Cord

- At E13 immunolabelling with GAP 43, PGP 9.5, peripherin and RT97 is restricted to the ventral horn and to the dorsal root entry zone which ramifies to form the Bundle of His at E14
- At E14 dorsal root collaterals first penetrate the grey matter. Peripherin and RT97 labelled fibres are found extending into the grey matter of the dorsal horn from the ventro-lateral aspect of the Bundle of His
- Major collateral ingrowth occurs at E15 and E16
- Collaterals project from the lateral dorsal column in a ventrolateral arc to the lateral columns and from the medial dorsal column to the ventral motor pools
- As development proceeds from E16-E17 collaterals emerge from the dorsal columns in a lateral to medial progression. The exception to this is peripherin, whose fibres originate from the medial aspects at the outset and do not occupy the lateral region of the dorsal horn. Some RT97 positive clumps are located in the SG
- TrkA positive collaterals first grow into the SG at E17/E18. These become denser over E19-E20
- IB4 collaterals also found in the SG at E18
- CGRP positive collaterals are first observed at E19 and are found throughout the lateral to medial extent of the SG

Tables 4.3a, b, and c show the onset and location of immunolabelled fibres in the spinal cord at each developmental age.

Table 4.3a: Onset and Location of Immunolabelling in the Spinal Cord at each Developmental Age

	E13 & E14	E15 & E16
GAP 43	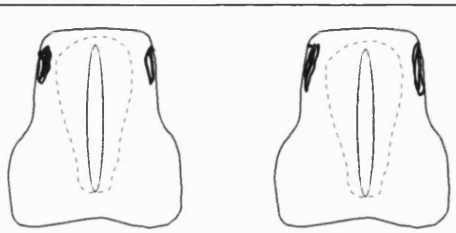	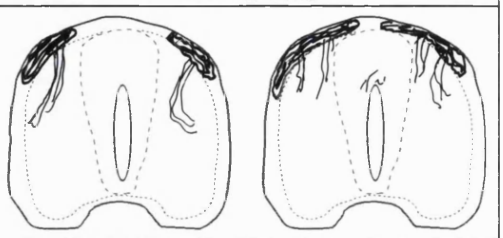
PGP 9.5	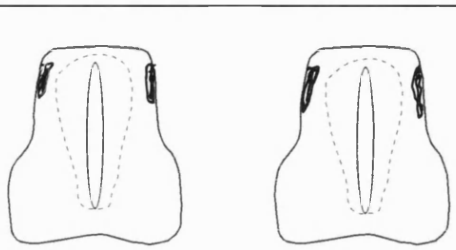	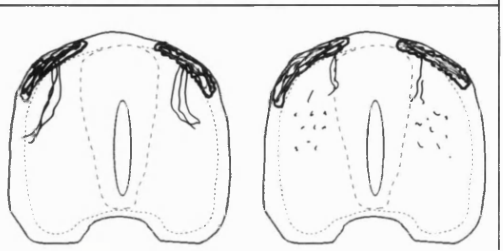
PER	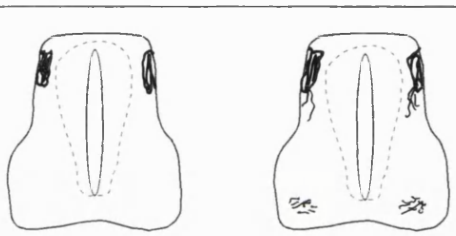	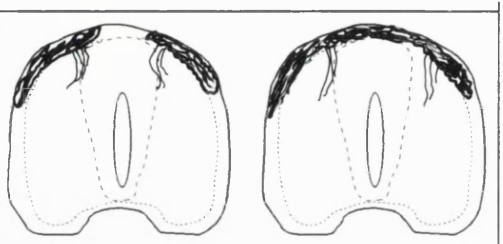
RT97	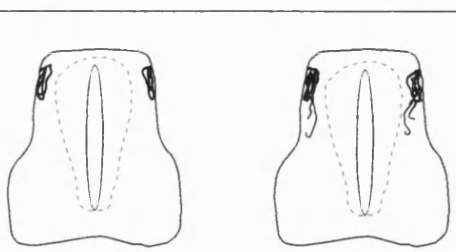	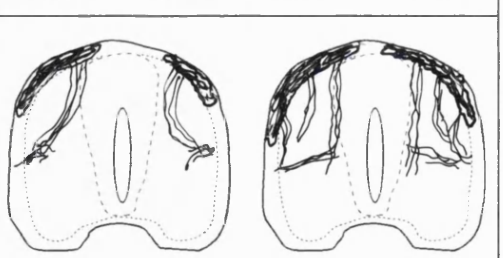
Trk A	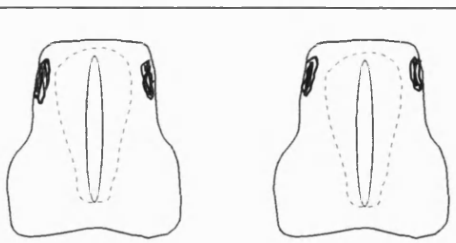	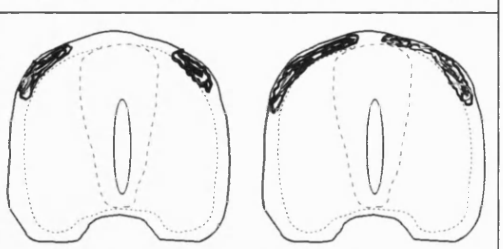
CGRP	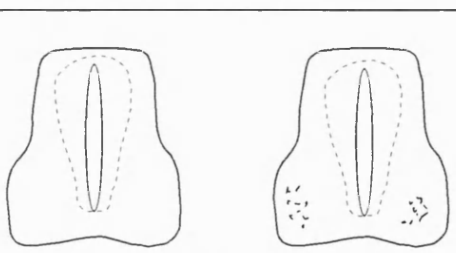	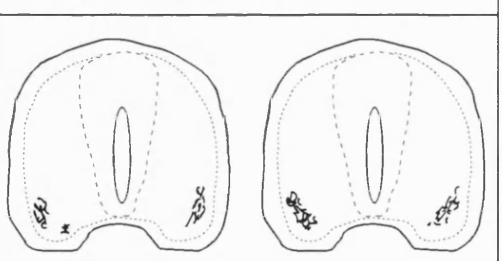

Table 4.3b: Onset and Location of Immunolabelling in the Spinal Cord at each Developmental Age

	E17 & E18	E19, E20 & E21
GAP 43	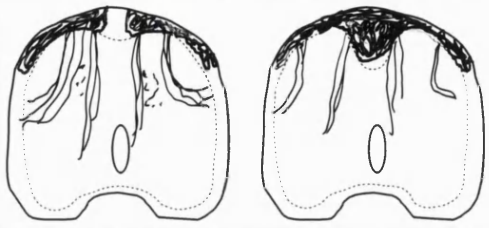	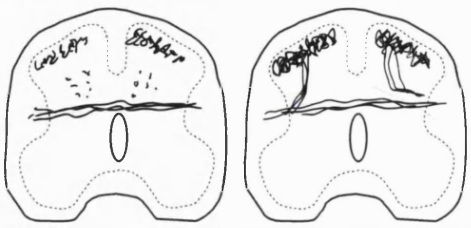
PGP 9.5	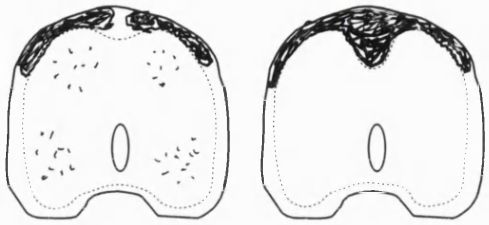	
PER	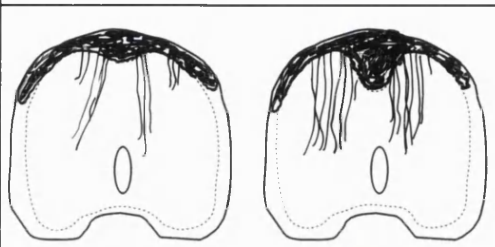	
RT97	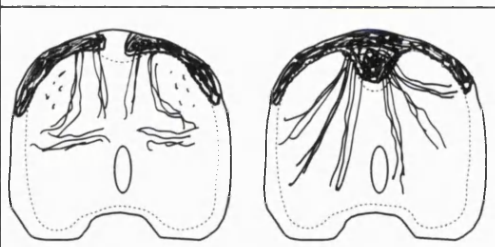	
Trk A	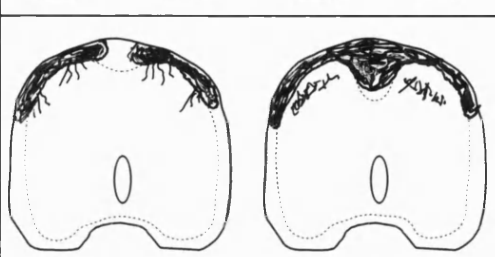	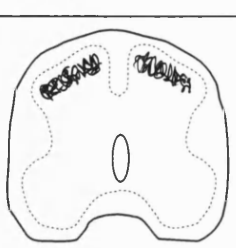
CGRP	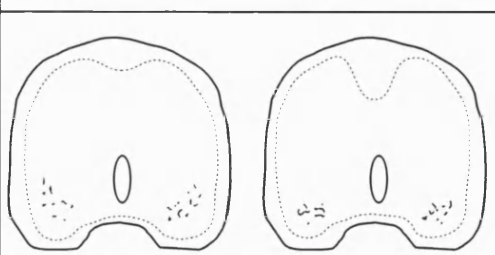	

Table 4.3c: Onset and Location of Immunolabelling in the Spinal Cord at each Developmental Age

	E18	E19, E20 & E21
SP	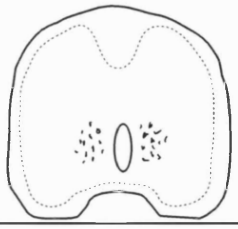	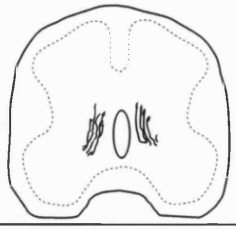
IB4		

4.16 Analysis of peripheral innervation according to A-fibre and C-fibre phenotype

The immunohistochemical markers GAP 43 and PGP 9.5 label all growing axons regardless of phenotype. The remaining markers used in this study were included because of their ability to distinguish between A-fibres and C-fibres.

The marker RT97 is selective for A-fibres in the adult and embryo (see Chapter 3). Analysis of the C-fibre population was complicated by the lack of adequate markers. This was due to the different expression patterns in development of characteristic small fibre markers, as described in the adult. The peptides CGRP and SP, and the lectin IB4 are not expressed in early development, so these would not determine if small diameter axons are part of the early innervation. Peripherin was chosen as an ideal candidate because, like RT97, is a structural component of the small diameter fibre. However, its extensive labelling pattern during development excluded it as a selective marker. The remaining small fibre label is trkA. It also labels more extensively in the embryo than the adult, however, in the adult its expression practically overlaps with CGRP and the extra expressing cells during development are thought to later become IB4 positive. Therefore, this marker appears to be the only available determinant of small fibre development.

The results of the developmental series show that RT97-IR fibres are found to be among the earliest to be expressed in the periphery. These fibres continue to grow in a pattern mirroring the progression of the fibres labelled with the general markers. RT97 labelling reaches the toes at E18 and is expressed in the epidermis, even though it is primarily described as a large fibre marker.

TrkA-IR fibres are also found in the periphery in the same timeframe as the earliest innervation. The fibres are very fine and loosely fasciculated revealing the relative paucity compared to other markers. They do not reach the skin target until E15. In contrast to many of the other labels, epidermal innervation at E17 consists of many fine axons parallel and close to the surface. The skin innervation as detected with trkA increases considerably by E19, coincident with the first expression of the peptide CGRP in the skin.

CGRP labelling appears in the muscle at E17, but is not located in the skin until E19 where firstly, the intensity is very strong, and secondly, unlike the gradual proximo-distal progression of other fibres it appears in all regions simultaneously, including the distal skin. The other difference in comparison to other labels, is that epidermal fibres grow towards the adjacent perpendicular fibre as if wrapping around another structure.

In conclusion, since RT97 has been confirmed to preferentially label the large fibre population during development (see 3.4.4.), and these fibres are found from the outset, the phenotype of innervating axons must include the A-fibres. The presence of the small fibre label trkA, in the early nerve bundles should also suggest that the C-fibre phenotype is represented in these axons. However, a more cautious interpretation is required because a size-frequency histogram is not available for trkA during development.

4.17 Analysis of central innervation according to A-fibre and C-fibre phenotype

The first afferents to enter the grey matter of the spinal cord were RT97 positive with some peripherin positive fibres. These originated in the lateral dorsal column and moved ventrally along the lateral wall.

At E15, the major collateral ingrowth occurs and is revealed by peripherin. Peripherin is the only marker to originate from the medial dorsal column and projects ventrally along the edge of the neuro-epithelial zone. From the projection pattern, these are putative 1a afferents. The remaining labels, RT97, GAP 43 and PGP 9.5 all originate from the lateral dorsal column, project ventro-laterally and correspond to putative Aβ afferents. There is no evidence of afferents labelled by any of the small diameter markers nor in locations consistent with C-fibres.

By E17, collaterals with Aβ projection patterns originate from progressively more medial positions. The peripherin labelled fibres originate from the same position but project deeper into the dorsal horn, although some RT97 positive fibres may also label 1a fibres. Until this point it was clear that only A-fibres were represented, but a few faint,

short fibres labelled by trkA appear in the lateral region of the superficial dorsal horn, possibly revealing the first non-peptidergic C-fibres.

At E18, this assumption is reinforced by the presence of IB4 labelling confined to the SG and increased labelling with trkA. Hence, it appears that while A-fibres display a two day wait in the DREZ before afferent entry, it is four days before the first C-fibres are detected.

4.18 Correlation between peripheral and central innervation at each age

Examination of the pattern of labelling in the spinal cord and the hindlimb with each immunohistochemical marker at different developmental ages, allows comparisons to be made about the relative timing of events. This analysis has identified two areas where analogous events occur both centrally and peripherally. The first is the correlation between the sequence and position in which nerve fibres enter the spinal cord, and the relationship of peripheral innervation to a specified target type and location.

Peripherin-IR and RT97-IR fibres are the only nerves that enter the proximal epidermis of the hindlimb at E14, and these markers are the only ones that show afferents penetrating the lateral grey matter of the spinal cord at E14. By E15, GAP 43 and PGP 9.5 labelled fibres are located in the epidermis proximally and they now also project into the lateral grey matter. The coincident appearance of fibres in the proximal skin and the lateral grey matter could suggest that innervation of the proximal skin promotes afferent entry into the lateral grey matter.

This theory is further supported with the extension of peripherin labelled fibres to a more distal location, coinciding with afferents entering the grey matter from the medial dorsal horn. This evidence implies that presence of innervation in a proximal peripheral target is related to the occupation of the lateral dorsal horn and the appearance of innervation in the distal target stimulates the emergence of afferents in the medial dorsal horn. However this may be an oversimplification, the peripherin fibres although in a more distal position, are also located in the centre of the hindlimb, over the muscle region and have a projection pattern consistent with 1a fibres. At E16, when RT97-IR fibres are detected in a muscle region quite proximally, RT97-IR fibres are found projecting into the

dorsal horn from a more medial aspect but with a projection pattern similar to 1a's and distinct from the ventro-lateral Aβ type originating from the lateral dorsal columns. Therefore, the appearance of afferents in the dorsal horn in a medial to lateral progression, may not just be linked by the growth of afferents peripherally in a proximal to distal direction, but by the presence of innervation in the skin followed by muscle.

At the earlier developmental stages described above, a connection is now established between the presence of afferents in progressively medial positions in the dorsal horn and the appearance of peripheral innervation of muscle. It is important therefore to distinguish what is meant by the distal target. By separating the distal innervation into its cutaneous and muscular components allows a more detailed analysis of the affiliation with the central innervation.

Distinguishing between the type of peripheral target to which innervation projects distally, in fact shows that a reversal in the sequence of target innervation that occurs in the proximal region. Proximally, skin is innervated before muscle, resulting in occupation of the lateral dorsal horn by ventrolaterally directed afferents (Aβ) prior to occupation of the medial dorsal horn by ventrally directed afferents (1a). In the distal region, however, at E17, the large GAP 43 and peripherin labelled nerve bundles particularly are located in a central position over muscle in the foot, which is combined with novel ventrally directed projections in the medial dorsal horn. These observations are reproduced a day later with RT97. This muscular innervation distally is followed a day later by increased skin innervation in the region and a shift medially of the ventrolateral directed fibres in the dorsal horn.

In summary, this analysis implies that proximal hindlimb skin is the first peripheral target innervated and is associated with growth of spinal cord afferents from the lateral dorsal column in a ventrolateral arc. The second target innervated is muscle, both proximally and distally which is equated with medio-ventral and ventral directed afferents emerging from the medial dorsal columns. The third peripheral target is distal skin, which at E18, is combined with a medial shift in the ventro-laterally directed afferents. These patterns are valid for A-fibres. The late onset of C-fibre entry is not

equated with peripheral events since at E19, axonal labelling in the substantia gelatinosa occurs after large diameter and small diameter fibres are found in the distal skin.

Fig. 4.1: GAP 43 labelling in the Spinal Cord and DRG of embryos aged E13-E20

In E13 and E14, arrows point to the bundle of His. Arrowheads in E14 are directed towards the developing innervation in the ventral horn. At E15 the dorsal columns (DC), dorsal roots (DR), dorsal root ganglia (DRG), ventral column (VC) and ventral root (VR) are clearly visible. Long arrows point to ventrally directed fibres. Short arrows to the laterally directed fibres. By E16 the lateral columns (LC) are labelled except for the dorsal funiculus marked with an asterisk. Arrowheads show transient labelling above the central canal.
The prominent feature at E17, is the clumps of staining which are circled. Arrows indicate the two afferent pathways, ventrally and ventro-laterally. At E19 the clumps of staining in the dorsal horn are delineated by the dotted lines. Arrowheads point to labelling in the superficial dorsal horn. Arrows in E19 and E20 show contralateral crossing fibres. Scale bars =100μm.


E13
BOH

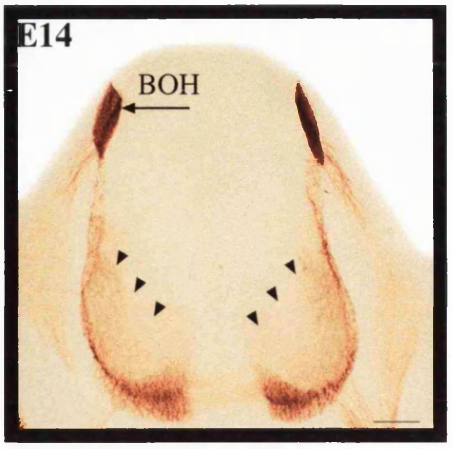
E14
BOH

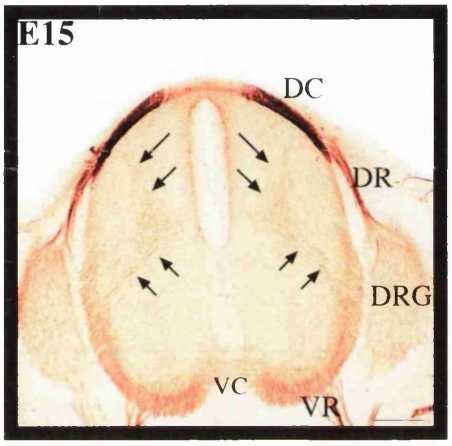
E15
DC
DR
DRG
VC
VR

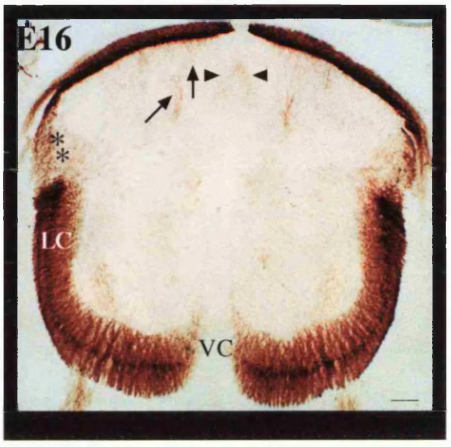
E16
LC
VC


E17

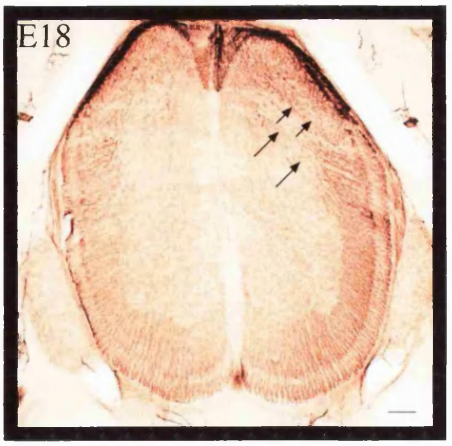
E18


E19


E20

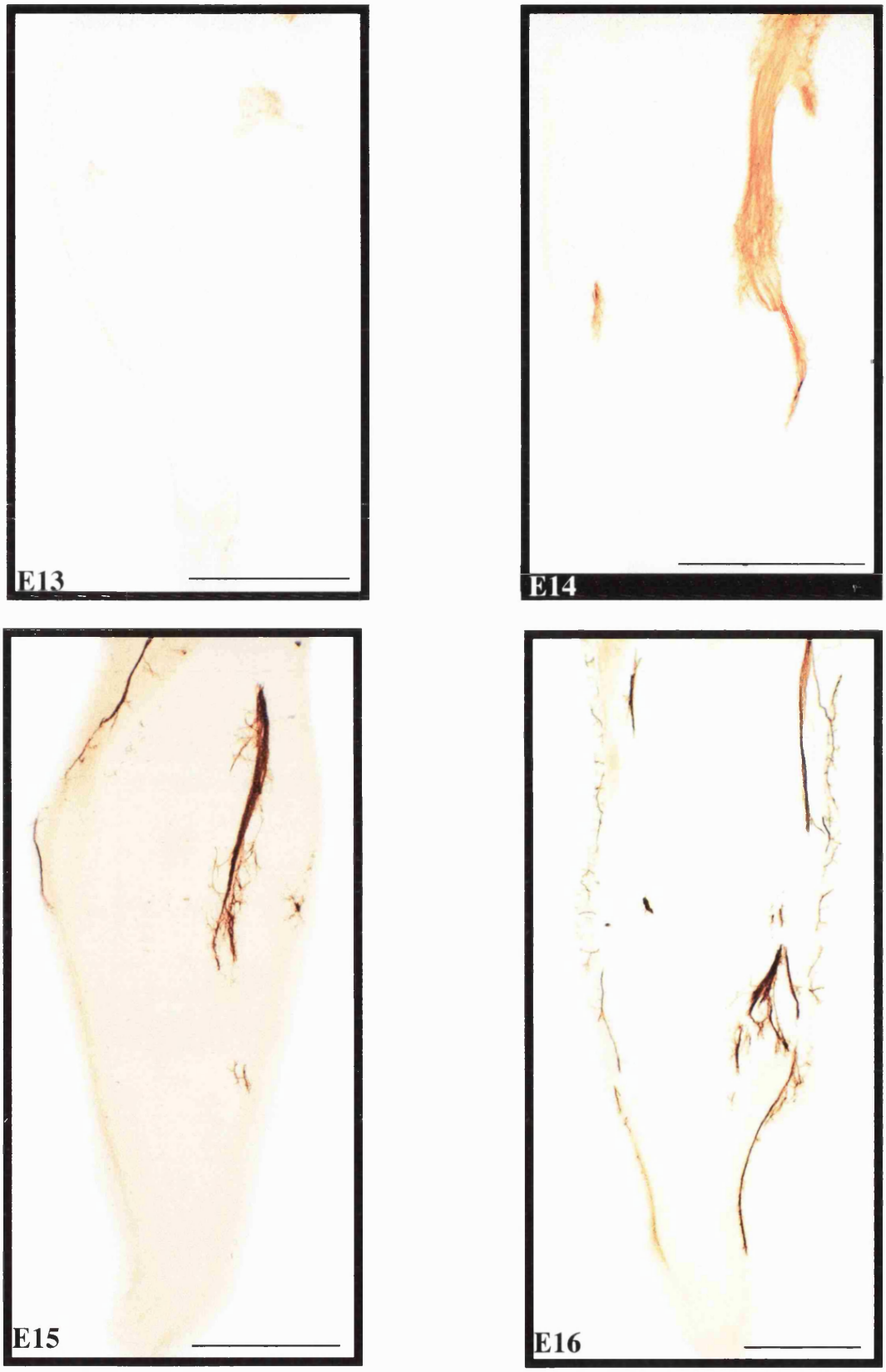

Fig. 4.2: GAP 43 labelling in the hindlimb of embryos aged E13-E16

Scale bar=500μm

Fig. 4.3: GAP 43 labelling in regions A-D of the hindlimb at E17 (top) and E18 (bottom)

In A, B, C and D of E17 the edge of the epidermis is marked with arrowheads. A dotted line separates the epidermis (E) from the dermis (D). The orientation of the region in relation to the hindlimb is indicated by the compass directions, L=lateral; M=medial; D=distal and P=proximal. In B a large nerve bundle (NB) is located along the epidermal-dermal border giving rise to perpendicular (P) branches. In C, axons ending in visible growth cones (GC) are circled.

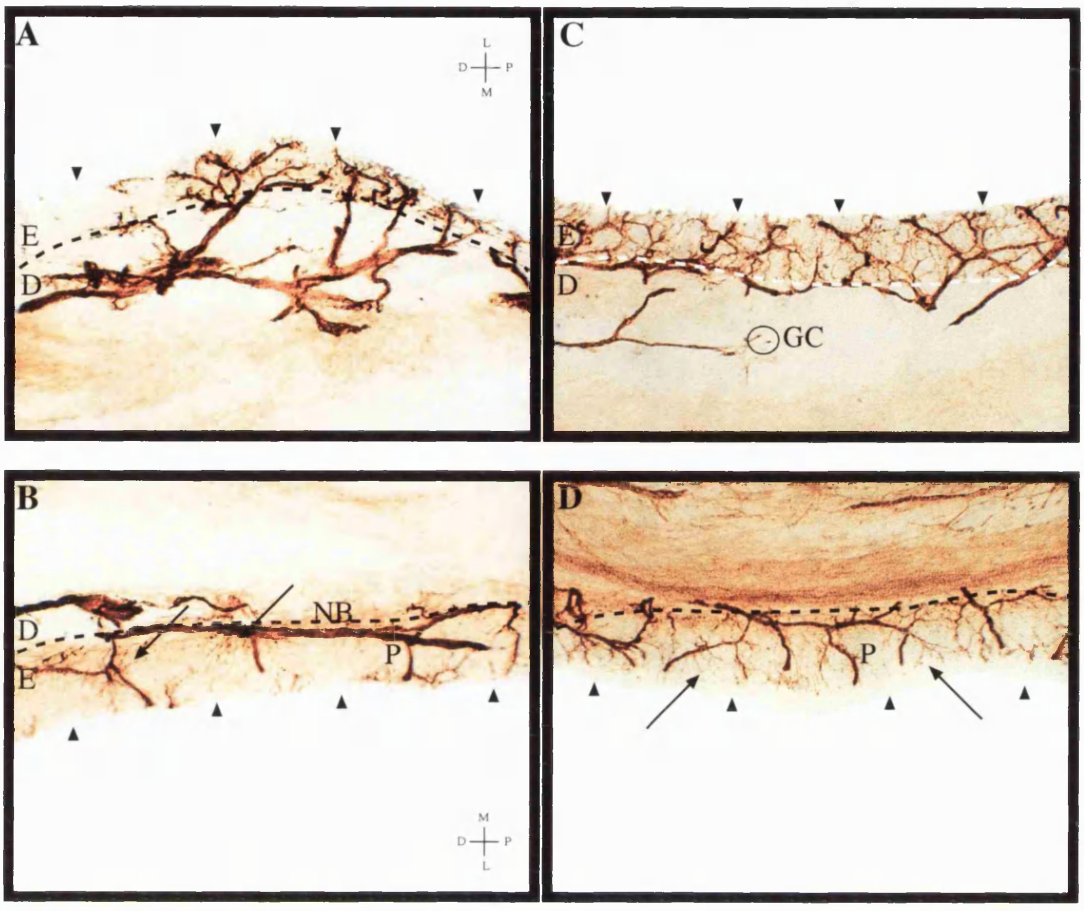
A
L
D
P
M
E
D
C
E
D
GC
B
D
NR
P
E
M
D
P
L
D
P

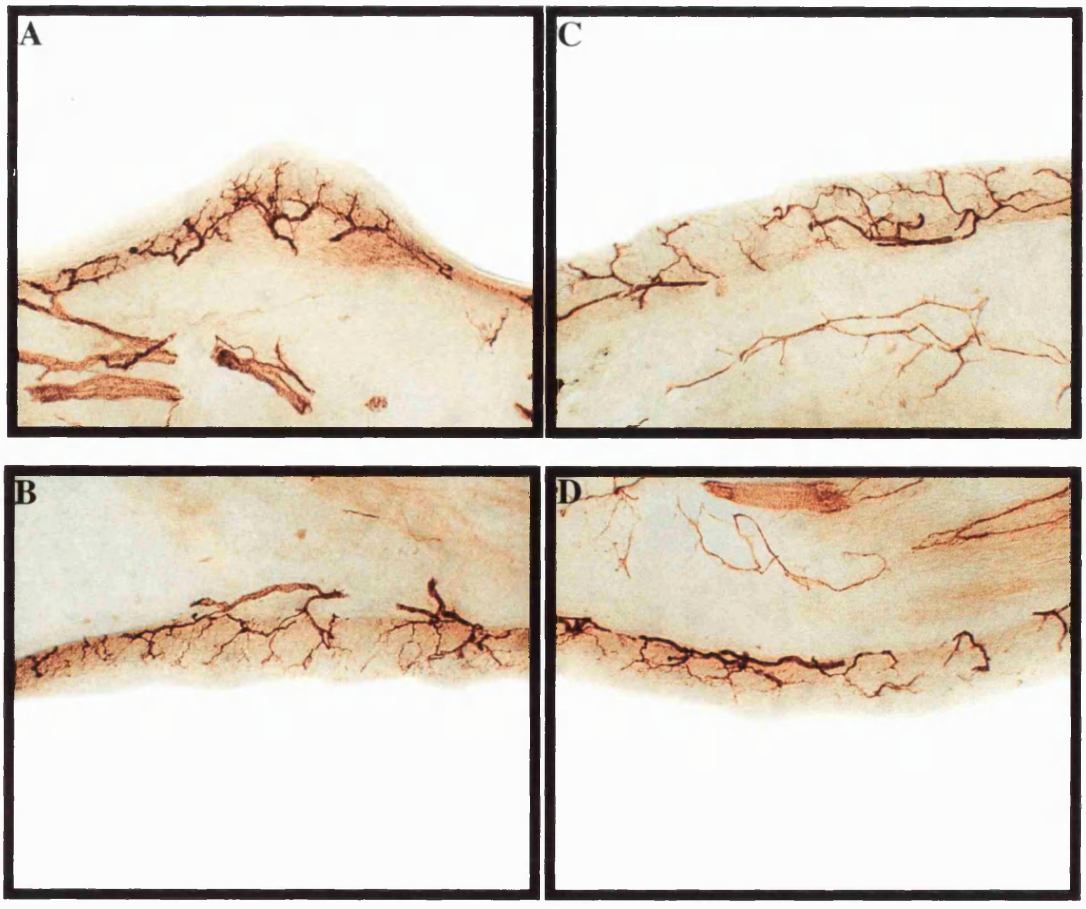
A
C
B
D

Fig. 4.4: GAP 43 labelling in regions A-D of the hindlimb at E19 (top) and E20 (bottom

Details as for legend of Fig. 4.3.

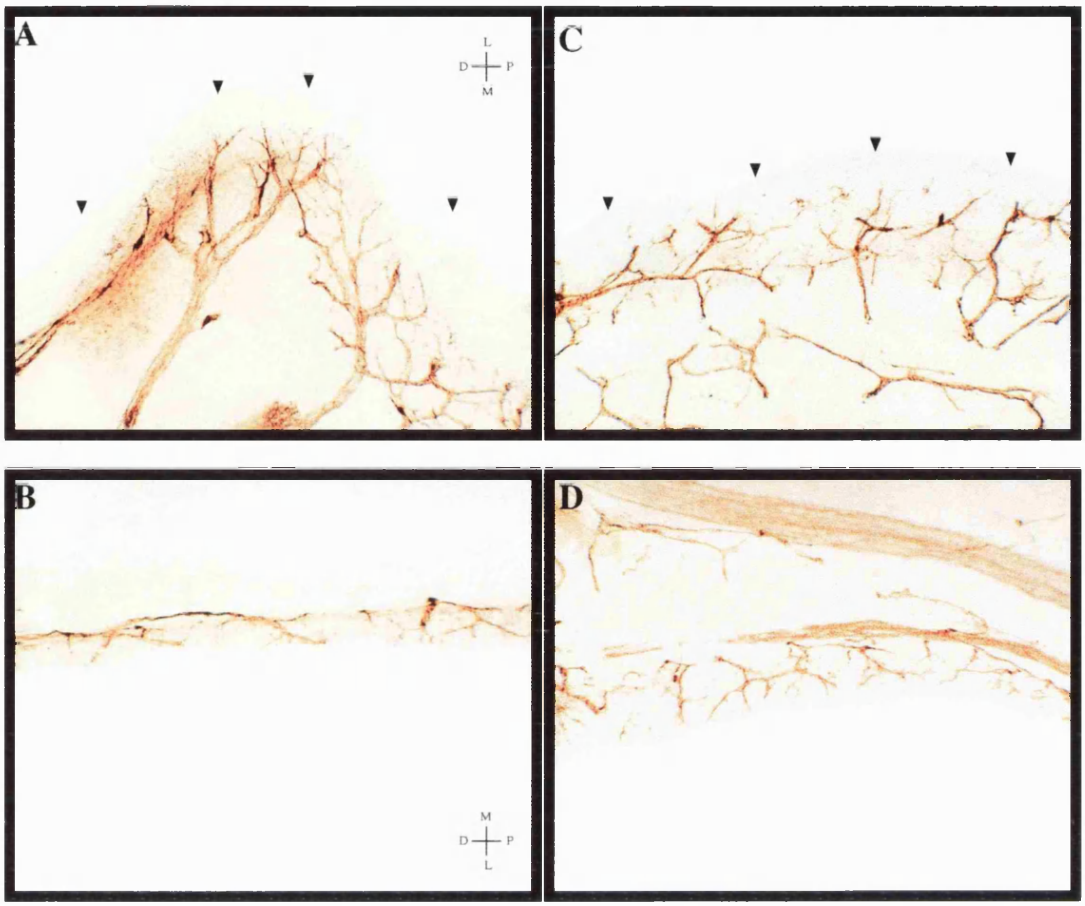
A
L
D
P
M
C
B
M
D
P
L
D

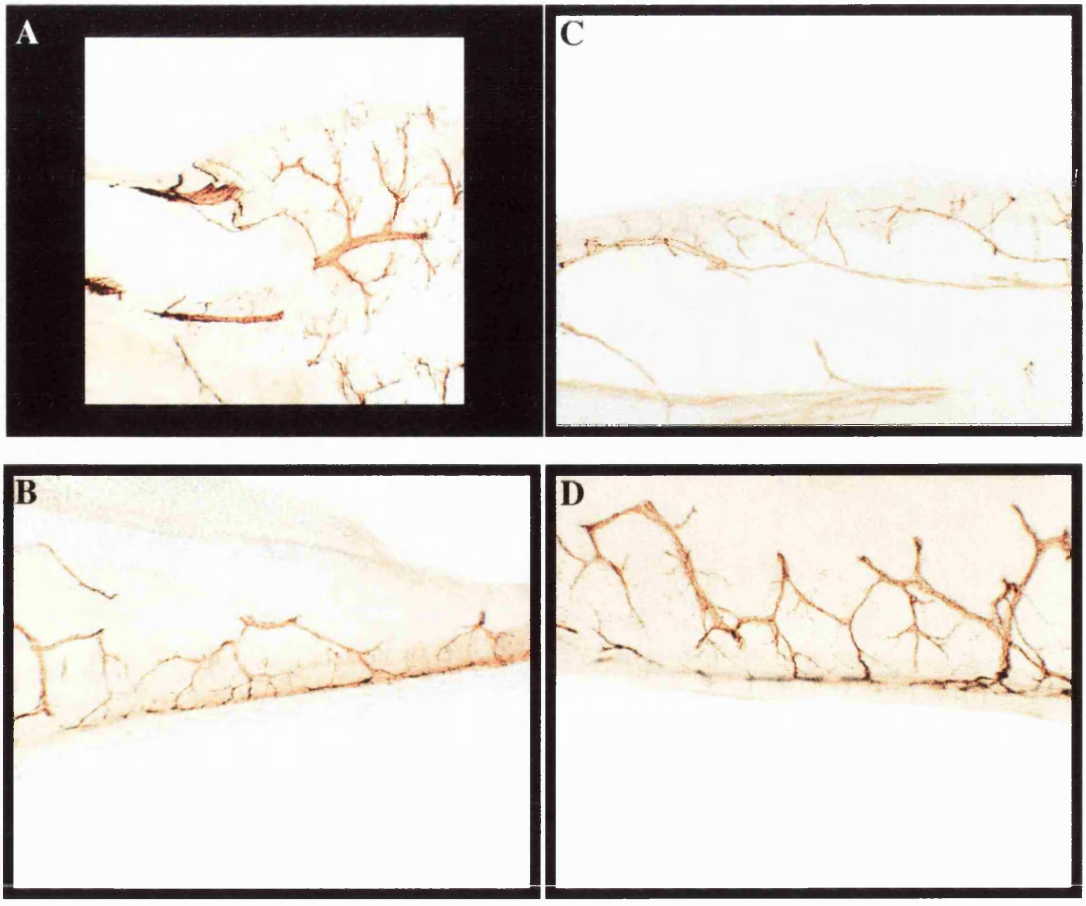
A
C
B
D

Fig. 4.5: PGP 9.5 labelling in spinal cord and DRG of embryos aged E13-E18 and E20.

Details as for legend of Fig. 4.3. In E17, cellular staining extending into the ventral horn is circled.

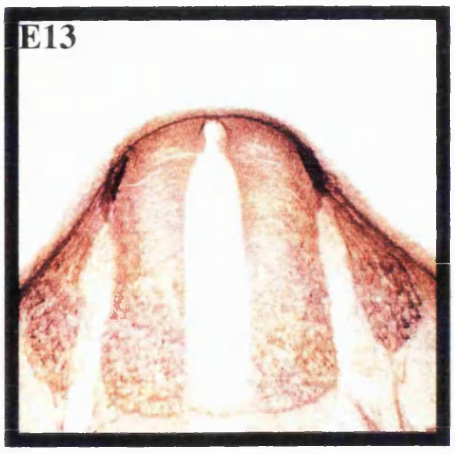
E13

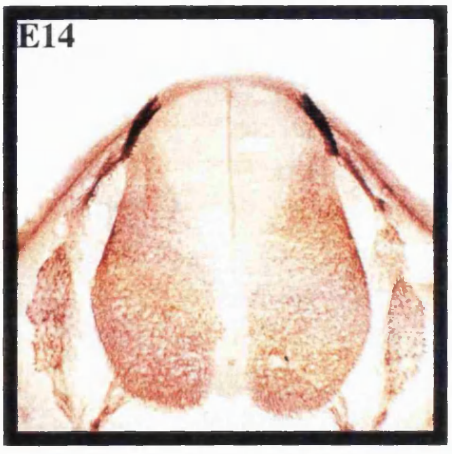
E14

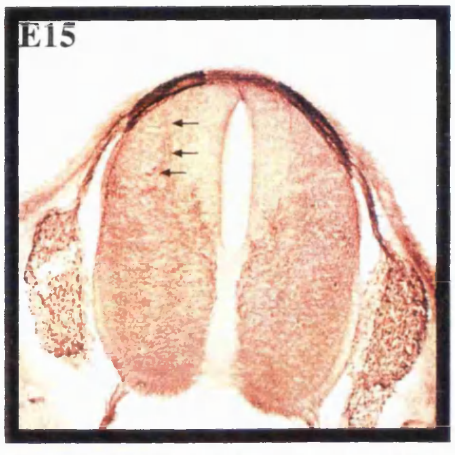
E15


E16

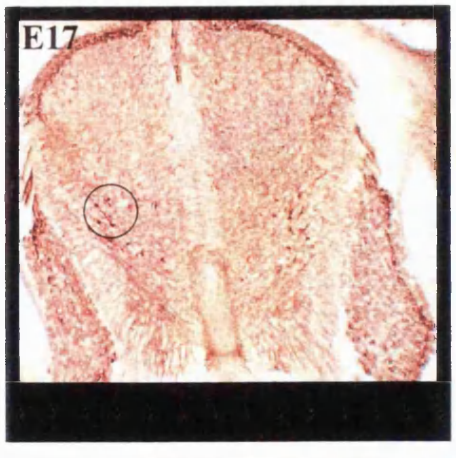
E17


E18

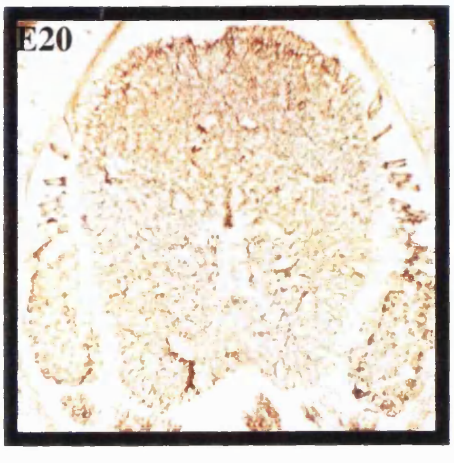
E20

Fig. 4.6: PGP 9.5 labelling in the hindlimb of embryos aged E14-E17.

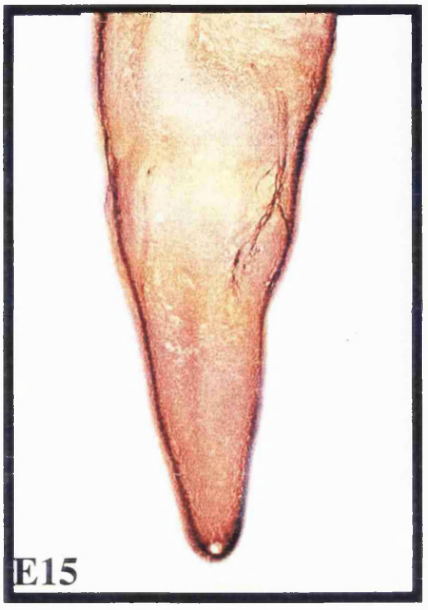
E15

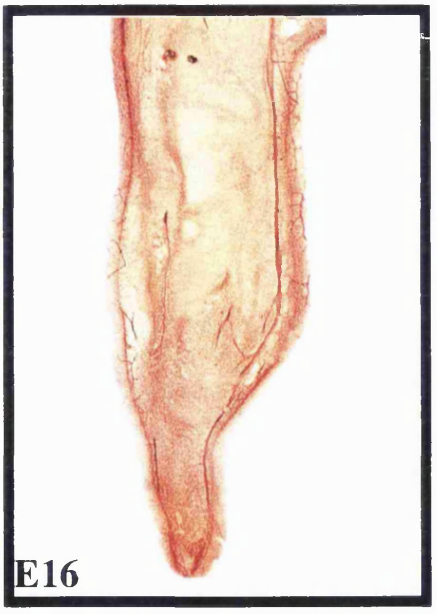
E16

Fig. 4.7: PGP 9.5 labelling in regions A-D of the hindlimb at E17 (top) and E18 (bottom).

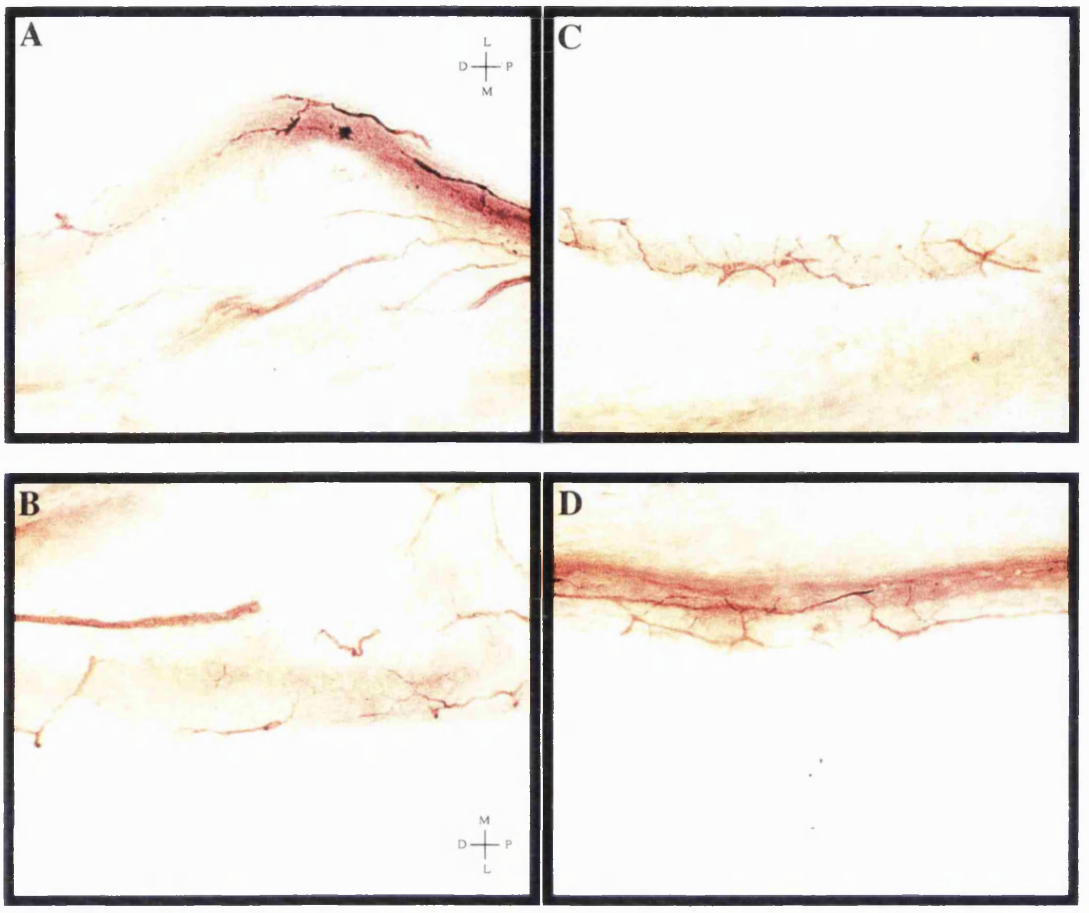
A
L
D
P
M
C
B
M
D
P
L
D

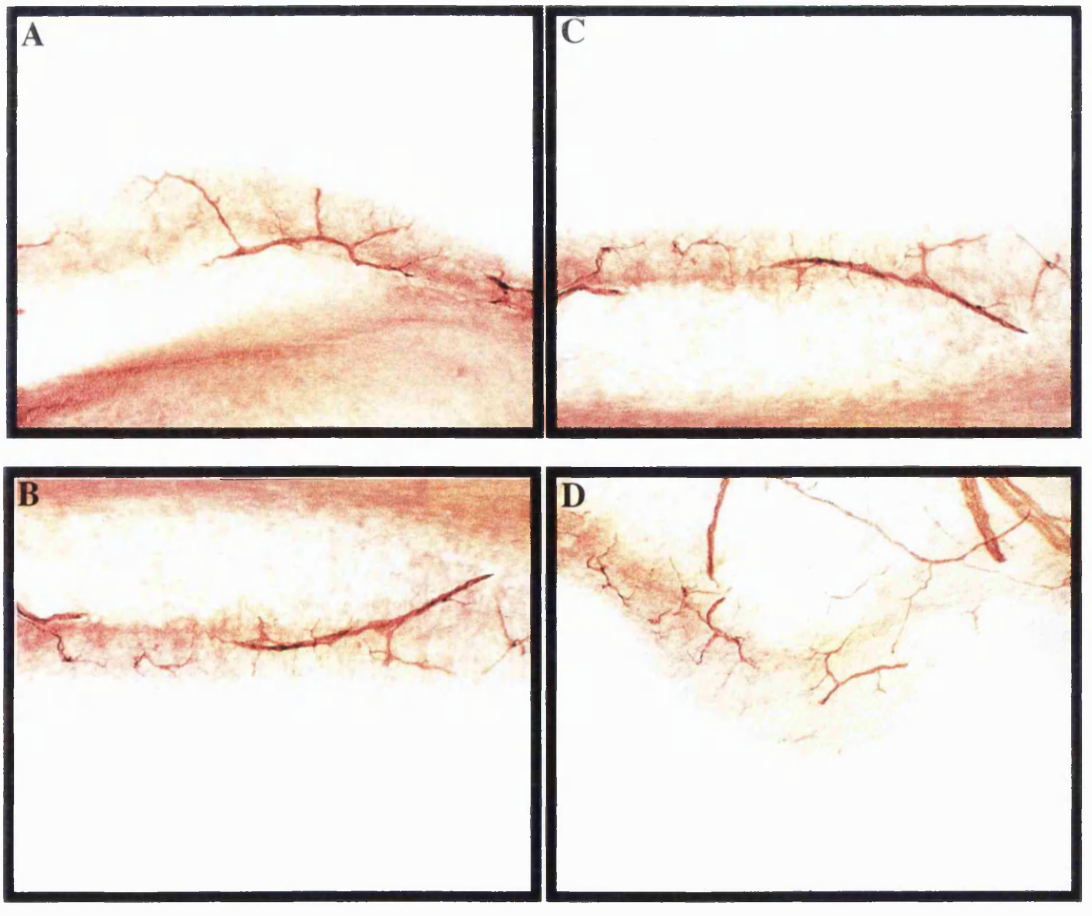
A
C
B
D

Fig. 4.8: PGP 9.5 labelling in regions A-D of the hindlimb at E20.

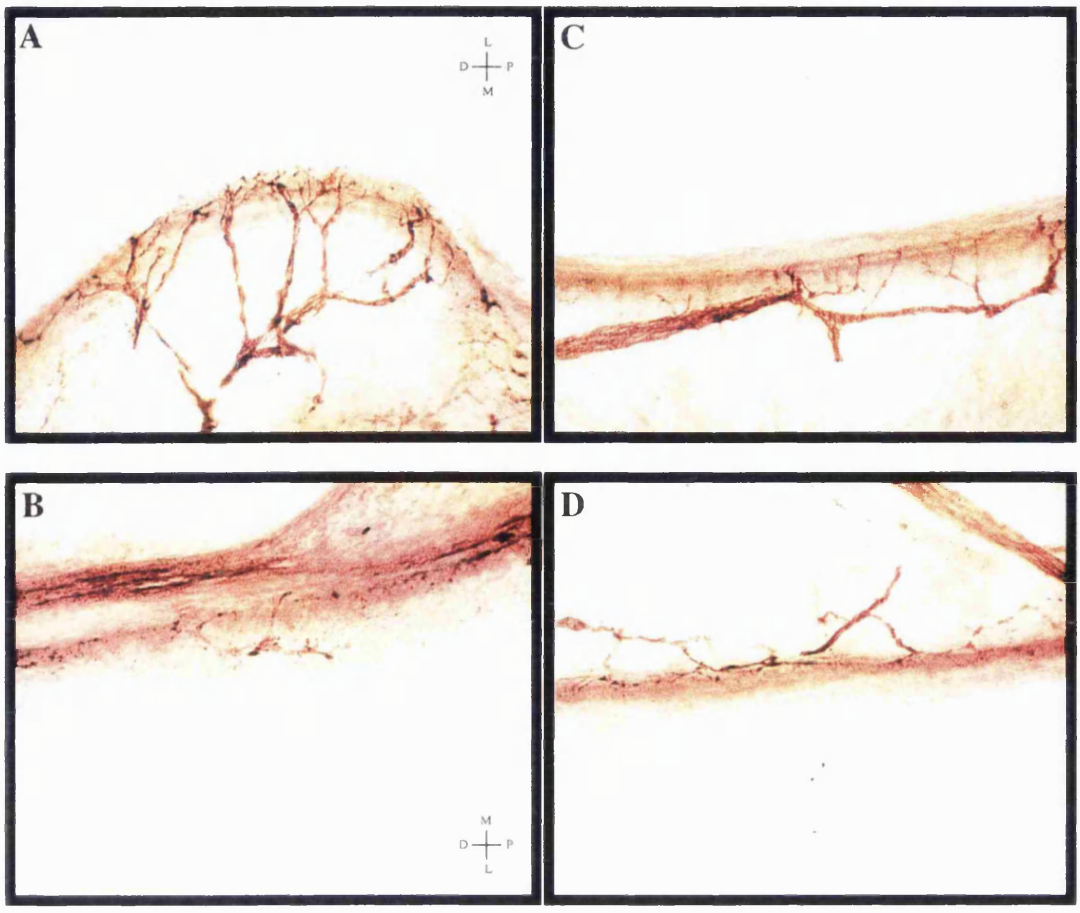
A
L
D
P
M
C
B
M
D
P
L
D

Fig. 4.9: Peripherin labelling in spinal cord and DRG of embryos aged E13-E19.

Main details as for legend of Fig. 4.1. In E14, the enlargement of the boxed area shows labelling of motoneurons. The asterisks in E15-E19 signify areas in the lateral dorsal horn where afferents are not found with this label.
In E17 the afferents directed towards the ventral horn begin to defasciculate, which continues as shown in E19. Also in E19, the dotted area delineates the superficial labelling and scale bar = 100μm.

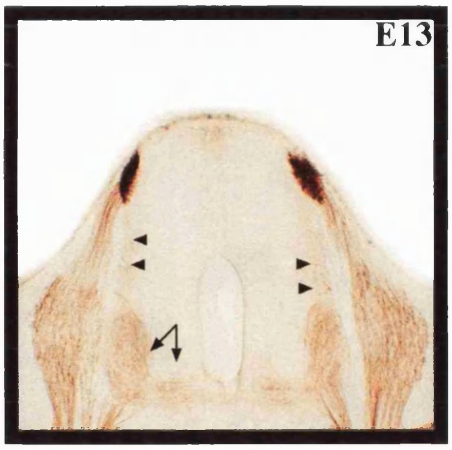
E13

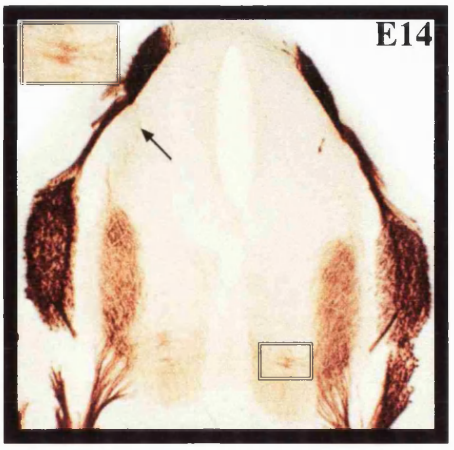
E14

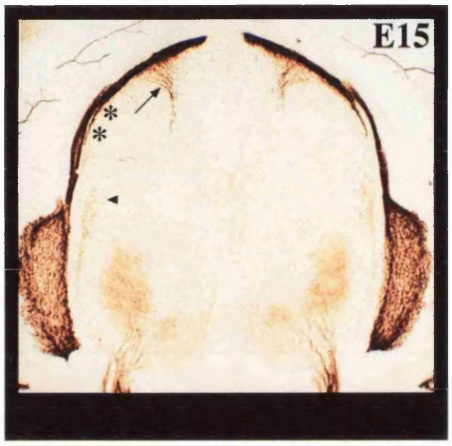
E15


E16


E17


E18

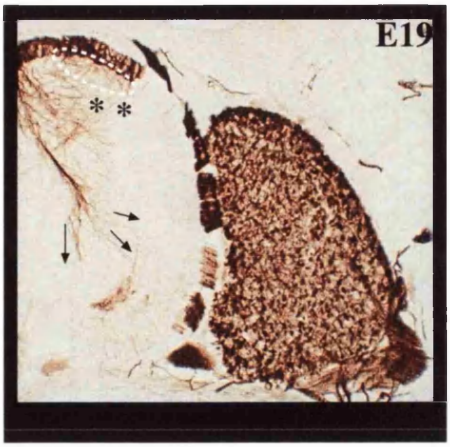
E19

Fig. 4.10: Peripherin labelling in the hindlimb of embryos aged E13-E16.

Main details as for legend of Fig. 4.2. In E13, peripherin labelling is found over presumptive muscle (PM), but cutaneous (C) branches are also evident. Growth cones are circled on axon terminals.


PM
C
C
E13


E14

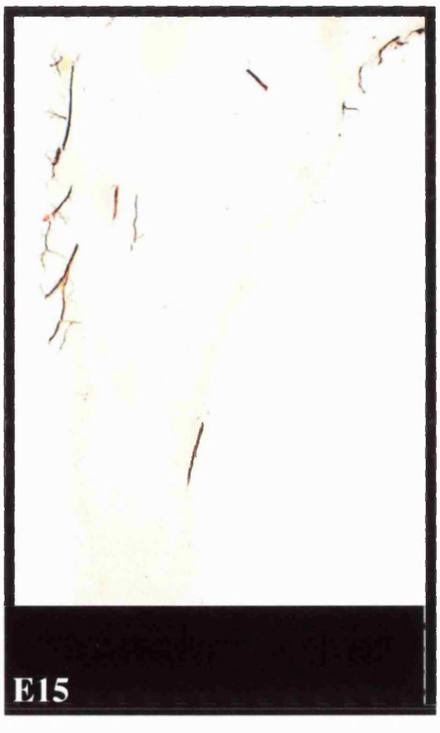
E15


E16

Fig. 4.11: Peripherin labelling in the hindlimb of embryos aged E17-E19.

Details as for legend of Fig. 4.3. Scale bar = 500μm.


E17


E18


E19

Fig. 4.12: Peripherin labelling in regions A-D of the hindlimb at E17 (top) and E18 (bottom).

Details as for legend of Fig. 4.4

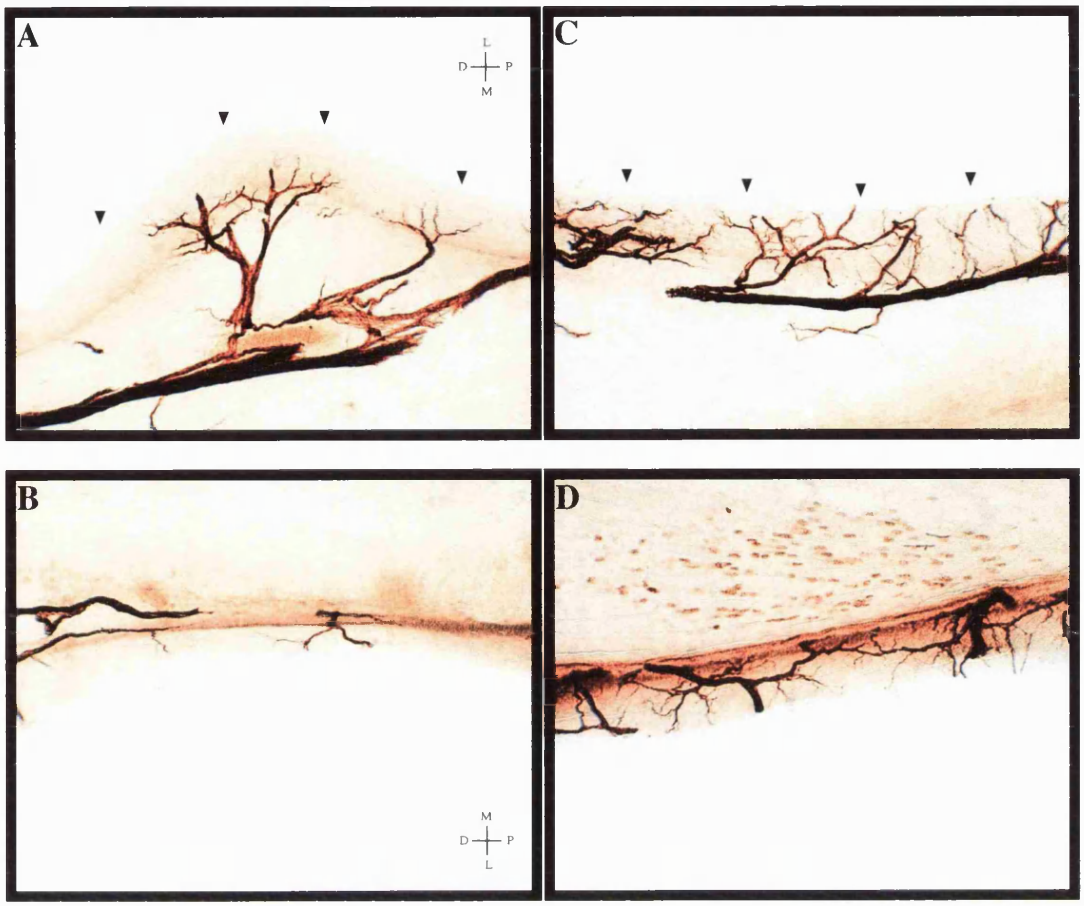
A
L
D
P
M
C
B
D
M
D
P
L


A
B
C
D

Fig. 4.13: Peripherin labelling in regions A-D of the hindlimb at E19 (top) and E20 (bottom).

Details as for legend of Fig. 4.4

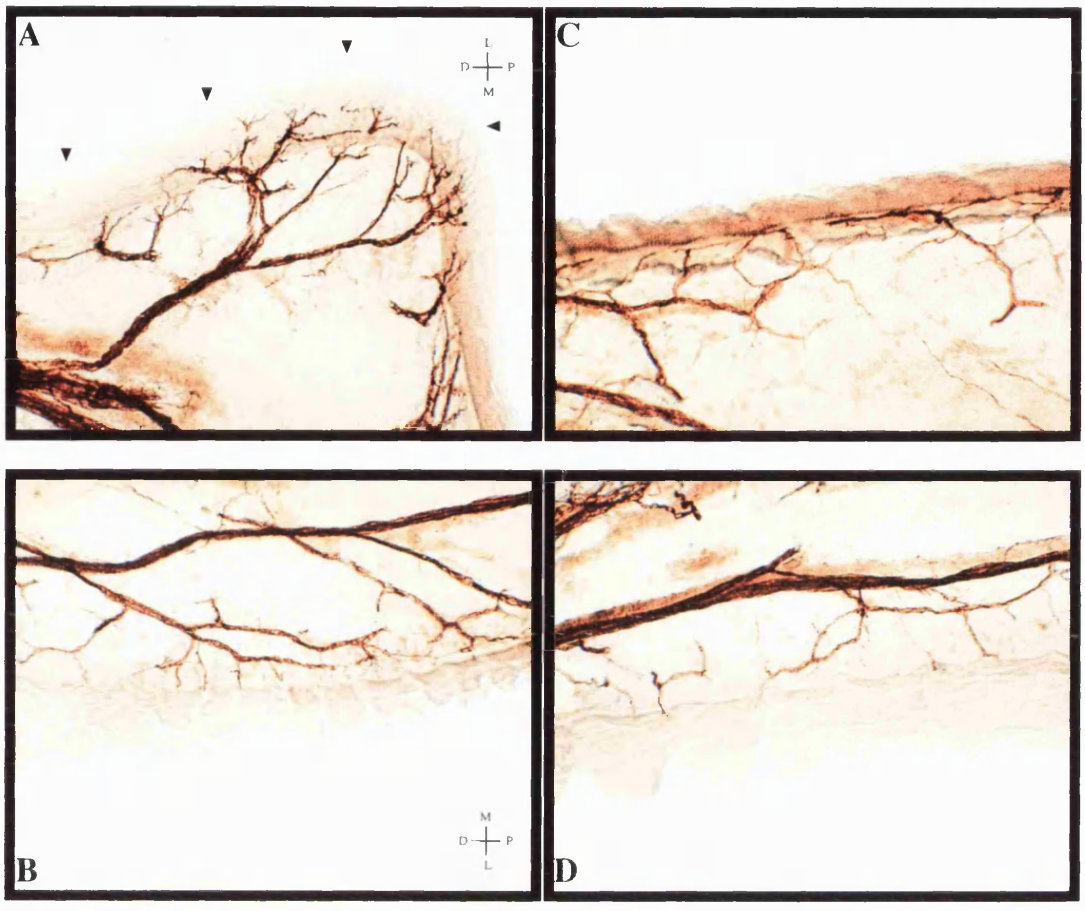
A
L
D
P
M
C
B
M
D
P
L
D

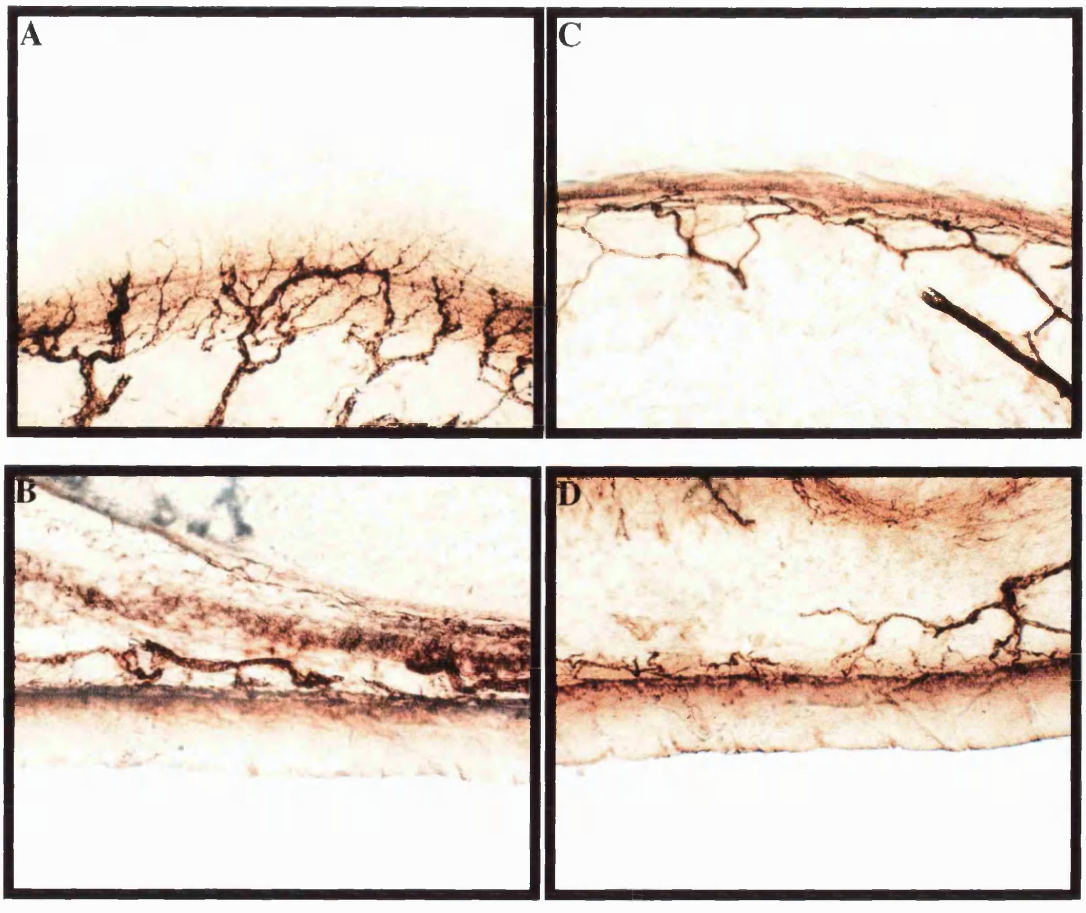
A
C
B
D

Fig. 4.14: RT97 labelling in spinal cord and DRG of embryos aged E13-E20.

Main details as for legend of Fig. 4.1. At E19 and E20, RT97 positive cells in the DRG are indicated by short arrows. Cytoplasmic labelling of these cells is clearly visible.


E13

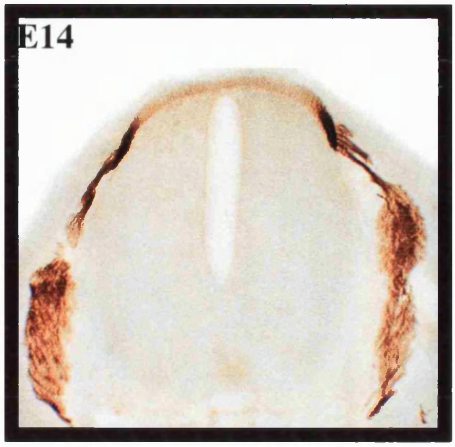
E14

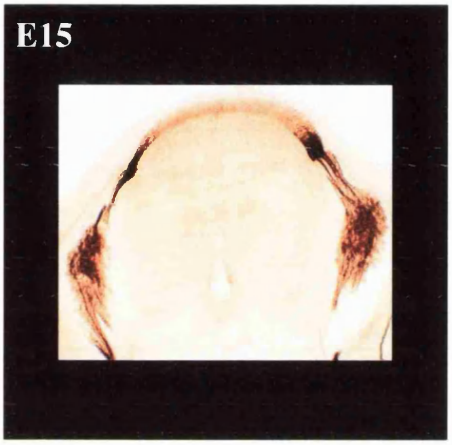
E15

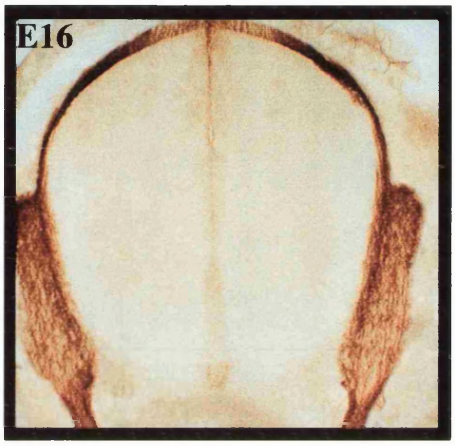
E16


E17

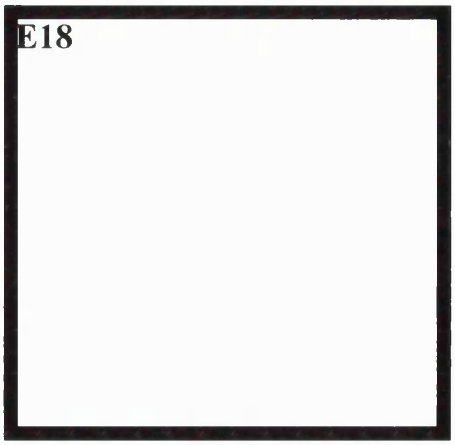
E18

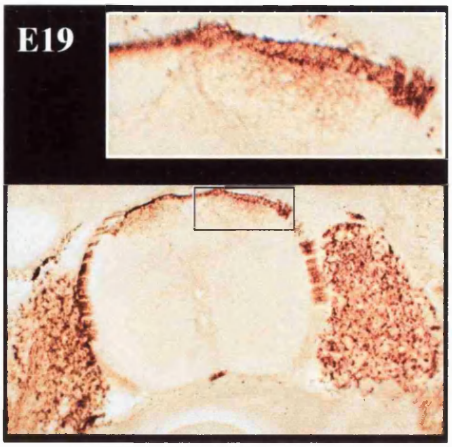
E19

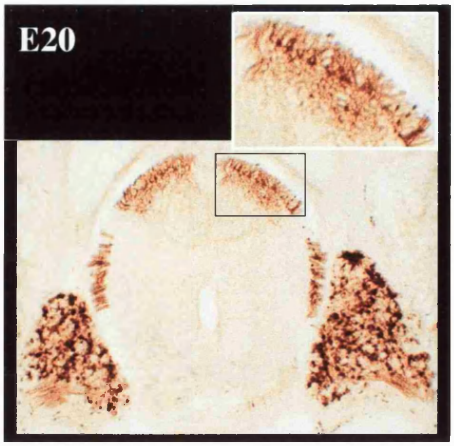
E20

Fig. 4.15: RT97 labelling in the hindlimb of embryos aged E14-E17.

Details as for legend of Fig. 4.2.


E14
P
L
M
D


E15

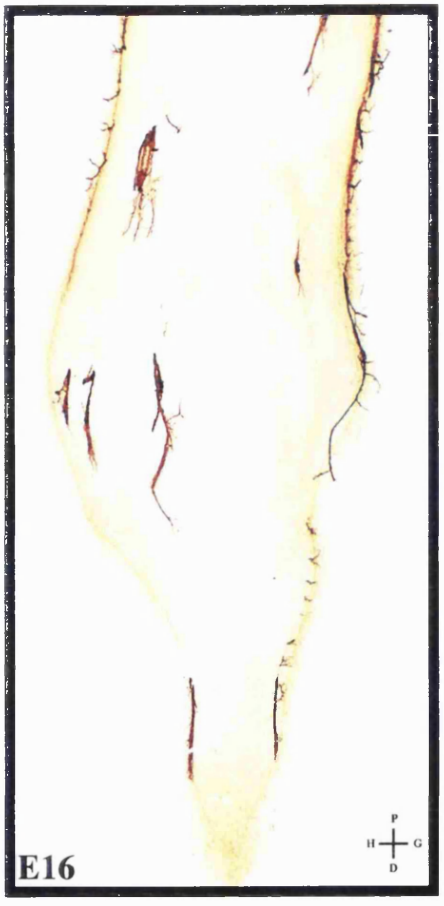
E16
P
H
G
D

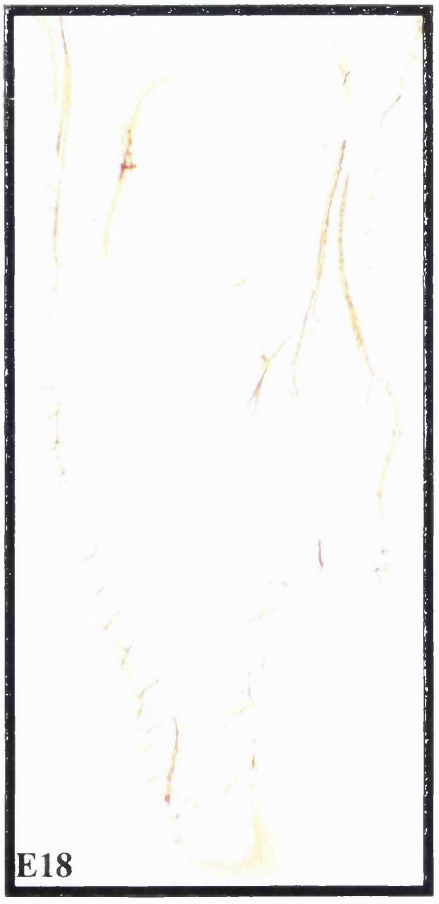
E18

Fig. 4.16: RT97 labelling in regions A-D of the hindlimb at E17 (top) and E18 (bottom).

Details as for legend of Fig. 4.3.

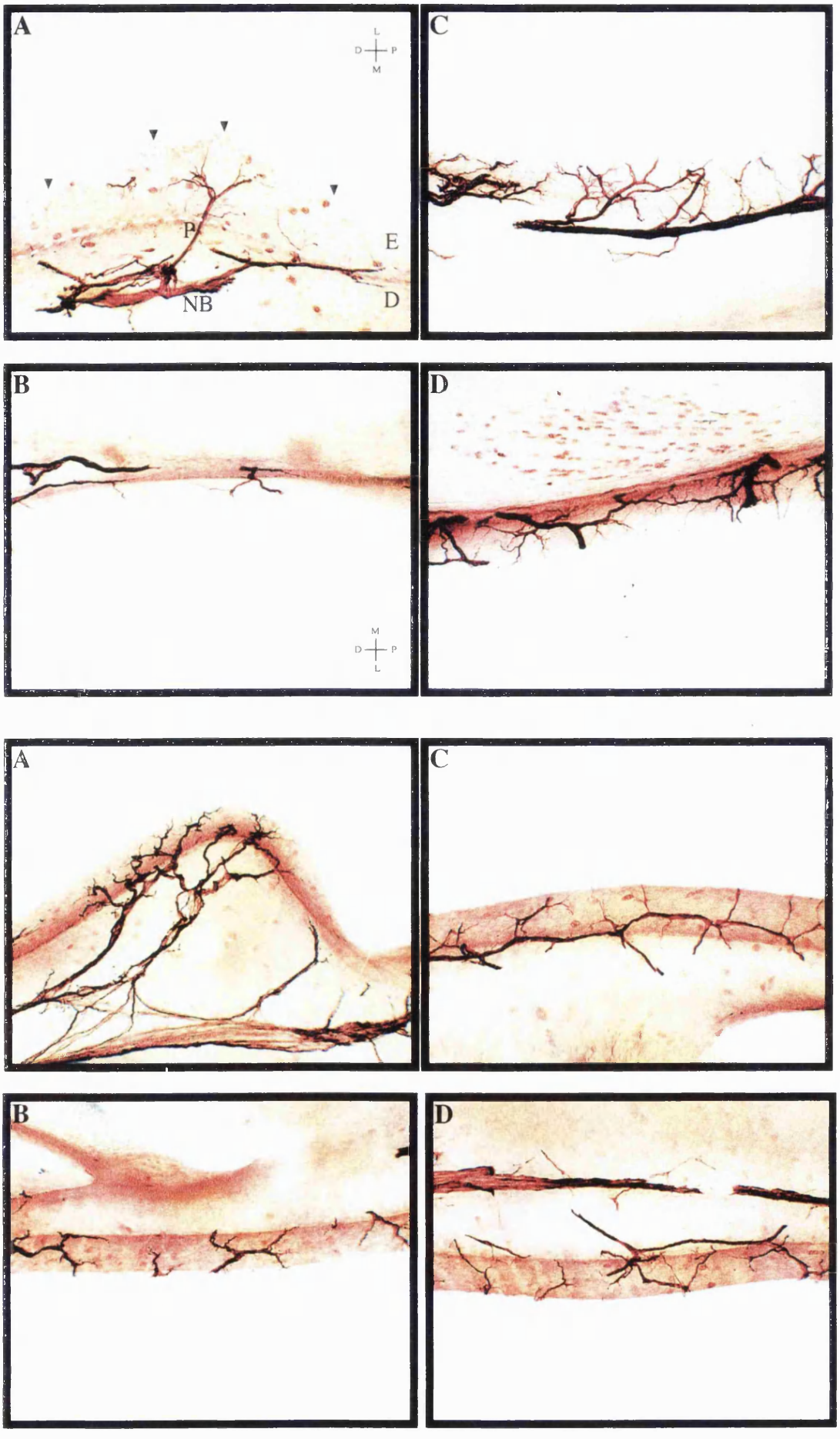
A
L
D
P
M
P
E
NB
D
C
B
M
D
P
L
D
A
C
B
D

Fig. 4.17: RT97 labelling in regions A-D of the hindlimb at E19.

Details as for legend of Fig. 4.3.

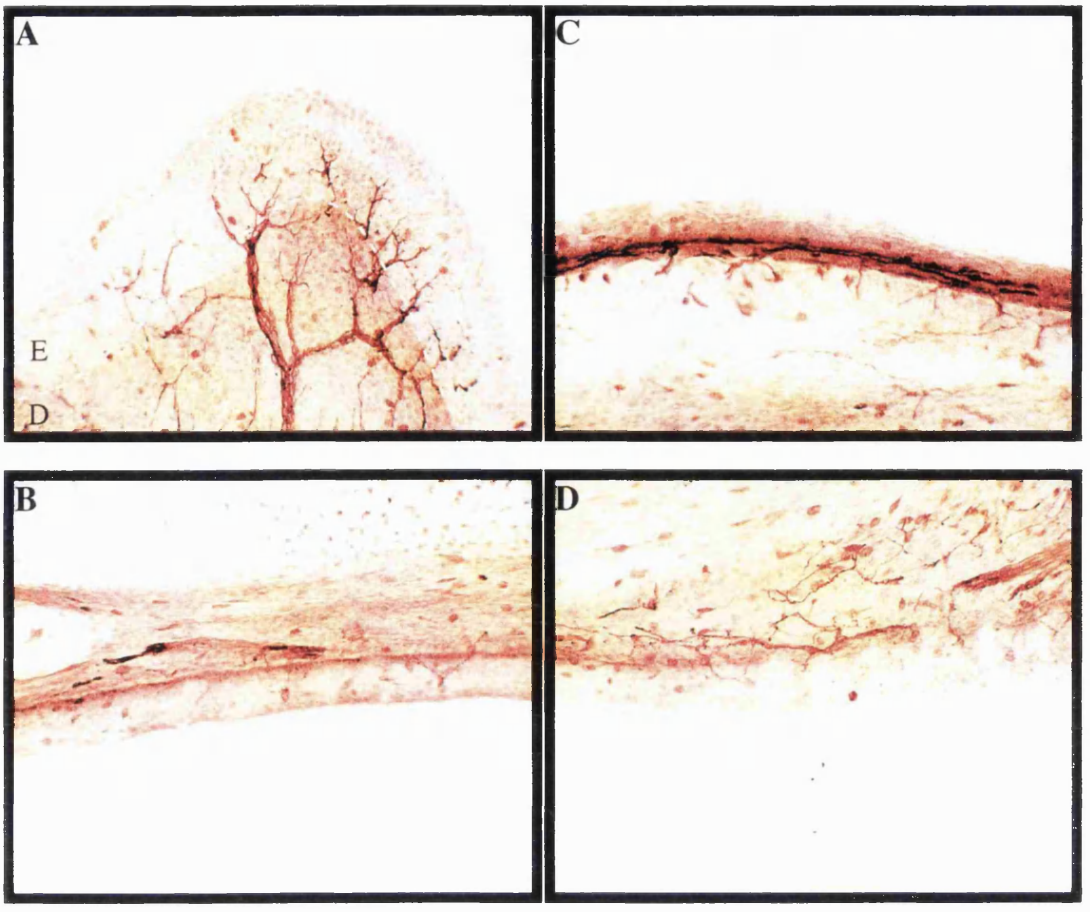
A
E
D
C
B
D

Fig. 4.18: TrkA labelling in spinal cord and DRG of embryos aged E13-E16, E19 and E20.

Details as for legend of Fig. 4.1. In E19 and E20 enlargements of the boxed areas show establsihed labelling of the superficial dorsal horn.


E13


E14

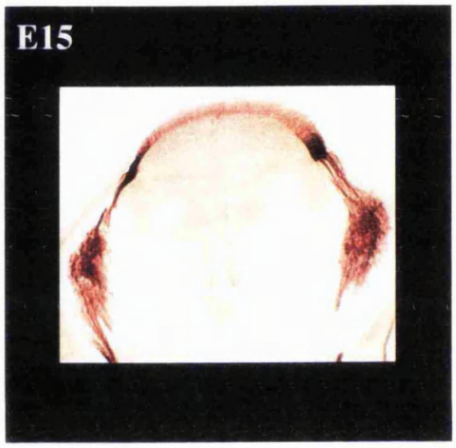
E15

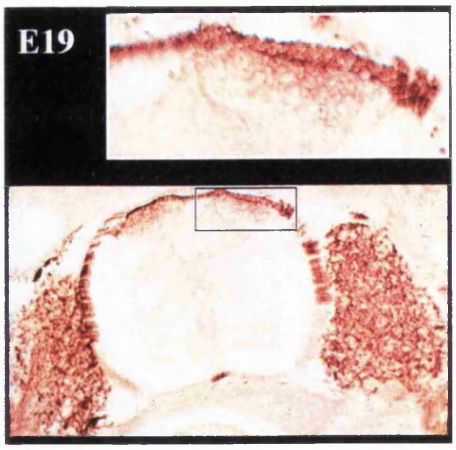
E19

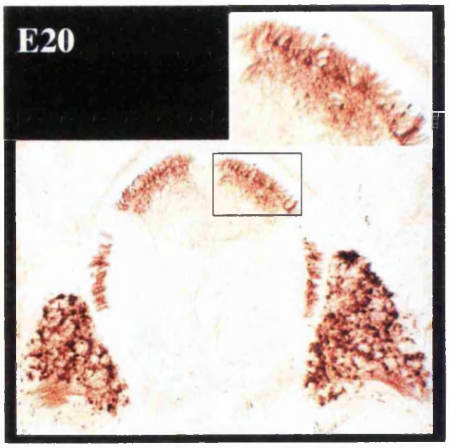
E20

Fig. 4.19: TrkA labelling in the hindlimb of embryos aged E13-E16.

Details as for legend of Fig. 4.2.


E13


E14


E15

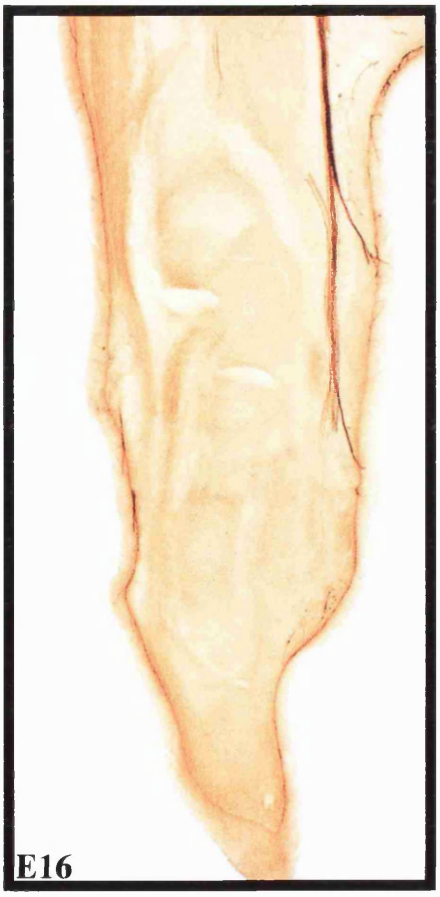
E16

Fig. 4.20: TrkA labelling in regions A-D of the hindlimb at E17 (top) and E19 (bottom).

Details as for legend of Fig. 4.3


A
L
D
P
M
E
D
B
C
M
D
P
L
D

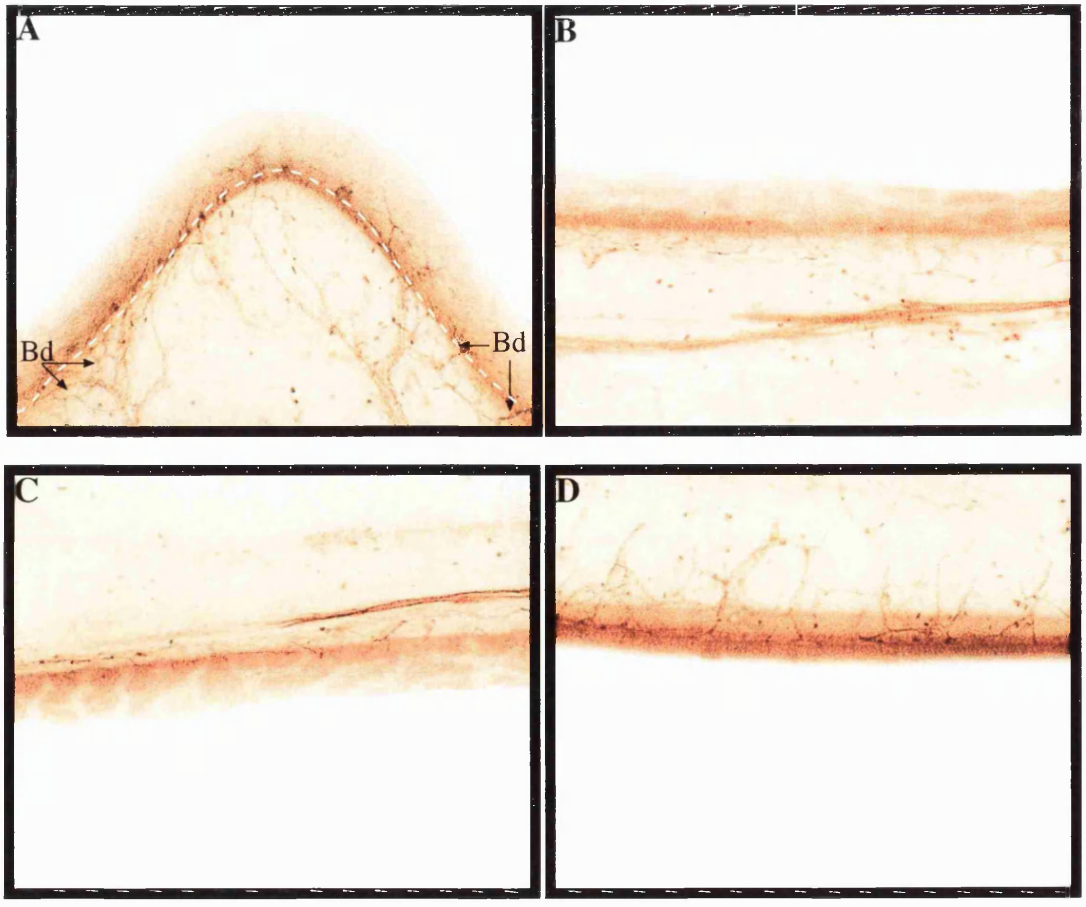
A
Bd
Bd
B
C
D

Fig. 4.21: CGRP labelling in spinal cord and DRG of embryos aged E14-E19.

Main details as for legend of Fig.1. In E17, the enlargement of the boxed area shows a labelled motoneuron cell body. The first immunoreactive DRG cells are also circled in E17 and E18.
In E19, the dotted line delineates labelling in the superficial dorsal horn. The short arrow points to motoneurons while the curved arrows shows some afferent fibres in the dorsal horn.

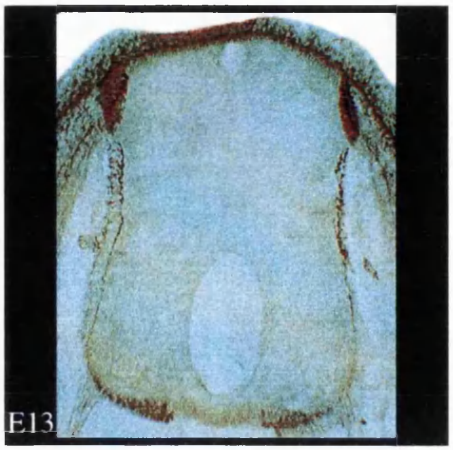
E13


E15


E16


E17


E18


E19

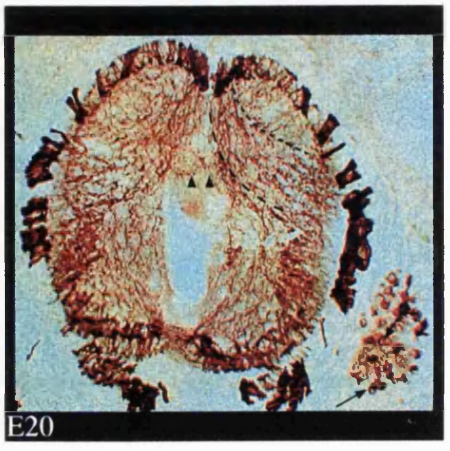
E20

Fig. 4.22: CGRP labelling in the hindlimb of embryos aged E18 and E19.

E17 is a higher magnification (x20) of a region in the proximal hindlimb. Arrowheads show the surface of the skin. Arrows define the path of a CGRP-immunoreactive (IR) fibre, which terminates in a circled growth cone (GC). In E18, arrows point to CGRP-IR fibres but none of these are present in skin until E19.

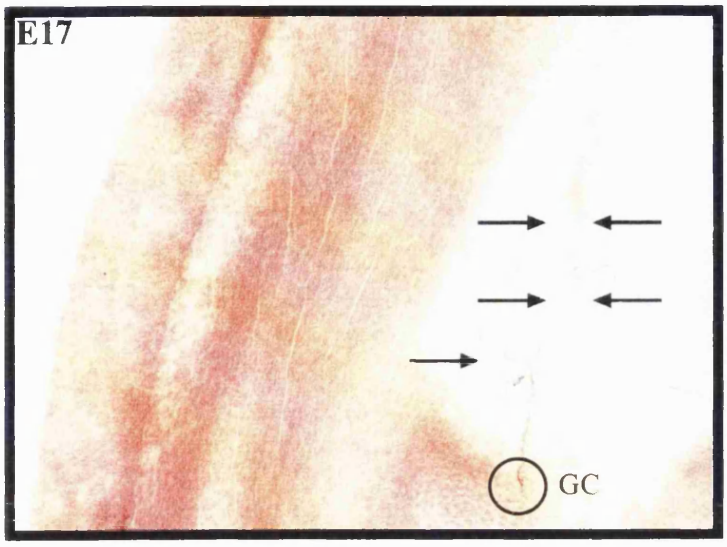
E17
GC

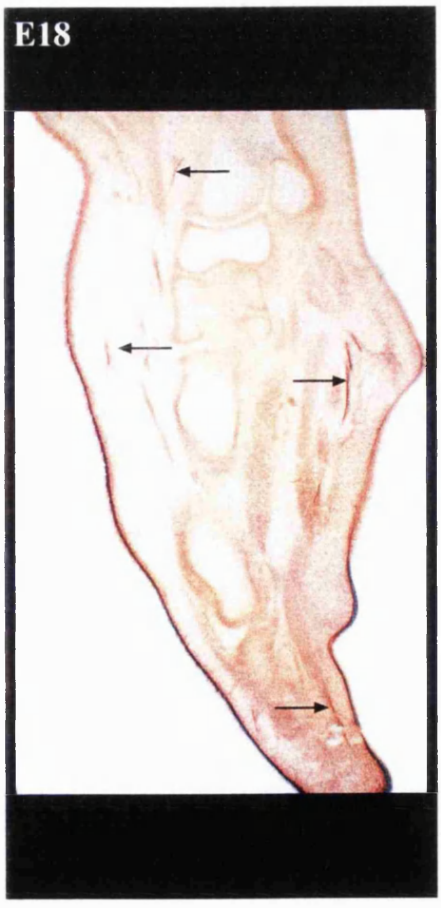
E18

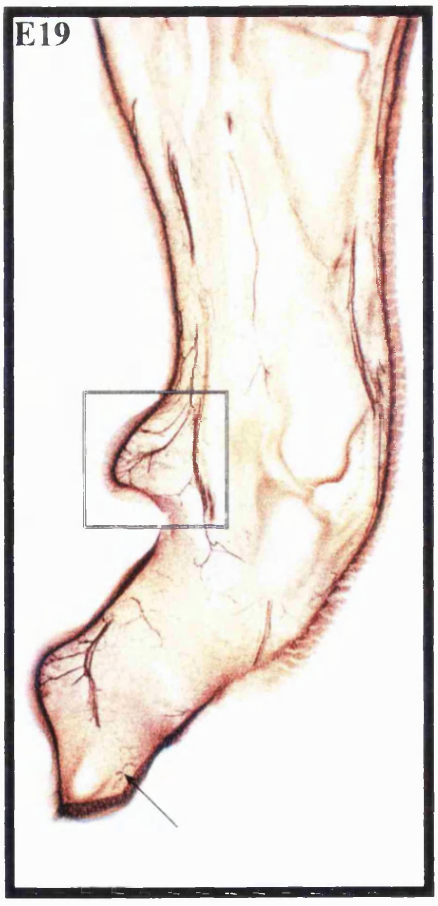
E19

Fig. 4.23: CGRP labelling in regions A-D of the hindlimb at E19.

Main details as for legend of 4.3. In region C the enlargement of the boxed area shows beaded fibres extending into the epidermis.

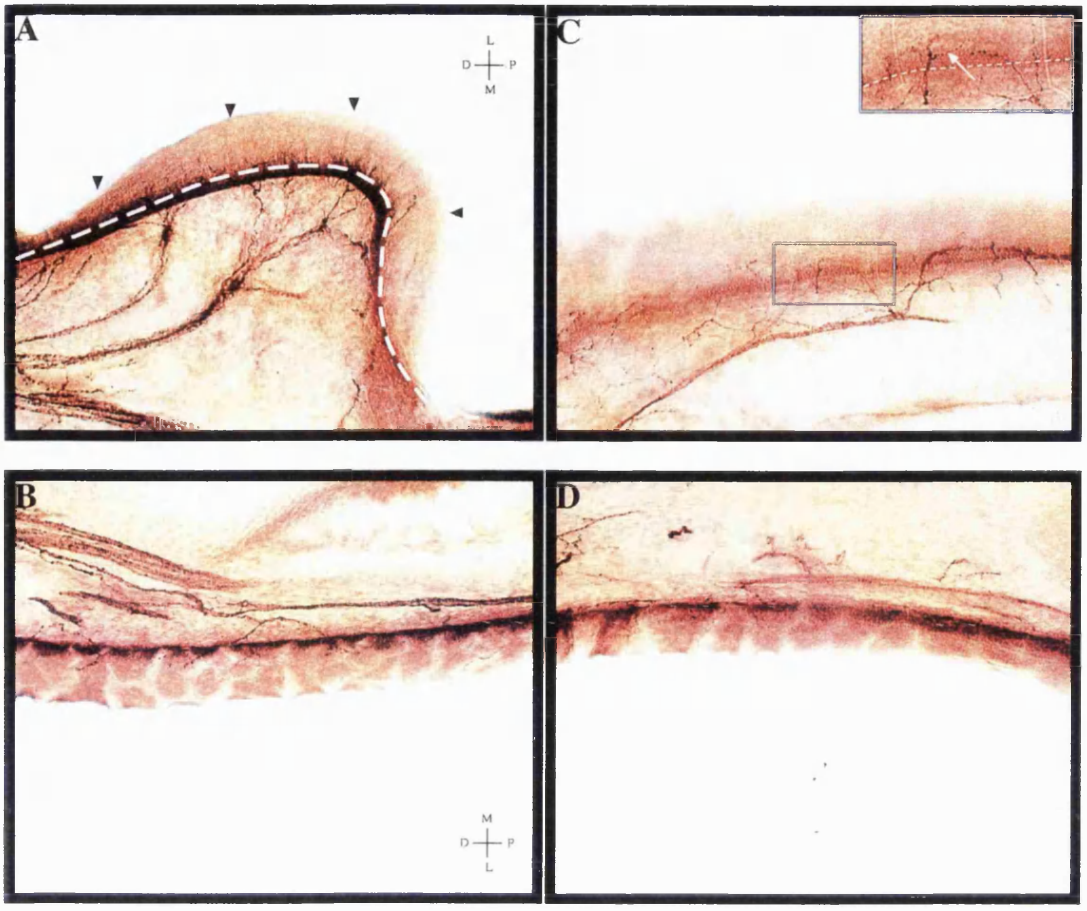
A
L
D
P
M
C
B
M
D
P
L
D

DISCUSSION

Previous studies examining the development of innervation in the periphery have not used markers selective for each of the DRG subpopulations (Honig, 1982; Scott, 1987; Wessels et al, 1990; Reynolds et al, 1991; Mirnics & Koerber, 1995a). This has meant that the onset and patterns of innervation have been described but there has been no discrimination between A and C-fibres. This study describes the timecourse of innervation for neuronal subpopulations and is achieved using a series of general and selective markers. The innervation of the spinal cord was also examined using the same markers and the relationship between central and peripheral innervation described.

The results of the developmental timecourse have revealed that the A-fibre phenotype is included in the earliest innervation of the hindlimb, as defined by RT97 labelling. The involvement of C-fibres, however, is less clear. Central innervation is detected earlier than in previous studies and follows a sequential pattern of collateral growth relating to each sensory subpopulation. The onset and pattern of central innervation corresponds to specific events occurring in the periphery.

4.19 Do A-fibres reach the peripheral target prior to C-fibres?

RT97 has been confirmed to label large diameter fibres during development (Chapter 3), in addition to the adult rat (Lawson et al, 1984). Most of the small diameter fibre labels are not expressed however, during early development or their expression is not appropriately selective. This situation means that only one remaining small fibre marker, trkA, was a suitable candidate for inclusion in this study. TrkA labelling was found in the periphery in the same timeframe as the earliest innervation, but this result is ambiguous as the presence of trkA does not automatically mean that C-fibres were labelled.

TrkA is expressed in 40-50% of adult DRG cells (Verge et al, 1992; Mu et al, 1993; McMahon et al, 1994; Wright & Snider, 1995; Molliver et al, 1995; Averill et al, 1995; Bennett et al, 1996b) and from co-expression data, these cells are in the size range of CGRP expressing cells (Verge et al, 1989; Crowley et al, 1994; Averill et al,

1995; Silos-Santiago et al, 1995). In development, 70-80% of cells express trkA (Verge et al, 1989; Averill et al, 1995; Bennett et al, 1996b), though a recent study has shown that the extra 30% of trkA expressing cells become IB4 positive postnatally (Bennett et al, 1996b). This indicates that during development, trkA is probably expressed in cells of CGRP size range, and additionally, cells in the IB4 positive size range which are of small diameter (Silverman & Kruger, 1988).

This leaves three feasible options as to the phenotype of fibres labelled by trkA: Firstly, there are no C-fibres and trkA is merely labelling a small proportion of A-fibres that are found in the CGRP size range. CGRP is predominantly found in small-medium sized cells, however, it labels some 25% of A-fibre cells (McCarthy & Lawson, 1990). Secondly, trkA is labelling the fibres from the 30% of DRG cells that become IB4 positive and are non-peptidergic. Thirdly, trkA labels small fibres that will become peptidergic but are not expressing peptides yet because the target influences are not switched on.

The most favourable explanation is that trkA is labelling small diameter non-peptidergic C-fibres. The reasons for this are nonetheless complex. Evidence supporting the first option is limited to the knowledge that in the adult the trkA size distribution overlaps with CGRP, which labels some A-fibres, and by deduction trkA must also label A-fibres. More convincingly, it is known that trkA is co-expressed with RT97 in 18% of DRG cells (Averill et al, 1995). However, neither CGRP nor trkA size distributions have been determined during development. The trkA labelling is sparse compared to other markers, which could be interpreted as labelling a few A-fibres but it is known that trkA cell bodies are very heavily labelled in comparison to their central axons (Molliver at al, 1995) and this could equally apply to the peripheral terminals. The fact that trkA labelled fibres are found in the periphery three days before their appearance in the SG also favours the possibility that it may label A-fibres, yet trkA is not found anywhere in the dorsal horn characteristic of A-fibre terminations and these may still be C-fibres waiting to grow ino the spinal cord. The final reason for discounting the first proposition is that the sudden appearance of peptidergic labelling at

E19 throughout the hindlimb, suggests that the C-fibres were resident before E19 and that peptide expression was rapidly induced.

Evidence supporting the latter options is much stronger therefore trkA posistive fibres could be part of the IB4 group or future peptidergic fibres, it is simply not possible to tell. The pattern of trkA labelling is consistent with that of small diameter fibres, particularly in the skin and the fine calibre of the fibres. I have shown that peptidergic labelling, as defined by CGRP, is not detected in skin until E19. This event is coupled to a large increase in the expression of trkA in the skin, suggesting that trkA now encompasses these CGRP fibres. This also implies that trkA was not previously labelling fibres in the CGRP size range. Moreover, the fact that trkA would label fibres later destined to become IB4 positive is not an unfeasible concept, since IB4 is a surface marker of C-fibres, and therefore is a structural component comparable to RT97, and may be one of the reasons it is detectable prior to peptide expression. In addition, trkA is not found terminating over muscle in this study and it is known that IB4 labelling of small unmyelinated fibres is exclusive to those innervating skin (Plenderleith et al, 1992).

This explanation raises interesting questions as to when the C-fibres that express peptides are found in the hindlimb. There are two possibilities. Firstly, all C-fibres are established and express trkA. They are then able to utilise NGF to trigger induction of peptides in a selective population, this is consistent with the rapid diminution of trkA labelling soon after peptide expression commences.

The second implies that the chemical differentiation of DRG neurons is intrinsic, some early C-fibres will remain non-peptidergic and postnatally will switch expression from trkA to IB4. This is followed by a second wave of C-fibres which will become peptidergic after reaching their target. This theory is particularly attractive because of information derived from a recent neurogenesis study (Kitao et al, 1996). This determined that contrary to previous reports (Lawson et al, 1974; Altman & Bayer, 1984) three separate neuronal populations are generated during development. The first are large RT97 positive cells, the second are small IB4 positive cells and the third are

also small, but both RT97 and IB4 negative. The authors suggested the third population may be peptidergic. In this context, the currently accepted view that large DRG cells are born before small DRG cells and that large A-fibres enter the CNS prior to small C-fibres is still perfectly valid, the small DRG cell population and C-fibres have merely been sub-classified according to the sequence of development. Nonetheless, although this theory reinforces the possibility that trkA is labelling non-peptidergic C-fibres from the outset of hindlimb development, the stage at which peptidergic fibres occupy the hindlimb is unresolved. A realistic timeframe for peptidergic C-fibre arrival can be deduced by examination of the other immunohistochemical markers both peripherally and centrally.

DRG axons reach their peripheral target in advance of their central target, hence if non-peptidergic C-fibres reach the hindlimb before peptidergic fibres then they should also reach the central target in advance of peptidergic fibres. My results show that trkA labelling is found in the lateral substantia gelatinosa (SG) at E17. By E18, the trkA labelling has extended to the medial SG and IB4 is found in the same location. This indicates that ingrowth of non-peptidergic small diameter afferents begins at E17, in advance of peptidergic labels, if my assumption that trkA is labelling non-peptidergic fibres is correct. At E19, CGRP is found in the muscle and skin of the complete hindlimb and simultaneously in the substantia gelatinosa of the spinal cord. This demonstrates that peptide expression was switched on concurrently in the central and peripheral target, but that the central afferents must have penetrated the SG at least one day previously at E18. If the general rule of peripheral before central target destination is applied, then putative peptidergic axons must have reached the hindlimb at least one day before the spinal cord, at E17. This timeframe is also expected if there are three separate neuronal populations generated, as discussed above. The third population characterised was born between E14 and E15, therefore if it follows the developmental pattern of the other populations, its axons would arrive in the hindlimbs two days after their birthdate - E16-E17.

Despite availability of an adequate marker for the peptidergic population prior to expression of peptide, endorsement of this timescale is possible by examination of novel growth in the hindlimb at E17 using GAP 43. Increased labelling is observed at E17 proximally, especially of fine axons in the skin. A day later this new growth, including some short beaded axons intra-epidermally, is found more distally and is quite distinct from the pattern of the A-fibre label, RT97. At E19, many of the larger fibres express much less GAP 43, consistent with the downregulation associated with the completion of novel innervation. This also eliminates the remote possibility that peptidergic fibres only entered the peripheral target at E19. By E20, PGP 9.5 fibres with a beaded appearance are found in the glabrous footpad. PGP 9.5 co-localises with CGRP in the adult (Dalsgaard et al, 1989), and these type of beaded fibres are found in the developing human epidermis at 10-12 weeks (Terenghi et al, 1993). GAP 43 labelling is not as revealing about growth to the central target as no fibres are observed in the SG until E19, when CGRP fibres already occupy that area. Some formerly unexplained cellular labelling in the superficial dorsal horn emerges at E17 and is more localised at E18. There is a possibility that this represents the afferent terminals, and the fibres observed subsequently are collateral axons.

The final inference from this data is that initiation of peptide expression in the DRG, results in simultaneous transport to the peripheral and central axons, but importantly that this does not occur until both the peripheral and central processes of the DRG cell have reached their target. SP is found in the spinal cord at E18 but not in the SG, it is noteworthy that SP is not located in the peripheral target at this stage. SP has been reported in the DRG and SG at E21 but not in the epidermis of the foot pad until P1 (Marti et al, 1987). These findings are in contrast to the present study where SG labelling is not observed until the periphery is innervated. This means that it is not conclusive whether the peripheral target initiates afferent entry into the spinal cord and if both these targets must be innervated prior to peptide expression (see Chapter 6).

4.20 Do A-fibres reach the central target prior to C-fibres?

This question has been addressed in the spinal cord by a number of previous studies, using many different methods (Smith, 1983; Fitzgerald, 1987; Davis et al, 1989; Fitzgerald et al, 1991; Snider et al, 1992; Mirnics & Koerber, 1995b). The results are easier to interpret than in the periphery because each of the physiologically defined neuronal populations have characteristic terminations in the spinal cord (see Chapter 1). This study, using a range of immunohistochemical markers is in broad agreement with earlier descriptions that A-fibres penetrate the central target in advance of C-fibres, but additionally provides evidence that the non-peptidergic fibres are present prior to peptidergic fibres.

The first collaterals seen entering the grey matter at E14, were RT97 and peripherin positive. These were followed at E15-E16 by GAP 43 and PGP 9.5. All these collaterals grew ventrally and laterally into the dorsal grey matter, locations consistent with 1a and Aβ fibres. The identification of collateral ingrowth at E15 is consistent with previous reports (Smith et al, 1983; Fitzgerald et al, 1991; Mirnics & Koerber, 1995b), but no previous studies have described fibre intrusion at E14. The former studies concluded that the earliest fibres in the spinal cord were A-fibres based on their projection patterns, however, this study is more unequivocal because of the presence of RT97 which I have shown to selectively label large DRG cells (Chapter 3).

In agreement with the studies above, no small diameter markers were detected at these early ages, nor was any labelling found in the SG, the terminal location of C-fibres. Contrary to those studies where C-fibre ingrowth is not observed until E19, trkA was first detected in the superficial and lateral region of the grey matter at E17, albeit a few faint fibres until E18. The position of this labelling suggests that these are C-fibres and as discussed above, there is much supporting evidence to indicate that these trkA fibres are non-peptidergic. This proposal is further strengthened by the appearance of the lectin IB4 in the SG at E18. The trkA collaterals then become denser over E19-E20 when labelling with the peptide CGRP is first detected. The appearance of the peptide label does correspond with the earlier descriptions, and in this study with the presence of GAP 43,

PGP 9.5 and peripherin in the SG. These results imply that there are three waves of collateral ingrowth to the spinal cord from the DRG. The first are A-fibres, the second are non-peptidergic C-fibres followed swiftly by more extensive ingrowth of peptidergic C-fibres.

4.21 Are peripheral and central events correlated?

Examination of the developing innervation in the hindlimb and spinal cord shows that entry of DRG axonal subpopulations to these targets is sequential, and that a number of events centrally and peripherally are temporally correlated. The ingrowth of afferents to the dorsal horn in a lateral to medial progression is temporally linked to the proximal-distal extension of hindlimb innervation and the orientation of the dorsal horn afferents is spatially linked to the type of peripheral target. Evidence supporting a causal link between these events is difficult to determine.

Previous accounts of the relationship between the peripheral and central targets (Honig, 1982; Wessels et al, 1990; Fitzgerald et al, 1991; Reynolds et al, 1991; Snider et al, 1992; Mirnics & Koerber, 1995a; 1995b) have focused on the somatotopy of the system - the laminar terminations and the spatial occupation in the dorsal horn, in addition to the segmental origin of innervation to the peripheral target. This study does not encompass these aspects of the relationship but focuses on the use of selective labels to define the ontogeny of central projections in relation to the events in the periphery.

To simplify this argument it is preferable to specify the type of fibres and describe them individually since A-fibres are the first to enter the spinal cord followed by C-fibres after a longer waiting period, and to consider the target type - skin and muscle separately. The developmental series indicates that since skin and muscle targets are innervated within a short time interval, so the growth of the central component of these targets will be initiated at approximately the same time, hence distinguishing between these afferents may be difficult using only a global marker.

A-fibres

Based on my results, the following model is proposed and is deduced from the selectivity of markers and the characteristic termination patterns of collaterals. Aβ afferents are the first to penetrate the grey matter from lateral dorsal column followed by 1a afferents from the medial dorsal column. These are linked temporally to peripheral contact with skin and muscle respectively. The Aβ afferents first originate from the lateral dorsal column but progressively arise from more medial locations as peripheral axons extend proximo-distally into the hindlimb. The projection pattern of the Aβ collaterals are maintained in a ventro-lateral arc. Meanwhile as muscle targets are innervated more distally, the 1a collaterals still originate from the medial dorsal column but grow deeper into the dorsal horn towards the motor pools.

The concept of sequential entry of afferents to the spinal cord (Smith, 1983; Smith & Hollyday, 1983; Fitzgerald, 1987; Davis et al, 1989; Fitzgerald et al, 1991; Snider et al, 1992; Mirnics & Koerber, 1995b) has been well described. It is also obvious from these studies that a delay or waiting period exists for all of the afferents once they reach the dorsal root entry zone (DREZ) of the spinal cord. The stimulus for ingrowth has been linked to innervation of the periphery (Smith and Frank, 1988), and the lateral-medial ingrowth of collateral afferents has been proposed to be linked to the proximo-distal growth of peripheral axons (Fitzgerald et al, 1991). In the model above I am also suggesting that the lateral-medial displacement of central afferents is specific to the proximo-distal progression of cutaneous axons. Inconsistent with this hypothesis was the recent DiI study by Mirnics & Koerber (1995) who concluded that innervation of specific targets on the limb are not essential factors for the initiation of fibre growth into the grey matter, although peripheral cues may direct central growth.

Their conclusion was based upon differential labelling of the proximal and distal hindlimb at E15, with DiI crystals placed a week later in the proximal target than the distal target. The results showed that the afferents grew synchronously into the dorsal horn and had penetrated to the same depth. It was also deduced from this observation that the peripheral target was not required because labelling was achieved from the paw

before innervation was detected. There are a number of problems with this assumption. The first is that the DiI crystals were in place for one week in the paw before labelling was attempted in the proximal skin. From my results it is known that innervation reaches the toes only four days after commencing in the hindlimb, therefore it is probable that innervation was present in the paw and labelled back to the spinal cord. Accordingly this does not negate the role of the peripheral target in inducing central innervation. The fact that collaterals extend the same depth into the dorsal horn after the labelling may not be as important as the origin of the fibres in determining whether they are from a proximal or distal site in the hindlimb, if the model suggested is correct. In addition, the DiI placed in the paw and thigh may have labelled both skin and muscle afferents, the differences between the targets then become indistinguishable.

The reason that the extent of peripheral and central innervation could be confidently compared in this study, was because they were both visible in one section due to the technique of sectioning the embryo (see Fig. 2.1). This model is further reinforced by a more recent study in the mouse using lipophilic carbocyanine dyes (Ozaki & Snider, 1997). Muscle afferents penetrate from the medial portion of the dorsal funiculus while cutaneous afferents penetrate from the lateral portion. Moreover the lateral dorsal horn is the appropriate location for fibres innervating the proximal skin (Koerber & Brown, 1980; 1982).

C-fibres

In contrast to the A-fibres which begin to form collaterals in the spinal grey matter two days after reaching the DREZ, no C-fibres enter for a further three days, yet small fibre labels were detected in the Bundle of His at the same time as A-fibres. All ingrowth to the substantia gelatinosa (SG) starts in the lateral part then extends throughout the laminae which is consistent with the findings for the A-fibres. There are significant differences however between these groups of fibres. The lateral to medial development of labelling within the SG occurs within 24 hrs. Even though this pattern may correspond to that of the A-fibres, the proximal-distal extension of C-fibres throughout the hindlimb could not occur within this short period of time. In fact most of

the periphery including the toes are labelled with trkA before ingrowth. It is obvious that the presence of labelling in the periphery does not initiate ingrowth of C-fibres.

If this is not true for C-fibres, it is also possible that peripheral target innervation is not required for A-fibres either, but merely temporally correlated. Labelling of A and C-fibres are detected in the dorsal roots in the same timeframe, but C-fibres wait at the DREZ for 3-4 days compared to 2 days for A-fibres, which confirms previous findings in many species (Smith & Frank, 1983; Davis et al, 1989; Fitzgerald et al, 1991; Mirnics & Koerber, 1995b; Ozaki & Snider, 1997). This may not be due to the axons or what target they have contacted but to the intrinsic properties of the spinal cord. Before these factors are considered, the fact that A-fibres only wait for a short period means that the spinal cord is sufficiently developed. The fact that A-fibre afferent development mirrors the progress in the periphery so closely, argues that they enter during the period when the peripheral projections are forming and can influence the collateral formation, therefore it is probable that this peripheral influence is limited to the A-fibres.

4.22 Why do C-fibres exhibit longer waiting periods? If C-fibres are present in the peripheral target, why is there a delay in afferent entry to the central target?

Three possibilities are apparent for the C-fibres. Firstly, the destination of the C-fibres - the SG, is not developed. Secondly, A-fibres occupy their target, and finally the spinal cord is selectively non-permissive to C-fibres.

SG development

The SG is the last region in the spinal cord to mature (Nornes & Das, 1974; Bicknell & Beal, 1984) and it is logical that afferent entry would be delayed until the destination is sufficiently developed. In the mouse it has been reported that "onset of collateral branching does not occur until well after differentiation of certain cell groups suggesting that spinal neuronal differentiation is a prerequisite to appropriate targeting and branching of sensory axons" (Ozaki & Snider, 1997). However, this analysis was

not able to be conducted in the superficial dorsal horn and a definitive association formed between the development of the target field in relation to the innervation.

Results of *in vitro* experiments also shift the emphasis onto the spinal cord as the primary determinant of sensory axon projections (Sharma et al, 1994). These organotypic co-cultures are difficult to interpret since if DRG and spinal cord are cultured at stage 28 prior to peripheral contact, appropriate central afferents do not materialise but neither is the dorsal horn mature. When cultured at stage 30, the chick spinal cord has differentiated and sensory projections are correct yet the DRG had previous contact with the periphery. An attempt to dissociate these responses by using isochronic (age-matched) or heterochronic (non-age matched) co-cultures showed that the age of the spinal cord is the critical variable in determining the ability of afferents to make connections (Redmond et al, 1997). This study found that rat DRGs aged E14, E16 and E18 could only grow into spinal cords aged E14-E18 and not PO. This suggests that after a critical window of development the spinal cord is non-permissive to all growth (also see below).

The drawbacks with this study that showed growth of E14 DRG into older spinal cords was firstly that at E14 some peripheral contact would have been made. Secondly only CGRP-IR afferents were examined and the exact projections of these afferents were not considered. Finally, cultures were conducted over 6 days and the results only reported at the end of this period when tissue was the equivalent *in vivo* age of postnatal animals, so it was not ascertainable when exactly ingrowth was detected.

Apart from the limitations of that particular study, all culture experiments involve the addition of neurotrophic factors for survival, however the presence of these factors may stimulate premature ingrowth into the spinal cord as they may mimic the *in vivo* contact with target and exposure to neurotrophic factors, if indeed neurotrophins are a stimulus for afferent ingrowth.

A-fibre occupation

Somatotopy of the developing neuronal connections is appropriate from the outset with respect to the establishment of dermatomes and the medio-lateral and

rostro-caudal extent of terminal fields of different nerve origin (Fitzgerald & Swett, 1983; Shortland & Fitzgerald, 1994). More recently, it has been established that Aβ fibres enter the dorsal horn and when they make their characteristic flame-shaped arbors they extend into lamina II, which in the adult exclusively contains C-fibre terminals. A and C-fibre terminals share lamina II for the first three postnatal weeks before A-fibres withdraw and are restricted to laminae III-V (Fitzgerald et al, 1994). These terminals make synaptic contact in the neonatal lamina II (Coggeshall et al, 1996) and low-threshold stimulus in the periphery elicits fos expression from dorsal horn neurons in lamina II (Jennings & Fitzgerald, 1996).

It is possible that the presence of the A-fibre terminals may be a deterrent for the entry of C-fibres, however they clearly grow in at stages when the A-fibres are still occupying these laminae and indeed the A-fibres do not reach LII until late in foetal development . There is an opportunity then for C-fibre terminals to enter and compete for the target before this.

Spinal cord is non-permissive

In Chapter 1 influences on neurite outgrowth are described and the recognition of inhibitory or negative factors in the development of the nervous system are discussed. The prevention of innervation reaching inappropriate areas by repulsive activity appears to play as large a role in shaping the final pattern of innervation as attractive cues. Inhibitory influences are specific to certain classes of sensory and motor afferents. They are also temporally expressed and so may only operate within defined timepoints. In the spinal cord, a ventral inhibitory factor has been isolated which prevents non-proprioceptive innervation from projecting to the ventral horn. This factor is thought to be semaphorin III/D and is part of a large family. Evidence now suggests that localised expression of these semaphorins may contribute to the control of the "waiting period" displayed by dorsal root afferents.

Sema III is selectively inhibitory to non-proprioceptive or non-NT3-dependent axons and excludes them from the ventral horn. It is transiently expressed by cells near the DREZ in the rat embryo prior to any afferent entry (Wright et al, 1995). For this

molecule to contribute to the waiting period for all axons, its actions would need to be developmentally regulated to provide total inhibition of afferent entry. Recent research has shown that both NT3 and NGF-dependent neurites are inhibited by Sema D at E12.5 in the mouse, yet only NGF-dependent neurites are responsive at E14.5 (Puschel et al, 1996). This suggests that the sensitivity of sensory neurons is stage-dependent and that a selective desensitisation to Sema D occurs in the NT3-dependent population. The fact that NT3 neurons are also inhibited by Sema D before afferent ingrowth implies that it may be involved in preventing an early penetration to the spinal cord by sensory afferents. In the chick the Sema D homologue, collapsin-1 is also found near the DREZ *in vivo* shortly before and during the waiting period (Sharma et al, 1996). In culture, addition of recombinant Collapsin-1 prevents the normal ingrowth of collaterals to the spinal cord after a two day period, and both trkA and trkC positive axons were similarly affected.

The loss of sema D/collapsin-1 expression at the DREZ site and the subsequent loss of sensitivity of NT3 afferents to Sema D, allows the entry of these fibres to the spinal cord. Sema D is subsequently restricted to the ventral horn although it is thought that a diffusible gradient still exists. The reason that the remaining non-NT3 dependent afferents, i.e. small diameter afferents, do not enter at this point is most likely because they are exposed to different inhibitory factors, also likely to be members of the semaphorin family.

The semaphorin gene family are differentially expressed in the developing mouse spinal cord. Seven members of the semaphorin family (Puschel et al, 1996) as well as novel family members (Zhou et al, 1995; 1996) are expressed in distinct laminae and downregulated after E17 in the mouse. This is the age when nociceptive afferents are first detected in the superficial dorsal horn of the mouse (Ozaki & Snider, 1997). The regionalised and developmentally regulated expression of semaphorins in addition to their known effects on sensory subpopulations *in vitro,* is consistent with roles in preventing the entry of all sensory collaterals to the immature spinal cord by forcing them to wait in the DREZ, and a role in determining the subsequent lamina-specific

innervation of different subpopulations by repelling afferents from inappropriate areas (Puschel et al, 1996).

It has been shown that semaphorins are expressed in the periphery (Wright et al, 1995). These may not be the same complement as expressed in the spinal cord since trkA positive axons are found in the hindlimb at E13, yet trkA positive axons wait at the DREZ for four days, although it is also possible that they are expressed but downregulated earlier. Nonetheless similar molecules could be expressed in both targets because peptidergic sensory fibres do not enter the central or peripheral target until after the remaining subpopulations, although inhibitory actions may only be a contributory factor in this case (see 4.4.1). The detection of CGRP-IR fibres in the muscle of the hindlimb at E17 may reflect motor rather than sensory axons, since the levels of CGRP in the motoneurons decrease at this stage suggesting axonal transport into the peripheral axons. If CGRP does label motor neurons at E17, the fact that motor neurons show a differential responsiveness to Sema D (Vareala-Echavarria et al, 1997) and possibly other members of the family, may explain why these are found in the hindlimb before sensory fibres.

A different type of inhibition may operate after collateral ingrowth as shown by the *in vitro* experiments of Redmond and colleagues (1997). In their experiments, no growth could be induced in spinal cords aged P0. This is not likely to be due to semaphorins whose activity is downregulated, but due to an axonal barrier in the DREZ mediated by proteoglycan expression and responsible for failure of axons to regenerate after nerve injury (Pindzola et al, 1993).

4.23 What are the general features revealed by each of the antibodies in this series and how do they compare to previous studies?

i) GAP 43

GAP 43 immunolabelling of developing innervation in the spinal cord and periphery has been examined previously in two companion papers (Fitzgerald et al, 1991; Reynolds et al, 1991). Many aspects of this study substantiate the findings of

those papers, although differences were noted particularly in central innervation. These differences are outlined below and reasons for the discrepancies discussed.

In contrast to my study, they found that from E14, stray axons could be detected leaving the Bundle of His. In addition, differences were observed in the location of clumped staining in the dorsal horn in the late foetal period (see iv below). The largest variations however, were found in the ventral horn. The previous study showed a medially located motor pool at E14 and medially directed afferents originating from the lateral columns. These were absent in my study, yet I detected novel contralateral staining at E19 and E20, originating from the lateral columns and projecting towards the mid-central canal. Furthermore I found that collaterals from the white matter extended further into the grey matter at each stage.

In the periphery, I detected innervation at the most distal extremity of the toes at E17 but not in the skin until E18, yet Reynolds and colleagues did not observe any labelling in this region until E19. In general, both the central and peripheral labelling in the previous companion papers (Fitzgerald et al, 1991; Reynolds et al, 1991) was much stronger and intense at all comparative stages and they found intense labelling at E12 and E13, some 48 hrs prior to this study.

These differences can be accounted for in part by the use of different antibodies. The previous study used a polyclonal antibody which recognised epitopes arising from post-translational processing. In this study a monoclonal antibody was employed, which is insensitive to postranslational modification, detecting both phosphorylated and unphosphorylated subtypes. The differences between these two antibodies were discussed further in a paper by Chong et al, 1994. That paper highlighted the large variances in intensity that occurred between using the sheep and mouse antibodies at high titres, at which both this and the previous study used. The importance of postranslational modification to the detection of GAP 43 has been discovered by several recent studies. Firstly, motile growth cones contain very low levels of phosphorylated GAP 43 compared to stationary growth cones. Phosphorylated GAP 43 is differentially distributed within the growth cone so that increased immunoreactivity to phosphorylated

GAP 43 can be detected in the neck of the growth cone, whereas it is only heterogeneously expressed in the lamellae and filopodia (Dent & Meiri, 1992). This means that if an antibody only detects the active phosphorylated form that it may not pick up the lamellepodial extensions, and therefore some studies may detect fibres in advance of, and with increased intensity than others. Additionally from regeneration studies it has been noted that GAP 43 can be transcribed but not necessarily translated (Woolf et al, 1992; 1994), therefore care must be taken when interpreting investigations using GAP 43 mRNA.

ii) PGP 9.5

PGP 9.5 labelling is very similar to the pattern of GAP 43 in the hindlimb. It has been described as a general neuronal marker however, it is not as effective in the spinal cord. Axons were only detected until E15, after which only cellular labelling was recognised. This meant that for this study its inclusion did not contribute to information about the development of the central projections. Although, in late development of the periphery, a general marker was required because the remaining markers are restricted to specific populations and GAP 43 is downregulated when novel innervation is completed.

iii) Peripherin

Peripherin is a structural component of the neuron and is one of the first elements to be expressed (see 4.8.6). In this study, I found that peripherin-IR was detected in the DRG, spinal cord and periphery at the earliest age examined. Recently, it has been reported that peripherin is downregulated during development and that DRG expression becomes restricted at E20 (Goldstein et al, 1996). In agreement with those findings, I observed the downregulation of peripherin. This was not quantified but changes in expression levels were detected slightly earlier at E17-E18. However, another study using protein levels, also determined that peripherin increases from E14 until stabilisation at E20 (Escurat et al, 1990). At E17, coincident with the observed onset of peripherin restriction in the DRG, some transient labelling was found in the

ventral horn. This consisted of intensely staining cell bodies and some short ventrally directed fibres projecting from them, these disappeared by E18. E17, is also the earliest age when innervation reaches the toes. It is possible that contact with the distalmost target by sensory and motor axons, resulted in a retrograde signal to the spinal cord, involving a transient response in the ventral horn followed by the initiation of restricted protein expression in the DRG. It is also significant that mRNA continues to be expressed in 80% of cells of the DRG (Goldstein et al, 1996), implying that protein downregulation is due to increased transport to the periphery in the expanding peripheral axons, or decreased translation rather than decreased transcription.

Escurat and colleagues, (1990) detected peripherin in peripheral nerves from E14, but they did not describe the patterns or extent of peripheral projections. This study is the first to extensively analyse this aspect, and that of the spinal innervation in the rat with peripherin, although a study involving central innervation has been undertaken in the mouse (Troy et al, 1990a).

Peripherin and a NF, were the first markers demonstrating afferent entry into the grey matter of the spinal cord at E14. This is significant for two reasons. Firstly, these are observed in advance of GAP 43 which labels all new axonal growth, and secondly because it was detected at E14, when previously afferents were not detected until E15 (Smith, 1983; Fitzgerald, 1987; Snider et al, 1992; Mirnics & Koerber, 1995). The reasons for this are discussed in 4.4.6 below, however, this finding makes peripherin an important marker for axonal growth. The pattern of peripherin labelling in the dorsal horn is also notable. Apart from the first few axons at E14, which originate from the lateral part of the Bundle of His, all subsequent axons are derived from the medial dorsal horn, and unlike any of the other markers they do not occupy the lateral dorsal horn or have laterally directed fibres at any stage. Reasons for this are only speculative, but at the early stages it is known that only the axons from the large DRG cells reach their central target. Even though peripherin may label all DRG cells at these stages, it is only the A-fibres expressing peripherin which will project to the spinal cord. The projection pattern then suggests that only the Ia fibres are labelled and not the Aβ fibres.

This is consistent with its position in motoneurons from E14 and extensive labelling of muscle in the hindlimb (see below). Moreover, it implies that during development the only A-fibres it labels are derived from muscle and not skin.

Peripherin is expressed in the hindlimb from E13 and is detected in the epidermis at E14. It is unique between E14 and E16 because it simultaneously labels skin and muscle. The labelling in muscle may partly be motor derived because there is strong staining in the motoneuron cell bodies from E14 which decreases rapidly, suggesting transport to the periphery. However, some of the labelling must also be sensory as from E15, there is clear labelling in the spinal cord corresponding to 1a afferents, directed towards the ventral horn. It was suggested above that peripherin may not label A-fibres in the skin, but skin is labelled from the outset although is characterised by much finer fibres than seen with either GAP 43 or PGP 9.5. This rationale would imply that labelling of fibres in the skin is confined to C-fibres. This observation, in addition to the proposal above, leaves the question as to what peripherin is staining in the skin. It is possible that until E19 it overlaps with trkA positive non-peptidergic fibres. If it does not label A-fibres in the skin and peptidergic fibres are not yet present then the fine axons would be consistent with the portrayal of non-peptidergic fibres. At E19 however, there is a large increase in the peripherin labelling particularly in glabrous skin and some additional bundles found in the hairy part of the foot, which corresponds with the onset of CGRP expression indicating the presence of peptidergic fibres. It is likely that the peripherin increase included the peptidergic fibres and is further supported by peripherin located in the SG at E19.

Peripherin labels all DRG neurons (Troy et al, 1990) and theoretically all peripheral processes during early development. It is quantitatively the most important IF in sympathetic neurons (Escurat et al, 1990) and the only type III IF found exclusively in motor, sensory and sympathetic neurons (Portier et al, 1993). These findings imply that it is an excellent general marker, possibly better than PGP 9.5 because of superior axonal staining in the spinal cord. Results from this study indicate that this may not be the case as there is no evidence of A-fibre terminals derived from skin in the dorsal

horn. Double-labelling with RT97 or the physiological identification of peripherin-IR processes would resolve this.

iv) RT97

RT97 labelling was problematic in two respects. Firstly, in the periphery it showed a slight temporal delay compared to other markers from E14 -E16, and also in reaching the toes at E18, even though using general markers the presence of innervation was established in that region at E17. RT97 immunolabelled fibres were among the first to colonise the target so this does not necessarily infer that A-fibres lagged behind, but merely that their visualisation with the NF-H component was a delaying factor (see 4.8.6).

Secondly, RT97 was found in the epidermis even though in the adult this region is restricted to unmyelinated sensory afferent fibres, namely the C-fibres and Aδ fibres. RT97 labels myelinated afferents (Lawson et al, 1984) so their detection in the epidermis was not anticipated, especially since a recent report revealed there was no intraepidermal labelling (Sann et al, 1995). The specificity of RT97 during development was evaluated in the previous chapter (3) and was ascertained to be large fibre specific. This means that occupation of the epidermis is transient during development (see Chapter 5). Comparison of these fibres to those of GAP 43 and PGP 9.5 showed that axons in the glabrous skin were not as thick and clumpy ended, nor did they reach the epidermal edge suggesting that the largest fibres were not labelled. Furthermore they were thicker than axons in hairy skin detected with GAP 43, indicating that they were also not labelling the finest axons. Taken together, these observations indicate the fibres are probably Aδ, supported by the knowledge that electrophysiologically identified Aδ fibres in the adult are all RT97-IR (Lawson & Wadell, 1991). By E20, labelling with GAP 43 and PGP 9.5 decreased in the epidermis. This is expected with GAP 43 as novel growth declines, but due to the parallel decrease with PGP 9.5, it must also be attributed to the relative growth of the epidermis. Partial sub-epidermal retraction of RT97 fibres occurs earlier at E19. One reason for this could be the co-incident arrival of the peptidergic C-fibres (also see Chapter 5).

In the spinal cord, RT97-IR fibres, like peripherin, are observed at E14. This is a significant observation as afferent entry has not previously been reported this early. Section 4.4.6 below, includes discussion on why labelling could be found at this age with these markers. From E15, the pattern of axonal labelling with RT97 becomes more complex, most obvious are the ventrolateral directed afferents, however, the typical flame-shaped arbors associated with Aβ fibres are not detected making a U-turn dorsally at any point. These have previously been observed during development using the DiI procedure (Ruit et al, 1992; Konstantinidou et al, 1995; Mirnics & Koerber, 1995) and from golgi studies (Beal, 1982). Afferent fibres with terminals ending in laminae III-IV were found at E18, and these extended dorsally to the laminae II-III border by E21 (Ruit, et al, 1992). This suggests that ingrowth of these afferents is somatopically correct when compared to the adult, which is consistent with the conclusion reached in an earlier study on the C and Aδ fibres (Fitzgerald, 1987). Although, in the most recent study even though fibres in laminae III-IV did not change significantly throughout development, it was E20 before the fibres made a full dorsal U-turn (Mirnics & Koerber, 1995).

The reasons these fibres are not detected in this study may be twofold. Firstly, this may be a methodological issue concerning the use of IHC as opposed to fibre tracing. This view is supported by unexplained cellular labelling in the dorsal horn. Some cellular staining was transiently detected with peripherin at E15 in the dorsal horn, this was followed at E17 by RT97 and GAP 43. The RT97 labelling had a clumped appearance and was confined to the lateral and superficial dorsal horn, similar to most of the GAP 43 labelling which increased at E18. Larger clumps of GAP 43 labelling were also found in the medial dorsal horn at E17, these had moved ventrally at E19 and E20. This type of clumped cellular labelling may be the terminal arbors of the cutaneous mechanoreceptors, which supports a procedural reason for the lack of afferent visualisation. Their location is consistent with the terminals of Aβ fibres described in the adult (Brown et al, 1977; Woolf, 1987; Shortland et al, 1989; Fitzgerald et al, 1994) and are similar to the type of staining of nerve terminals obtained

after injections of Horseradish Peroxidase (HRP). The presence of terminals may additionally explain why from E16 the lateral part of the dorsal horn appeared devoid of staining with RT97, meaning that it is not because there are no fibres there but that they were not visualised. The clumped staining in the dorsal horn has also been reported in a previous GAP 43 study (Fitzgerald et al, 1991) where it was suggested that these aggregates are likely to represent sensory projections to the spinocervical, spinovestibular, spinotectal and possibly spinocerebellar tracts. The location of cells in that study were widespread throughout the dorsal horn and some fibres were detected projecting from them indicating that they were dorsal horn cells, in comparison to the type and location of labelling in this study.

Secondly, the number of of RT97 positive cells in the DRG were determined to be half that of the adult (Chapter 3), therefore it is possible that RT97 does not reflect all of the A-fibres present in either the periphery or the spinal cord. Although, the size distribution indicated RT97 were amongst the largest cells, several of the largest cells were RT97 negative. These could be the Aβ population and therefore the majority would go undetected in this study. The density measurements in the next section may resolve this issue, by comparison of the level of innervation with that of PGP 9.5 If these are comparable, then it seems that the technique is responsible for failing to demonstrate the full extent of the afferents and also that the adult expression levels may be inaccurate due to profile counts.

v) TrkA

TrkA in its capacity as a small diameter fibre marker has been discussed in 4.4.1. It has been used extensively in labelling of DRG cells (Averill et al, 1995; Molliver & Snider, 1995; Silos-Santiago et al, 1995; Bennett et al, 1996b; White et al, 1996; Bergmann et al, 1997) however, only one previous study has examined its distribution in peripheral nerves.

Consistent with the observations of White and colleagues (1996) in the mouse hindlimb, this study showed that trkA labelling in the rat was present in a comparable developmental timeframe. Whilst trkA-IR fibres were among the first in the hindlimb

they did not extend as far distally as the other IHC markers in this study or as far as DiI (White et al, 1996). This is probably due to the earlier or more extensive outgrowth of non-trkA expressing axons. In the mouse, trkA positive axons were also confined to cutaneous targets in close proximity to regions of NGF mRNA synthesis and gradually grew into the limb in a proximo-distal manner. Similarly, trkA positive axons were present in the dorsal roots from E11.5, but did not penetrate the grey matter of the spinal cord until E15.5 when the distalmost part of the hindlimb had been colonised. This finding is also substantiated in this rat study, where the distal-most target is reached at E17, coincident with the first appearance of trkA in the superficial dorsal horn.

vi) CGRP & SP

The peptides CGRP and SP were both examined in this study. CGRP was found in each of the targets by E19 and is fully discussed in Chapter 6 along with the mRNA data. SP however, was only detected in the spinal cord. This is consistent with a previous study that did not detect SP in the DRG until birth and in the skin until P1, which is beyond the age range examined in this study (Marti et al, 1987). In contrast a recent study has reported 13% expression in the E19.5 DRG (Hall et al, 1997).

The SP-IR fibres in the spinal cord were only transiently expressed at E18, while cellular labelling persisted until E19. The position of this labelling was not characteristic of the superficial dorsal horn in the mature animal but was localised in the deep medial dorsal horn. A putative trophic role in development of the spinal cord has been advocated (Jessel & Yamamoto, 1980; Wall & Fitzgerald, 1982; Marti et al, 1987) and the expression of SP is consistent with cell groups in areas undergoing differentiation in the dorsal horn (Ozaki & Snider, 1997). Alternatively it may be involved in chemotropism (DePhilipe & Hunt, 1995).

vii) IB4

The IB4 label was included in this study as it is a structural component of the small diameter neurons and it was hoped to be a definitive marker of this population in

the embryo. Onset and patterns of labelling in the DRG and spinal cord are in agreement with a previous study (Plenderleith et al, 1992). This is the first time that IB4 labelling has been examined in embryonic skin. No labelling was found at these stages although postnatally fine short axons are located in hairy skin but they are infrequent (results not shown). Plenderleith & Snow (1993) determined that IB4 positive axons labelled the skin by retrogradely labelling skin afferents, and staining the DRG neurons. The fact that axons have not been detected directly in the adult and were not detected here embryonically may be due to the levels required for exposure by immunohistochemistry.

4.24 Why does labelling of the intermediate filaments peripherin and RT97, precede that of GAP 43?

Regeneration studies are often helpful to developmental studies because many aspects of regeneration are mere recapitulation of events and processes that occur in development and in a context easier to manipulate. After sciatic nerve injury GAP 43 expression is not fully elevated until axon elongation is under way, so induction of GAP 43 may be a secondary consequence of axon outgrowth (Skene, 1989). If this is applied to the situation during development, it may explain why GAP 43 labelled afferents are detected after those of peripherin and RT97.

In the PNS peripherin is important for the dynamic changes occurring in axons during axogenesis and NF proteins are implicated in the stabilization of a more rigid filamentous network in mature fibres (see 4.3.5; 4.8.6). These proteins are essential for the actual outgrowth of neurites whereas GAP 43 may be required slightly later to direct this growth. If GAP 43 expression is prevented, cells can still extend neurites (Baetge & Hammang, 1991). Moreover, a transgenic knockout of GAP 43 had a grossly normal CNS and normal neurite outgrowth but defective pathfinding (Strithmatter et al, 1995).

5

QUANTITATIVE ANALYSIS OF CUTANEOUS INNERVATION DENSITY IN THE DEVELOPING HINDLIMB

INTRODUCTION

5.1 Aim

The aim of this chapter was to analyse developing peripheral innervation in a quantitative manner, to complement descriptions of the patterns of developing innervation described in Chapter 4. In the previous chapter, subpopulations of sensory neurons were identified on the basis of their selective immunolabelling. In this chapter, sections of hindlimb and hindpaw immunolabelled with those selective markers were quantitatively analysed. Two clear objectives of the analysis were:

- **To determine any differences in innervation density through development and in different regions.**
- **To establish if there are any differences in innervation density between identified subpopulations.**

5.2 Previous Studies

A search through recent literature identifies many papers describing innervation density, especially during development (e.g. Albers et al, 1994; Mirnics & Koerber, 1995a), however, only occasionally do these refer to quantitative analysis. One of the reasons that this analysis is not routinely undertaken is that it is fraught with technical difficulties. This type of data is of widespread interest if it can be systematically and reliably generated for comparative purposes, however the range of variables in any such study makes this difficult to achieve. Previous work reporting quantitative data on neurite outgrowth has mainly been confined to *in vitro* studies (Leskawa & Hogan, 1985) where conditions are reproducible and variable factors can be controlled. Other approaches have been to count the number of neurites in a given area or to count the number of branch points (Jones & Marfurt, 1991; Andrews & Cowen, 1994; Bonner et al, 1994; Deller et al, 1996), however these techniques give no idea of the calibre of individual fibres or the range of axon diameters. A more comprehensive analysis recently, is the examination of the volume occupied by nerves using laser scanning confocal microscopy, through optical sectioning of tissue at a range of focal increments (Navarro et al, 1997).

Quantitative innervation analysis *in vivo* has been previously conducted in this research group. The analysis of skin hyperinnervation following neonatal wounds (Reynolds & Fitzgerald, 1995), employed a method similar to here, except that wounded skin was compared only to age matched controls in the neonates that show more advanced skin development, and a fixed area for analysis in the region of the wound was utilized. More recently, adult skin in IGF II overexpressing transgenic mice displaying an enlarged skin area, and controls, were analysed using the same paradigm as 1995 (Reynolds et al, 1997). A fixed area of skin was examined at a landmark region, showing clearly the reduction in sensory terminal arborization. Another approach in comparing adult cutaneous innervation in control and transgenic mice, has been to selectively remove a piece of skin prior to immunolabelling. Labelled fibres were then similarly drawn with a camera lucida and the area encompassed by the fibres calculated (Bergmann et al, 1997).

Direct image analysis of immunolabelled sections is also problematic as these are subject to large variances, primarily because the intensity of the labelled reaction product varies according to the antibodies used, the calibre of the axons and background staining and is therefore not consistently reproducible. Hence, many researchers use qualitative methods to describe immunolabelled differences in the amount of innervation, whereas most attempts at quantitative density analysis described above, have used a camera lucida to record the presence of innervation. This technique ensures that the number and calibre of axons are accurately recorded ignoring the intensity of labelling. This is especially pertinent in developmental studies since the intensity of labelling for any particular marker may be up or downregulated throughout maturation (see section 3.6.1 and Chapter 4).

5.3 Parameters of Study

After compilation of the image analysis data, it became apparent that the results were difficult to interpret in relation to the patterns of innervation described in Chapter 4. Density, in this thesis, refers to the amount of innervation per unit area of tissue, hence its value is intimately linked to the relationship between innervation and measured tissue area. One unexpected but important factor was that using the calculation given in the Methods section (Chapter 2) the density of innervation was found to be inversely

proportional to the measured area which can change with age and tissue shrinkage. Due to the dependence on the measured area, scale bars were included on all camera lucida drawings so the actual area of the region analysed could be determined and compared with the eventual density measurements.

The relationship between density, innervation and area is comprehensible if one uses the balloon hypothesis analogy (see diagram below). If a partially inflated balloon has a finite number of nerve fibres drawn on it (B), then the balloon is inflated (C), the actual amount of innervation is unchanged but its density is decreased. If however, as the balloon is inflated, nerve fibres are drawn on at the same rate (D), even though the absolute innervation has increased the density remains constant. Conversely, if the balloon is deflated (A), innervation would be unchanged but the density would increase.

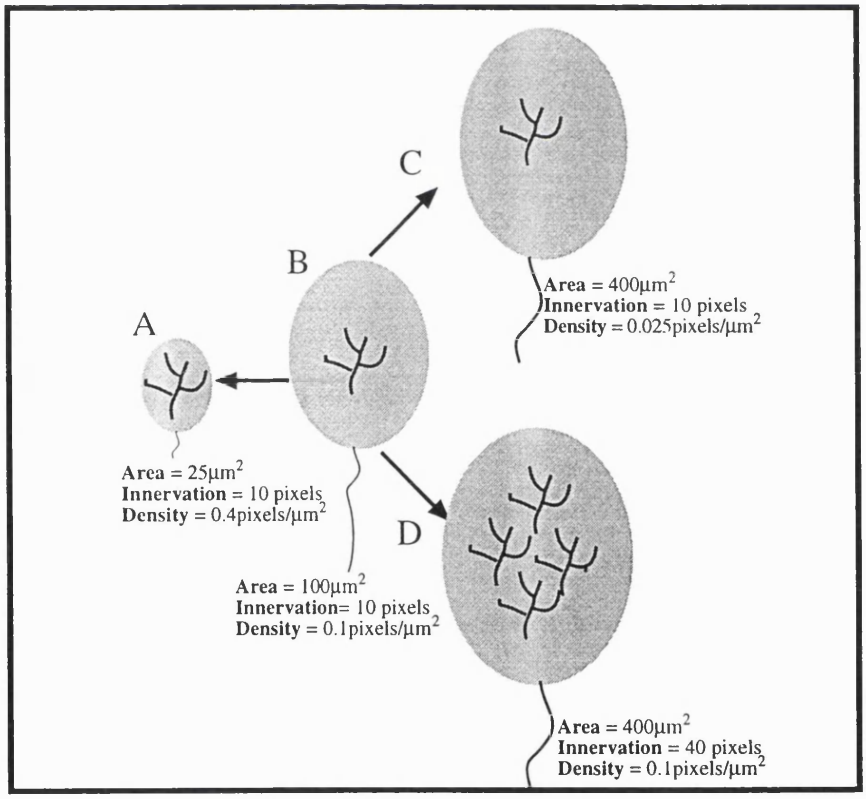

The balloon model explains why the size of the measured tissue area needs to be presented together with the density measurements, especially since the measured area varies with each section analysed. The method of innervation analysis is outlined in Chapter 2, however, relevant aspects are discussed here. This study was designed to examine innervation at different points in development, and to compare proximal/distal

and glabrous/hairy sites. It was desirable to select some landmark regions for consistent identification, particularly as there are many structural changes in the developing limb that make reproducible measurements difficult. To avoid biased selection of areas for analysis once the landmark region was identified, everything observed under x200 magnification was drawn with a camera lucida.

E15 was the age selected for early innervation since the immunohistochemistry (IHC) data in Chapter 4 indicated that all markers included in the study were expressed in the hindlimb and that cutaneous innervation had been initiated. E18 was considered the age when cutaneous innervation was established since during the late foetal stages of E17 to E21, terminal formation occurs within the epidermis and the gross structure of the epidermis resembles that of the adult by E18 (Martin et al, 1987).

Why does the area of the epidermis progressively change with age or even at the same age? Firstly, there may be different degrees of histological shrinkage in the tissue, this may artificially reveal an increased density when innervation is really unchanged. Secondly, there is inter-animal variation, this is more crucial in the embryo as the tissue may be harvested even with a few hours difference at a given plugdate. Thirdly, during this period of rapid development, growth of skin occurs. Epithelial proliferation between nerve terminals may separate and stretch the terminals so decreasing density, unless innervation increases in tandem. Finally, there may be biological compaction. This is the most difficult aspect to account for. The nature of the skin itself is subject to change, from the water content, protein complement and the presence of extracellular matrix molecules. The fact that many of these factors are unknown and uncontrollable *in vivo*, require that a cautious approach be taken to interpretation of innervation density in isolation.

Density alone is also uninformative about the degree of projection to the epidermal surface. From Chapter 4 and the image analysis, it is realised that the distance of terminals from the epidermal surface also changes (Fig. 5.5) and may be of functional importance. I have included a graphical representation of how far innervation extends into epidermal regions at different ages with different subpopulations, referred to as a projection ratio.

Definitions of Terminology:

Absolute/Actual Innervation: The physical amount of nerve terminals irrespective of area, in a designated region. This refers to all attributes such as number, branches and calibre.

Area: The size of the region analysed for innervation density, measured in microns squared (μm^2).

Density: The amount of innervation measured in pixels, in a micron square of tissue.

Epidermis: The demarcation of the epidermis was decided upon from the immunolabelled sections (for example see Fig. 4.3A). A brown deposit accumulates along the basal edge of the epidermis and this was verified from histological staining.

Growth Index: A numerical factor by which the area of a designated region increases with age.

Projection Ratio: The distance that axon terminals project into the epidermis relative to the depth of the epidermis.

5.4 Epidermal innervation of a defined region - change with age

Innervation of the epidermis in the first glabrous pad (region A) as visualised with antibodies to PGP 9.5 and CGRP, was quantified to examine any changes in density with increasing age. CGRP innervation was also quantified in four selected regions A-D from E19-P0 (these regions are described and illustrated in the methods [Fig. 2.3], but briefly these are: A and B the first glabrous pad and the hairy skin immediately opposite and one glabrous and one hairy site in the ankle region denoted C and D respectively). This analysis was intended to reveal the process by which subpopulations of sensory terminals achieve their final density in skin from their initial arrival at the target, through the period of cell death and the changes taking place in the composition of the target itself. The comparison between regions, was proposed to identify any innervation differences in the type of target: glabrous or hairy skin.

Table 5.1: Innervation Density in Region A from E17-E20 with PGP 9.5

AGE	INNERVATION DENSITY (pixels/μm^2)	AREA (μm^2)
E17	1.84	13320.50
E18	1.71	28973.72
E19	0.65	56740.82
E20	2.71	36298.68

n=3 at each age

Density of innervation decreases slightly from E17-E18 (Fig. 5.1), with a further large decrease at E19. By E20 however, density has increased substantially to exceed E17 levels by 37%. Comparisons of all ages E17 to E20 with PGP 9.5, show statistically

significant differences in innervation density (Table 5.1a). These decreasing innervation density results from E17-E19 appear anomalous considering it is known that epidermal innervation is underway, (see immunohistochemistry data). Inclusion of the area of skin under analysis (Fig. 5.2) shows that between E17 and E18, the skin area increases by 50%. Although a small decrease in innervation density was detected, the absolute innervation in this region must also have increased. The area of the region increased another 48% by E19, but this only partially accounts for the large decrease in innervation density, hence the absolute innervation must have remained unchanged while the area increased, or even have decreased through terminal regression. By E20, the region area is slightly larger than the size at E18, yet innervation density is increased 37%, therefore the large density value is probably a reflection of increased terminal area, possibly a second wave of innervation from putative C-fibres.

Table 5.1a: ANOVA Factorial Analysis of Innervation Density in Region A from E17-E20 with PGP 9.5

AGE	Mean Difference	p-Value
E20/E19	2.06	<0.001*
E20/E18	1.00	<0.001*
E20/E17	0.87	<0.001*
E19/E18	-1.06	<0.001*
E19/E17	-1.19	<0.001*
E18/E17	10.13	<0.001*

* shows statistical significance

Innervation of the same region as visualised by CGRP-IR was also examined for the same trends as above, and also to determine the proportion of C-fibres in comparison to the total.

Table 5.2: Innervation density in Region A from E19-P0 with CGRP

AGE	INNERVATION DENSITY (pixels/μm^2)	AREA (μm^2)
E19	0.23	95272.58
E20	0.21	81611.14
P0	0.28	40412.64

n=3 at each age

There is little change in density between E19 and E20, with a small increase by P0, though none of these show statistical significance. Examination of the area in region A importantly shows that there is a 51% decrease between E20 and P0 (mirroring the decrease observed from E19-E20 with PGP 9.5), yet no real change in density, hence it is likely that absolute innervation has decreased. Confirmation of this conclusion is found by visual inspection of the regions under analysis (Fig. 5.5). The footpad changes shape from E19 to P0 by elongating and becoming less prominent. As a consequence, the epidermal depth decreases which explains the decrease in area. By P0, there is less innervation in the epidermal region but the density per square micron remains the same due to the change in area.

A full examination of CGRP development in other regions during this period, was conducted to determine whether there are differences between the proximal/distal regions or between hairy and glabrous skin.

Table 5.3: Innervation density in Regions A-D from E19-P0 with CGRP

	INNERVATION DENSITY (pixels/ μm^2)			
AGE	**REGION A**	**REGION B**	**REGION C**	**REGION D**
E19	0.23	0.23	0.22	0.27
E20	0.21	0.28	0.23	0.26

P0	0.28	0.37	0.56	0.50

n=3 at each age

There is little difference both between the regions at E19 and E20, or for each region between E19 and E20 (Fig. 5.6). At P0, there appears to be slightly higher densities in the proximal ankle region (regions C and D) than in the distal part of the foot (regions A and B). These proximal values increased by 50% from E20 compared to 25% for the distal regions, however these are not statistically significant. Due to the similarities between regions at each age, these were combined to give an overall value for the hindpaw at each age. This analysis also confirmed that selection of the foot pad (region A), is representative of innervation throughout the hindpaw.

Table 5.4: Effect of Age on CGRP Innervation Density from combined regions

Age	Mean Innervation Density (pixels/μm^2)	Area (μm^2)
E19	0.24	59747.43
E20	0.23	55431.04
P0	0.43	30604.68

n=12 at each age

Table 5.4a: ANOVA Factorial Analysis of Innervation Density from E19-P0 in Combined Regions with CGRP

AGE	Mean Difference	p-Value
P0/E20	0.198	0.0036*
P0/E19	0.187	0.0066*
E20/E19	-0.011	0.8565

* shows statistical significance

Combination of innervation density from each region (Fig. 5.7), allowed the effect of age to be isolated. This analysis shows that there are significant changes in innervation density between E19-P0 and E20-P0. To determine whether or not these were real changes in innervation it was necessary to examine the effect of area as shown in Table 5.4 above and Fig. 5.8.

Table 5.4b: ANOVA Factorial Analysis of Area size from E19-P0 in Combined Regions with CGRP

AGE	Mean Difference	p-Value
P0/E20	-24826.363	0.0019*
P0/E19	-29142.749	0.0005*
E20/E19	-4316.386	0.5568

* shows statistical significance

Consistent with the analysis of the CGRP region A alone, the overall area of regions A-D decreased at progressively older ages. These changes were significant between P0 and E20 (45%) and P0 and E19 (49%), corresponding with the observed changes in density. The decrease in area at P0, is a contributory factor for the observed density increase, therefore it is likely that similar to region A, actual CGRP innervation is decreased.

Additionally, these measurements show a trend in the epidermal area of regions A-D. The area increases from E17 to E19, then decreases from E19 to P0. This suggests proliferation of the epidermis from E17 which is then balanced possibly by some biological compaction from E19 to birth. Furthermore, the density levels relative to the

regional area are much lower for CGRP than PGP 9.5. This is consistent with CGRP labelling only a subpopulation of dorsal root ganglion sensory axons.

5.2 Differences in innervation density between identified subpopulations

The previous chapter focused on the immunohistochemical identification of different subpopulations of sensory neurons and their onset and localisation. Two timepoints have been selected for innervation density analysis. The first at E15, during the ingrowth of nerve bundles and the beginning of skin innervation in the hindlimb, and the second in the late foetal period at E18 when cutaneous innervation has been established.

i) Differences in subpopulation innervation densities at E15

At E15, the whole limb was analysed, using camera lucida drawings of innervation immunolabelled with PGP 9.5, RT97 and trkA, which are representative of total, A-fibre and C-fibre populations respectively. Using embryos of the same age with the same approximate target area, it was possible to examine the relative contribution of each subpopulation. At this early stage of ingrowth, the amount of innervation in the whole limb is small compared to the amount of uninnervated areas, nonetheless, the degree of cutaneous innervation was analysed for each marker.

Table 5.5: Innervation Density of sensory neuron subpopulations in the E15 Hindlimb

Innervation Density (pixels/μm^2)

Marker	Total	Skin	Skin Area (μm^2)
PGP 9.5	0.04	0.15	187334.00
RT97	0.06	0.14	417959.70
TrkA	0.02	0.02	598463.67

n=3 for each antibody

Table 5.5A: ANOVA Factorial Analysis of Innervation Density in the E15 Hindlimb

MARKER	p-Value for Total	p-Value for Skin
RT97/PGP 9.5	0.032*	0.566
RT97/TrkA	0.009*	0.014*
PGP 9.5/TrkA	0.018*	0.008*

*shows statistical significance

The total innervation density for the hindlimb is significantly different with the three markers examined. The surprising finding is that the A-fibre label RT97 shows a higher density than that of the general marker PGP 9.5. Although RT97 labels the putative myelinated fibres, and at all ages in the developmental timecourse shows heavy labelling of thick fibres, it is more likely that these differences arise from the plane of section. In some sections, larger bundles are present which may skew the data. TrkA however, has a much lower density value and in the sections only have thin loosely fasciculated fibres.

The skin region is more clearly defined and does not contain the large bundles which may alter data significantly by their presence or absence. The density of the skin innervation (Fig. 5.9) is not significantly different between PGP 9.5 and RT97 which suggests that the amount of A-fibres is similar to the total. There are significant differences between RT97 and trkA, and between trkA and PGP 9.5. The low density of trkA fibres is consistent with their fine calibre and maybe if the suggestion in Chapter 4 is correct, may be restricted to non-peptidergic fibres and therefore contribute less to the total than A-fibres. The area of the skin region must also be considered. From Fig. 5.10, the area of PGP 9.5 labelled skin appears less than both RT97 and trkA but this is only significant between PGP 9.5 and trkA. It is possible that the large area of trkA measured may have diluted its density, however the density is still eight-fold less than PGP 9.5 so the trend is likely to be unaffected.

In summary, at E15, the density of A-fibres is greater in both the whole limb and the skin than C-fibres. A-fibres contribute more to the total innervation than putative C-fibres.

ii) Differences in subpopulation innervation densities at E18

At E18, the epidermis from regions A-D were analysed as described above for each marker. From the IHC data, it was ascertained that all the markers utilised in this innervation analysis showed immunolabelled fibres in the epidermis at this age. In this analysis comparisons of innervation density with each marker were made in the four selected regions.

Table 5.6: Innervation Density of Sensory Neuron Subpopulations in Regions A-D of the E18 Hindlimb

REGION	PGP 9.5	RT97	TrkA
A	1.71	2.31	1.61
B	2.45	4.45	0.99
C	1.95	6.16	2.16
D	1.80	2.30	2.68

n=3 for each region and antibody

Examination of the data in Table 5.6 showed no statistical significance between the regions for any of the individual markers at 5% significance levels. Therefore, similar to the results presented above for CGRP, the data for each of the regions was combined to provide a mean value of innervation density for the hindpaw.

Table 5.7: Contribution of Different Sensory Neuron Populations to Innervation Density in the E18 Hindpaw

Marker	Mean Innervation Density (pixels/μm^2)	Area (μm^2)
PGP 9.5	1.98	43152.10
RT97	3.81	38453.98
TrkA	1.87	23703.70

n=12 for each antibody

Table 5.7a: ANOVA Factorial Analysis of Innervation Density in Subpopulations of Sensory Neurons in the E18 Hindpaw

Marker	Mean Difference	p-Value
RT97/PGP 9.5	1.828	0.224
RT97/TrkA	1.945	0.198
PGP 9.5/TrkA	0.117	0.947

Table 5.7b: ANOVA Factorial Analysis of Area Size for Different Sensory Neuron Subpopulations in the E18 Hindpaw

Marker	Mean Difference	p-Value
RT97/PGP 9.5	-4698.12	0.197
RT97/TrkA	14750.28	0.002*
PGP 9.5/TrkA	19448.40	0.002*

* shows statistical significance

The innervation density and area measured in the hindpaw are shown in Figs. 5.11 and 5.12. It appears that RT97 innervation density is greater than the total measured

by PGP 9.5, however there is no statistical significance between any of the markers for innervation density in the E18 hindpaw. This is surprising since peptidergic C-fibres are still not detectable at this age (see IHC data), therefore it was anticipated that the level of C-fibres detected with trkA would be less than both the total and A-fibres. The data was not affected by combination of the regions, as statistical analysis of each region with the different markers was similarly not significant.

The area of the region under analysis is found to be crucial to the interpretation of this innervation density, since as indicated in the previous analysis above, density may be artificially low due to an enlarged measurement area. In this case, there is no statistical significance in density between the different subpopulations at E18, however, from Fig. 5.12 it can be seen that differences exist in the size of regions analysed for each subpopulation. These differences are significant between RT97 and trkA, and PGP 9.5 and trkA (Table 5.7b). The fact that RT97 and PGP 9.5 areas are not statistically different, supports the density data suggesting that the amount of A-fibres are similar to the total. Conversely, the finding that trkA area is significantly smaller than both RT97 and PGP 9.5 means that the density values are theoretically higher than the absolute amount of innervation since such a small area was analysed. The E18 data follows the same trend as E15 where A-fibres are in higher density than C-fibres.

5.3 Epidermal innervation in relation to the corneal surface of the skin

The analysis of CGRP epidermal innervation from E19-P0 (Fig. 5.5) strikingly showed that the absolute innervation decreased in that it was withdrawing below the epidermal/dermal border, yet there was a small increase in density because of skin shrinkage. From Fig. 5.5, it is apparent that the number of evenly spaced axons projecting into the epidermis has increased from E19, but that these terminate further away from the skin surface than before. To examine whether this was a general feature of late development, the length that axons projected from the basal layer into the epidermis was measured and expressed as a ratio of the depth of the epidermis. This is referred to as the projection ratio, ranging from 0-1, where 1 represents axon terminals projecting the full depth of the epidermis to reach the surface. This measurement was conducted on one

section in each region and plotted against age, from E17-E20 for all markers used in Chapter 4 and also on CGRP from E19, (Fig. 5.13). Although, only a single section was measured for each marker and region, this was all that was required to establish whether there was a trend. Fig. 5.13 consistently shows that for each region, and with each marker the ratio decreases with age, indicating that axons terminate further away from the epidermal surface.

Although, the data in Fig. 5.13 is merely a general representation, it is interesting that in region A (the glabrous pad), the only markers showing an increase in projection are GAP 43 and CGRP between E19 and E20. This is consistent with CGRP as a marker for the second wave of growth. The GAP 43 labelling infers that these are new fibres, projecting further into the epidermis. CGRP then follows the trend as the other markers by retreating sub-epidermally. There are two other instances of increased projection ratio in Fig. 5.13, these are also between E19 and E20 and are both found with the marker peripherin. At this stage peripherin labels most neurons, its increase in the proximal region (C and D) of the hindpaw is consistent with the ingrowth of small diameter fibres. Another, interesting observation is that in Regions C and D, the projection ratio at E19 is identical for trkA and CGRP.

The conclusion is that less absolute innervation is found in the epidermis with maturity, due to the retraction of most fibres to a sub-epidermal plexus although there may still be changes in calibre or terminal number.

5.4 Summary

Innervation density increased in the presence of growth of the region undergoing innervation, from E17-E20 as detected by PGP 9.5, however, a substantial decrease was detected from E18-E19, suggesting that skin growth overtook innervation at this age. Slightly later, between E19-P0 no significant density change was detected with CGRP although due to area changes it is thought that actual innervation decreases from previous levels by P0. A contributory factor to actual innervation decreases may be the withdrawal of fibres to a sub-epidermal plexus, as indicated by the projection ratios. Regional

analysis showed no differences between the proximal and distal area of the foot, nor between glabrous and hairy skin during the period E19-P0.

At both E15 and E18, A-fibres are in greater density than C-fibres which contribute more to the total innervation. No regional differences were detected with the subpopulation markers.

Fig. 5.1: PGP 9.5 Innervation Density in Region A from E17-E20

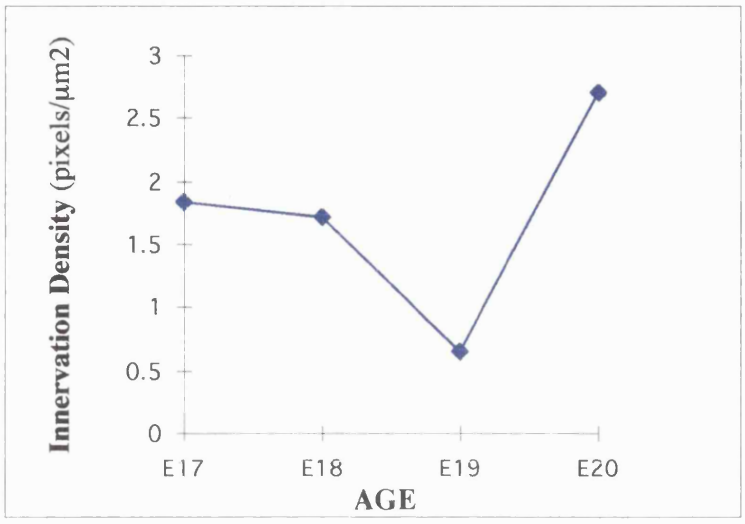

Fig. 5.2: Area of Region A from E17-E20 with PGP 9.5

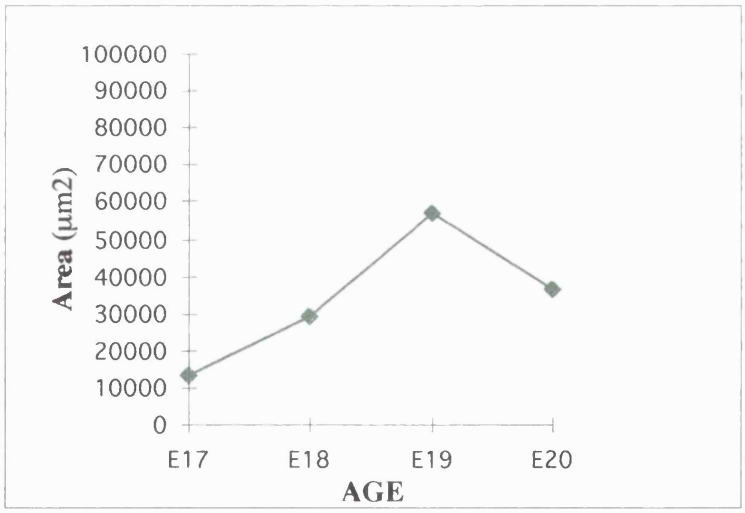

Fig. 5.3: CGRP Innervation Density in Region A from E19-P0

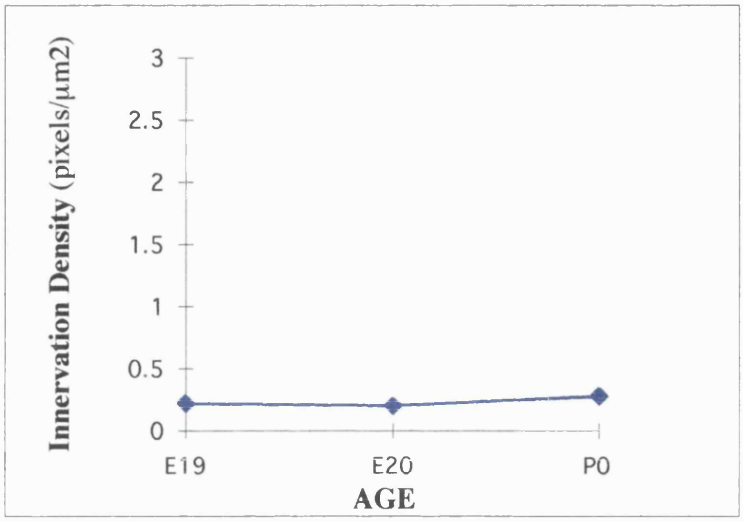

Fig. 5.4: Area of Region A from E19-P0 with CGRP

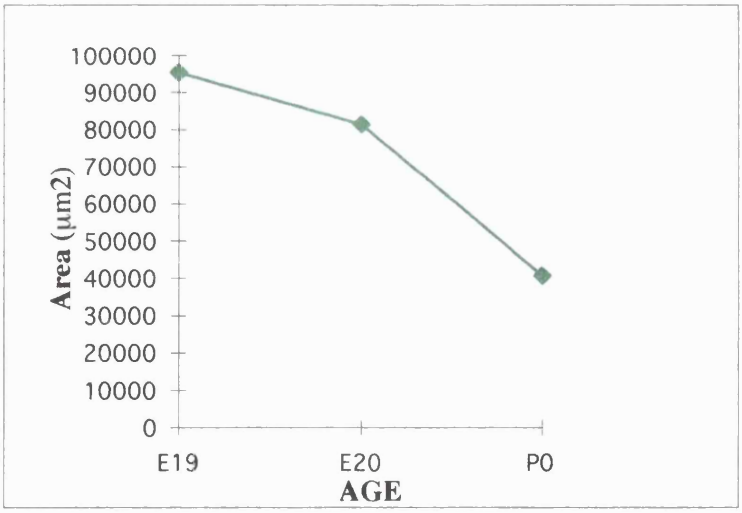

Fig 5.5: The Relative Thickness of the Epidermis Changes During Development

Camera lucida drawings of innervation in the first glabrous pad of the rat hindpaw, as visualised with anti-CGRP. The red lines delineate the epidermis, white lines represent the innervation. Epidermal innervation progressively retracts from E19-P0.

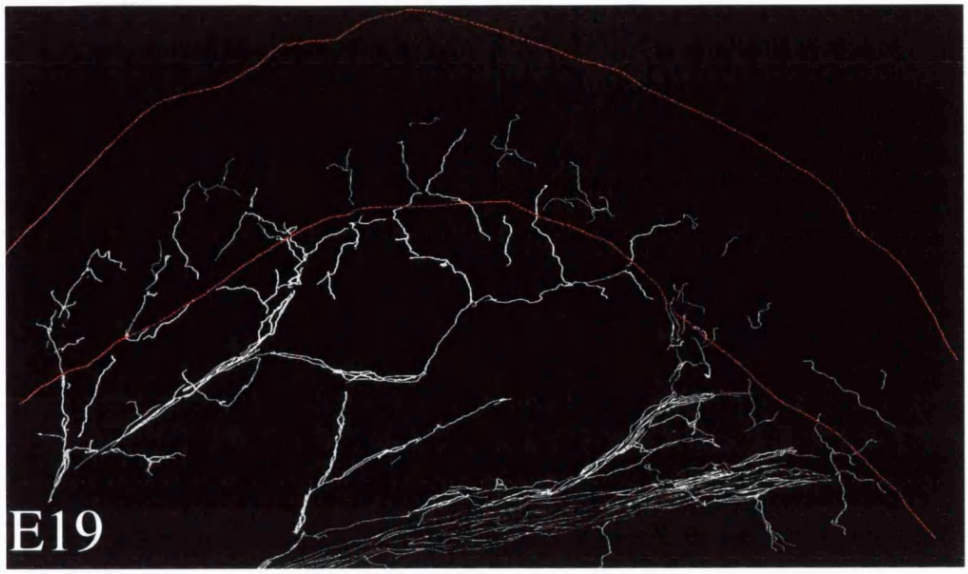
E19

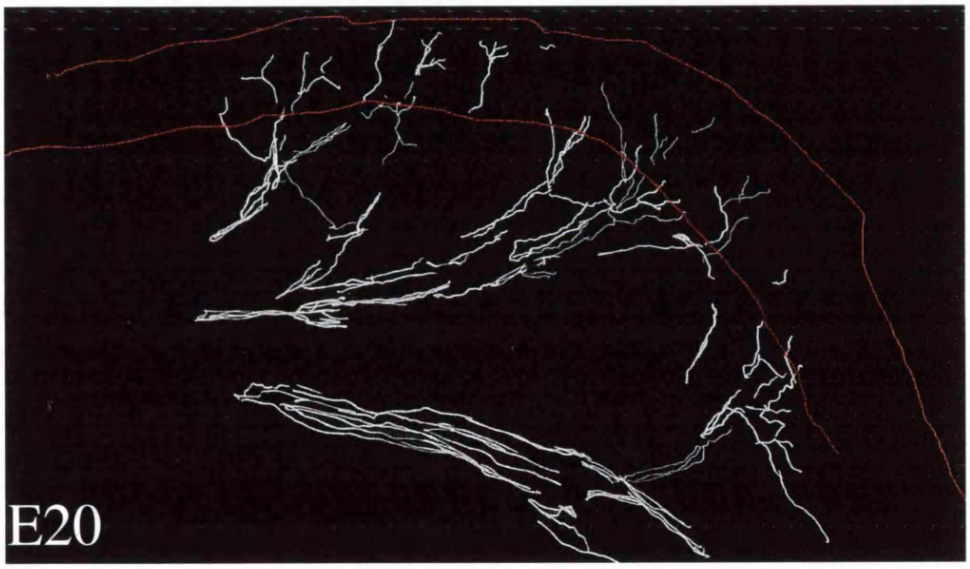
E20

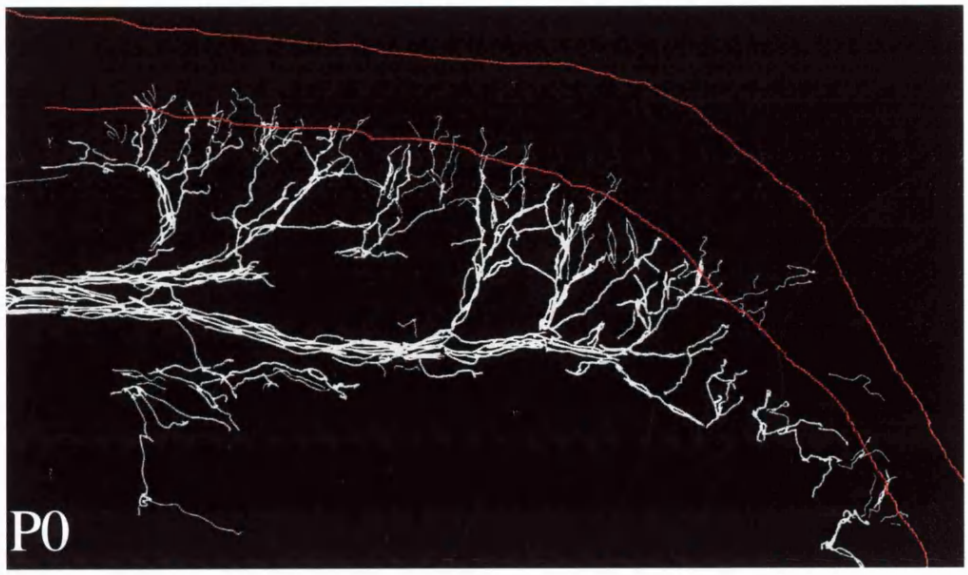
P0

Fig. 5.6: Innervation Density in Regions A-D from E19-P0 with CGRP

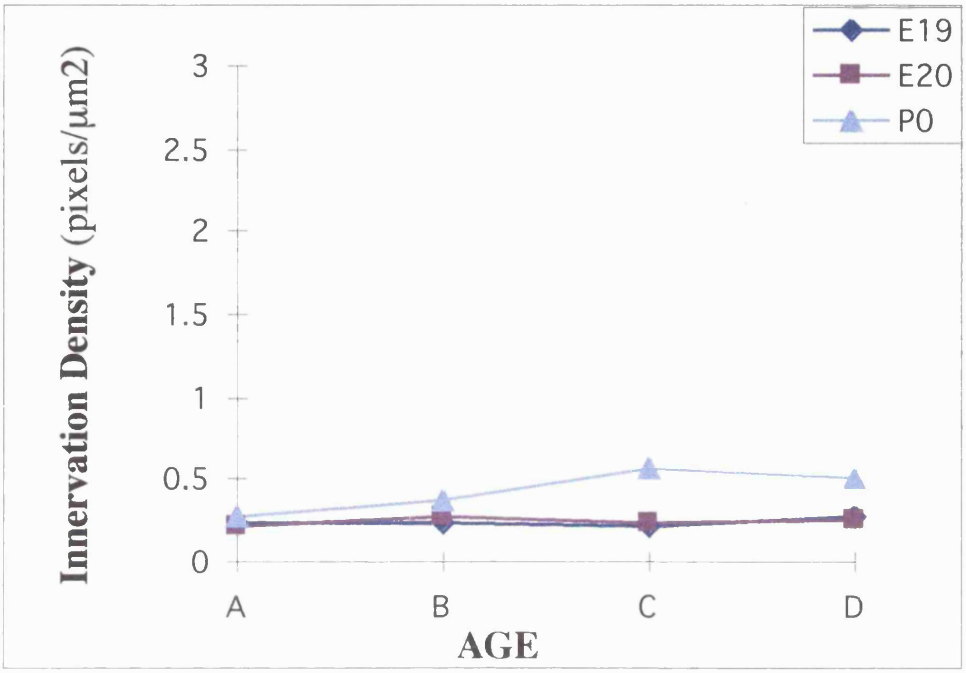

Fig. 5.7: CGRP Innervation Density in Combined Regions from E19-P0

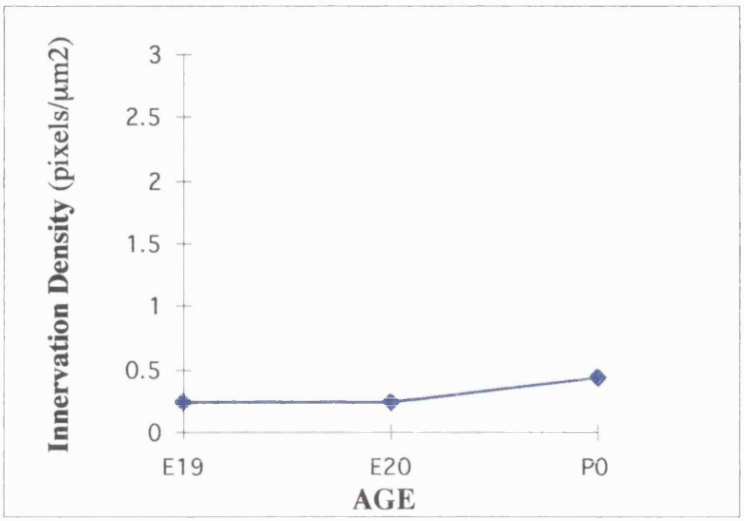

Fig. 5.8: Area of Combined Regions from E19-P0 with CGRP

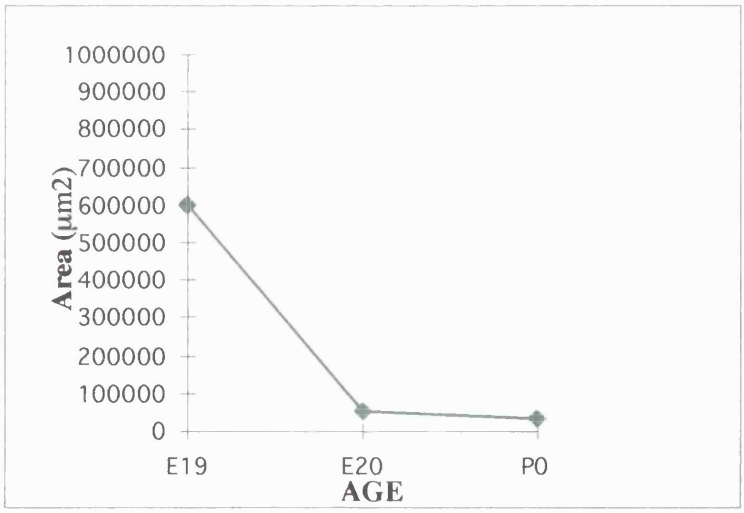

Fig. 5.9: Innervation Density of Sensory Neuron Subpopulations in the E15 Hindlimb

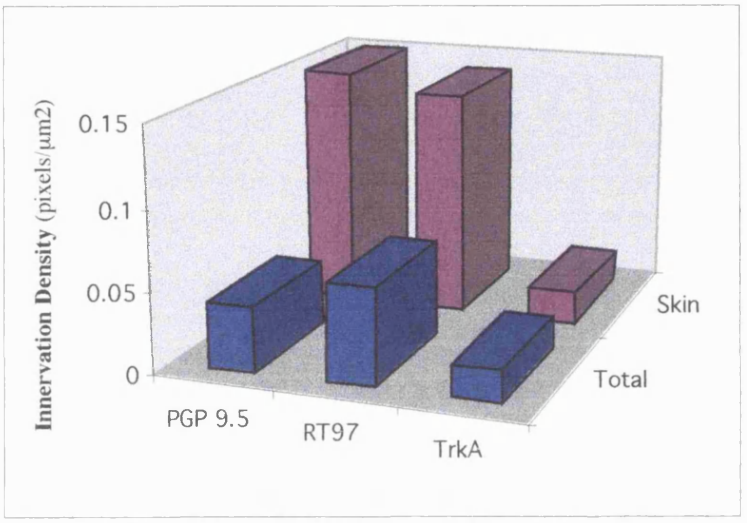

Fig. 5.10: Area of Skin in the E15 Hindpaw

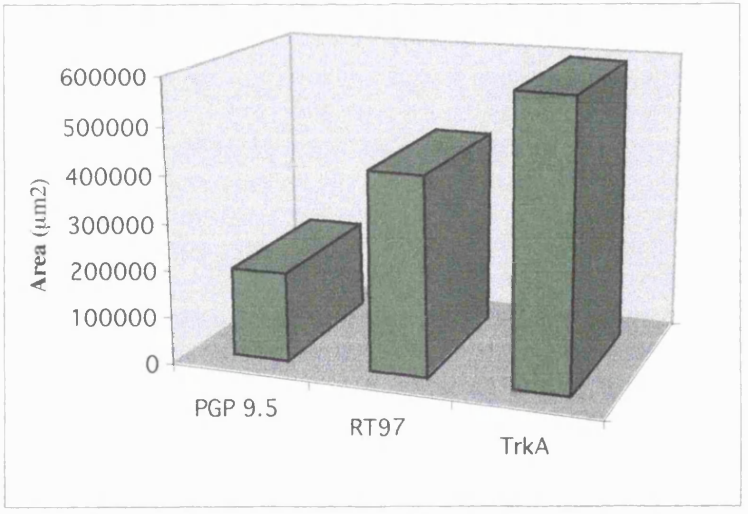

Fig. 5.11: Innervation Density of Sensory Neuron Subpopulations in the E18 Hindpaw

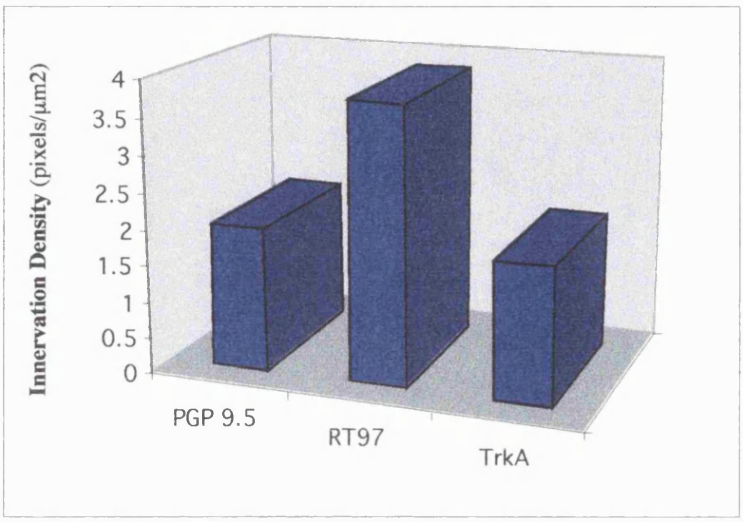

Fig. 5.12: Area of Skin in the E18 Hindpaw

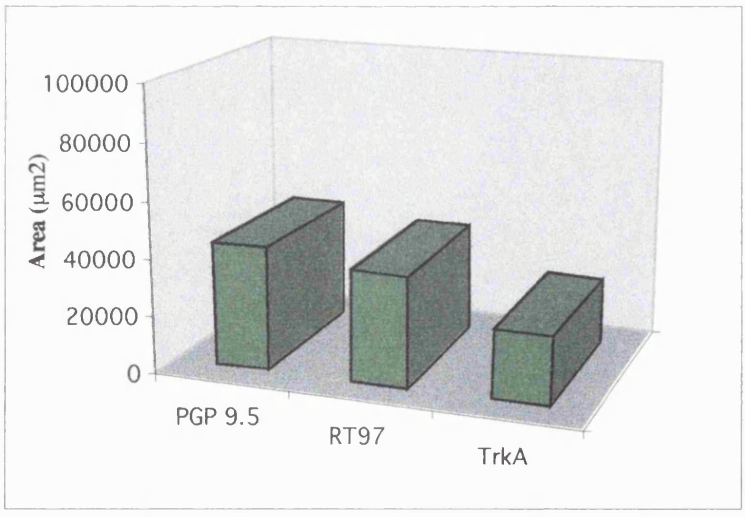

Fig. 5.13: The Projection Ratio of Epidermal Fibres to Epidermal Depth with Age

Regions A-D refer to the same as in methods (Chapter 2; Fig. 2.3).

Region A

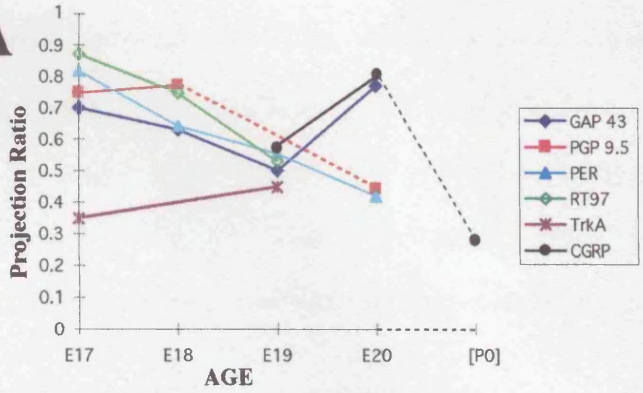

Region B

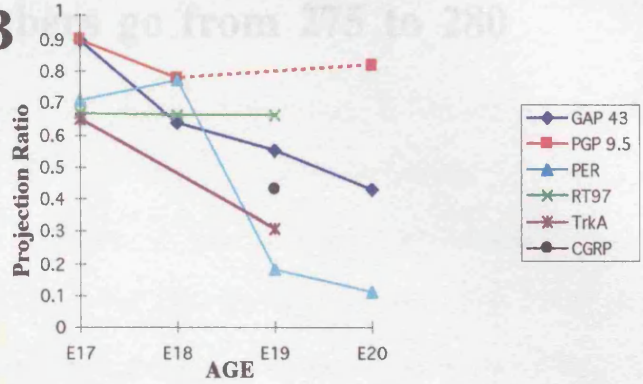

Region C

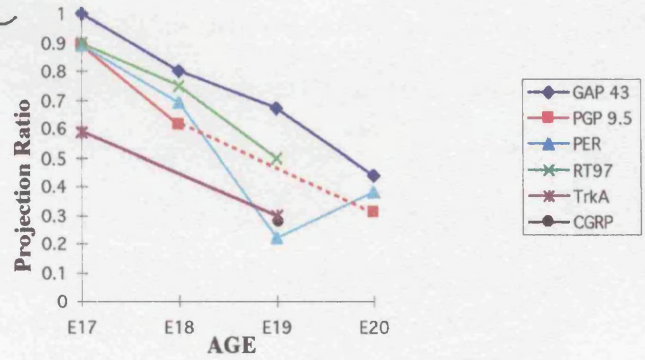

Region D

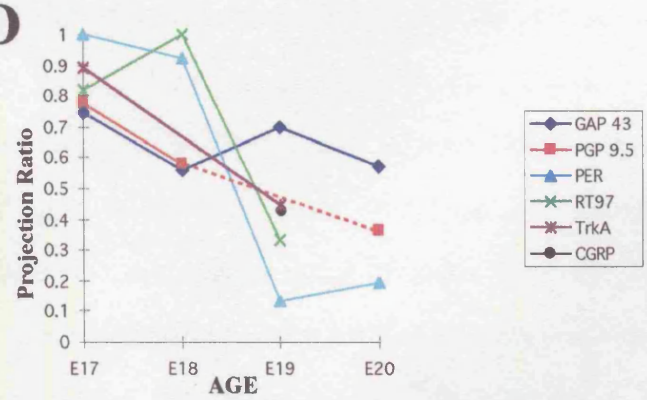

ERRATUM:
Page numbers go from 275 to 280

DISCUSSION

The innervation density analysis drew attention to three key aspects of epidermal terminal formation and to the caution required when interpreting this type of data. This analysis also succeeded in fulfilling its aims of examining innervation during foetal development and in detecting differences between subpopulations at selected ages.

5.5 Why is it important to differentiate between the innervation density at a particular age, the total volume of the tissue innervated and the actual amount of innervation?

This question is the pivotal technical issue to emerge from this analysis. In the introduction, I described the balloon hypothesis (section 5.2) which illustrated how changes in the size of target can alter the density while absolute innervation remains unchanged. This leads us to the point where we can ask which of the parameters is more informative? Initially, the density measurement was expected to reflect changes in innervation, as selection of a similar landmark region was thought to exclude large variations in the area of the region analysed. Subsequently, it was realised that the skin tissue in the region itself was undergoing radical development, some of which may lead to differing shrinkage during histological preparation and that while density is still important, it does not necessarily reflect what is happening to the actual innervation. Therefore, during development it is important to consider both aspects.

5.6 How does epidermal innervation of a defined region change with age?

Innervation of the epidermis changes in three aspects as development proceeds, density, innervation levels and terminal position. Firstly, the density decreases from levels at E17, but increases again at E20 to a stable level until another increase is detected at P0. As described above, this is not necessarily what happens to the actual innervation, since the area of the epidermis is altering during the same timeframe, however, density does reflect the amount of innervation within a micron squared piece of tissue. The fact that density changes during this period means there may be different functional thresholds. At E17 for example, a high density of nerve terminals might allow a greater

functional response to stimulation of a small area of skin than at E18. Although it has also been shown in regeneration studies, that presence of immunolabelled axons in skin does not always imply corresponding function (Kinnman & Wiesenfeld-Hallin, 1993). A striking feature of the DRG in foetal life is the presence of spontaneous activity (Fitzgerald, 1987). This might arise from sensitive, superficial nerve terminals in high densities in the skin at E17.

The second aspect of the developmental process of terminal formation that can be inferred from this study, is the absolute amount of innervation. This was deduced from the relative changes in density and area. While density decreased from E17-E19, the absolute innervation is likely to be unchanged, refuting the inference from the density data above that growth is exuberant. From E19-E20 an increase is innervation is deduced with PGP 9.5 but not CGRP. This may be explained by the sudden onset of CGRP expression at E19 (Chapter 4). It's levels do not change from E19-E20, but those of PGP 9.5 do as they now encompass the CGRP innervation. It is obvious that for the innervation to increase some form of growth occurs whether this is in calibre, branching or number.

The third aspect of epidermal development is the movement of terminals within the target. When axons first grow into the skin, they gradually grow deeper towards the skin surface. The projection ratio (Fig. 5.13) for each of the four regions from E17-E20 showed a general trend of withdrawal with all markers, also clearly illustrated in Fig. 5.5. The fact that this was a feature of all markers suggests that this occurs within all subpopulations. It had previously been reported that a postnatal retraction of fibres occurs with GAP 43 (Reynolds et al, 1991). It appears that this may occur much earlier, although the process in the neonate is accompanied by the growth of thin, unmyelinated axon terminal branches up into the epidermis (Reynolds et al, 1991) and other studies have shown fibre projections in the epidermis during the neonatal period (Marti et al, 1987).

These apparently conflicting results can be resolved since the retraction observed in this study is not complete and secondly the presence of postnatal epidermal fibres may be due to the presence of more peptidergic C- fibres. SP is not found in the skin

prenatally (Marti et al, 1987) so its ingrowth would also be accompanied by extended GAP 43 labelling whose late withdrawal may be the basis of the observation in Reynolds (1991) study. The purpose of this withdrawal in the embryo is not apparent but in the neonate may coincide with the development of receptor organs such as hair follicles and touch domes (Payne et al, 1991; Fitzgerald and Fulton, 1992), and may be causally related if the receptor organs replace the epidermis as the sensory surface. Some fibres expressing peptides obviously remain in the epidermis into adulthood (Cuello, et al, 1978; Dalsgaard et al, 1983; Marti et al, 1987; Bergmann et al, 1997). Intraepidermal axons can be traced as branches of a single fibre. Many axons end in the stratum spinosum as terminal knobs, larger than the beaded staining of the main fibre which are found solely in this layer below the stratum lucididum (Kruger et al, 1989).

This study does imply that withdrawal is a major contributory factor to the apparent decrease in the amount of innervation within the epidermis and not just death of terminals. What causes the onset of withdrawal remains unknown, however it may be linked to levels of neurotrophins particularly NGF (see Chapter 7). This would also be consistent with the two waves of cell death in the DRG that occur prenatally from E17-E19 and postnatally from P0-P3 (Chapter 3). It is also possible that the prenatal retraction of epidermal fibres primarily occurs in the A-fibre population, since these are putative myelinated axons whose terminals are not found in the adult epidermis. These fibres would need to withdraw prior to myelination which begins in individual axons at birth (Ziskind-Conhaim, 1988). Compatible with this proposal, RT97 terminals are subepidermal from birth yet CGRP branching continues in the neonatal epidermis (Reynolds & Fitzgerald, 1995).

5.7 Is it significant that changes are not detected between regions?

Density levels were not significantly different between the regions analysed, in addition, the same projection ratio trends were observed in each region. Perhaps this is not surprising, since during foetal life the characteristics of hairy and glabrous skin have not yet emerged. The hair on the dorsum of the rat foot is confined to one type and produces a simple and consistent pattern of innervation in the adult (Millard & Woolf,

1988). Hairy skin only develops postnatally with waves of hair growth following the prenatal waves of hair follicle production (Payne et al, 1991). A principle similar to that of innervation density exists where hair follicle density depends on the balance between production of new hair follicles and the change in skin area. Hair follicle density does show regional differences in the rat hindlimb, whereas human hair follicle growth stops prenatally and is diluted by the skin growth.

Axons wait for a week then grow from the dermal plexus towards the hair follicles at P3, reaches them at P5 and even extend into the epidermis by P7. The number of axons innervating a single follicle increase until P19, however, no exuberant growth is detected, in agreement with the prenatal innervation data presented here (Payne et al, 1991). The signal stimulating this dermal growth is equally as elusive as the opposite signal stimulating epidermal withdrawal in the embryo. It has been suggested that differential proteoglycan expression along the dermal-epidermal border and around developing follicles may contribute to this process (Couchman et al, 1990). This is not inconsistent with the reports of proteoglycan expression in chick skin where appendages develop (see Chapter 1.6.4) and that some inhibitory influence may propel the retraction of epidermal fibres. These events are nonetheless postnatal and support the finding that hairy and glabrous skin are similar in the foetal rat.

5.8 What are the differences between subpopulations?

The results of this aspect of the analysis are very clear. A-fibre markers have higher densities than C-fibre markers, and contribute more to the total innervation as detected with PGP 9.5, at both E15 and E18. The reason for this pattern is the greater absolute amount of innervation found with A-fibres during these periods. From the immunohistochemical data in Chapter 4 it was determined that A-fibres (RT97) were among the earliest innervating fibres, and that while C-fibres (trkA) were also present they were faint with thin loosely fasciculated bundles. The calibre of these axons alone could lead to different density measurements. The proposal in Chapter 4 that trkA is only labelling a subgroup of C-fibres may also explain the low density. It is suggested that trkA initially only labels non-peptidergic fibres then may also label peptidergic fibres that

have not begun to express their peptides. Peptide expression is detected at E19 after the density analysis was conducted.

Another difference between the subpopulations which suggests that the growth pattern of A-fibres and C-fibres is responsible for the disparity in density levels, is the subepidermal retraction of terminals. As stated, the overall trend for each marker was a decrease in the projection ratio with time, however this was postponed for CGRP and GAP 43, indicating that this was new growth undergoing the same programmed response but in a delayed timeframe.

5.9 What evidence supports changes in target structure as an influence on innervation levels?

The target of innervation evaluated in this study is the epidermis of the hindpaw. Since area of the target is crucial to the understanding of density, it is relevant to ask how much growth of skin occurs during this period in order to determine whether innervation is increasing in parallel when density is unchanged. A simple measurement of the depth and length of epidermis between two identifiable points on the hindpaw at four ages was conducted and used to calculate area and then to construct a growth index. These measurements were used to establish the framework for epidermal growth. From the diagram below, it can be seen that the area increases at progressive ages mainly due to elongation of the limb, however, the growth index, indicates that that the rate of growth defined by epidermal area is slowing. The growth index is the numerical factor by which the area changes from the previous age.

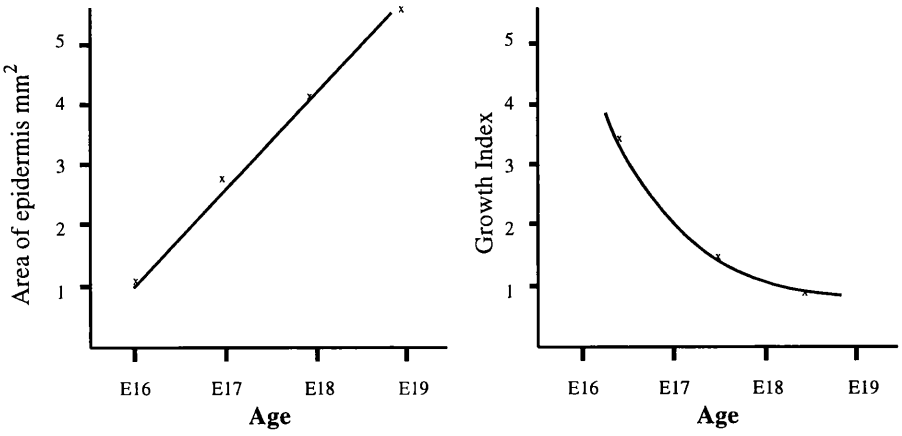

How does this apply to observations in this study? Firstly, it establishes that real changes are taking place in the target. Secondly, it may explain why density increases at E20 other than from a second wave of ingrowth. If growth of skin is slowing down and innervation is increasing a steady rate then at some point density will increase. Beforehand when growth was increasing rapidly, the addition of terminals was not sufficient to maintain density levels.

Changes in innervation in relation to the skin target have been the subject of investigation for a long time. In 1961, Fitzgerald (M.J.T.) examined the development of epidermal innervation in the pig skin. It was determined that the greatest number of epidermal ridges were formed in the foetus but that the concentration of nerve fibres beneath them did not peak until one month postnatally. The growth of nerve fibres into the ridges would have had to increase rapidly since there was none at day 0 but this rose steeply by 30 days to maximal at 160 days, yet the surface area increased 20 fold while the number of epidermal axons only increased 14 fold. The source of the axons penetrating the epidermal ridges were specified as collateral sprouts from the dermis that provided a neuronal pool from which the epidermis can acquire more fibres. It remains unclear however, why this process does not begin more gradually in the foetus when the target is being formed. The sudden projection postnatally resembles the sequence that occurs with innervation of the hair follicles. However in this case, since there is no indication of previous innervation, this area has suddenly become permissive and is actively recruiting collaterals possibly under the influence of neurotrophins.

Recent molecular studies have manipulated different aspects of the skin innervation model but have succeeded in complicating the issue. If the target is unchanged, but the neurotrophin NGF is overexpressed in the skin, hypertrophy of innervation occurs independent of changes in the volume of skin (Albers et al, 1994). Gross histological analysis of skin shows no abnormalities, so NGF production by the target tissue can control neuronal survival and establish the level of innervation. Another transgenic mutant where the low affinity neurotrophin receptor p75 was knocked out, showed a large reduction in the epidermal innervation, supporting the necessity of

neurotrophins to direct innervation levels, but the thickness of the skin was also decreased by 31% (Bergmann et al, 1997). This result raised the question of whether the lack of innervation, principally due to depletion of neurotrophins can affect epidermal proliferation (Bergmann et al, 1997) or whether the decreased target as a secondary effect of p75 removal, prevents innervation.

A third transgenic study involving innervation of skin, used overexpression of IGF-II. In this mutant, the skin is enlarged, the number of DRG neurons and NGF levels same as controls yet innervation is markedly reduced particularly in the superficial dermis and epidermis (Reynolds et al, 1997). This demonstrates how increased target and sufficient availability of neurotrophins do not increase innervation in the presence of IGF-II, a putative growth suppressant (Reynolds et al, 1997). Finally, the development of hairy skin innervation is associated with thinning of the epidermis (Reynolds & Fitzgerald, 1995) which is not suggestive of innervation having a positive influence on epidermal proliferation.

However, a role of innervation in promoting keratinization may not be excluded. A series of studies indicated that epidermal cells can be induced to differentiate *in vitro* into stratified squamous and keratinised epidermis (Hennings et al, 1983a; b; c) and *in vivo* these conditions may be partially regulated by peptidergic axons (Kruger et al, 1989). Peripheral release of the peptide CGRP from axons where tachykinins are co-localised, promotes cellular mitosis (Nitson et al, 1985) and may stimulate fibrosis and epidermal proliferation in normal and injury circumstances. This is consistent with the observation that changes in epidermal thickness occur in capsaicin-treated rats lacking CGRP-IR axons (Yeh & Kruger, 1984). Tissue maintenance is also compromised by lack of innervation as differentiation can impair epithelial repair of the cornea (Beuerman & Schimmelpfennigal, 1980).

5.10 Why are changes in innervation anticipated and what evidence is there for continued development of nerves?

Immunohistochemical studies of the development of innervation in the rat hindlimb show that markers of certain subpopulations display different temporal onset. It

has been evident for a long time that two principle waves of innervation occur in the spinal cord and data in Chapter 4 is consistent with a similar scenario in the periphery. These broadly correspond to A-fibre and C-fibre growth. Hence, until the C-fibre innervation is established the adult-like densities of innervation cannot be attained. From what is known about the number of processes that are occurring in the last few days of embryonic life and the first postnatal week, it is apparent that we should expect many changes in the innervation density levels. The process by which the balance of growth and innervation of target is achieved, is of importance not just to the understanding of development but to regeneration after injury, where regenerating axons recapitulate many aspects of development.

The first wave of innervation is incorporated into the target and may undergo trophic competition before the next surge of innervation, resulting in prenatal cell death of parent neurons. The second wave of innervation begins in the late foetal period, but continues to develop postnatally from evidence of peptidergic expression. At this time, the onset of sympathetic innervation is also underway (Schotzinger & Landis, 1990), although epidermal innervation is sparse so this should not be a major participant in the establishment of density levels. In the first few postnatal days, a second period of cell death occurs and this reinforces the observations made by Fitzgerald, M.J.T. (1961) where it was noted that during the growth period regressive features are normal and that degeneration is frequent in cutaneous nerve plexes. Taking all these rapid changes into account with the development of the target outlined above, it is not surprising that developmental studies are difficult to interpret.

Regeneration studies, help to identify the underlying processes as these arise from denervation solely and not changes in target. One study illustrates this clearly. Navarro and colleagues (1997), examined density and the depth of projection into the epidermis of the footpad with PGP 9.5 and CGRP in naive and sciatic nerve crush/axotomy rats. Post-crush, PGP 9.5 labelled axons penetrated a short distance into the epidermis after 17 days, by four weeks the number of axons had increased and extended 50% of the epidermal depth. CGRP axons took four weeks to reach the epidermis, showing the same

process of delay as in development. It was a further three weeks before a few fibres extended to the corneum as before. The abnormal pattern of reinnervation tended to regress to a near normal distribution long after injury where late changes were attributed to retraction of terminal axons or even a change in the synthesis and expression of the neuropeptides in the primary sensory neurons that are possibly not labelling the original type of nerve fibres. However, intraepidermal axons are confined to the basal layer after sciatic crush/axotomy (Stankovic et al, 1996), suggesting that although the target is unchanged the factors required to induce extension into the epidermis are absent, for example neurotrophins. This aspect is entirely consistent with the transgenic models described above.

6

ONTOGENY OF CGRP mRNA IN LUMBAR SPINAL CORD AND DRG

INTRODUCTION

6.1 Aim

The late onset of Calcitonin Gene Related Peptide (CGRP) protein expression in the DRG detected in Chapter 4, prompted the question of when CGRP synthesis begins. Possibly, initial levels of protein are below those detectable by immunohistochemistry (IHC). The aim of this chapter was to examine the expression of CGRP mRNA in the embryonic rat DRG and spinal cord and compare this to the IHC expression data. The results were used to determine when the peptide is available relative to the development of the peripheral and central targets.

6.2 Neuropeptides

The discovery of substance P (SP), CGRP and other neuropeptides in a restricted population of sensory neurons and their axons is of special interest since these peptides are predominantly found in small cells and unmyelinated axons that include a substantial proportion of nociceptors. The tissues innervated by peptidergic axons are largely sites from which pain can be elicited and unmyelinated/thinly myelinated axons possess nociceptive properties which have been identified electrophysiologically. The link between these aspects has meant that nociceptive or small diameter axons can now be anatomically identified by using immunohistochemistry for the neuropeptides. Another prominent feature of peptidergic endings is their relation to autonomic targets including smooth muscle, glands and blood vessels. This implicates them in effector roles and indeed they are released after nociceptive stimulation and have a number of potent biological actions attributed to them.

The neuropeptides CGRP and SP are co-expressed in 80% of DRG neurons and most studies investigating the expression, action or influence of neuropeptides examine both these peptides in parallel. Below is an account of CGRP that details its expression,

function and plasticity and is followed by a brief account of SP as much information is common to both.

6.3 Calcitonin Gene Related Peptide (CGRP)

6.3.1 Identification and structure

Calcitonin Gene Related Peptide (CGRP) is a 37 amino-acid neuropeptide related to the gene encoding the hormone calcitonin. It was discovered by Amara et al in 1982 from analysis of the primary calcitonin gene transcript, but differs from calcitonin as the mRNA for CGRP predominates in the peripheral nervous system (PNS). The calcitonin gene has two closely related CGRP mRNA transcripts, denoted α-CGRP, the first to be discovered and the most dominant in sensory ganglia, and β-CGRP differing by 1 (rat) and 4 (human) amino acids (Amara et al, 1985; Morris et al, 1984).

6.3.2 CNS expression

CGRP expression in rat CNS appears in a caudo-rostral direction in late gestation (Hares & Foster, 1991). More specifically, CGRP is initially localised to the motor neurons between E15 and E17 in the rat (human 6-14 wks), then subsequently decreases towards birth (Marti et al, 1987). By E18 CGRP expression is observed in the forebrain and diencephalon with continued expression developing perinatally and into adulthood at P56 where it is expressed abundantly in both cells and fibres (Inagaki, 1988). In contrast, Kubota (1988) found that maximum expression in cells of the brainstem peaked between P2 and P6, then decreased into adulthood although expression in fibres increased to reach and maintain adult levels by P14. This indicated that the possible function of CGRP in this region of the adult was neurotransmission or neuromodulation, whereas in the Inagaki study the high density of embryonic cellular CGRP suggests it is a more important factor in the developing organisation of the CNS.

CGRP is detected in the fibres and presynaptic terminals of laminae I, II and V of the spinal cord (Skofitsch & Jacobowitz, 1985) and in some cases fibres connect medial lamina V with the dorsal extent of lamina X in addition to fibres running between lamina

II and X (Gibson et al, 1984). Expression in the axons and terminals of the lumbar spinal cord of the adult rat is restricted to lamina I and II outer of the medial dorsal horn while in lamina I only laterally. Cell bodies were labelled in the ventral horn but absent in the dorsal horn (McNeill et al, 1988a; Piehl et al, 1992), although CGRP-IR fibres are most concentrated in the dorsal horn and show the highest concentration after radioimmunoassay (Gibson et al, 1984).

6.3.3 DRG expression

CGRP expression in the DRG cell bodies begins at E16 and is maintained into adulthood (Marti et al, 1987). This study compared the developmental pattern of peptides in motor and sensory (DRG, dorsal horn & epidermis) areas. Coincidental with the increase in DRG and fibre expression, is the earliest appearance of CGRP in the rat epidermis.

CGRP mRNA is found in a large number of small to medium sized neurons in the DRG (Rethelyi et al, 1989) with a reported 50% of all DRG cells expressing CGRP mRNA (Kirchmair et al, 1994). Adult neurons expressing CGRP have areas ranging from 300-2750μm^2, while at P2 they range from 150-700μm^2 (Goldstein et al, 1991). Although all the β-CGRP mRNA neurons also express α-CGRP, they have different size-distributions, with the α-CGRP occurring in the larger CGRP+ve neurons, suggesting they are differentially regulated and have different roles (Noguchi et al, 1990).

Using immunohistochemistry, McCarthy and Lawson in 1990 showed that 46.5% of all DRG neurons were CGRP positive. The distribution of CGRP-IR within the DRG sub-populations was described by Fang, 1987; Ju et al, 1987; Lee et al, 1985; Gibbins et al, 1987; Gibson et al, 1984 as largely unmyelinated or small myelinated but mainly reported in small to medium sized neurons of diameter 15-65mm. The exception to this conclusion was Lee (1985) who presented a distribution biased to large cells. McCarthy & Lawson (1990) detected CGRP-IR in all sizes except the very largest. Using RT97 to discriminate between small dark and large light DRG cells, they found 62% of RT97 negative(-ve) cells (small dark) were CGRP-IR. The weight of distribution was therefore towards the smaller cells and towards C-fibres since Lawson (1985; 1988) established

that all RT97-ve cells were C-fibres. Furthermore, they also found 30% of RT97 positive(+ve) cells (large light) to be CGRP-IR. This indicated that a proportion of CGRP-IR cells might have A-fibres, in agreement with evidence that it is localised in myelinated and unmyelinated nerve fibres (Kakudo et al, 1988; McNeill et al, 1988a; 1988b).

Electrophysiological studies revealed that conduction velocities of CGRP-IR cells ranged from a slow C-fibre velocity of 0.5m/s to a fairly fast A-fibre velocity of 28.6m/s. The number of CGRP+ve neurons in the electrophysiology study was 29% which despite being lower than the mean number (46.5%) identified immunohistochemically, is probably the inevitable result of sample bias in recording neurons with larger soma. Of the electrophysiologically identified C-fibres 46% were CGRP+ve, which is less than the IHC study (62%) most likely due to the small population of C-fibres recorded. The electrophysiology and IHC data on A-fibres were more closely associated. 25% of A-fibres observed had CGRP-IR, correlating well with the percentage of RT97+ve neurons that were also CGRP+ve (30%).

The conclusion reached from all these studies is that CGRP is a marker for fine afferent fibres but is not completely selective. It appears to label all fibres except those with the largest diameters.

6.3.4 Peripheral expression

Molander and colleagues, (1987) discovered that CGRP projections reached cutaneous and muscular targets in addition to autonomic ganglia. In a later study, O'Brien (1989) determined the type and proportion of CGRP+ve afferents from these targets. 50% of large light CGRP+ve afferents were from muscle and skin, 50% of small dark skin afferents were CGRP+ve and 100% of small dark muscle afferents were CGRP+ve.

CGRP co-localised with SP is found in axons around blood vessels in the dermis of hairy skin, and is also present in the plantar skin of the foot with their axons penetrating the epidermis (Gibbins et al, 1987; Kruger et al, 1989). Radioimmunoassay has been used to determine the relative levels of CGRP in rat epidermis where it is present

in decreasing levels from the following tissues: nose, footpad, face, tail and back (Mulderry et al, 1984).

In the human, a few CGRP fibres were observed in the dermis at 7 weeks, but it was not until 17 weeks that these were demonstrated in the sub-epidermal plexus (Terenghi et al, 1993). CGRP-IR fibres alone were reported around eccrine sweat glands while in the dermis and around hair follicles they were identified with SP (Tainio, 1987). In contrast, Dalsgaard (1987) demonstrated CGRP in the dermis and epidermis as free nerve endings and also determined that CGRP fibres surrounding sweat glands were of sympathetic origin due to the Vasoactive Intestinal Polypeptide (VIP)-like pattern.

The distribution of peptides in a variety of species reveals differences in the density of innervation to the epidermis and dermis. However, in all species CGRP forms the largest population in comparison with other peptides (Karanth et al, 1991).

6.3.5 Plasticity

Manipulation of the peptide levels through capsaicin application, injury or inflammation can result in phenotypic changes of the primary afferent nociceptor (Levine et al, 1993) and as a consequence, changes in function.

The local application of capsaicin, a selective neurotoxin which destroys a sub-population of DRG neurons with unmyelinated axons, to an adult peripheral nerve (Wall, 1987) or neonate (Nagy et al, 1983, Franco-Cereceda et al, 1987; Hammond & Ruda, 1989; 1991) reduces CGRP expression in the spinal cord. CGRP in the superficial dorsal horn (laminae I, II & V) and dorsal roots is also depleted by dorsal rhizotomy (Gibson et al, 1984; Chung et al, 1988; Traub et al, 1989; Verge et al, 1985). This procedure reveals the likely origin of CGRP-IR fibres and terminals in the spinal cord because the affected areas are those which receive terminals from primary sensory neurons that are disconnected from source by the rhizotomy. It is therefore reasonable to assume the greatest quantity of CGRP is derived from dorsal root ganglia, which itself shows elevated levels following rhizotomy (Inaishi et al, 1992).

Furthermore the ventral horn CGRP levels are not affected by this manipulation, nor ventral rhizotomy (Piehl et al, 1993) and can be enhanced by colchicine treatment,

indicating that at this location the peptide is synthesised in the cell body (Gibson et al, 1984). Evidence supporting this proposal arises from CGRP mRNA detection in motor neurons of the adult, confirming the motoneuron involvement in CGRP manufacture, contrary to previous assumptions since CGRP-IR in human motor nerve terminals was poor compared to the rat (Gibson et al, 1988).

A long-term study after dorsal rhizotomy reported the reappearance of CGRP in the superficial dorsal horn. CGRP re-emerged with a local density gradient showing higher levels towards neighbouring intact segments (Piehl et al, 1992). These authors proposed the recovered CGRP is derived from proliferating collateral branches of primary afferents from neighbouring intact segments. Also supporting an external source is the site of mRNA synthesis which rules out an intrinsic source.

Axotomy also leads to the downregulation of CGRP, SP and TMP in the adult DRG (Barbut et al, 1981; Jessel et al, 1979; Devor & Claman, 1980). This is attributed to the withdrawal of trophic factors, specifically NGF which has been directly shown to regulate peptide neurotransmitter/neuromodulator levels in the adult (See 6.3.6).

However, after neonatal axotomy there is only a transient decrease of neuropeptide levels in the spinal cord (Himes & Tessler, 1989; Reynolds & Fitzgerald, 1992) despite complete depletion of thiamine monophosphate (TMP) resembling the adult nerve section. The absence of TMP indicates that the signal response to the cell bodies of the neonate are comparable, therefore it is the neuropeptides that are responding differently. Reynolds & Fitzgerald proposed that the transient neuropeptide reduction could be associated with the substantial DRG cell death. It is known that 30% of axotomised adult neurons compared to 75% of neonatal neurons die after sciatic nerve section, and that neuron loss is both more rapid and more extensive in neonates, 5-10 days compared to 10-60 days for adults (Himes & Tessler, 1989). Hence, the extent of cell death alone is sufficient to temporarily deplete levels of the neuropeptide and so may not reflect actual downregulation but more likely upregulation in the surviving neurons to replenish peptide levels. A recent study confirmed the 50% neuron death in the neonate post-axotomy and ascertained that gene/peptide levels in the DRG did not exceed

constitutive levels. This verifies that upregulation does not occur, and regaining of dorsal horn peptide expression is attributed to rostral and caudal sprouting of L4 and L5 DRG's (Nothias et al, 1993).

Manipulations that increase the peptide levels also have profound effects. Hindlimb injections of formalin resulted in elevated levels of neuropeptide mRNA in the DRG (Noguchi et al, 1988). In another inflammatory model Smith and colleagues reported an increase in CGRP and SP in DRG neurons that innervated joints affected by adjuvant-induced arthritis (Smith et al, 1992). Axotomy, as described above, diminishes CGRP and SP but increases levels of VIP and galanin (Hokfelt et al, 1987; Noguchi et al, 1989) in DRG neurons that previously expressed CGRP (Doughty 1991), which is the strongest indication that phenotypic switching occurs. Changes in function can be anticipated from modification of peptide levels as a study directly applying anti-CGRP to the spinal cord, mimicking the injury models, established that this had an antinociceptive action (Kuraishi et al, 1988).

6.3.6 Regulation of Neuropeptide levels

NGF has been directly shown to regulate peptide neurotransmitter or neuromodulator levels in the adult. (Heumann et al, 1984; Lindsay & Harmer 1989; Noguchi et al, 1990; 1993). Basal levels of CGRP production occur *in vitro* in the absence of NGF, suggesting an additional regulating factor. However, when rhizotomy is preceded by a sciatic nerve cut (that decreases DRG CGRP levels), the normal increase in CGRP did not occur. When NGF is applied to the sciatic stump before the rhizotomy, the increase in CGRP occurs indicating that rhizotomy stimulated synthesis requires peripheral integrity. So CGRP regulation requires co-operation of centrally derived factors and peripherally derived NGF (Iniashi et al, 1992).

Another study that examined the effects of NGF on specific DRG sub-populations found that NGF infusion after a sciatic cut counteracts the CGRP and SP depletion of the DRG but not Somatostatin (SOM). This is consistent with the absence of trk A receptors on SOM+ve neurons. NGF also prevented up to 50% induction of other peptides not normally expressed, hence the peptides are differentially regulated by NGF which may be

part of a cascade normalising the response to injury (Verge et al, 1995). A very detailed study has clarified the intracellular process by which NGF regulates neuropeptides by examining the upstream transcription factors and their regulation, for review see Kashiba et al, 1996. The evidence supporting NGF as an inductive signal for CGRP expression is persuasive, although it may not be the only peripheral signal, and is not likely to be the central factor.

6.3.7 Co-localisation

CGRP is often found overlapping with the smaller sub-population of sensory neurons containing SP (Lee, 1985; Dalsgaard, 1988). They co-exist in the primary afferent dorsal horn terminals (Merighi et al, 1988; Fried et al, 1989; Plenderleith et al, 1990). Secretoneurin is another peptide concentrated in laminae I & II and motor neurons, with highest expression in lamina II and the DRG. It overlaps with CGRP and SP in the outer lamina of the dorsal horn and some motor neurons (Marksteiner et al, 1994).

Merkel cells in the cat contain CGRP in addition to and co-localised with VIP yet in the rat these cells are not immunoreactive to CGRP (Alvarez et al, 1988) nor VIP (Hartschuh et al, 1979) despite both having been found in the cell bodies of rat sensory ganglia (Ju et al, 1987). CGRP+ve DRG neurons also share expression with small neurons identified with NPY-R mRNA and protein (Zhang et al, 1994).

6.3.8 Function

The sensory function of CGRP has yet to be localised to a particular group of neurons and defined, although a majority of CGRP-IR neurons have a slow conduction velocity of less than 2-5m/s (Hoheisel et al, 1994). Its effector role both peripherally and centrally has been better described. The peripheral release of CGRP has been linked to vasodilatation and control of blood flow (Brain et al, 1985) and has a synergistic action on Substance P (SP) release (Gamse & Saria, 1985). CGRP is the best example of a neuromodulator as it has limited effects by itself but dramatically increases and potentiates effects of other compounds (Levine et al, 1993) notably SP, where CGRP retards its enzymatic breakdown (Le Greves et al, 1985).

The central release of CGRP occurs in the dorsal horn after a noxious thermal/mechanical/electrical stimulus from the periphery (Morton & Hutchinson, 1990). This, or iontophoretic application, produces a slow-onset, long-lasting excitation of nociceptive dorsal horn neurons, suggesting a role in transmission or processing in the spinal cord (Miletic & Tan, 1988; Ryu et al, 1988a & 1988b). CGRP and SP are co-localised in the same vesicles in DRG somas, axons and terminals of the guinea pig (Gulbenkian et al, 1986) and act synergistically on the spinal cord in behavioural studies (Wiesenfeld-Hallin et al, 1984; Woolf & Wiesenfeld-Hallin, 1986). These studies suggest a possible role for C-afferent neuropeptides in long-acting gain modulation of nociceptive inputs into the spinal cord.

The task of defining the sensory role of CGRP is complicated by the fact that it is apparently not restricted to neurons with a particular sensory function. In 1990, McCarthy & Lawson also found CGRP in 25% of A-fibres studied. If CGRP is in A-fibres then it could be involved in neurogenic vasodilatation, as a previous study presented evidence that this can be produced by Aδ-fibre involvement (Janig & Lisney, 1989). However, since CGRP is found in the soma of C, Aδ and Aα/β fibres its presence does not correlate to a specific type of sensory receptor suggesting a diversity of roles for this neuropeptide.

A new trophic role has been suggested by Nitsos, 1994. This study involved examination of the ontogeny of CGRP receptors. It was found from binding studies that CGRP receptor expression begins in foetal life before the primary afferent uses CGRP as a fundamental neurotransmitter. Therefore it is suggested that initially this peptide is important for growth, differentiation, connectivity or synapse maturation and these roles are later replaced by that as a neuromodulator. Examination of CGRP receptors is also paradoxical as there is an apparent mismatch in the distribution of CGRP-containing terminals and dorsal horn binding sites. In fact, these are especially low in the substantia gelatinosa (Kruger et al, 1988a) increasing only after dorsal rhizotomy (Charlton & Helke, 1985).

There is also a possible trophic role in muscle. CGRP mRNA is detected when neuromuscular synapses are forming, in the neuromuscular junction (NMJ) and motor

neurons of the week old rat. Levels gradually diminish in both and is negligible in the adult NMJ, but the decreases are related (Matteoli et al, 1990). Moreover, CGRP is thought to regulate synthesis of acetylcholine (ACh) receptors in nerve-muscle junctions in chick (Fontaine et al, 1986; New & Mudge, 1986). If axonal flow is blocked with vinblastine, α-CGRP mRNA accumulates in motor neurons (Kato et al, 1992); in addition the rate of CGRP anterograde axoplasmic transport decreases with age, which is consistent with changes in CGRP delivery contributing to age-related changes in the junctional ACh receptor (Fernandez & Hodges-Savola, 1994). The anterograde CGRP transport although slower in the mature animal, remains in the fast transport system as it is located in the LDCV (large dense cored vesicles) (Gulbekian et al, 1986) of diameter 100nm (Smith, 1980) which are part of the regulated exocytotic pathway indicative of fast transport (De Camilli & Jahn, 1990). These studies confirm the importance of CGRP in the immature NMJ and indicate that motoneuron-derived CGRP acts as an anterograde muscle trophic factor.

6.4 Substance P (SP)

6.4.1 Identification and structure

Substance P (SP) is an undecapeptide, was the first neuropeptide structurally characterised and is a member of the tachykinin/neurokinin family (Levine et al, 1993). It is translated from a precursor gene, preprotachykinin (PPT). The neurokinin receptors are NK1 (Masu et al, 1987); NK2 (Yokota et al, 1989) and NK3 (Buck et al, 1984), but it is NK1 that preferentially binds SP.

6.3.2 Expression

SP is first observed between E16 and E18 during development, in both cells and fibres of the spinal cord, and continues to increase in intensity until birth, but it is only expressed in the DRG at E21 (Marti et al, 1987). After birth, the number of immunoreactive cells in the spinal cord decreases until only a few are detectable at P7-10, so there is only a transient expression during development (Ni & Jonakait, 1988; Du et al,

1987, Inagaki et al, 1982). A similar distribution of SP in perikarya is seen in the developing and adult chick cords (Du & Dubois, 1988). Although, the co-existence pattern differs considerably among species. In general, the pattern of peptide content is developmentally regulated (Hammond & Ruda, 1991).

In the adult, SP terminals are found in laminae I and IIi of the dorsal horn (Hokfelt et al, 1975a; 1975b; 1976); confirmed by many subsequent studies (see Willis & Coggeshall, 1991). The origin of this SP labelling has been ascertained, and found to be to be equally from primary afferents and intrinsic axons (Tessler et al, 1980; 1981; Mantyh & Hunt, 1985a; Ruda et al, 1986). 20% of adult DRG cells, of small to medium diameter express SP (Hokfelt, 1975). This is confirmed by finding most SP+ve neurons in the RT97-ve population although a small percentage can be found in the RT97+ve population (McCarthy & Lawson, 1989).

In the periphery SP is found in 3/4 of muscle afferents, 2/3 of joint afferents and only 1/3 skin afferents (O'Brien et al, 1989). SP is also found in thin unmyelinated fibres in peripheral nerve and in the connective tissue of skin, (Hokfelt et al , 1976).

6.4.3 Plasticity

Axotomy of the sciatic nerve led to depletion of PPT mRNA in the DRG (Noguchi et al, 1989) and a corresponding decrease in SP-IR in the dorsal horn terminals (Barbut et al, 1981).

In contrast to the depletion associated with nerve injury, tissue injury induced by inflammatory agents increase both PPT mRNA (Noguchi et al, 1988) and SP (Smith et al, 1992) in the DRG. Neonatal capsaicin treatment significantly decreases SP in the DRG and dorsal spinal cord (Kesser & Black, 1981), and also reduces the severity of reaction to induced arthritis (Levine et al, 1986). NGF treatment however, increases the SP content in DRG and dorsal spinal cord, suggesting a link between SP release and elevated NGF levels.

6.4.4 Co-localisation

SP co-localisation with CGRP may be greater than 80% (Wiesenfeld-Hallin et al, 1984; Gibbins et al, 1987b; Ju et al, 1987b) but it is not found with SOM in the rat (Hokfelt et al, 1976) and only occasionally with cholecystokinin-octapeptide (Tuchscherer & Seybold, 1985; Gibbins et al, 1987b). SP is co-localised with galanin (GAL) in the DRG (Ju et al, 1987).

6.4.5 Function

The functions of SP have not been categorically proven for a number of reasons outlined below but it has been associated with roles in peripheral neurogenic reactions and nociception (see Willis & Coggeshall, 1991) and as a central neurotransmitter of primary afferent neurons (see Levine et al, 1993 for review). SP is associated with nociception because it is found in the appropriate location in the spinal cord, but also because it is released in the dorsal horn after excitation of unmyelinated fibres, following noxious mechanical/thermal/chemical stimulation of skin or administration of capsaicin (Duggan et al, 1987; 1988a; 1988b).

The release of an individual peptide such as SP has not been correlated with activity of a physiologically identified afferent phenotype, even though it is located in primary afferent nociceptors (Hunt & Rossi, 1985; Leah et al, 1985; Plenderleith et al, 1990). Reasons for this are twofold, firstly SP is not restricted to nociceptors and secondly most sensory receptors contain up to four different peptides (Cameron et al, 1988), implying that a combination of these are required for physiological activity.

In addition, Jessel & Yamamoto (1980), proposed that SP could regulate the differentiation of surrounding neurons and later it was suggested that SP may be involved in regulatory or developmental events (Wall & Fitzgerald, 1982).

Recently its role in inflammation has been clarified (Woolf, 1996). Acute inflammation results in altered levels of neuropeptides. The upregulation of neuropeptides and SP specifically, occurs through an NGF-mediated mechanism resulting in phenotypic changes and contributes to the cascade of cytokine-mediated inflammatory response. The novel expression of neuropeptides in cells that did not occur previously

(Neumann et al, 1996) provide a clear indication of how the central excitability component of inflammation may be augmented.

RESULTS

CGRP mRNA was detected using two approaches. The first was to use Digoxygenin (DIG) labelled riboprobes. While delivering better cellular resolution, this method is not as sensitive as radiolabelled probes, so the latter method was employed for the youngest embryos examined. Radiolabelling was achieved using S-35 labelled oligoprobes.

6.5 Ontogeny of CGRP mRNA expression in the DRG and Spinal Cord

The earliest embryonic tissue to be examined was E14. From E14-E16 labelling was only attempted using the S-35 labelled oligoprobes. At E17 and E18 both radiolabelled oligoprobe and Dig-labelled riboprobe methods of analysis were applied. In addition, adult DRG was processed with the Dig-labelled sections.

A small amount of labelling is found in the motor neurons at E14. (Fig. 6.1). This is located on the most ventral aspect of the ventral horn. By E15, the labelling is again confined to the motor neurons, but in a slightly more dorsal position relative to the ventral boundary of the spinal cord (Fig. 6.2). The intensity of labelling increased twofold and an enlargement of the labelled area indicates a cluster of 4 - 5 cells (Fig. 6.2B). At E16, the ventral horn labelling is still restricted to motoneuron pools, but two distinct pools are identifiable (Fig. 6.3A). The position of labelled cells also changed with some lateral and dorsal displacement. One pool is detected in a more dorsal position while the other remains on the ventrolateral region of the ventral horn. Closer examination reveals that up to 10 cells are labelled (Fig. 6.3C).

E17 is a significant age as this is when S-35 labelled transcripts are first detected in the DRG. An average of between 4 and 5 cells were positive at this time, when 20 random sections were counted. (Fig. 6.4B). No clustering was observed, but the heavy labelling precluded closer examination of the labelled cells. Two separate motor pools were still strongly labelled, but their position had shifted to immediately dorsal to the ventral column (Fig. 6.4A). These were not adjacent, as one was situated on the ventrolateral region and the second more medially. Results at E17 using the Dig-labelled

riboprobe were not as clear, only a few motoneuron cells were labelled in over 30 sections examined, while only one DRG showed labelling of two cells. Adult DRG sections were analysed simultaneously, to ensure the lack of labelling at E17 was not due to technical error.

One day later at E18, mRNA levels had increased sufficiently for 10-16 cells to be detected in the DRG using Dig-labelled riboprobe (Fig. 6.6A). These are located throughout the DRG showing no clustering (Figs. 6.6C, D). This finding was reinforced by the radiolabelled results also showing a mean number of 11 cells per DRG (Fig. 6.5). Cellular localisation with the S-35 labelled probe was also enhanced.

Motor neurons were still labelled but only one pool was identified in the ventrolateral region of the ventral horn (Fig. 6.5B & 6.6B).

6.6 Comparison of CGRP mRNA and peptide onset and expression

A summary comparing the ISH and IHC results are found in Table 6.1 and schematically in Fig. 6.7. The important finding from this study is that the temporal onset of mRNA and peptide expression is simultaneous in the motor neurons and in the DRG. This result indicates that the CGRP antibody used in Chapter 4 detected the peptide as soon as it was synthesised, and that the delay in expression in comparison to other histochemical markers is a genuine developmental event.

Table 6.1: Comparison of *in situ* hybridisation and immunohistochemical expression results

	mRNA Expression (ISH)		Protein Expression (IHC)	
	MN	**DRG**	**MN**	**DRG**
E14	✓	×	✓	×
E15	✓	×	✓	×
E16	✓	×	✓	×
E17	✓	✓✓	✓	✓
E18	✓	✓✓	✓	✓✓

Key
ISH: *In situ* hybridisation
IHC: Immunohistochemistry
MN: Motoneurons
DRG: Dorsal Root Ganglia

It can not be determined from this study precisely when CGRP mRNA is first expressed in motor neurons since it was already present at the earliest timepoint examined. The first detection of the CGRP transcript in the DRG however, is observed at E17 which coincides with the first detection of CGRP immunoreactivity. The proportion of cells in the DRG expressing both mRNA and peptide increase rapidly by E18. The intensity of labelling shows a similar evolution. Although, at E17 the expression of mRNA is slightly greater than peptide expression.

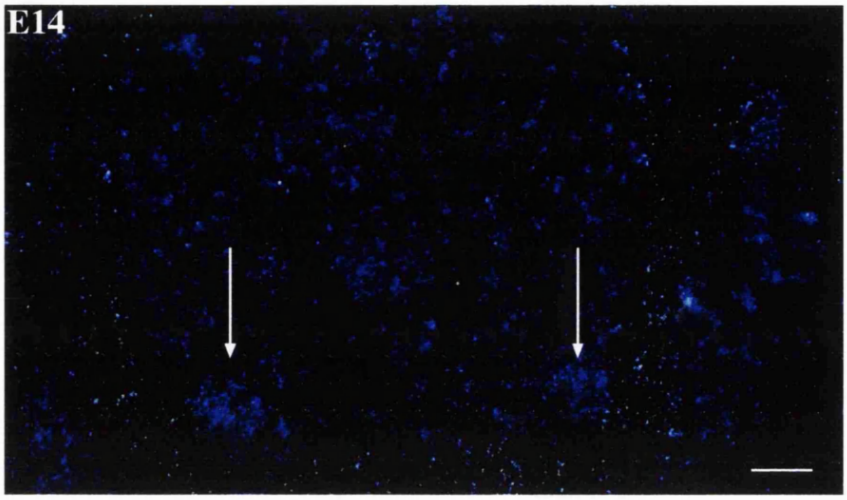

Fig. 6.1: CGRP mRNA Expression in the E14 DRG and Spinal Cord.
Arrows point to the labelled motoneuron pool in the darkfield photograph of spinal cord. Scale bar = 100μm

Fig 6.2: CGRP mRNA Expression in the E15 DRG and Spinal Cord

A is a darkfield photograph of DRG and Spinal Cord; B is an inversed darkfield photograph of the same section with an enlarged inset; C is a brightfield photograph of a spinal cord hemisection. Arrows denote labelled motoneurons in A, B and C. Scale bar = 100 μm

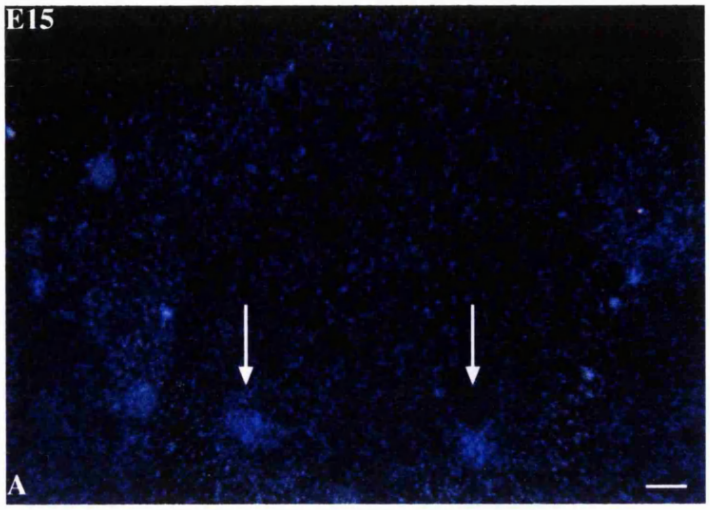
E15
A

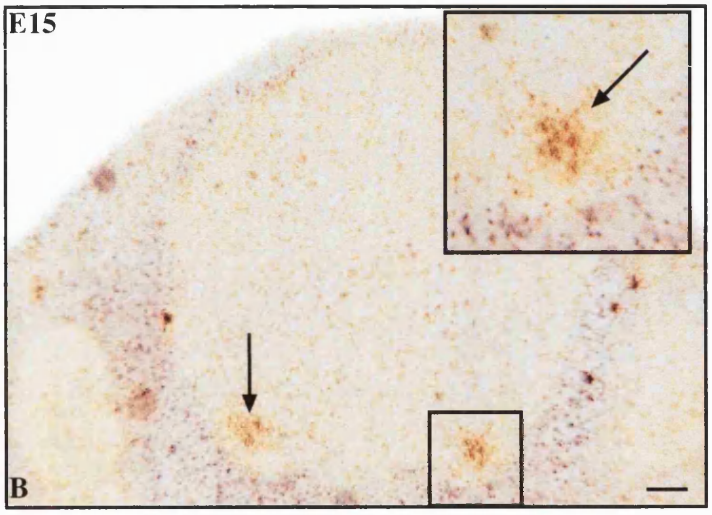
E15
B

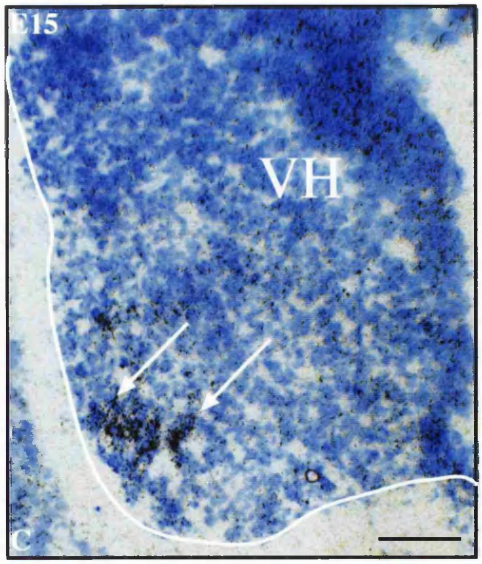
E15
VH
C

Fig. 6.3: CGRP mRNA Expression in the E16 DRG and Spinal Cord

A is a darkfield photograph; B is an inversed darkfield photograph of the same section containing an inset that is enlarged in C. Arrows point to labelled motoneurons. Scale bar = 100μm

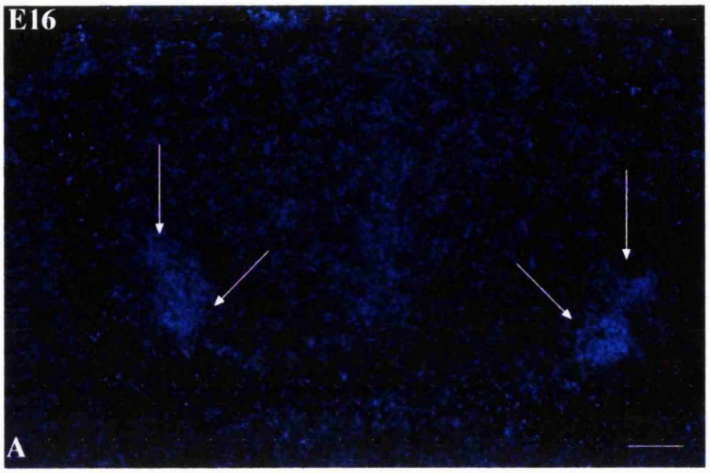
E16
A

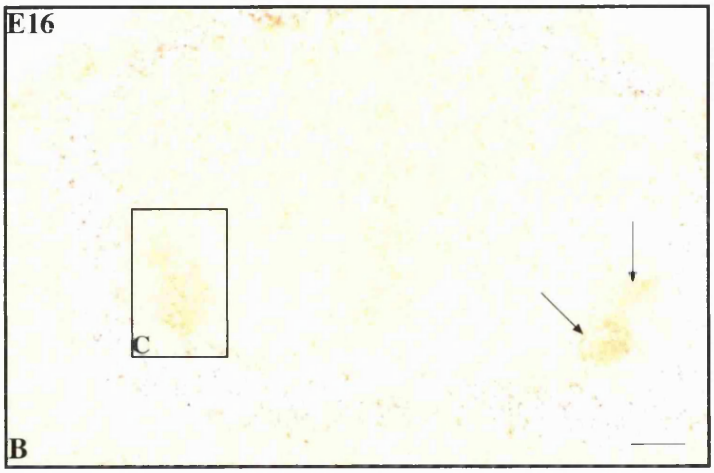
E16
C
B

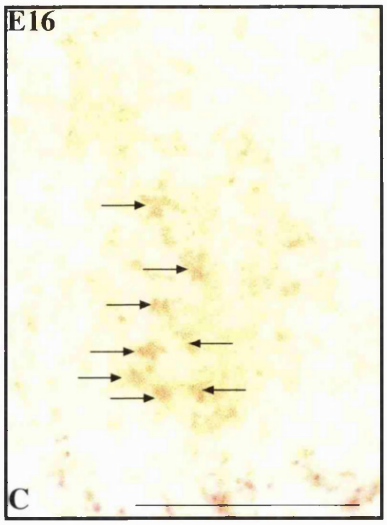
E16
C

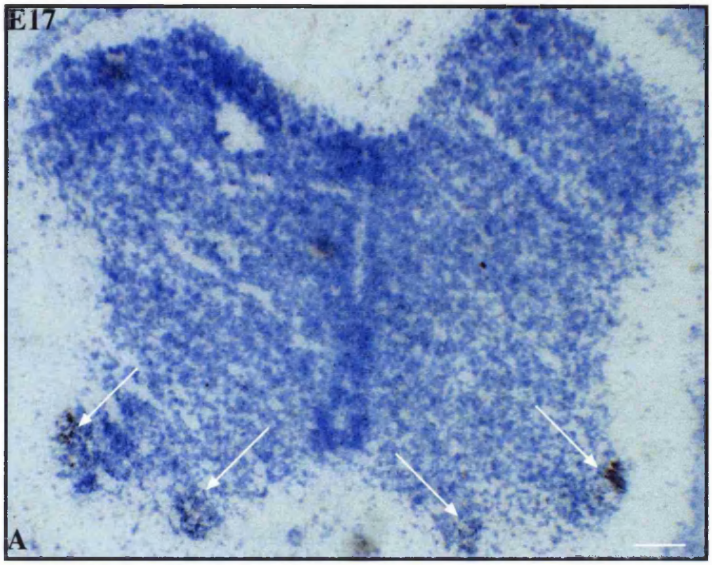

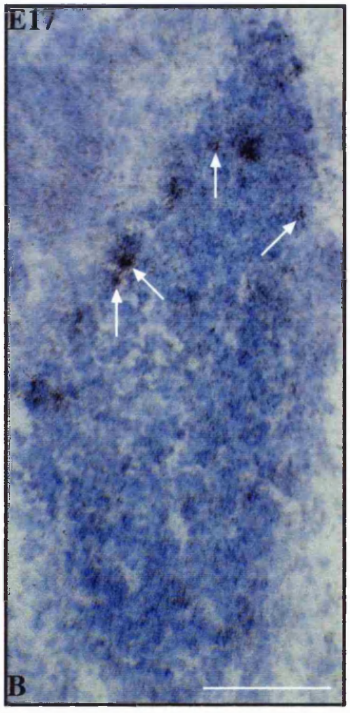

Fig. 6.4: CGRP mRNA Expression in the E17 DRG and Spinal Cord
A is a brightfield photograph of the spinal cord; B is a brightfield photograph of DRG. In A arrows point to labelled motoneurons while in B they point to labelled DRG cells. Scale bars = 100μm

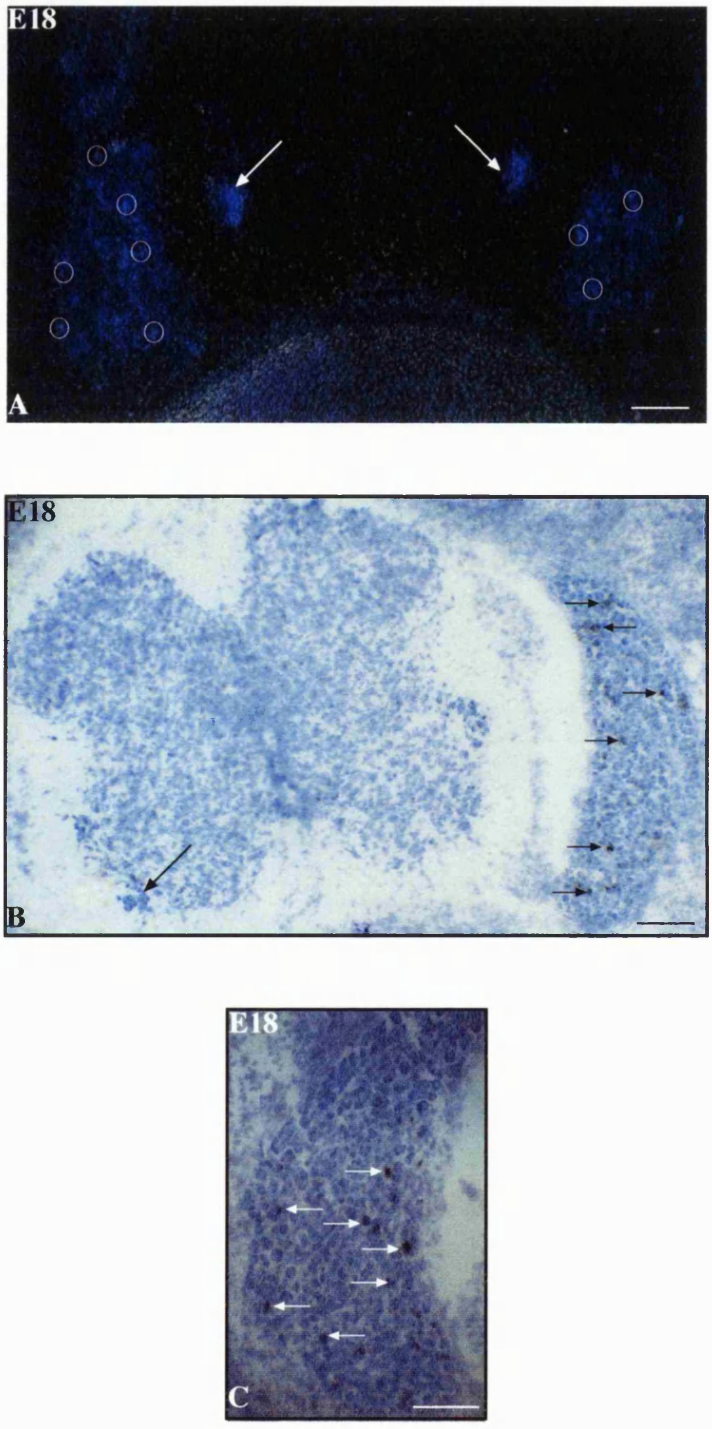

Fig. 6.5: CGRP mRNA Expression in the E18 DRG and Spinal Cord
A is a darkfield photograph of DRG & spinal cord; B and C are brightfield photographs of DRG & spinal cord and DRG respectively. Arrows denote labelled motoneurons in A, circles indicate position of labelled DRG cells. In B, the long arrow points to motoneurons and short arrows point to DRG cells. In C, arrows are directed towards labelled cells. Scale bar = 100μm

Fig 6.6: Digoxygenin-labelled CGRP mRNA Expression in the E18 DRG and Spinal Cord

A is a brightfield photograph of spinal cord and DRG treated with sense probe; B is a brightfield photograph of spinal cord treated with antisense probe; C and D are DRG labelled with antisense probe. In B arrows point to labelled motoneurons while in C and D they are drected towards examples of labelled cells. Scale bar = 100 μm

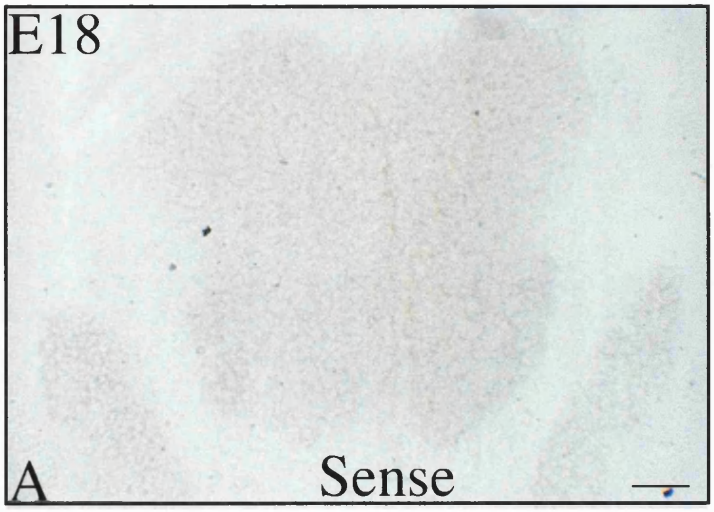
E18
A
Sense

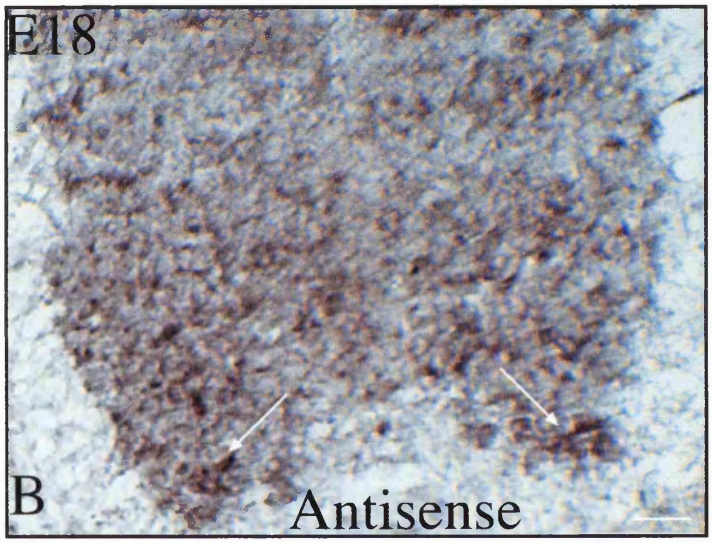
E18
B
Antisense

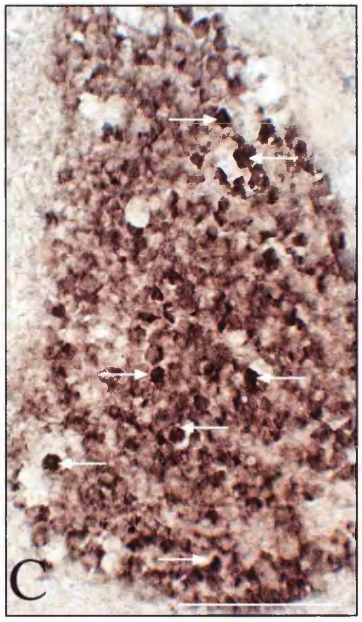
C

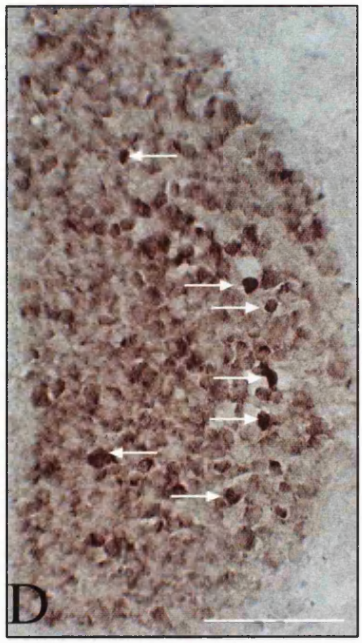
D

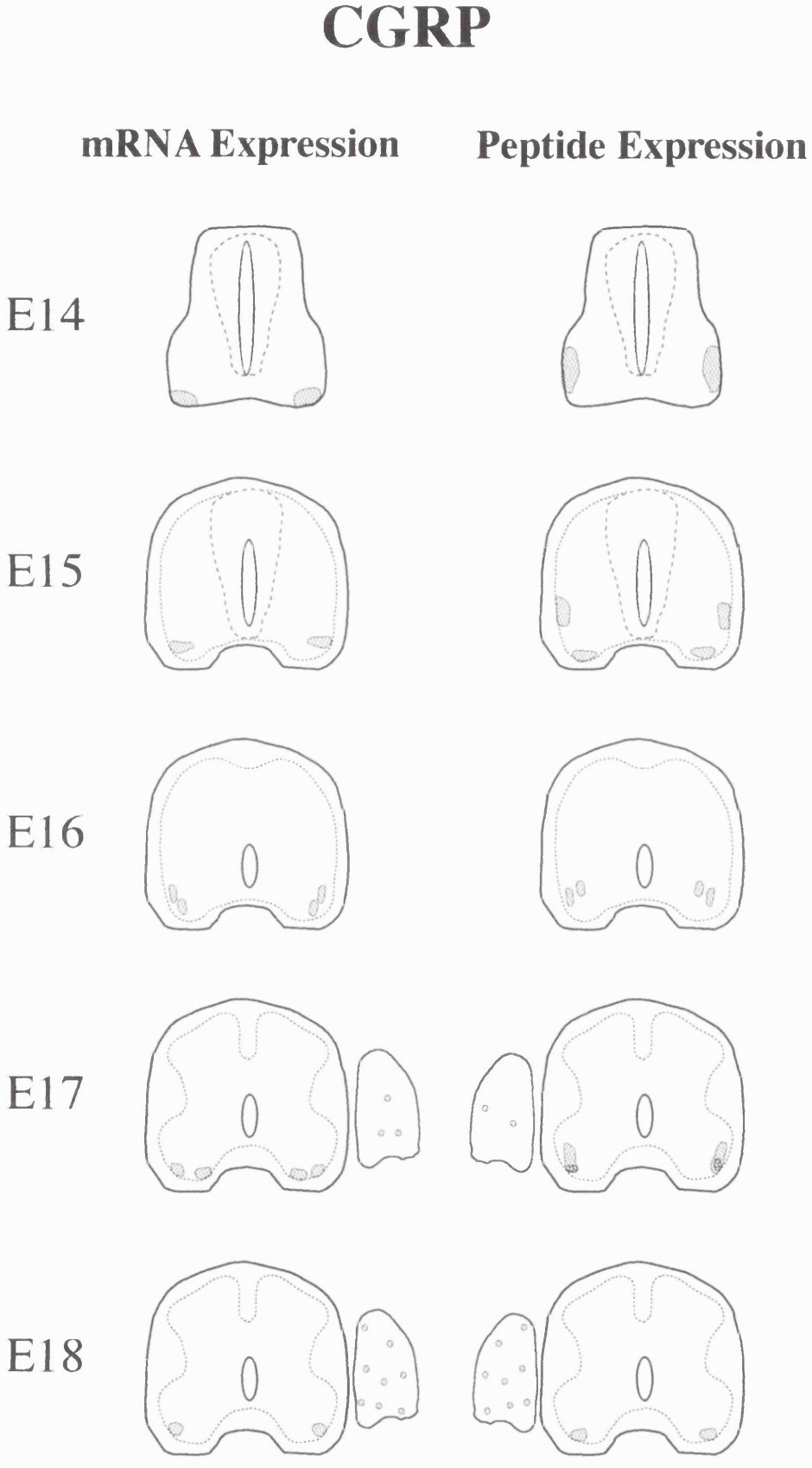

Fig. 6.7: Comparison of CGRP mRNA and peptide onset and localisation

DISCUSSION

In this chapter I have examined the expression of CGRP mRNA in the embryonic rat DRG and spinal cord and compared this to the protein expression data in Chapter 4 demonstrated with IHC. The results show that mRNA and peptide expression is switched on in a corresponding sequence in the regions analysed. This confirmed that CGRP is expressed later than many of the other DRG cell neurochemical markers.

6.7 Does the in situ data correlate with the immunohistochemical data on embryonic CGRP expression?

CGRP mRNA and protein are both detected at the same age. Their onset is simultaneous in the DRG, and at the earliest stage examined are both expressed in motor neurons. The fact that no delay is discovered between the expression of mRNA and protein in the DRG, refutes the proposal that the late identification of CGRP may have been due to an inability to detect low expression levels of protein with IHC. This confirms that CGRP is not synthesised in the DRG until E17, much later than the other histochemical markers examined in chapter 4. It was important to clarify this as a delay can exist between onset of CGRP mRNA expression and the subsequent detection of protein. In the mouse olfactory pathway mRNA is first detected at E13, yet this is not followed by the peptide until E15 (Denis-Donini et al, 1993).

6.8 Why is CGRP expressed late in DRG development?

The functions of CGRP have been described in 6.3.8, and these functions are primarily as neurotransmitters or neuromodulators in physiological activity. It is understandable that CGRP is not required earlier, when physiological attributes of sensory neurons have not matured and spinal cord processing is not required. Nonetheless, in the motor neurons CGRP is expressed from E13 (Chapter 4) which is consistent with a role in development of the neuromuscular junction (Fontaine et al, 1986; New & Mudge, 1986), although there is a delay of some 4 days before CGRP is found in the target muscle. A further trophic role is suggested for CGRP as receptor binding studies indicate that initially this peptide is important for growth, differentiation,

connectivity or synapse maturation and these roles are later replaced by that of neuromodulator (Nitsos, 1994). Indeed, it was suggested by Wall & Fitzgerald (1982) that the introduction of peptides into the CNS could have a trophic effect. If this role was verified, the timing of CGRP transport to the dorsal horn at E19 is compatible with synapse maturation and the onset of recorded activity (Fitzgerald, 1991). In Chapter 5, the role of neuropeptides in the differentiation of the epidermis is discussed with reference to the changes in innervation density. The presence of CGRP in the skin at E19, may stimulate further growth of the epidermis to accommodate the later arriving C-fibres and may explain why density decreases from levels at E17.

6.9 What is the signal for the onset of DRG expression?

The DRG first expresses CGRP in a few cells at E17, by E18 both the number and intensity of expression increases, yet no axonal CGRP is detected until E19. At E19, both peripheral and central axons express CGRP. In the periphery even the most distal axons show full expression. These findings pose two questions. Firstly, what is the stimulus for the onset of DRG expression and secondly what determines the appearance in axons?

The sudden arrival of CGRP throughout the peripheral axons indicated that the peptide was rapidly transported within 24hrs in existing axons, and unlike many of the other structural markers that reflect the gradual proximal-distal progression of nerves into the hindlimb. Since this occurs in both central and peripheral axons, it is obvious that the putative CGRP expressing axons have reached their target destinations prior to the expression of peptide. Evidence for the presence of fibres in the substantia gelatinosa prior to CGRP expression is derived from co-culture experiments of DRG and spinal cord explants. If E14 DRG and E14 spinal cord are cultured together for 6 days, fibres grow into the dorsal horn and can be visualised by DiI labelling. These show laminar specific targets are reached, yet the DRG does not express CGRP (Redmond et al, 1997). The combination of peripheral and central target contact *in vivo,* must produce some signal to inform the cell soma to start synthesising CGRP. This may be why in the co-culture experiment above, the E14 DRG had not been exposed to any peripheral signal, therefore

although fibres grew appropriately compared to an equivalent P0 *in vivo*, CGRP expression was not initiated in the DRG. The nature of this signal or signals is unclear, however, one candidate is the presence of NGF in the peripheral target.

Evidence for the influence of NGF on neuropeptide levels is outlined in section 6.3.6. It is known that the CGRP content of DRG cells increases after rhizotomy (Villar et al, 1991) and that this is associated with increased mRNA expression (Iniashi et al, 1992), indicating that some regulatory factors are derived from central processes. It is understood however that CGRP regulation requires co-operation of centrally derived factors and peripherally derived NGF (Iniashi et al, 1992). This position is clearly consistent with the peripheral and central axons of CGRP-expressing DRG neurons reaching their target and of exposure to the required factors prior to peptide synthesis.

The peripheral regulation of peptides has generally been deduced from their reaction to nerve injury. Axotomy results in a decrease in CGRP levels within the DRG, however this can be reversed by NGF infusion (Fitzgerald et al, 1985; Wong & Oblinger, 1991). In addition, some peptides appear to be maintained by NGF derived from the peripheral target (Goedert et al, 1981). The role of NGF in controlling density of dorsal horn CGRP immunoreactive fibres has also been documented in co-culture experiments where increasing concentrations of NGF were added to the culture medium. This resulted in an increased number of fibres, although, it was not clear whether this was a result of increased DRG expression (Redmond et al, 1997).

The appearance of the peptide, once synthesised, in the central and peripheral axons is a different issue. This study determined that peripheral and central onset of CGRP expression was simultaneous (Chapter 4). However, a previous study examining a number of peptides found that peripheral expression followed some days after central expression, except for CGRP where a delay of only one day was observed (Marti et al, 1987). Those results suggested no influence of the peripheral target on initiation of central afferent ingrowth. The stimulus for afferent growth into the spinal cord has been discussed in Chapter 4 and a different conclusion is reached as it is thought that peptides are expressed after the axons have already formed and therefore do not influence the

initiation of central afferent ingrowth. Nonetheless, this does not address the issue of why the peptide is simultaneously transported through to its central and peripheral target.

It may be that while CGRP simultaneously appears in the central and peripheral axons, peripheral transport is initiated first. The peripheral target, skin, is further away from the DRG than the spinal cord, so for CGRP to be simultaneously detected in both targets, transport to the periphery may have begun first. If this occurs, it might be expected that partially completed transport would be detected, i.e. CGRP in axons *en route* to the skin, however this is not the case. Speed of axonal transport in the periphery is also a reason why peripheral transport could be initiated earlier than central transport, but is not applicable since CGRP is found in the fast transport system that uses large dense cored vesicles (LDCV) which is even faster in the immature animal (Gulbekian et al, 1986). It is much more likely that the stimulus for axonal transport is intrinsic to the DRG neurons once peptide synthesis has been induced.

Evidence supportive of an intrinsic response in DRG neurons has clarified the requirement of the target in modulating the established peptide levels. No neurons in newly formed DRG express neuropeptides, yet by the time that axons connect with their peripheral target neuropeptides are detectable *in vivo*. If DRG neurons are isolated and cultured before target connections are formed, they express neuropeptides in a similar timecourse to the *in vivo* situation. This infers that some neurons in the embryonic DRG seem to be intrinsically specified to later express CGRP and SP (Hall et al, 1997). These findings are not in conflict with the co-culture experiments described above when using E14 DRG and spinal cord where CGRP is not expressed even after six days, (equivalent to P0). This is because in the Redmond (1997) experiment the E14 DRG was co-cultured with spinal cord. Since CGRP increases in the DRG after rhizotomy, this is indicative that the spinal cord may exert an inhibitory or downregulatory influence. So the potential for the E14 DRG, that had not experienced target contact, to express CGRP intrinsically may have been perturbed by the presence of the spinal cord.

If it is accepted that some neurons are intrinsically predetermined to express peptides then it is logical that they are intrinsically programmed to transport those peptides

to the targets at a particular stage of development. Furthermore, as discussed in 3.1.2 and 4.19, the existence of a third neuronal population categorised by birthdates and identified as peptidergic, is consistent with the finding that embryonic DRG isolated from targets, intrinsically become peptidergic.

6.10 Does the existence of intrinsic peptidergic neurons undermine the data suggesting peptidergic expression is influenced by peripheral target-derived NGF?

The role of extrinsic influences has also been studied in culture. In the same series of experiments where it was determined that DRG neurons intrinsically express peptides, Hall and colleagues (1997) cultured DRG neurons with potential target tissues. Co-culture of DRG with an epidermal cell line increases the proportion of CGRP-containing neurons whereas addition of neurotrophins to the DRG in isolation does not change the percentage of CGRP-IR neurons. Again, the finding that neurotrophins do not alter the expression levels of CGRP is not inconsistent with the results of the DRG-spinal cord co-cultures as in this case a target is present. These studies show that a target connection must be made in order to achieve modulation of the intrinsic expression pattern and reinforces the role of neurotrophins and specifically NGF in the peripheral target.

7

EFFECT OF FOETAL ANTI-NGF TREATMENT ON DRG CELLS AND INNERVATION OF THE SKIN

INTRODUCTION

7.1 Aim

The aim of this chapter is to investigate the interactions of different subpopulations of DRG neurons with the peripheral target. The consequences of selective removal of the small DRG cell and C-fibre population with embryonic anti-NGF treatment, upon the remaining DRG cell population is examined. Furthermore, the effect of such removal upon the target innervation is investigated.

7.2 Background

This study is based on the dependence of developing neurons upon growth factors. The removal of growth factors during a critical period of neuronal development has profound effects, culminating in cell death. A family of related growth factors called the neurotrophins and their receptor family, have been the subject of intense investigation since the discovery of the second neurotrophin member in the early 1980's (Barde et al, 1982). There is an extensive amount of literature describing the actions of these families on sensory, motor and autonomic innervation and even in non-neuronal tissues. Studies extend over many species including both *in vitro* and *in vivo* investigations. Due to the amassing literature, this account focuses on the *in vivo* effects of neurotrophins and their receptors on rodents.

There are currently six identified neurotrophins: nerve growth factor (NGF); brain-derived neurotrophic factor (BDNF); neurotrophin-3 (NT-3); NT-4/5 and NT-6. There are three high-affinity neurotrophin tyrosine kinase receptors: trkA; trkB and trkC and a low-affinity receptor p75. The trk receptors are discussed together with the appropriate neurotrophin and p75 is discussed separately.

7.3 Neurotrophic Hypothesis

The central theory of the neurotrophic hypothesis is that the survival of developing neurons depends on the supply of a neurotrophic factor that is synthesised in limiting

amounts in the target. This hypothesis was initially based upon studies with NGF and has been substantiated by inclusion of newly identified neurotrophins. It provides an explanation for how the target can regulate the size of the neuronal populations that innervate them. However, the roles of neurotrophins outlined below shows how these range beyond this hypothesis, both at timepoints before and after cell death, and how the fate of a neuron is constantly under review even after it has survived target competition and cell death. The levels of neurotrophins in their target or elsewhere in their environment may determine neuronal function long after survival to the extent that excess or depletion of levels may cause phenotypic changes other than their own intrinsic program.

7.4 NGF and trkA

Nerve growth factor (NGF) was discovered as a growth factor for neural crest derived cells, promoting their survival and neurite elongation. It has occupied a central position in developmental neurobiology because of the number of important neuronal functions it has been shown to regulate. In addition to the specific roles outlined in the sections below, NGF is exceptional in that it is synthesised at a considerable distance from the cell body. Peripheral tissues or other target neurons synthesising NGF are then innervated by NGF-sensitive neurons. The secreted NGF is thought to have local effects on axons of innervating neurons as well as more general influences on gene expression after it reaches the cell body via the process of retrograde transport.

The actions of NGF are restricted to a few populations of neurons and its role of survival during development has been deduced from *in vitro* survival assays and *in vivo* analysis of receptor profiles and gene activation studies (for review see Purves, 1988; Davies, 1994).

7.4.1 Embryonic development

i) Neurogenesis & Proliferation

One of the unique features of NGF as a growth factor is that it only regulates the functions of differentiated cells and does not influence proliferation.

ii) Cell Death & Neurotrophic Hypothesis

The regulation of neuronal survival plays a key role in matching the relative sizes of different groups of neurons in the vertebrate nervous system. During development, neurons are generated in excess and those superfluous to requirements die shortly after axons reach their targets. Survival of neurons depends on adequate supply of an appropriate growth factor, which is the basis of the neurotrophic hypothesis described above. It remains paradoxical that such large numbers of neural cells are generated during development only to be lost some days later.

The death of cells occurs in two distinct ways, apoptosis (programmed cell death or PCD) and necrosis. These modes of death are distinguishable by their morphology, biochemistry and molecular changes. Apoptosis is the most common form of eukaryotic cell death and is essentially an inherent physiological suicide mechanism. Necrosis, which is normally regarded as pathological, results in cell swelling and lysis of intracellular contents into the extracellular space, inducing an inflammatory response. Apoptosis which occurs during development, manifests itself by shrinking and nuclear fragmentation, resulting in chromatin and DNA cleavage followed by phagocytic ingestion by neighbouring cells and macrophages. Consequently, apoptotic cells remain histologically inconspicuous (Raff, 1992) until recent detection methods where the fragmented DNA is labelled using the TUNEL technique (Gavrieli et al, 1992).

Two members of a family of proteins known to be important regulators of the apoptotic cascade have recently been identified. Bcl-2 has been demonstrated to have antiapoptotic properties while Bax tends to enhance cell death. *In vitro* experiments have shown that overexpression of Bcl-2 is protective (Garcia et al, 1992). The importance of Bcl-2 to neuronal survival is shown by the fact that Bcl-2 protein expression is widespread in both the CNS and PNS (Merry et al, 1994). The genetic manipulation of these genes is already in progress with null mutations for both genes reported (reviews: Henderson, 1996; Silos-Santiago et al, 1995). Interestingly, neurons of the PNS that are capable of regeneration following injury express high levels of Bcl-2 protein outside the developmental period.

Sensory neurons however are not equally influenced by the growth factor NGF, whose presence or absence determines whether or not an apoptotic cascade is initiated as described above. Results from a series of experiments using an NGF deprivation paradigm, have established that nociceptive neurons selectively require NGF for survival.

By using systemic application of antibodies to anti-NGF at birth, a 40% cell loss in the DRG was observed (Hulsebosch et al, 1987, Johnson et al, 1989). If the anti-NGF was administered to the pregnant mother, many more neurons failed to survive in the neonate (Gorin & Johnson, 1979). The apparent discrepancy between the outcome of these experiments can be reconciled by the result of timing differences in NGF requirement. It has since been ascertained that anti-NGF treatments beginning at P2 are even less effective in reducing the number of neurons in the DRG (Lewin et al, 1992), this highlights the fact that a critical window for NGF survival action on neurons exists.

The initial anti-NGF experiments revealed the importance of NGF as a survival factor for a population of neurons. The identity of these neurons as nociceptive, was determined from the greater effect on the small cells in the ganglion (Goedert et al, 1984; Hulsebosch et al, 1987; Ruit et al, 1992). This is in agreement with the fact that cells providing projections to the substantia gelatinosa are lost after embryonic anti-NGF treatment (Ruit et al, 1992). In earlier studies, the peptide-containing cells were selectively depleted after anti-NGF treatment, consistent with the data suggesting a selective effect on nociceptive neurons (Otten et al, 1980; Goedert et al, 1984).

This action would require interaction with a receptor for the trophic factor. Several reports indicate that the high affinity receptor trkA is localised to nociceptive neurons (see sections 4.4.1, 4.19, 4.23.v). TrkA is found co-localised with CGRP expressing neurons (Verge et al, 1989; McMahon et al, 1994). More conclusively it was shown that neurons expressing trkA are selectively lost in the same embryonic anti-NGF model (Carroll et al, 1992).

7.4.2 Postnatal development

i) NGF Deprivation

The administration of anti-NGF at P2, does not result in detectable cell death, indicating that the action of NGF on neuron survival are limited to the period before this, however it still has an effect on the physiological development of selective neurons.

Neonatal deprivation of NGF has no effect on the large myelinated Aβ fibres but the properties of Aδ fibres are changed. Aδ fibres are composed of three receptor subgroups in control animals. 40% are high threshold mechanoreceptors (HTM), 30% are low threshold hair afferents (D-hairs) and the remaining 30% are subcutaneous deep receptors. The effect of treatment was to produce a decrease in HTM receptors with a reciprocal rise in D-hair afferent receptors. As stated above, no cell death occurred, hence the lack of NGF effectively caused a phenotypic switch from HTM to D-hair units (Ritter et al, 1991; Lewin et al, 1992). The effect on the remaining class of neuron, the C-fibres, is also very specific. Anti-NGF given during the same neonatal period results in a loss of C-fibre mechanoreceptors, that are replaced however, with a novel group of low threshold mechanoreceptors (Lewin & Mendell, 1994). These experiments clearly illustrate the necessity of NGF for the development of the physiological phenotype of both Aδ and C-fibres. In the absence of NGF, the putative Aδ phenotype changes to D-hair by default. The different physiological receptor types are identifiable at birth (Fitzgerald & Fulton, 1992) and the mechanical nociceptors are recognisable before the critical period of anti-NGF action on the Aδ HTM receptor (Lewin et al, 1992) therefore it is likely that the HTM phenotype is intrinsically determined but reliant upon NGF for continued development postnatally.

ii) NGF levels and location

The interpretation of these results is further supported by reference to the normal development of the skin target which is the source of NGF. Skin is well innervated by birth, as evidenced by the developmental timecourse in Chapter 4 of this thesis. However, the organisation of terminals continues for the first two postnatal weeks (Reynolds et al, 1991), coincident with the period that leaves the nociceptors susceptible to anti-NGF treatment. During this period new peptidergic processes grow into the epidermis, followed by the withdrawal of some terminals from the epidermis to a sub-epidermal position (as discussed in Chapter 6.3). NGF levels are high in the skin in the postnatal period (Davies et al, 1987; Constantinou et al, 1994), the terminals of axons reside in the epidermis and have exposure to NGF. The effect of anti-NGF in altering the phenotype of the Aδ HTM receptors may be to allow migration of these terminals to the dermis in conjunction with the natural withdrawal of other cutaneous terminals, and therefore the role of NGF may be deduced as promoting the continued projection of HTM receptors in the epidermis and in the vicinity of NGF. This theory is also fundamental to the argument for the changes in the depth of projection outlined in Chapter 6. Alternatively, the anti-NGF may change the membrane or transduction processes involved in the maintainance of the Aδ response.

iii) Exogenous NGF treatment

To ensure that the effects of anti-NGF on nociceptors were direct, these experiments can be compared to studies where excess NGF has been administered in the same period (Lewin et al, 1993; Vedder et al, 1993). The findings are practically reciprocal to those of anti-NGF. No changes are observed on Aβ fibres while C-fibre mechanoheat receptors are increased. Contrary to the anti-NGF result, the numbers of HTM and D-hair afferents are unchanged suggesting that complete depletion leads to the phenotypic switch while addition of NGF is ineffective if NGF is already expressed in excess normally (Lewin et al, 1993). Significantly the threshold levels of Aδ afferents decrease, which together with the increased proportion of C-fibres sensitive to noxious heat results in behavioural changes. These behavioural differences as a result of increased

NGF are similar to the hyperalgesic state observed in adults after injury and inflammation (see below).

iv) Behavioural Changes

Surprisingly, there are no behavioural changes in response to a nociceptive stimulus in anti-NGF treated animals even though the phenotypes of nociceptors have changed (Lewin et al, 1993). It had been anticipated that low threshold stimulation would inappropriately activate nociceptive pathways and elicit an behavioural response to a painful stimulus and additionally the loss of C-fibres to reduce the response to noxious heat. The fact that anticipated changes were not realised indicated that connections in the spinal cord had also changed. D-hair input to lamina I did not increase despite the larger number of these afferents, suggesting that their central action was regulated to maintain the appropriate modality. Moreover, afferents responding to noxious heat magnified their central effects so that fewer surviving afferents activated the same proportion of lamina I cells.

This compensatory effect maintained the relatively normal spectrum of inputs to lamina I despite the peripheral changes (Lewin & Mendell, 1996). The peripheral effector function however was disrupted. The amplitude of antidromic vasodilatation was significantly reduced after neonatal anti-NGF treatment, consistent with phenotypic changes (Lewin et al, 1992a). This effect is also supportive of the selectivity of anti-NGF treatment as this response occurs in peptidergic neurons, and was at risk since this vasodilatory response only develops postnatally. Also, excess neonatal NGF is known to upregulate tachykinins in sensory ganglia (Vedder et al, 1993).

v) Genetic manipulation of NGF / trkA gene

Transgenic mice show altered nociceptive functions, NGF overexpressors are mechanically hyperalgesic while underexpressors are mechanically hypoalgesic (Davis et al, 1993). These mutations also prove that experiments with systemically administered NGF / anti-NGF do act on skin. NGF -/- and trk -/- both result in hypoalgesia (Crowley et al, 1994; Smeyne et al, 1994). These animals are viable at birth but do not gain weight. They both have dramatically depleted populations of DRG neurons by the time of birth,

70-80% in the DRG, that is selective for small peptidergic neurons. The cell loss is selective for those neurons mediating nociception.

Downregulation of trkA postnatally explains how NGF and trkA knockout cell loss is greater than number of cells expressing trkA in the adult (Bennett, 1996b).

7.4.3 Adult

Roles in inflammation and pain

The potential ability to alter pain thresholds by altering levels of NGF or signal transduction by its receptor, trkA, represents one of the avenues for therapeutic application of neurotrophin research. Evidence is also available that the effects of NGF in modulating the function of physiological receptors and the function of neurons in the neonate also extends to the adult. Excess NGF in the adult promotes hyperalgesia by acutely affecting autonomic neurons and mast cells. The effects are pharmacological as NGF influences neurons directly, or by cells with the appropriate receptors that secondarily release transmitters that sensitise or activate sensory neurons. This role is also physiological since it is upregulated as a consequence of injury (for review see Woolf, 1996; McMahon, 1996).

7.5 BDNF and NT-3 - additional roles in development

The roles of NGF have been comprehensively described, however NGF alone is not the sole neurotrophic growth factor, nor does it provide for all classes of sensory neurons. The other members of the family, BDNF and NT-3 have complementary and additional roles. These roles do not restrict their actions to the conventional neurotrophic hypothesis action of NGF, although directed towards other sensory neurons. Instead they have roles outside the relatively brief developmental period with sources of neurotrophins other than the target.

The fact that neurons are initially responsive to either BDNF or NT-3 early in development, then respond to NGF, shows there is a developmental switch in neurotrophin dependence. Gene localisation and pharmacological studies have indicated

that some neurons may switch receptor expression and therefore growth factor dependence during development (Birren et al, 1993; DiCicco-Bloom et al, 1993).

The purpose of this switch on reaching the target appears to be intrinsically programmed, and may represent a strategy to maximise innervation of the target and thus provide a wider population of neurons to compete for limited trophic factors and ultimately selection of the final complement of neurons after a period of cell death (Mendell, 1996).

The other neurotrophins however do fulfil the survival criterion of neurotrophic factors. The following is the evidence outlining the groups of neurons responsive to NT-3 and BDNF.

7.6 NT-3 and trkC

DRG neurons that project to the primary endings of muscle spindles in the periphery, extend collateral branches to the motor pools in the ventral horn and are referred to as 1a afferents. These are the largest neurons within the DRG and are thought to mediate proprioceptive responses.

It has been hypothesised that these neurons are NT-3 dependent. NT-3 was the third member of the neurotrophin family to be identified (Rosenthal et al, 1990). Its identification was quickly followed by the identification of a new trk receptor, trkC, which mediates the effects of NT-3 (Lambelle et al, 1991). TrkC is expressed in novel tissues where other trk genes are silent. It is also detected at earlier stages than the other trk receptors and suggests that in addition to regulating neuronal survival, this receptor may have broader effects (Tessarollo et al, 1993).

7.6.1 Embryonic development

i) Neurogenesis & Proliferation

Several lines of evidence suggest that NT-3 is involved at much earlier stages of neural development than NGF. Blockade of trkC activity *in ovo* induces reductions in subpopulations of DRG neurons known to be dependent on NGF and NT-3 (Lefcort et al, 1996). Similarly, blocking NT-3 at the end of gangliogenesis causes a 30% decrease in the number of surviving neurons, demonstrating that endogenous NT-3 is required before the period of naturally occurring cell death (Gaese et al, 1994). These observations suggest an early function for NT-3 on immature DRG neurons, since at this early stage it supports most neuron survival. NT-3 mutants display cell loss greater than the number of cells expressing its receptor trkC. This implies that NT-3 is having effects on other neurons, possibly through interaction with another receptor early in embryogenesis on transiently responsive precursors (Farinas et al, 1994), see discussion 7.19(v). Sensory neurons in the trigeminal ganglia switch their growth factor dependence from NT-3 in early development to NGF at a later stage (Buchman & Davies, 1993), and NT-3 is known to promote survival of neuronal precursors (Birren et al, 1993; DiCicco-Bloom et al, 1993).

More direct evidence for a role of NT-3 in promoting neurogenesis originates from a series of studies involving neural crest cells. NT-3 can act as a mitogen for early neural crest cells (Kalcheim et al, 1992) and it is known that it can promote neuronal differentiation (Wright et al, 1992). Recently, a subpopulation of early migrating neural crest cells were found to express the trkC receptor (Henion et al, 1995). The restricted expression of trkC to cells on the medial pathway (which gives rise to all peripheral neurons) led to the suggestion that these represent a subpopulation of neurogenic precursors that give rise to a subset of DRG neurons. Furthermore, in the same study NT-3 partially rescues cultured neural crest cells in a medium that otherwise does not support neurogenesis.

NT-3 addition to embryos over the same time period as the studies above, causes even greater losses of sensory neurons (Ockel et al, 1996). The paradoxical effects of

NT-3 are attributed to a decrease in the number of proliferating neuroblasts in treated embryos, and therefore presumably induction of premature differentiation in postmitotic neurons. Thus, NT-3 may simultaneously play anti-proliferative and survival-promoting roles in these early ganglia (Henderson, 1996).

The theory to emerge from these observations is that neuronal precursors and early post-mitotic neurons depend on locally synthesised factors and then switch their dependence to target-derived factors for survival.

ii) Expression

NT-3 mRNA has been localised to muscle and motor neurons, i.e. the targets of these neurons (Ernfors & Persson, 1991). TrkC expressing neurons are the largest in the DRG (Carroll et al, 1992; Mu et al, 1993; Oakley et al, 1995) and NT-3 has been shown to support DRG neurons retrogradely labelled from muscle (Hory-Lee et al, 1993) and *in vitro* (LoPresti & Scott, 1994). In the adult, 15% of sensory neurons retrogradely labelled from skin also express trkC (Barbacid, 1994; McMahon et al, 1994).

Anti-NT-3 treatment was administered during the period of normal cell death. The survival of muscle sensory neurons were selectively reduced in the DRG while 1a afferent projections were also affected (Oakley et al, 1995). Antibodies to trkC inhibits its activation and when administered before the period of cell death, results in reductions of neuronal cell numbers (Lefcort et al, 1996). This data is consistent with proposal that NT-3 is a required survival factor for proprioceptors. The following transgenic studies confirmed this role.

iii) Transgenic manipulation

NT-3 (Farinas et al, 1994) and trkC (Klein et al, 1994) knockouts both possess phenotypes characterised by abnormal movements and postures. The similarity of these movements to those exhibited by humans with large fibre sensory neuropathies led to the suggestion that those animals were deficient in proprioceptive neurons (Klein et al, 1994). Loss of 1a afferents was confirmed in the NT-3 (Ernfors et al, 1994) and trkC (Klein et al, 1994) knockouts in addition to 50% loss of large myelinated dorsal root axons in the trkC null mutation. DRG markers associated with proprioceptive neurons, carbonic

anhydrase and parvalbumin are similarly deleted in NT-3 -/-, while their sensory end organs never develop (Ernfors et al, 1994; Farinas et al, 1994).

An overview of all these studies shows that distinct subsets of DRG neurons require NT-3 for survival. The fact that different DRG subpopulations require different members of the neurotrophin family means that neurotrophin dependency is another criterion upon which to classify DRG cells according to their sensory modality.

7.6.2 Postnatal development

Similar to NGF, NT-3 is also required for postnatal maintenance of specific cutaneous afferents, D-hair receptors and slowly adapting mechanoreceptors, known to subserve fine tactile discrimination (Airaksinen et al, 1996). Adult animals heterozygous for a mutation in NT-3, showed clear deficits in populations of cutaneous afferents and in those whose dependence on NT-3 commences postnatally. Physiological investigation in the heterozygote mice showed that two subtypes of afferents were substantially reduced while remaining afferents in these classes functioned normally. There was a 78% reduction in the Aβ slowly-adapting afferents (SA) and a 50% decrease in incidence of the Aδ D-hair afferents (D-hair). Merkel cell numbers were similar to wild-type at P2, but by P14 were virtually absent, suggesting that NT-3 is absolutely necessary for the postnatal development of Merkel cells as they are intact at birth. NT-3 though, is not required for the functioning of SA and D-hair afferents but for their survival.

These findings are supported by the increased number of Merkel cells and hypertrophied touch domes found in mice overexpressing NT-3 (Albers et al, 1996).

7.6.3 Adult

Roles

BDNF and NT-3 are expressed within peripheral ganglia (Ernfors & Persson, 1991; Schecterson & Bothwell, 1992). Thus, neurotrophin expression is not restricted to neuronal target fields. This finding raises the possibility of paracrine and even autocrine actions of neurons that was not perceived on the basis of the study of NGF. NT-3 is

synthesised in the DRG until birth (Schecterson & Bothwell, 1992), but is also found in the skin (Ernfors et al, 1992).

7.7 BDNF, NT4 and trkB

BDNF was the second neurotrophin identified (Barde et al, 1982). Culture experiments indicate that it promotes survival of embryonic DRG and nodose ganglion neurons, but is inactive on sympathetic or parasympathetic neurons (Lindsay et al, 1985b). All populations of neurons in these ganglia are responsive to BDNF application, but on comparison with NGF it was found that survival was only promoted in a subpopulation (Davies et al, 1986a). The possibility that BDNF-responsive neurons comprises a distinct subset was reinforced when effects of NGF and BDNF were found to be additive (Lindsay et al, 1985b).

TrkB is expressed in small to medium-sized DRG cells (Ernfors et al, 1992; Schecterson & Bothwell, 1992; Mu et al, 1993). BDNF mRNA is synthesised in dermal mesenchyme during development in regions particularly sensitive to touch (Schecterson & Bothwell, 1992). The survival effects of BDNF on DRG neurons have been difficult to determine.

Many classes of primary sensory neuron are lost in the BDNF and trkB knockouts as they show striking losses in vestibular, nodose, dorsal root and trigeminal ganglia (Klein et al, 1993; Ernfors et al, 1994; Jones et al, 1994). TrkB knockouts which have affected BDNF and NT-4 signalling, die in 24hrs due to defective feeding (Klein et al, 1993). BDNF knockout therefore has milder phenotype and a few survive for the first couple of postnatal weeks (Ernfors et al, 1994; Jones et al, 1994). Both show significant neuron loss in trigeminal and dorsal root ganglia, consistent with the *in vitro* and *in vivo* pharmacological findings (review Davies, 1992).

Neuronal loss in neonatal trkB knockouts appear to be minimal (Silos-Santiago, 1995) and dorsal horn afferents appear relatively normal (Snider & Silos-Santiago, 1996), yet there is 30% cell loss in P14 BDNF -/- mice (Ernfors et al, 1994; Jones et al, 1994). Surprisingly motor neurons which were predicted to require BDNF, NT-4 during

development are less affected. On the basis of differences between the BDNF and trkB knockouts it is concluded that NT-4 may be relatively more important for motor neuron survival, although its source is unclear (Henderson et al, 1993).

7.8 Neurotrophin requirement of central nervous system neurons (CNS)

An unexpected distinction between CNS and PNS neurons has emerged from the recent genetic manipulation studies. After neurotrophin or trk receptor knockout, there is a relatively normal complement of CNS neurons that survive, even though most CNS neurons express neurotrophin receptors (Snider et al, 1992; Jones et al, 1994; Klein et al, 1994). Suggestions to explain this anomaly centre on the complex cellular environment of a typical central neuron which means that it is dependent on multiple neurotrophic factors for its survival and can therefore easily compensate for the inactivation of a single gene (Snider, 1994). Another possibility is that neurotrophins may regulate aspects of development or function in the CNS other than survival that have as yet not been revealed.

7.9 The low-affinity neurotrophin receptor p75

The first neurotrophin receptor to be molecularly characterised and cloned was p75. It acts as a low-affinity receptor for all the neurotrophins (Meakin & Shooter, 1992). Its function and requirement for transduction of neurotrophic signals has been the subject of much debate and has been reviewed by Bothwell (1995); Chao (1994); Lee et al (1992); Greene & Kaplan (1995); Chao & Hempstead (1995). One of the more recent and controversial aspects which relate to the results presented in this thesis is considered below.

7.9.1 p75 mediated cell death

The structure of the p75 receptor was unique when initially sequenced (Chao et al, 1986; Radeke et al, 1987) but subsequently was found to be structurally related to the tumour necrosis factor (TNF) receptors CD40 and Fas from the same cytokine family.

These TNF receptors convey potent signals to the cell via the transcription factor NF-κB, resulting in apoptosis (Beutler & Huffel, 1994; Hsu et al, 1996). The sequence motif in the receptor responsible for this action, named the death domain, is also identified in p75. It is 60-70 amino acids in length and resembles a cytoplasmic protein identified with the cell death pathway in *Drosophila* (Martins & Earnshaw, 1997). It is also known that mutations in this domain prevent activation of apoptosis by these receptors (Brakebrush et al, 1992).

Recognition of this motif in p75 led investigations into whether p75 was also capable of promoting apoptotic cell death. The only previous indication that p75 could trigger cellular responses in the absence of trk receptors, was when Schwann cells that do not express functional trk receptors, responded to NGF by increased expression of adhesion protein L1 (Seilheimer & Schachner, 1994).

In neuronal cell lines different groups have found evidence supporting apoptotic activity of p75 (Rabizadeh et al, 1993; Barrett & Bartlett, 1994; Von Bartheld et al, 1994). Expression of p75 in specific neuroblastoma cell types increased cell death upon withdrawal of neurotrophin (Rabizadeh et al, 1993). In cultured mouse DRG neurons, a series of experiments clearly showed that while p75 was required for NGF mediated survival until E19 and during the period of target innervation, it subsequently switched function postnatally from survival to apoptosis in the absence of NGF (Barrett & Bartlett, 1994).

These experiments showed that p75 promotes cell death at a specific stage of development and this was also applicable to postnatal rat DRG neurons and chick at E11 (Barrett & Bartlett, 1994). The conclusion from this work was that p75 and trkA together form a receptor complex to transduce a survival signal to NGF; it is known that trkA is downregulated postnatally (Bennett et al, 1996b) so in the absence of trkA the free p75 receptor elicits an apoptotic signal. This concept is feasible since there is a wave of postnatal cell death (Coggeshall et al, 1994), however this apoptotic process in the mouse only occurs in the absence of trophic support indicating a ligand-independent process.

The role of neurotrophins in contributing to cell death was first referred to when in several cell lines not expressing trk receptors, the neurotrophins NGF, BDNF or NT-3 induced intracellular changes (ceramide production by conversion of sphingomyelin). These changes also accompany the TNF receptor-induced apoptotic cell death (Dobrowsky et al, 1994; 1995). The next significant step in restricting this effect to NGF, was a study directly demonstrating that NGF alone, of the neurotrophins, contributes to NF-κB activation through p75 (Carter et al, 1996). NF-κB is a homo/heterodimer of DNA binding proteins and part of the cell death pathway. It is cytoplasmically localised and exists as two subunits p65 and p50, bound to inhibitory proteins (collectively called IκB) that mask its localisation signal. Activation of NF-κB is through phosphorylation of IκB, leading to degradation by proteosomes and therefore removal of inhibition (Wallach, 1997).

The study by Carter and colleagues (1996) involved Schwann cells. These were suitable to study the response of p75 signalling since they do not express trkA and as described above they transduce signals through p75. Postnatal Schwann cells were cultured and on addition of NGF, NF-κB activation was detected. In p75 knockout mice, the addition of NGF provoked no response proving that p75 was required. The same experiment in PCNA cells that also express p75 only, led to NF-κB activation on addition of NGF. These effects did not materialise using BDNF or NT-3, prompting the question of why they do not elicit apoptotic signals.

BDNF and NT-3 stimulate ceramide production but not NF-κB activation through p75. It appears that although other neurotrophins result in similar intracellular changes as the TNF receptor with regard to ceramide production, it may be that both NF-κB and the ceramide are downstream effectors, and that while NGF activates both pathways, BDNF and NT-3 only activate the ceramide pathway. This subtle difference may arise since NGF is more strongly inhibited from binding to p75 using an antibody to p75 than the other

neurotrophins, suggesting they bind at different sites (Von Bartheld et al, 1996). Analysis of the TNF intracellular pathway has indicated two proteins that associate with the receptors. The first is TRAF which has been shown to activate NF-κB, the other is TRADD which itself is a branchpoint to FADD that initiates cell death, or signals through TRAF II to NF-κB. NF-κB is the master switch regulating the expression of a variety of genes, which does not always lead to cell death. p75 can transduce a more subtle signal in certain cellular contexts therefore the route by which it is activated may depend on a ligand-specific accessory protein (Carter & Lewin, 1997). Such a candidate is NRIF, a novel zinc finger protein that associates with p75 in a ligand depedent manner, is specific for NGF and may be the second messenger activated only after NGF binding to p75 (Carter et al, 1996b).

Further support for these observations were found in restricted stages of development. Early retinal cells expressing p75 and not trkA in the chick, undergo cell death that is preventable by application of antibodies to NGF (Frade et al, 1996). Expression data showed that p75 and NGF were expressed in the retina before E4, but trkA was not found until E14. Cell death occurs in the retina at E4, prior to the target innervation in the tectum, and the dying cells correspond to p75 positive cells. If anti-NGF or anti-p75 is administered at E2.5, cell death is decreased. However there are some p75 expressing cells that are not affected even if additional NGF is provided, therefore p75 alone may not be sufficient for NGF-mediated cell death (see above re: NRIF). At the other end of the age spectrum, mature but not immature oligodendrocytes are susceptible to NGF-mediated cell death (Casaccia-Bonnefil et al, 1996). This effect is specific to NGF and the intracellular hallmarks of this pathway, ceramide and c-jun, were detected. Oligodendrocytes do not normally express significant levels of p75 *in vivo* but do after injury, suggesting that this type of p75 mediated apoptosis is a functional response to injury in the adult. Similarly, NGF increases cell death of motor neurons after axotomy of the facial nerve in the P0 rat (Sendter et al, 1992).

Examples are also found in the CNS where NGF-p75 mediated cell death is responsible for apoptosis of developing cholinergic neurons (Van der Zee et al, 1996). An

increase in cholinergic neurons is detected in p75 knockout mice and this can be mimicked in wild-type mice by blockade of NGF binding to p75. Interestingly, the 25% of cholinergic neurons that are lost are p75 positive, trkA negative and they die postnatally. The authors suggest that trkA may inhibit the apoptotic signal, similar to the suggestion by Barrett & Bartlett (1994) in their postnatal ligand-independent example.

RESULTS

Intra-uterine injections of anti-NGF were administered at E15 and E18 as described in the Methods (Chapter 2) and the embryos harvested at E21. It was necessary to ascertain whether the treatment had successfully eradicated the small cell DRG population. Lumbar vertebral columns from treated and control embryos were wax embedded, sectioned and counterstained, then a size-frequency histogram of DRG cells constructed. This was used to determine if cells with a small area were absent compared to controls. In addition counts of DRG cells were conducted using the physical dissector method, to ensure that cell-death had occurred after the trophic factor deprivation.

If embryos satisfied these criteria, the innervation of the skin in the hindlimb was investigated using antibodies to PGP 9.5, RT97 and CGRP. Innervation with each of the markers were compared to controls and the pattern of axon termination described.

7.10 Information about experimental protocol

7.10.1 Size-Frequency Histograms

Due to technical difficulties the generation of anti-NGF treated embryos took place over an extended period of time. It was not possible to assess whether the treatment had been successful until analysis of the DRG could be undertaken after wax embedding. Treated embryos were stored in fixative and embedded together with controls in batches so that they did not stay for excessive periods in fixative. However, since all embryos included in this study (n=6 controls, n=11 anti-NGF treated) were not embedded simultaneously, treated embryos were only compared to controls from the same processed batch to avoid variation due to shrinkage and tissue histology. Size-Frequency histograms were produced (see Chapter 2) for all embryos and the patterns analysed. Data was pooled for two anti-NGF and two control embryos that had been processed together and is presented here.

7.10.2 Cell Counts

DRG cells were counted using the fractionator technique adapted from the physical dissector (see Chapter 2). These counts were conducted on the same sections as those used for the size-frequency analysis. Since the sections were derived from the wax-embedded vertebral columns, it was not possible to exactly pinpoint which lumbar segment each DRG belonged to, therefore counts were completed on three DRGs from each control (n=2) and anti-NGF treated (n=3) embryos and the counts averaged to illustrate total cells per lumbar DRG.

7.11 Size-Frequency histograms of control and anti-NGF treated DRG

The size-frequency histogram of control DRG at E21 has been described in detail in Chapter 3, cells range from 30-570μm^2 and have a mean size of 160.25μm^2. The population is not yet bimodal, but two populations begin to emerge with the second larger population starting at 180μm^2 determined from the intersection of the two curves. If this value of 180μm^2 is taken as the boundary between small and large cells, then 67% of cells fall into the small cell category.

After anti-NGF treatment there are profound changes in the distribution. Fig. 7.1 shows the size-frequency distributions of both control and anti-NGF treated DRG. The treated DRG distribution appears to have shifted to the right. Cells range in size from 60-850μm^2 with most small cells absent. Using the same criterion as above there are now only 23% of cells in the small cell category. The mean size of the distribution has increased to 292.63μm^2 and the modal value increased from 120μm^2 to 255μm^2.

These changes may not just due to the loss of small cells, as cells at the upper end of the distribution have increased from 570μm^2 in controls, to 850μm^2 after treatment. Statistical analysis of this data shows that the control DRG cells are clearly smaller than anti-NGF treated DRG cells [ANOVA: $F(1, 4394) = 1422.77$, $P < 0.001$]. Control DRG cells (mean: 160.25, n=1951) are significantly smaller than anti-NGF treated DRG cells (mean: 292.63, n=2445).

7.12 Examination of sections show larger cells in treated DRG

The increase in size of surviving cells (570-850μm^2) detected by the cross-sectional areas was also apparent upon observation of the cells. Fig. 7.2 shows toluidine blue stained control and treated sections. The appearance of the control cells at E21 have been described in 3.3.4. After anti-NGF treatment, the DRG at low magnification appears compacted with a more pronounced boundary cap. This is reflected in the reduced number of sections obtained from each DRG. Few small cells are found in any section at higher magnification. The most obvious feature is the predominance of very large cells which would not normally be seen in control tissue. These retain the same shape as control cells, possess a large, centrally placed nucleus with virtually no multiple nucleoli. Although it is not apparent in Fig. 7.2, the majority of anti-NGF treated DRG cells appeared more widely spaced than controls, giving the impression of fewer cells.

7.13 Cell counts reveal 43% loss of DRG cells in the anti-NGF treated embryos

The fact that larger cells appeared in the anti-NGF compared to control DRG made it important to determine whether the whole population had simply enlarged and the size frequency histogram shifted to the right, or whether selective cell death had occurred in the small DRG population (Ruit et al, 1992) and the remaining DRG neurons grown larger than controls. The observation that cells were spaced further apart in the treated embryos was not sufficient to conclude that cell death had occurred.

Table 7.2: Mean Cell Counts for Control and Anti-NGF Treated DRG

	CONTROL (n=2 animals; n=6 DRGs)	ANTI-NGF (n=3 animals; n=9 DRGs)	% DIFFERENCE of Mean
Mean cells per DRG	**17978**	**10184**	**43**
$Animal_1$	14913	9387	-
$Animal_2$	21164	10300	-
$Animal_3$	-	10868	-

The cells counts show that 43% of cells are lost after embryonic anti-NGF treatment. The absence of small diameter cells was evident from the size-frequency histogram, therefore it can be concluded that the cell loss was selective for small-diameter cells. However, this also means that the total cell population did not merely enlarge producing a shift to the right in the histogram. This infers that the larger cells found in the treated DRG are a novel feature.

Statistical analysis showed that cell counts were significantly different after treatment [ANOVA: $F(1,3) = 10.211$, $P < 0.05$].

7.14 Effects of anti-NGF treatment on skin innervation

The cell counts and size-frequency histograms confirmed that 43% of DRG cells were lost and these were confined to the small diameter cells. The loss of these cells means that most C-fibre axons will not innervate the peripheral target, and that A-fibres will reach and predominate in the peripheral target.

Hindlimb sections from control embryos (n=6) and anti-NGF treated embryos (n=8) were each immunolabelled with the general marker PGP 9.5, an A-fibre selective marker RT97, and the small diameter fibre marker CGRP. Regions A-D on the hindpaw were examined as selected in Chapters 4 and 5.

The most striking observation was that in anti-NGF treated embryos innervation failed to penetrate the epidermis as visualised by any of the markers and in any of the regions. Fig. 7.3 shows innervation of the glabrous foot pad (region A), with each of the markers. Labelling with PGP 9.5 in control tissue demonstrates axon terminals projecting into the epidermis. This aspect is completely absent after anti-NGF treatment except for a few stray fibres in a couple of sections throughout the analysis. Instead, the axon plexus terminates sub-epidermally, but there is no apparent difference in the pattern or density in the dermis compared to controls.

Differences in the density or calibre of the dermal axons may not be perceptible using PGP 9.5 as this is a general neuronal marker, the absence of the fine diameter axons may be masked by the larger remaining axons.

One way of overcoming this problem was to use markers selective for the A and C-fibre populations. The C-fibre label, CGRP, is appropriate at this stage of development since it is detected in the periphery from E19. In control tissue, it also reveals fibres projecting into the epidermis. After treatment however, normal CGRP labelling is found in muscle and in the dermis but not in the epidermis, similar to the observation with PGP 9.5. However, the labelling is less intense and appears to be less beaded. Fig. 7.3 shows the CGRP labelling of region A after treatment, and is an example of a section that has a few fibres extending into the epidermis.

RT97 positive fibres in the epidermis are also affected by anti-NGF treatment. The remaining RT97 labelling in the dermis, does not appear different to controls even though these A-fibres are theoretically exposed to a larger target area due to the removal of the C-fibres. The potential differences in sub-epidermal labelling between treated and control embryos was further investigated quantitatively by density analysis, using the PGP 9.5 labelled sections which are representative of the overall innervation.

7.15 Quantitative Analysis of Dermal Innervation

Visual analysis of the epidermis clearly showed that innervation was almost completely abolished in all sections after anti-NGF treatment. However, this was not due to a total lack of innervation, as the rest of the skin was innervated sub-epidermally. To

assess whether this dermal innervation had reached the skin similar to controls, it was analysed quantitatively.

Camera lucida drawings (Fig. 7.4) of three sections, immunolabelled with PGP 9.5, from each region A-D, from control (n=3) and anti-NGF treated (n=4) embryos were digitised and the density of innervation assessed. Density was determined as the percentage of pixels of innervation from the total number of pixels in the region analysed.

Fig. 7.5 shows the density of innervation in control and treated embryos in each of the regions. Similar to the observation from the immunolabelled sections, there is no difference in the dermal innervation between control and treated embryos. There is also little variation between the regions. Statistical analysis confirms that no difference in density is found between the control and treated groups, even when all regions are combined [ANOVA: $F(1,81) = 0.013$, $P = 0.91$]. This finding infers that the same amount of innervating fibres reach the dermis even after anti-NGF treatment, where 43% DRG cell death occurs. It also supports the theory that the epidermis has become non-permissive to growth and that lack of innervation is not due to insufficient fibres reaching the target area.

7.16 Changes in the target

In addition to the apparent absence of innervation in the epidermis, it is obvious that the depth of the epidermis also changed after the treatment (Fig. 7.4). The epidermal depth appeared to have decreased. Measurements of epidermal depth in region A of control (n=18) and anti-NGF treated (n=24) sections revealed that the mean depth decreased by 29%. This observation was also valid for the other regions examined.

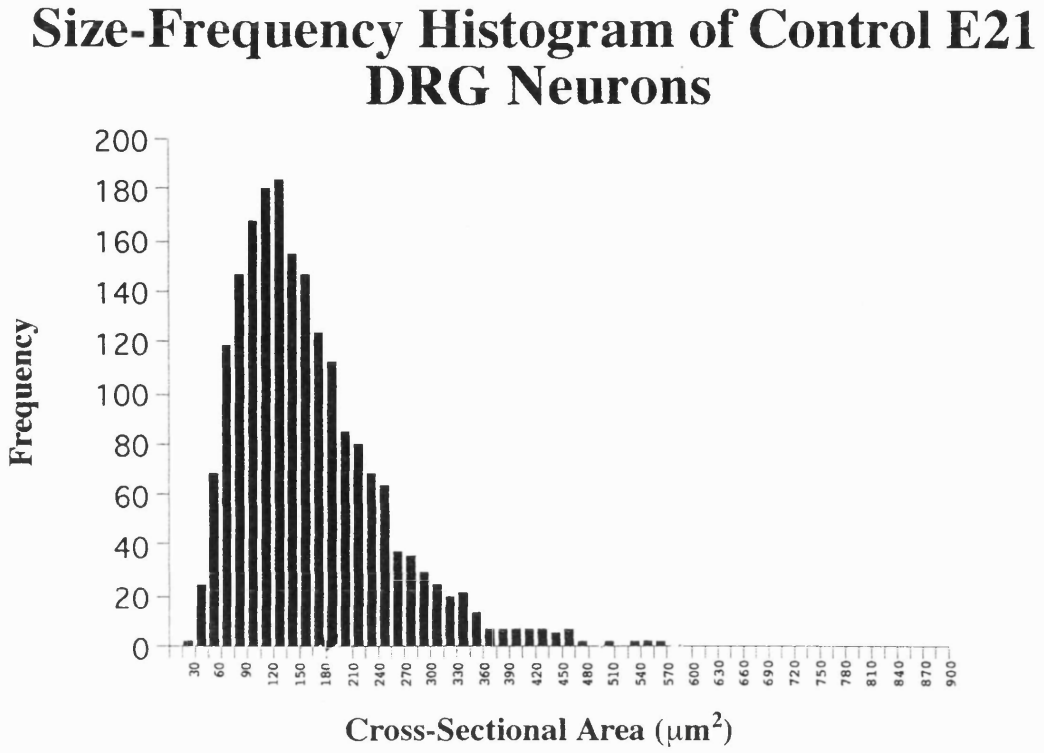

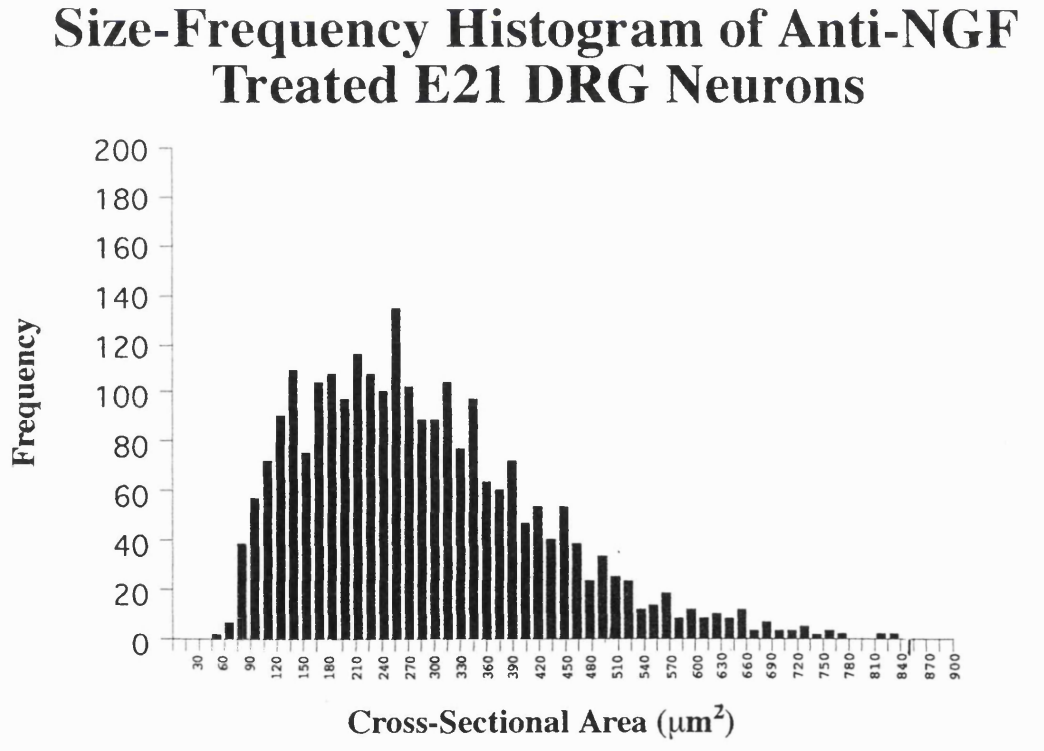

Fig. 7.1: Size-Frequency Distributions of Control and anti-NGF Treated E21 Dorsal Root Ganglia (DRG).
Anti-NGF treatment results in a selective loss of small diameter cells, and the appearance of cells larger than observed in the control DRG.

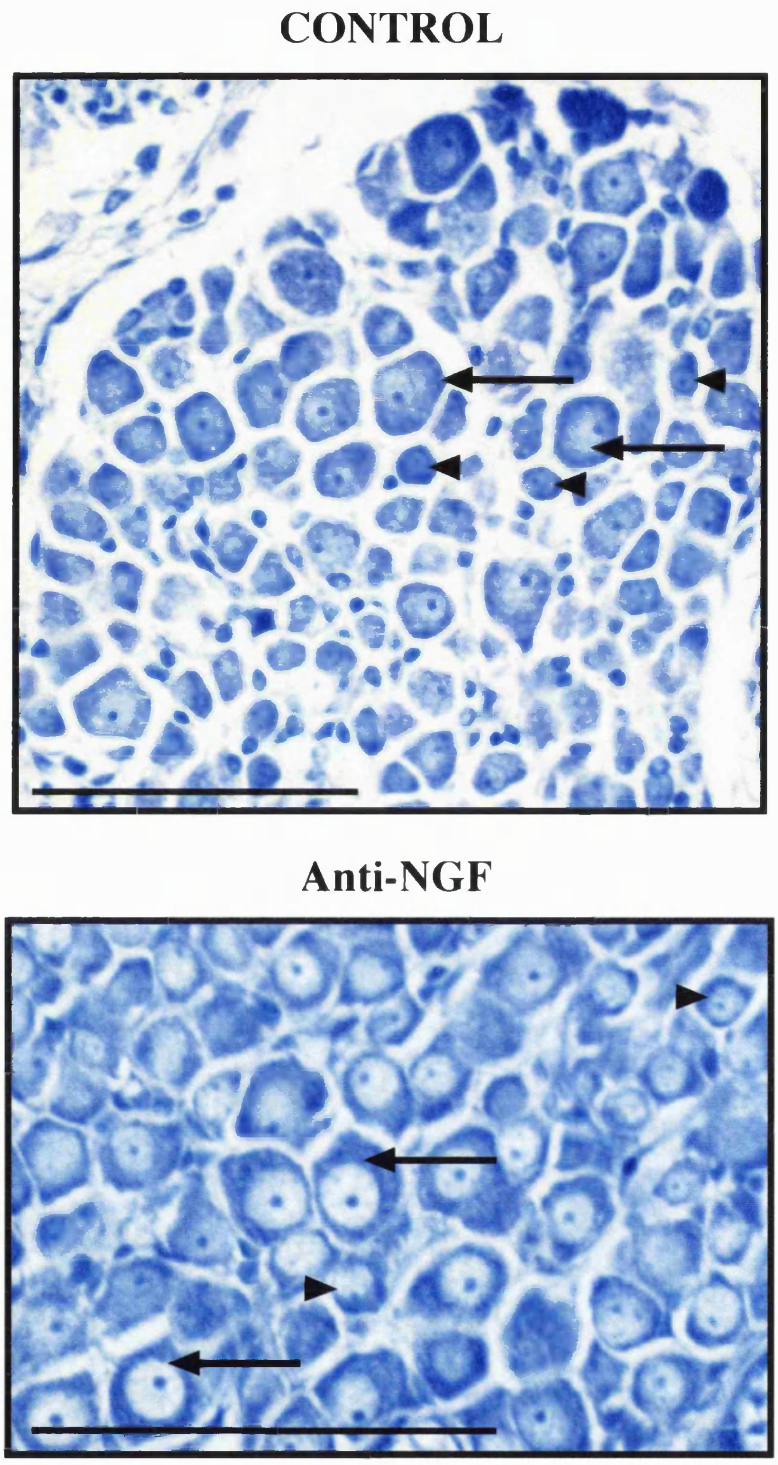

Fig. 7.2: Control and Anti-NGF Treated E21 DRG Sections counterstained with Toluidine Blue
These photographs are both at a magnification of x400. In the control, large and small cells are readily apparent, with larger cells denoted by an arrow and smaller cells by an arrowhead. After anti-NGF treatment, there are few small cells, arrowheads point to smaller cells in the section, however, these are much larger than the smallest cells in the control. In addition the largest cells (long arrows) are considerably larger than any observed in controls. Scale bar = 100μm.

Fig. 7.3: Localisation of immunoreactive (IR) nerve terminals in the E21 glabrous foot pad (Region A) of control and anti-NGF treated embryos

In control footpads labelled with PGP 9.5, CGRP and RT97, IR-terminals extend into the epidermis demarcated by the dotted line and are shown by the long arrows. Few axon plexus terminate in the dermal area. After anti-NGF treatment, terminals labelled by any of the markers are largely absent from the epidermis. Areas of epidermis denuded of innervation are shown with an asterisk. Axons now terminate in the dermal area and are marked with short arrows. The sub-epidermal innervation is apparently unchanged except with CGRP-labelled axons whose intensity has decreased. Scale bar = 100 μm.

Control **Anti-NGF**

PGP 9.5

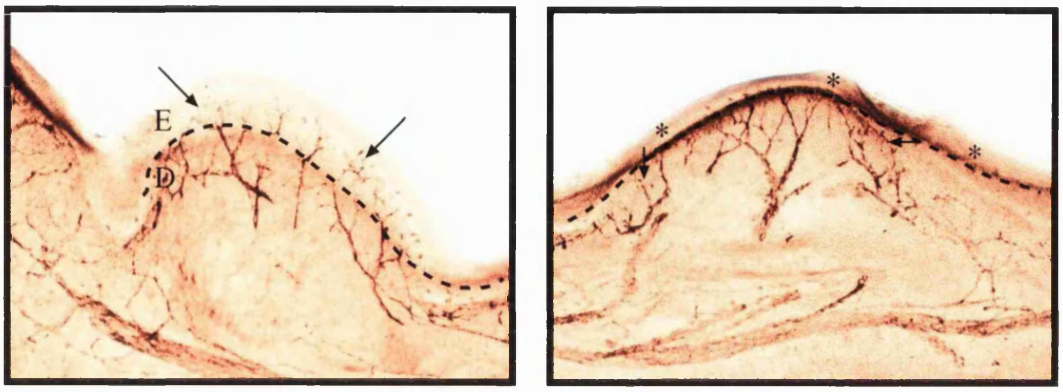

CGRP

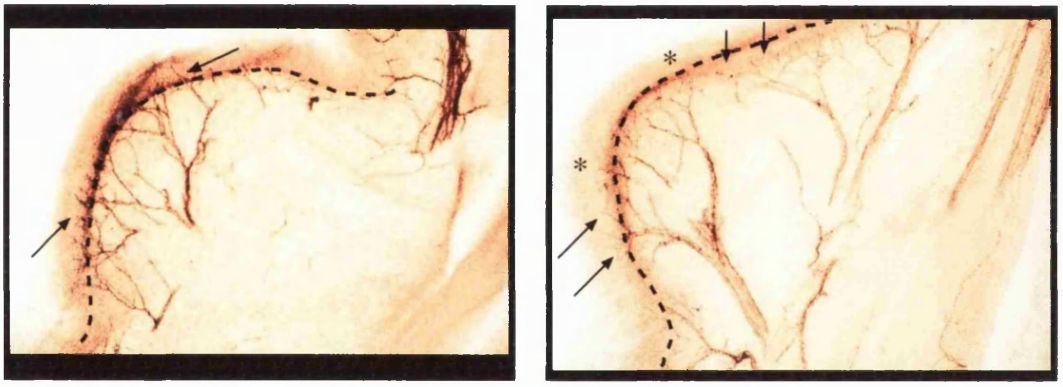

RT97

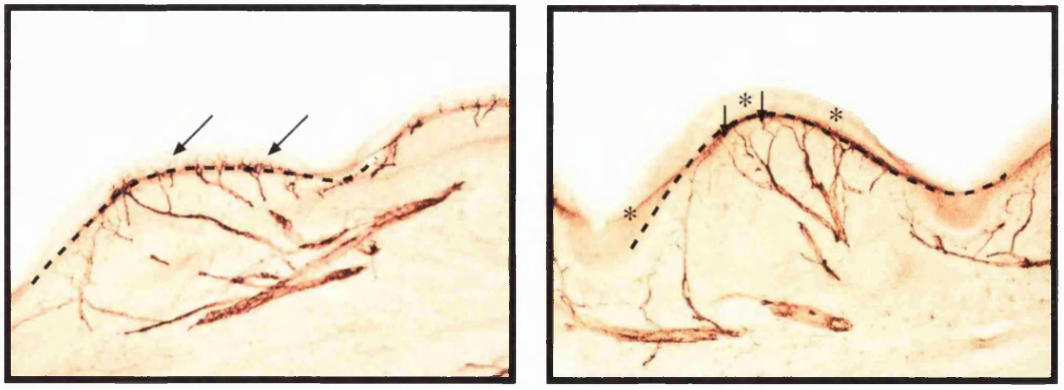

CONTROL

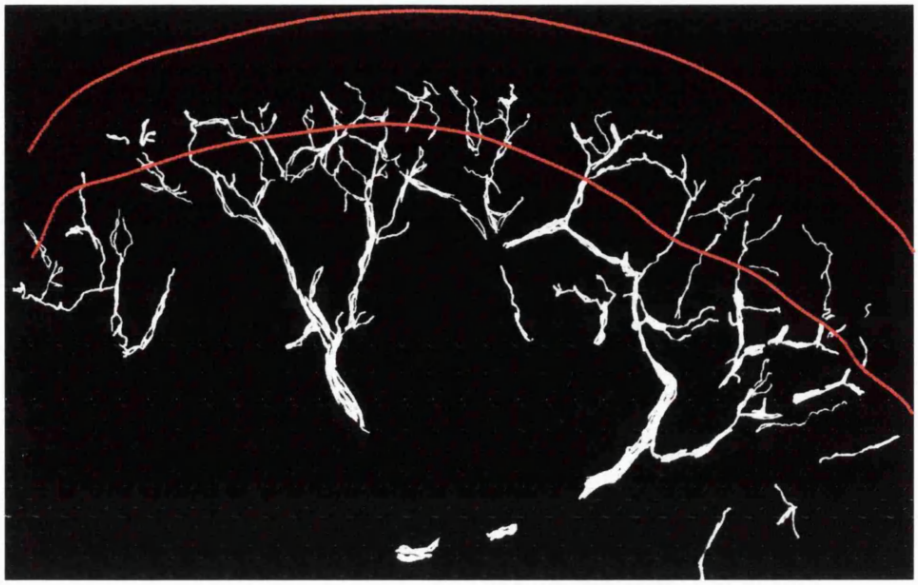

Anti-NGF TREATED

Fig. 7.4: Camera Lucida Drawings of Innervation in the E21 Glabrous Foot Pad of Control and Anti-NGF Treated Embryos
Innervation was visualised using PGP 9.5. The red lines delineate the epidermis, white lines represent the innervation. After anti-NGF treatment, axon terminals are absent from the epidermis, terminating sub-epidermally. In addition, the depth of the epidermis is reduced after anti-NGF treatment.

Innervation Density of the Sub-epidermis in Selected Regions of control and anti-NGF Treated Embryos

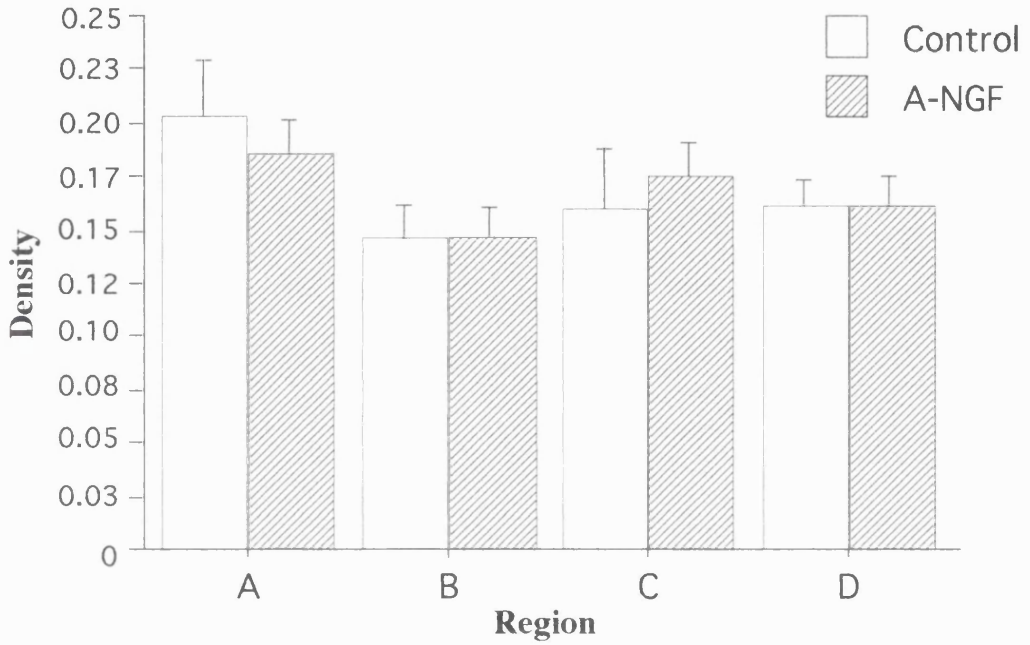

Fig 7.5: Sub-epidermal Innervation Density in Control and anti-NGF Treated Embryos
Innervation of the sub-epidermis in four regions A-D (defined in Chapter 2) of the hindpaw were visualised by PGP 9.5 and quantified. No statistically significant differences were found between controls and anti-NGF treated embryos.

DISCUSSION

The treatment of embryos with anti-NGF has four identifiable consequences.

A) 43% DRG cell loss restricted to the small cell population

B) The enlargement of surviving DRG neurons

C) The abolition of epidermal innervation of all neuronal subpopulations

D) No change in the dermal innervation density

7.17 Do the size-frequency histograms and cell counts reflect selective loss of small diameter neurons?

The size-frequency histogram showed a shift to the right after anti-NGF treatment with few cells in the small cell range, possibly indicating that all cells had enlarged. The results of cell counts however, show that a 43% DRG cell loss occurred. Together this information suggests that the cell loss is selective for small diameter neurons.

This finding is consistent with previous studies involving anti-NGF treatment (Johnson et al, 1980; Goedert et al, 1984; Carroll et al, 1992; Ruit et al, 1992) where cell loss after similar embryonic NGF deprivation occurred selectively in the small cells. Further verification of the selectivity of cell loss was provided by Ruit and colleagues (1992) after the central axonal projections were investigated with DiI. Their study confirmed that cell loss was selective as the superficial laminae of the dorsal horn were almost completely devoid of fibres in treated embryos, indicating that the entire functional class associated with this terminal location, namely the small diameter nociceptors which had been depleted yet central projections of other classes of DRG neurons were unaffected. Moreover, a separate study by the same group showed that 95% of the population of neurons expressing the high affinity NGF receptor trkA were lesioned under the same conditions (Carroll et al, 1992).

Size-frequency analysis of transgenic animals with null mutations of NGF and the receptor trkA also support the specificity of NGF dependent neurons. TrkA knockouts revealed that all of the smallest neurons as well as some medium-sized neurons in the

DRG are lost (Smeyne et al, 1994; Silos-Santiago et al, 1995), while NGF knockouts confirmed the loss of small to medium peptidergic neurons (Crowley et al, 1994).

Differences were noted in the actual size of the neurons recorded. In this study the mean area of control DRG neurons was 160.25μm^2 compared to 292.63μm^2 after anti-NGF. A discrepancy exists with the areas reported previously (Ruit et al, 1992) with both larger control and treated neurons, 275μm^2 : 394μm^2 at P0. This difference is most likely attributed to the technique for preparing the tissue since they used plastic embedded sections resulting in less shrinkage. Importantly, in both studies an increase in the mean size of cells is detected, reflecting the loss of small diameter cells. The establishment of selective small DRG loss was central to this experiment so that the effects of the interactions of A-fibre with the skin target could be examined.

7.18 Why is the DRG cell loss less than previous reports?

A 43% DRG cell loss was found in this study after anti-NGF treatment. This is considerably less than the reports of 70-80% cell death after similar prenatal immune deprivation of NGF (Goedert et al, 1984; Ruit et al, 1992) and from transgenic knockouts of NGF (Crowley et al, 1994) or trkA (Smeyne et al, 1994; Silos-Santiago et al, 1995).

The reason for this discrepancy may be twofold. Firstly it is possible that deprivation of NGF was not complete, allowing survival of more cells than in previous studies. If this is solely responsible then it is curious that size-frequency histograms mirror those in more successful attempts. Secondly, the technique for obtaining cell counts may be directly responsible for the disparity. The studies mentioned above all used profile counts to determine cell numbers whereas this study used unbiased stereological counting methods based upon the physical dissector technique (Coggeshall, 1992), which does not include assumptions or correction factors (see Chapter 2). The merits and differences between these techniques have been illustrated in a series of recent papers (Coggeshall, 1992; Pover et al, 1993; Tandrupp, 1993, Saper, 1996, Coggeshall & Lekan, 1996) and demonstrate how profile counts may overestimate the actual number of cells by up to 50%. Using the profiles measured for the size-frequency histograms in this study, the number of cells that fell into the small cell category (<180μm^2) reduced from

67% to 23% of the total, which is a 69% decrease, a figure within the limits of the cell death reported by the above studies. This finding substantiates the explanation of technical differences in coating for the observed small cell loss.

In addition, Ruit and colleagues stated that "the degree of cell death may have been slightly overestimated due to the severe atrophy accompanying trophic deprivation" (Ruit et al, 1992), explaining that some non-neuronal satellite cells may have been mistaken for atrophied neuronal cells. This factor was also taken into consideration in this study by only drawing profiles containing a clearly identifiable nucleolus.

7.19 Why are the surviving DRG neurons hypertrophied compared to those in controls?

The size-frequency histograms also illustrated how cell size at the upper end of the distribution increased from 570 to 850μm^2 after anti-NGF treatment. Since it has been established that cell death occurred selectively in the small cell population, this result indicated that some surviving cells had enlarged significantly, generating cells larger than observed in any age-matched controls.

It was important to establish if this effect had been observed in preceding NGF deprivation paradigms. In the NGF knockout study (Crowley et al, 1994) where size-frequency histograms were generated for the DRG, small cell loss occurred and the mean size of the population increased, but the size of surviving cells was unchanged because the number in the large cell categories did not change. In contrast, during NGF deprivation (Ruit et al, 1992) the number of cells in the largest size categories increased dramatically for surviving cells. If small cell loss alone occurred, then the mean cell size of the distribution would increase as observed, but the population that survives would not be expected to change size. These findings suggest that some process in addition to selective cell loss is occuring.

There are four possibilities to be considered. The first is target size, studies are described below where changes in DRG cell size occur after experiments affecting target size. This is important since the elimination of C-fibres increases the peripheral target available to surviving A-fibres. The second is the influence of increased cell survival, and

by implication how cell death in this paradigm could affect cell size. The third is that cell size is not changed, but these larger cells are novel cells that are not normally observed. Lastly, the effect of different neurotrophins when NGF is artificially deprived. The possibility that one or more of these processes may operate concurrently is also discussed.

i) Influence of target size

A 50% increase in the mean cross-sectional area of bladder DRG cell profiles was detected after a spinal cord injury that results in hypertrophy of the bladder muscle (Kruse et al, 1995). In this study, it is suggested that bladder hypertrophy drives the DRG cell enlargement since when the bladder hypertrophy is prevented after the spinal cord injury the DRG cell increase does not occur. Two explanations for the increase in bladder muscle and consequent cell size increases were pursued based upon previous research. The first possibility was that neuronal hypertrophy resulted from an increase in neurotrophic factors in the bladder muscle (Steers et al, 1991), and the second, that it was a result of increased axonal sprouting necessary to innervate the larger muscle (Gabella et al, 1992; Gabella & Uvelius, 1993).

Although bladder hypertrophy induced by urethral ligation is accompanied by increased NGF levels (Steers et al, 1991), and NGF affects the size of cultured bladder neurons (Tuttle & Steers, 1992), Kruse and colleagues (1995) showed how in their model, neurons have greater potential access to trophic factors but if this is allowed to occur without peripheral target hypertrophy, no increase in DRG cell size occurs. Therefore the hypertrophy is probably not solely driven by neurotrophic factors. Evidence supporting hypertrophy associated with peripheral afferent terminal sprouting is more persuasive. Urethral ligation leads to sprouting of efferent terminals intramuscularly and neuronal enlargement (Gabella et al, 1992; Gabella & Uvelius, 1993), if the efferent neuron ganglia is destroyed then remaining bladder neurons expand their innervation and increase in size (Gabella et al, 1992). This suggests that the terminal field may influence the size of the cell body. It also follows that the hypertrophied bladder is working harder so afferent fibres could have an altered firing pattern and have the potential to induce

morphological changes in the afferents and efferents (Gabella, 1984). In my study, the surviving neurons have no competition in the target from invading C-fibres, therefore they have the potential for increased occupation of the target. This point is fully discussed later in 7.23, but it is likely that collateral sprouting within the target did occur.

ii) Influence of cell survival

A number of the mediators of cell death have been identified and genes necessary to either promote or prevent cell death cloned (see Chapter 1). Bax is a gene that has been shown to enhance cell death. The Bax knockout (Deckwerth et al, 1996) has sympathetic neurons that survive for weeks in culture but shrink to 20% of normal volume, however NGF addition to these neurons restores their volume. This result shows that cell survival can be increased, but if there are insufficient growth factors, cell size is altered so that Bax inactivation may even result in functionally compromised neurons. This experiment is also important as it highlights how the role of neurotrophins are twofold. Firstly they are essential for survival, but if survival is guaranteed when cells don't have the machinery to die they can exercise their second function in growth, as demonstrated by the restoration of cell volume by NGF. The ratio between cell survival, cell death and availability of trophic factors may determine neuronal cell size beyond their intrinsic limits.

In my study the opposite occurs. There is increased cell death and therefore there should be increased trophic support available to surviving neurons. However, this study is more complicated as the cell death arises from trophic factor deprivation and cell death is selective, indicating that remaining cells do not require NGF. Nonetheless, the possibility of altered neurotrophin levels affecting the remaining cells is considered in section (iv) later.

iii) Cell size does not change, but neurons survive that would normally be eliminated by apoptosis

It is possible that these larger neurons are generated during development, but are normally eliminated by a natural process. How these larger neurons survive in this NGF deprivation experimental paradigm, may be due to the dual actions of survival and death displayed by the neurotrophins and the interactions with their receptors.

The role of neurotrophins in promoting cell death has received attention after several recent examples of cells susceptible to NGF-induced death through the p75 receptor. This theory was initially viewed with misgivings since all previous investigations of neurotrophins or their elimination, led to the conclusion that they were essential for survival (see introduction 7.4). The examples of neurotrophin-mediated p75 death promotion so far illustrate how specific the conditions and circumstances under which this process occurs and why it has remained unrecognised for so long. p75 can transduce signals leading to apoptosis in some cells though there is no general agreement on whether pro-apoptotic signals are transduced by the occupied (ligand-dependent) or unoccupied (ligand-independent) receptor or perhaps by both, as a function of the cell type involved (Henderson, 1996).

Evidence suggests that NGF signalling through p75 in the absence of trkA stimulates apoptosis (see 7.9), and should be considered as a possible mechanism whereby the larger cells are found by default in this experiment. If this process occurs, then removal of NGF would prevent the intracellular death signal and the cells that survive are these very large cells that otherwise would not.

The pertinent theme to emerge from the p75 mediated cell death studies outlined in 7.9, is that apoptosis transduced through the p75 receptor may or may not be NGF mediated. If we assume it is not NGF mediated, and the apoptotic response to p75 is a normal process applicable to the rat DRG development, then it is difficult to foresee why such a response is biologically necessary in the normal situation. From the size-frequency histograms of control DRGs at E18 and E21 shown in Chapter 3, none of these very large cells are observed. This is either because they are removed in the first wave of prenatal cell death, which is unlikely in a ligand-independent process since there are high levels of NGF and trkA. Alternatively, these may persist postnatally in the normal embryo but due to limited growth factors, appear to be of similar size as the remaining cells until their elimination. Postnatal elimination through the ligand-independent process is feasible, since NGF and trkA levels are downregulated and this process has been documented in two cases postnatally (Barrett & Bartlett, 1994; Van der Zee et al, 1996).

The timeframe in which the DRG is examined is important. It is possible that in the mouse example (Barrett & Bartlett, 1994) a ligand-independent process constitutes the mechanism behind the second wave of cell death (Coggeshall et al, 1994) and is promoted by the decrease in NGF and the downregulation of trkA. The likely reason for ligand-independent p75-mediated apoptosis not occurring in this study, is because it would have to occur during the period of target innervation and terminal competition when NGF is normally abundant. In addition, p75 is rarely expressed independently of trk receptors prenatally (Wright & Snider, 1995).

In my study, the cells survive in the absence of NGF and grow larger instead of dying. The artificial removal of NGF in this experiment could have mimicked the events postnatally and stimulated premature apoptosis in the trkA negative, p75 expressing cells in a ligand-independent model. However that did not occur as the larger cells are evident when examined at E21.

It is known that after anti-NGF treatment, even though there is 70% cell death, that only 28% is accounted for by p75 positive cells (Carroll et al, 1992) Therefore the fact that so many surviving cells are p75 positive is consistent with possible inhibition of ligand-dependent/NGF-mediated cell death generating these large cells. The percentage of cells known to be p75 positive and trkA negative in the adult is between 5-10% (Bennett et al, 1996b).

A 7% increase in the number of cells larger than 500μm^2 was found after anti-NGF treatment. Although ligand-independent death would be unlikely when target innervation is underway, it is possible that NGF-dependent apoptosis could occur in the normal embryo since there are high levels of NGF as required, and if the effect is normally as small as the 7% described here, then this fits within the percentage of p75 postitive trkA negative cells in the adult. This NGF-mediated elimination of p75 positive cells during the first wave of cell death would also explain why these large cells are not observed in the E18 and E21 controls. The problem with this assumption is that in the embryo, trkA levels are higher than p75, however in this anti-NGF experiment the

number of trkA expressing should be reduced due to trophic deprivation, and the ratio between the receptors sufficient to imitate the adult scenario.

It is not possible to determine if p75-mediated cell death occurred in this experimental paradigm but if we assume that it occurs prenatally through the prevention of NGF-mediated cell death, it explains the presence of these large cells. If p75 mediated cell death occurs postnatally when NGF levels are low, it suggests that the cells in this experiment were prenatally exposed to some other influence which causes hypertrophy above the normal state.

iv) Added exposure to a previously limited growth factor

Information about the expression patterns and temporal sequence of neurotrophin and receptor onset and duration, allow us to deduce how each class of neuron is supported throughout the period of cell birth to the final pattern of target innervation. If the removal of NGF by immune deprivation just prior to target innervation is considered, we can speculate about how this disrupts normal development and what happens to the sequence and pattern of neurotrophin and receptor while the underlying processes are continuing.

It had previously been accepted that the onset of DRG neuron dependence on NGF/trkA signalling occurs after axons arrive in the developing skin and that neurons could be dependent on another neurotrophin before that time. If we consider the possibility that NGF dependent neurons also utilise another neurotrophin prior to reaching the target, it is not inconceivable that they also receive other additional input upon reaching the target. Although another trophic factor is not sufficient to support the cells in absence of NGF, it will be in excess after the death of the NGF-dependent cells. This unknown neurotrophin could then act upon the remaining cells. The prime candidate for this unknown neurotrophin is NT-3. There are many pieces of information which together suggest that NT-3 could signal through trkA, and therefore in the absence of NGF/trkA expressing neurons, would be available in greater quantities for remaining neurons.

The evidence supporting NT-3 signalling through trkA is diverse. It is known that in addition to subpopulations of cells requiring a particular neurotrophin or receptor for

survival during target innervation, that at various stages in development they may require different neurotrophins and that switches in dependence may occur. Examples of this process have been documented in mouse trigeminal ganglion neurons where cells expressing BDNF/NT-3 for survival at E11 then switch to NGF dependence by E13 (Buchman & Davies, 1993). TrkC expressing sympathetic neurons are supported by NT-3 early in development yet require NGF later (Birren et al, 1993; DiCicco-Bloom et al, 1993). From these studies it was hypothesised that neurons may depend upon locally synthesised factors before arrival of axons in target fields and then switch to dependence on target-derived factors (Buj-Bello et al, 1994; Davies, 1994). This opened up the possibility that a different neurotrophin could signal to cells at a specific developmental stage but lose this as the animal matures. The order in which these developmental switches occur may reveal if there are periods of overlap when a neurotrophin may signal through more than one receptor.

The candidacy of NT-3 as the putative molecule signalling through trkA was initially established because of the observation that NT-3 null mutant mice show far greater cell loss than trkC null mutants. This led to the suggestion that NT-3 supports many DRG neurons via actions on the NGF receptor trkA rather than the preferred NT-3 receptor trkC (Davies, 1994; Farinas et al, 1994; Klein et al, 1994). The large cell death of neurons in NT-3 knockouts above the number that express NT-3, also demonstrated that some NGF-dependent neurons require NT-3 for survival at some stage (Ernfors et al, 1994; Farinas et al, 1994). There has been *in vitro* evidence that NT-3 can act via trkA (Ip et al, 1993; Davies et al, 1995). Retrograde transport of NT-3 by small diameter neurons suggests the existence of a population of small NT-3-dependent neurons while in NT-3 overexpressing mutants the number of unmyelinated axons increase by 65% in addition to the myelinated axons (Albers et al, 1996).

Expression data in the mouse does not reinforce these assertions. Initially at E11.5, neurons express trkC and require NT-3 for survival. NT-3 is expressed immediately adjacent to the ganglia and in the axon projection pathways (White et al, 1996). TrkC downregulation starts when trkA expression is first being detected, however

there is no survival dependence on trkA at E11.5. Onset of NGF/trkA dependence is synchronous at E13.5 when trkA-IR fibres are found in the hindlimb and NGF is expressed in developing skin.

This scenario does not support NT-3 signalling through trkA, but rather that dependence is sequential as if NT-3 did signal through trkA at early stages, the loss in trkA knockouts would be detected earlier at E11.5 and would be more extensive, yet it is the same loss as in NGF knockouts (White et al, 1996). However since the discrepancy between NT-3 and trkC knockouts is evident at E13.5, it is plausible that NT-3 could signal through trkA only when trkC is absent and would explain the smaller loss of cells in trkC knockouts. This is also possible due to the extensive co-localisation of trkA and trkC in neurons at E13.5. Co-localisation is further supported due to the transient detection of trkC in chick cutaneous sensory axons (Plouffe et al. 1995.) Subsequent to the period of peripheral innervation, the populations of DRG neurons expressing trkA and trkC are largely non-overlapping but before this there is a window of time where trkC is being restricted and trkA upregulated simultaneously, which also parallels the shift in responsiveness for survival from NT-3 to NGF (Philips & Armanini, 1996).

In the normal situation it appears that NGF dependency is acquired later and is associated with the peripheral target. A recent study has indicated that even when NGF dependency is established, NT-3 may influence these axons. This study (Fundin, 1997) consists of a series of experiments submitted for a PhD (manuscripts submitted/in preparation), and contains some new theories concerning the influence of neurotrophins and receptors in axonal development. Collectively, the experiments suggest that neurotrophins signal through different receptors at different developmental stages and that these can be switched several times between the receptors throughout development. A very complicated picture of axonal development nonetheless emerges, since tissue from all neurotrophin and receptor knockouts in addition to neurotrophin overexpressing mutants are examined with respect to fourteen sets of identified sensory endings immunostained with different markers. Some clear results however are of relevance to my study.

From comparison of the effects of elimination and excess expression of each of the neurotrophins and receptors on sensory endings in the mystacial pad, it was concluded that NT-3 has a major impact on formation of all sensory endings independent of survival or outgrowth. NGF overexpression increases the amount of dermal axons considerably (Davies et al, 1997) with little effect on epidermal endings while NT-3 overexpression increases endings significantly leaving dermal innervation unchanged (Fundin, 1997). In the NT-3 knockout, surviving innervation sprouts into the epidermis and is attributed to actions of NGF, but in the trkC knockout, sprouting of endings known to be dependent on NT-3 occurs, therefore they must have arisen as a result of NT-3 signalling via trkA.

In this anti-NGF study, if neurons express trkA and manage to reach the target expressing NT-3, it is not clear why they could not use NT-3 instead of NGF to promote survival. Activation of trkA by NT-3 requires relatively high concentrations of NT-3 compared to NGF (Birren et al, 1993; Davies et al, 1993; Dechant et al, 1993; DiCicco-Bloom et al, 1993; Davies et al, 1995), but this criterion is fulfilled since NGF has been neutralised by antibodies. The reason that this does not occur is that there is no evidence that NGF/trkA dependent axons reach the target then degenerate, they must require NGF prior to target innervation. Neurons were thought to acquire dependence on target-derived factors after reaching the target, but NGF and trkA knockouts show that DRG neurons die some 48 hours before the time when axons arborise in the hindlimb (White et al, 1996). Therefore these neurons require a signal from the target before innervation is complete suggesting it must be a diffusible source or an auto-paracrine source. NGF/trkA dependent neurons probably do not reach the target in this experiment - they die during their NGF-dependent growth through the hindlimb.

The surviving neurons reach the target as normal, only there is no competition from small diameter neurons and they have access to a larger uninnervated territory. The normal developmental sequence would have involved a signal to downregulate trkC expression on DRG cells and NT-3 in the skin while simultaneously upregulating trkA and NGF. This signal was postulated to be the onset of NGF synthesis itself. TrkA

upregulation corresponds to peripheral target innervation, yet it is not initiated by NGF since the profile of trkA expression is normal after targeted disruption of NGF gene (Davies et al, 1995). The fact that the downregulation of trkC/NT-3 and the upregulation of trkA/NGF may be prevented in the absence of NGF suggests that there still may be a connection to NGF. When NGF levels do not increase in this experiment, trkC and NT-3 should continue to be expressed, all NT-3 is then available to a smaller population of cells that can signal through trkC only.

NT-3 is in excess because there it is more than required for survival purposes, therefore it could initiate collateral sprouting as suggested above, resulting in greater retrograde transport to the soma and hypertrophy. Consistent with this speculation, the soma areas of trigeminal neurons increase by 23% in NT-3 overexpressing mutants (Albers et al, 1996). More convincingly, administration of NT-3 in a similar *in utero* paradigm as used here, preferentially increases soma area of DRG neurons at the larger end of the spectrum. In addition, 6% of cells had soma areas larger than 250μm^2 which were never observed in controls (Zhang et al, 1994).

v) Combination of factors to increase size of selective surviving cells

The four possibilities detailed previously, together provide clues as to what may be happening in this experiment to generate these large cells. The fact that NGF deprivation results in 43% selective cell death of small cells means that a larger target is available to surviving neurons. Due to the changing neurotrophin dependence of neurons, NT-3 levels have normally decreased by late foetal stages so very little signalling occurs through the downregulated trkC receptors. However, if NGF levels are kept low due to the antibody treatment then the signal for the NT-3 to decrease does not occur. NT-3 levels are maintained, trkC expressing cells (i.e. A-fibres) do not die as expected since the first wave of cell death is not complete at the outset of this experiment. NT-3 is unable to compensate for the loss of NGF, but its expression in the target is thought to influence terminal formation (Fundin, 1997). Therefore NT-3 may cause collateral sprouting of the surviving axons to invade the enlarged target. Sprouting would mean greater access to target-derived factors for retrograde transport to the cell, and direct enlargement by

continued exposure to NT-3. The one problem with this model is that only a small proportion of the cells grow larger than observed in controls, therefore it is also possible that there are a subpopulation of cells that are particularly susceptible and that otherwise would be eliminated by an apoptotic mechanism.

7.20 What is the stimulus for the abolition of epidermal innervation?

Two recent studies also describe the complete eradication of epidermal innervation specifically, after manipulations of neurotrophins or their receptors. The low affinity neurotrophin p75 receptor null mutant showed no selective cell loss yet epidermal innervation was severely compromised (Bergmann et al, 1997). Null mutants of NGF, trkA or NT-3 produced similar results in the epidermis of the mystacial pad (Fundin, 1997). These studies mainly attribute the suppression of epidermal innervation to loss of the parent cell bodies by trophic deprivation. Indeed, it would appear that this has occurred in my study except that there are surviving cells, and the NGF-independent axons labelled by RT97 are also affected, suggesting there may be another underlying reason.

The common feature of these studies is that manipulation of trophic factors has altered the epidermal environment rendering it seemingly non-permissive to neuronal growth. If the effect were restricted to NGF or trkA knockouts, it would be consistent with a requirement for transducible NGF in the epidermis. It has been shown that NGF is not an attractant for early sensory fibres (Lumsden & Davies, 1983) but it may be required at the site of terminations when axons have acquired their NGF dependency. In both the knockout experiments and in this anti-NGF paradigm, sub-epidermal innervation appears normal. In section 7.19(iv) above, it was suggested that NT-3 may cause collateral sprouting. Consistent with this explanation, NT-3 overexpressing mutants increase the innervation density but do not induce aberrant projections even though the source of the NT-3 is inappropriately expressed in keratinocytes, suggesting that NT-3 regulates density but not location of innervation (Fundin, 1997). This is reinforced in my study since, although not raised above normal, NT-3 levels may be maintained beyond

the usual expression timeframe and continue to be expressed in the deeper layers of skin (Albers et al, 1996; White et al, 1996) where all innervation terminates in this experiment.

This would suggest that innervation intrinsically terminates at the appropriate site and, if excess trophic factor is available, that they will undergo sprouting at that site but will not change their position. This explanation is not sufficient to account for the loss of epidermal innervation in the NT-3 and p75 null mutants.

It is possible that trophic levels regulate some other factors that either confer a permissive or non-permissive environment to neurite growth. Examples of such inhibitory factors could be semaphorins (see Chapter 1.6.3[ii]), while influences to promote a permissive environment may be due to laminins (see Chapter 1.6.2[ii]).

In rat E11-E13 Sema III is intensely expressed in peripheral tissues. At E14, developing muscle and superficial skin appear to downregulate Sema III until undetected at birth (Wright et al, 1995). The relationship between neurotrophins and semaphorins has not been clearly defined, but NGF, BDNF, NT-3 and GDNF are all expressed in the peripheral target adjacent to the DRG axons when Sema III is detected. Wright and colleagues (1995) suggest that neurotrophins may attract and support axons but not promote branching, while Sema III co-ordinates the timing and appropriate location of innervation within the target. Hence an association exists between neurotrophin levels and expression of molecules that are non-permissive to neurite growth.

Laminins may be responsible for neurons distinguishing their target and consistent with this differential role, different isoforms are restricted to particular tissues. Interestingly, laminin isoform up/downregulation is associated with keratinocyte differentiation (Tennenbaum et al, 1996). Laminins can be used as markers of keratinization but importantly certain laminins are only expressed when keratinocytes are differentiated, indicating that a sign of epidermal permissiveness to growth may be the expression of laminins once keratinocytes have differentiated.

The significance of this feature to the lack of epidermal innervation after anti-NGF treatment is in the regulation of keratinocyte differentiation. Developmental changes in levels of NGF mRNA in whisker pad epidermis are paralleled by changes in keratin

expression (Schornig et al, 1993). Although the induction of NGF is not linked to epithelial differentiation it is clear a relationship exists between them after NGF initiation. Moreover, receptor tyrosine kinases such as c-met, c-ros and keratin growth factor receptor are preferentially expressed in epithelia and if the ligand-binding domain of these receptors are partially substituted with that of trkA, then NGF addition leads to cell motility and branching of epithelial cells (Sachs et al, 1996). This latter finding provides a explanation for the influence of the NT-3 knockout on epidermal innervation since it also acts via a receptor tyrosine kinase, trkC.

7.21 Why should A-fibres affected by this treatment?

RT97 projections to the epidermis were equally affected by this anti-NGF treatment. This result was not anticipated because RT97 labels the large diameter axons that are not dependent on NGF signalling. Also, from the size-frequency histogram there was no loss of large diameter cells and in fact even larger cells were observed. This indicates that failure to innervate was not due to the lack of cells to generate axonal fibres. RT97 does however label some smaller axons and cells (see Chapter 3). If therefore these are the fibres that normally extend into the epidermis, they may have been susceptible to the anti-NGF treatment and resulted in the same effect as observed with other markers.

Alternatively, the lack of epidermal innervation observed with the A-fibre marker may be a reflection of the epidermis being non-permissive to any innervation as described above. Large and clumpy RT97-IR fibres project into the epidermis during the embryonic period (Chapter 4 and Chapter 5), and even though they withdraw subepidermally as development proceeds, it is surprising that these are also affected in this experiment. Evidence to suggest that these are not NGF independent arises from two studies. Firstly, there is a 17% increase in myelinated dorsal root axons after neonatal anti-NGF (Hulsebosch et al, 1987) and secondly NGF/trkA signalling is required for some sets of Aβ innervation to the mystacial pad (Fundin, 1997).

7.22 Is the presence of CGRP-IR neurons an indication that all C-fibres were not eliminated?

It is probable that not all small cells were eliminated by this anti-NGF treatment regime. Examination of the DRG sections (Fig. 7.2) and the size-frequency histogram (Fig. 7.1) reveals that some small cells survive. It may also be the case that the few remaining small cells underwent substantial collateral sprouting (see 7.23 below), alternatively the CGRP may be labelling the A-fibres that it normally does (McCarthy & Lawson, 1990). The CGRP innervation may also be maintained as some CGRP innervation requires NT-3/trkC signalling for survival (Fundin, 1997). As also discussed in 7.23, the intensity of CGRP labelling is decreased and CGRP levels are regulated by NGF, therefore in the absence of NGF, the levels of CGRP may not be physiologically relevant.

7.23 How is the dermal innervation density unaffected after 43% cell death?

The lack of changes in innervation density in the dermis even after 43% cell death leads to two conclusions. Either there are small differences but these are not being identified using this technique or the axons from the surviving cells have branched or undergone collateral sprouting at the target.

Differences in the density of innervation may be very subtle because the DRG cell loss was selective for small cells which give rise to thin unmyelinated axons. These may be very difficult to detect with immunohistochemistry amongst the larger myelinated axons. Since the unmyelinated axons are so fine they may not contribute significantly towards overall density in the control situation and therefore statistically significant differences would not be picked up even after loss of the small cell population. The use of selective markers should overcome this problem but as discussed above and in Chapter 4, at this stage of development and even in the adult to some degree, there is not an adequate antibody available.

CGRP mostly labels small to medium sized cells, although some 25% of A-fibres are included. The density of CGRP labelling was not quantitatively analysed in this study

but qualitative analysis did not indicate any differences in density although the intensity of labelling was decreased. The decrease in CGRP intensity is consistent with a previous analysis in the trkA knockout where CGRP was vastly reduced in the DRG and central projections (Silos-Santiago et al, 1995) and similarly infrequent and weakly labelled cells in DRG of NGF knockout (Crowley et al, 1994). More relevant to this study was the complete loss of CGRP-IR processes in the hairy skin of the mice (Crowley et al, 1994). The reason for this may be due to the synthesis of the peptide in the DRG cells and not due to differences in the axons themselves. As discussed previously in Chapter 6, the production of neuropeptides is influenced by growth factors from the target, specifically NGF. The decrease in NGF due to the antibody treatment may be the cause of the intensity changes.

The other reason for the unchanged dermal innervation density may be that some form of sprouting has taken place. A study in 1987 indicated that after neonatal anti-NGF treatment, 38% of DRG cells were lost yet counts of axons in the dorsal root revealed 17% more myelinated and 40% more unmyelinated than control dorsal roots (Hulsebosch et al, 1987). This was interpreted as the remaining DRG cells emitting more processes than normal since all axons in dorsal roots arise from DRG cells (Langford & Coggeshall, 1979), and therefore after anti-NGF, cells must produce 50% more processes than normal. Some of this increase may be accounted for by the cessation of the normal developmental loss in the first two postnatal weeks (Hulsebosch et al, 1986). In contrast, a follow-up study examining the effects of neonatal anti-NGF treatment on peripheral processes found a 48% decrease selective for unmyelinated fibres (Urschel et al, 1991). The peripheral nerve distal to the origin of the dorsal primary ramus was examined and the loss attributed to the result of DRG cell loss in the same small cell population.

The finding that sprouting occurred in the central processes after DRG cell loss was controversial and generated much debate. Subsequently, physiological studies have validated this finding by Coggeshall's research group. Some researchers Devor, Wall and McMahon find minor branching while others, Pierau and Lawson suggest there is considerable branching (Coggeshall, personal communication). These paradoxical effects

of anti-NGF treatment may be because NGF is not the only target-derived trophic factor. The dorsal roots and peripheral nerve fibres have different targets so it is not inconceivable that the sprouting response of the dorsal roots after DRG cell loss was stimulated and directed by a centrally-derived factor - possibly BDNF (Davies, 1986). The importance of these investigations to this study is the implication that axonal sprouting does not occur. However this does not rule out collateral sprouting within the target.

Another study manipulating the amount of innervation destined for the target involved removal of the L4 DRG in a P0 rat pup. The innervation of the hindlimb skin is equally derived from the L4 and L5 DRG (Wessels et al, 1990), therefore the removal of the L4 DRG would result in 50% less innervation supplied to the target. Counts of the axons in the sciatic nerve revealed a decreased number, however, no difference in innervation was detected in the skin between control and operated rats (Payne, 1993). This finding particularly, suggests that cutaneous terminals have the capacity for local terminal sprouting if target availability increases and that collateral sprouting compensates for the reduced innervation due to loss of DRG cells. This response was looked for since the reaction of surviving fibres in the target was the premise behind this experiment. The experimental paradigm utilised (Ruit et al, 1992) was expected to selectively remove the small DRG cell population and therefore C-fibres, leaving A-fibres to innervate the skin target. Whether or not the A-fibres would respond to the increased target or at least decreased competition for target was the basis for examination of the peripheral effects of anti-NGF. Although the density of innervation is the same as controls, it is not clear whether there was greater sprouting from any surviving small fibres or whether all classes of fibres sprouted equally.

The stimulus or the source of factors influencing sprouting in this situation are unknown. Measurements of known neurotrophin levels in the skin were not determined. Previously, NGF onset and levels have been investigated in skin (Davies et al, 1987) and collateral sprouting has firmly been associated with NGF (for review see Diamond et al, 1992). When NGF has been removed from the target, the ability of remaining trophic

factors to promote collateral sprouting *in vivo* has not been ascertained. It is known that in transgenic animals that signalling of NT-3 through trkA stimulates terminal branching of primary sensory afferents (Fundin et al, 1997a; Rice et al, 1997). This was determined from comparisons of effects with NT-3 knockouts/overexpressors and trkC knockouts. Each type of afferent is dependent upon a unique combination of receptors and neurotrophins, yet the overall distribution of the various sets of sensory innervation appears to be due to a balance of differential neurotrophin dependencies and by competition for the same neurotrophin by different sets of afferents.

7.24 Are the structural changes in epidermal depth a primary consequence of trophic factor deprivation?

A similar decrease in epidermal depth (31%) has been reported after the null mutation of the low affinity neurotrophin receptor p75 (Bergmann et al, 1997) as was found in this anti-NGF study (29%). This observation may have arisen by two processes. The first is a direct effect of trophic withdrawal on either the structure of the epidermis or of molecules expressed within it. The second is an indirect effect by which trophic withdrawal reduces innervation and it is innervation that determines the depth of the epidermis.

These influences have been addressed in previous sections of this thesis. The direct influence of trophic factors is discussed in section 7.19(iv). The effect of innervation has been discussed in Chapter 5, but additionally in the p75 knockout study (Bergmann et al, 1997) the authors provide further support for an indirect cause by referring to nerve injury studies where decreases in skin thickness are associated with reduced synthesis of several housekeeping enzymes of keratinocytes following nerve section in rats (Hsieh et al, 1994).

Concluding Remarks

The work presented in this thesis has been directed towards characterisation of sensory cells and axons that constitute the DRG and its central and peripheral target and an understanding of how the specific innervation patterns are established.

Chapters 3 and 6 of this thesis dealt with aspects of DRG development and the methods of reliably identifying different neuronal phenotypes. The unequivocal classification of cells and axons based on their histochemical profile was central to the subsequent descriptive analysis of different DRG subpopulations. In recent years the ability of one neuronal phenotype to change features such as trophic requirements of chemical profile during periods of development or injury has underlined the necessity of scrutinising the techniques and materials used to describe such populations. Results from these chapters indicated that cells at E18 and E21 cannot yet be classified by the morphological criteria large light and small dark. The size-selectivity of the neurofilament marker, RT97 is however established early in development. The peptide CGRP is also an appropriate label as it is detected within the same timeframe that it is synthesised.

Chapter 4 contained descriptions of the patterns of innervation in both the hindlimb and spinal cord and enabled a comparison of events at the peripheral and central target of the DRG. The density of the skin innervation was investigated in Chapter 5 and these two chapters used as a basis for the examination of the interactions between innervation and the target in Chapter 7. The summary of these results are found in the relevant chapters but together allow models of DRG neurite outgrowth to be constructed. The following models are representative of possible interactions and sequential events between the DRG and target based on the interpretation of results in this thesis.

Model 1: Outgrowth of DRG subpopulations to appropriate targets

The peripheral processes of the A-fibre (RT97) and non-peptide expressing C-fibres (trkA) grow together to reach the skin at E14. Innervation is established in a proximo-distal direction with skin innervation preceding muscle innervation. Peptidergic labelling is detected throughout the limb at E19 and its onset is stimulated by the contact with target and

a signal (NGF) to modulate the intrinsic expression pattern. Innervation of the skin epidermis proceeds by projection towards the skin surface but by late embryonic stages, terminals retract to a sub-epidermal position.

The central processes of A-fibres and non-peptide expressing C-fibres also grow towards the spinal cord at the same time peripheral processes are initiated. The A-fibres wait at the dorsal root entry zone (DREZ) for two days before they enter the lateral dorsal horn at E14. A-fibres quickly establish projection patterns consistent with their physiological modality but are correlated with the position of their peripheral process. As proximal skin is innervated, afferents innervate the lateral dorsal horn, when distal skin is reached afferents enter the dorsal horn from the medial dorsal column. Muscle innervation is correlated with the appearance of ventrally directed 1a afferents. Meanwhile C-fibres wait 4 days at the DREZ until a few trkA fibres are detected in the superior dorsal horn. These increase at E18 and are joined by IB4 positive fibres. By E19 a dense network is found in the substantia gelatinosa and is the first stage when peptidergic labelling is detected.

In model 1, it is not known what stimulates the onset of peptidergic labelling, however the literature reviewed in earlier chapters indicates that this factor is consistent with a role of NGF. It is also unclear whether trkA is labelling only non-peptidergic axons at this stage, or whether future peptidergic axons are included. There are two implications for this model of outgrowth if only non-peptidergic axons are labelled. Firstly, in the periphery there are two waves of growth, A-fibres and non-peptidergic fibres together followed by peptidergic fibres. Centrally, this would mean there are three waves of ingrowth: A-fibres, non-peptidergic fibres and then peptidergic C-fibres. Furthermore this implies that non-peptidergic C-fibres are a separate phenotype from the outset, perhaps even with different trophic requirements.

Another unexplained feature of the sequential phenotypic ingrowth to the spinal cord is what is responsible for establishing the waiting periods of C-fibres. It had previously been thought that cells born later in the DRG were contributing to the waiting period, but in this study central axon outgrowth clearly begins in tandem with peripheral

outgrowth. This implies that it is the target that determines the waiting period, which is consistent with the proposed roles for the extensive semaphorin family.

Model 2: The effect of anti-NGF on DRG cells and cutaneous innervation

Embryonic anti-NGF treatment results in the death of 43% of small DRG cells due to trophic deprivation by E21. The consequence of this cell loss is the selective decrease in C-fibres innervating their targets. The surviving cells (A-fibres), innervate an enlarged target area due to the absence of competition from C-fibres.

The removal of NGF additionally prevents the decrease of NT3 and trkC levels in the peripheral target that normally accompanies the detection of NGF in the skin. The continued expression of NT3 and trkC beyond that required for survival, results in sub-epidermal terminal collateral sprouting. The sprouting allows increased access to target-derived factors for retrograde transport to the soma and potentially may be the stimulus for the hypertrophy of a small population of surviving neurons. The lack of NGF may in addition regulate factors such as semaphorins or laminins that render the epidermis non-permissive to all neuronal phenotypes.

In model 2, unknown factors include the stimulus for the downregulation of NT3 and trkC. This event is correlated with the upregulation of NGF, but its effect may not be direct. There is accumulating evidence that NT3 causes terminal sprouting and may also cause hypertrophy of cells but the small proportion of cells that displayed hypertrophy above controls in this study suggest these may be responding to some additional target-derived factor. The lack of epidermal innervation observed in this study and in several studies involving transgenic manipulation of neurotrophins and their receptors suggests that a particular neurotrophin is not responsible for inducing epidermal innervation but that neurotrophins regulate expression of molecules within the skin target that determines permissiveness to growth.

Reference List

Acheson A., Barker P. A., Alderson R. F., Miller F. D. and Murphy R. A. (1991) Detection of Brain-Derived Neurotrophic Factor-like Activity in Fibroblasts and Schwann Cells: Inhibition by Antibodoes to NGF. Neuron **7**, 265-275.

Adams J. C. and Watt F. M. (1993) Regulation of development and differentiation by the extracellular matrix. Development **117**, 1183-1198.

Adams R. H., Betz H. and Puschel A. W. (1996) A novel class of murine semaphorins with homology to thrombospondin is differentially expressed during early embryogenesis. Mech Dev **57**, 33-45.

Aigner L. and Caroni P. (1993) Depletion of 43-kD growth-associated protein in primary sensory neurons leads to diminished formation and spreading of growth cones. J Cell Biol **123**, 417-429.

Aigner L., Arber S., Kapfhammer J. P., Laux T., Schneider C., Botteri F., Brenner H. R. and Caroni P. (1995) Overexpression of the neural growth-associated protein GAP-43 induces nerve sprouting in the adult nervous system of transgenic mice. Cell **83**, 269-278.

Airaksinen M. S., Koltzenburg M., Lewin G. R., Masu Y., Helbig C., Wolf E., Brem G., Toyka K. V., Thoenen H. and Meyer M. (1996) Specific subtypes of cutaneous mechanoreceptors require neurotrophin-3 following peripheral target innervation. Neuron **16**, 287-295.

Albers K. M., Perrone T. N., Goodness T. P., Jones M. E., Green M. A. and Davis B. M. (1996) Cutaneous overexpression of NT-3 increases sensory and sympathetic neuron number and enhances touch dome and hair follicle innervation. J Cell Biol **134**, 487-497.

Albers K. M., Wright D. E. and Davis B. M. (1994) Overexpression of nerve growth factor in epidermis of transgenic mice causes hypertrophy of the peripheral nervous system. J Neurosci **14**, 1422-1432.

Aletta J. M., Shelanski M. L. and Greene L. A. (1989) Phosphorylation of the peripherin 58-kDa neuronal intermediate filament protein. Regulation by nerve growth factor and other agents. J Biol Chem **264**, 4619-4627.

Alexander K. A., Cimler B. M., Meier K. E. and Storm D. R. (1987) Regulation of calmodulin binding to P-57. A neurospecific calmodulin binding protein. J Biol Chem **262**, 6108-6113.

Alexander K. A., Wakim B. T., Doyle G. S., Walsh K. A. and Storm D. R. (1988) Identification and characterization of the calmodulin-binding domain of neuromodulin, a neurospecific calmodulin-binding protein. J Biol Chem **263**, 7544-7549.

Altman J. and Bayer S. A. (1982) Development of the cranial nerve ganglia and related nuclei in the rat. Adv Anat Embryol Cell Biol **74**, 1-90.

Altman J. and Bayer S. A. (1984) The development of the rat spinal cord. Adv Anat Embryol Cell Biol **85**, 1-166.

Amara S. G., Arriza J. L., Leff S. E., Swanson L. W., Evans R. M. and Rosenfeld M. G. (1985) Expression in brain of a messenger RNA encoding a novel neuropeptide homologous to calcitonin gene-related peptide. Science **229**, 1094-1097.

Ambalavanar R. and Morris R. (1992) The distribution of binding by isolectin I-B4 from Griffonia simplicifolia in the trigeminal ganglion and brainstem trigeminal nuclei in the rat. Neuroscience **47**, 421-429.

Ambalavanar R. and Morris R. (1993) An ultrastructural study of the binding of an alpha-D-galactose specific lectin from Griffonia simplicifolia to trigeminal ganglion neurons and the trigeminal nucleus caudalis in the rat. Neuroscience **52**, 699-709.

Anand P. (1995) Nerve growth factor regulates nociception in human health and disease. Brit J Anaesth **75**, 201-208.

Anderson K. D., Alderson R. F., Altar C. A., DiStephano P. S., Corcoran T. L., Lindsay R. M. and Wiegand S. J. (1995) Differential Distribution of Exogenous BDNF, NGF, and NT-3 in the Brain Corresponds to the Relative Abundance and Distribution of High-Affininty and Low-Affinity Neurotrophin Receptors. J Comp Neurol **357**, 296-317.

Andres K. H. (1961) Untersuchungen den Feinbau von spinal ganglion. Z. Zellforsch Mikrosk Anat. **55**, 1-48.

Andrews T. J. and Cowen T. (1994) Nerve growth factor enhances the dendritic arborization of sympathetic ganglion cells undergoing atrophy in aged rats. J Neurocytol **23**, 234-241.

Angulo A. W. (1951) A comparison of the growth and differentiation of the trigeminal ganglion with the cervical spinal ganglia in albino rat embryos. J. Comp. Neurol **95**, 53-71.

Anton E. S., Sandrock A. W. J. and Matthew W. D. (1994) Merosin promotes neurite growth and Schwann cell migration in vitro and nerve regeneration in vivo: evidence using an antibody to merosin, ARM-1. Dev Biol **164**, 133-146.

Averill S., McMahon S. B., Clary D. O., Reichardt L. F. and Priestly J. V. (1995) Immunocytochemical Localization of trkA receptors in Chemically Identified Subgroups of Adult Rat Sensory Neurons. Eur J Neurosci **7**, 1484-1494.

Baas P. W. and Black M. M. (1989) Compartmentation of alpha-tubulin in neurons: identification of a somatodendritic-specific variant of alpha-tubulin. Neuroscience **30**, 795-803.

Baetge E. E. and Hammang J. P. (1991) Neurite outgrowth in PC12 cells deficient in GAP-43. Neuron **6**, 21-30.

Bambrilla R., Schnapp A., Casagranada F., Labrador J. P., Bergemann A. D., Flannagan J. G., Pasqual E. and Klein R. (1995) Membrane-bound LERK2 ligand can signal through different Eph-related receptor tyrosine kinases. EMBO **14**, 3116-3126.

Barbacid M. (1994) The TRK Family of Neurotrophin Receptors. J Neurobiol **25**, (11):1386-1403.

Barbut D., Polak J. M. and Wall P. D. (1981) Substance P in the spinal cord dorsal horn decreases following peripheral nerve injury. Brain Research **205,** 289-298.

Barde Y. A., Edgar D. and Thoenen H. (1982) Purification of a new neurotrophic factor from mammalian brain. EMBO **1**, 549-553.

Barrett G. L. and Bartlett P. F. (1994) The p75 nerve growth factor receptor mediates survival or death depending on the stage of sensory neuron development. Proc Natl Acad Sci U S A **91**, 6501-6505.

Bartsch T., Habler H. J. and Janig W. (1996) Functional properties of postganglionic sympathetic neurones supplying the submandibular gland in the anaesthetized rat. Neurosci Lett **214**, 143-146.

Bartsch U. (1996) Myelination and axonal regeneration in the central nervous system of mice deficient in the myelin-associated glycoprotein. J Neurocytol **25**, 303-313.

Baumert M., Takei K., Hartinger J., Burger P. M., Fischer von Mollard G., Maycox P. R., De Camilli P. and Jahn R. (1990) P29: a novel tyrosine-phosphorylated membrane protein present in small clear vesicles of neurons and endocrine cells. J Cell Biol **110**, 1285-1294.

Beal J. A. (1982) The pre and postnatal development of flame-shaped hair-follicle primary afferents in the rat dorsal horn: a golgi study. Soc. Neurosci. Abstr **3,** 92.

Beal J. A., Knight D. S. and Nandi K. N. (1988) Structure and development of central arborizations of hair follicle primary afferents fibres. Anat Embryol **178**, 271-279.

Beaudet L., Cote F., Houle D. and Julien J. P. (1993) Different posttranscriptional controls for the human neurofilament light and heavy genes in transgenic mice. Brain Res Mol Brain Res **18**, 23-31.

Beauvais A., Erickson C. A., Goins T., Craig S. E., Humphries M. J., Thiery J. P. and Dufour S. (1995) Changes in the fibronectin-specific integrin expression pattern modify the migratory behavior of sarcoma S180 cells in vitro and in the embryonic environment. J Cell Biol **128**, 699-713.

Behar O., Golden J. A., Mashimo H., Schoen F. J. and Fishman M. C. (1996) Semaphorin III is needed for normal patterning and growth of nerves, bones and heart. Nature **383**, 525-528.

Bendotti C., Servadio A. and Samanin R. (1991) Distribution of GAP-43 mRNA in the brain stem of adult rats as evidenced by in situ hybridization: localization within monoaminergic neurons. J Neurosci **11**, 600-607.

Bennett D. L., Averill S., Clary D. O., Priestley J. V. and McMahon S. B. (1996b) Postnatal changes in the expression of the trkA high-affinity NGF receptor in primary sensory neurons. Eur J Neurosci **8**, 2204-2208.

Bennett D. L., Dmietrieva N., Priestley J. V., Clary D. and McMahon S. B. (1996c) trkA, CGRP and IB4 expression in retrogradely labelled cutaneous and visceral primary sensory neurones in the rat. Neurosci Lett **206**, 33-36.

Bennett D. L., French J., Priestley J. V. and McMahon S. B. (1996a) NGF but not NT-3 or BDNF prevents the A fiber sprouting into lamina II of the spinal cord that occurs following axotomy. Mol Cell Neurosci **8**, 211-220.

Benowitz L. I. and Routtenberg A. (1997) GAP-43: An intrinsic determinant of neuronal development and plasticity. Trends in Neurosciences **20**, 84-91.

Bergmann I., Priestly J. V., McMahon S. B., Brocker E.-B., Toyka K. V. and Koltzenburg M. (1997) Analysis of cutaneous sensory neurons in transgenic mice lacking the low affinity neurotrophin receptor p75. Eur. J. Neurosci. **9**, 18-28.

Beutler B. and van Huffel C. (1994) Unraveling function in the TNF ligand and receptor families. Science **264**, 667-668.

Bicknell H. R. J. and Beal J. A. (1984) Axonal and dendritic development of substantia gelatinosa neurons in the lumbosacral spinal cord of the rat. J Comp Neurol **226**, 508-522.

Birren S. J., Lo L. and Anderson D. J. (1993) Sympathetic neuroblasts undergo a developmental switch in trophic dependence. Development **119**, 597-610.

Boisseau S., Nedelec J., Poirier V., Rougon G. and Simonneau M. (1991) Analysis of high PSA N-CAM expression during mammalian spinal cord and peripheral nervous system development. Development **112**, 69-82.

Bonner P. H., Friedli A. F. and Baker R. S. (1994) Botulinum A toxin stimulates neurite branching in nerve-muscle cocultures. Brain Res Dev Brain Res **79**, 39-46.

Booth C. M. and Brown M. C. (1993) Expression of GAP-43 mRNA in mouse spinal cord following unilateral peripheral nerve damage: is there a contralateral effect? Eur J Neurosci **5**, 1663-1676.

Bossy B., Bossy Wetzel E. and Reichardt L. F. (1991) Characterization of the integrin alpha 8 subunit: a new integrin beta 1-associated subunit, which is prominently expressed on axons and on cells in contact with basal laminae in chick embryos. EMBO J **10**, 2375-2385.

Boudreau N., Sympson C. J., Werb Z. and Bissell M. J. (1995) Suppression of ICE and apoptosis in mammary epithelial cells by extracellular matrix. Science **267**, 891-893.

Brain S. D., Williams T. J., Tippins J. R., Morris H. R. and MacIntyre I. (1985) Calcitonin gene-related peptide is a potent vasodilator. Nature **313**, 54-56.

Bronner-Fraser M. (1986a) An antibody to a receptor for fibronectin and laminin perturbs cranial neural crest development in vivo. Dev Biol **117**, 528-536.

Bronner-Fraser M. (1986b) Analysis of the early stages of trunk neural crest migration in avian embryos using monoclonal antibody HNK-1. Dev Biol **115**, 44-55.

Bronner-Fraser M. (1993) Enviornmental influences on neural crest cell migration. J. Neurobiol **24**, 233-247.

Bronner-Fraser M. and Lallier T. (1988) A monoclonal antibody agaginst a laminin-heparan sulphate proteoglycan complex perturbs cranial neural-crest migration in vivo. J. Cell Biol. **106**, 1321-1330.

Bronner-Fraser M., Artinger M., Muschler J. and Horwitz A. F. (1992) Developmentally regulated expression of alpha 6 integrin in avian embryos. Development **115**, 197-211.

Brown D. G., Willington M. A., Findlay I. and Muggleton Harris A. L. (1992) Criteria that optimize the potential of murine embryonic stem cells for in vitro and in vivo developmental studies. In Vitro Cell Dev Biol **28A**, 773-778.

Bruses J. L., Oka S. and Rutishauser U. (1995) NCAM-associated polysialic acid on ciliary ganglion neurons is regulated by polysialytransferase levels and interaction with muscle. J Neurosci **15**, 8310-8319.

Buchman V. L. and Davies A. M. (1993) Different neurotrophins are expressed and act in a developmental sequence to promote the survival of embryonic sensory neurons. Development **118**, 989-1001.

Buck S. H., Helke C. J., Burcher E., Shults C. W. and O'Donohue T. L. (1986) Pharmacologic characterization and autoradiographic distribution of binding sites for iodinated tachykinins in the rat central nervous system. Peptides **7**, 1109-1120.

Buck S. H., Walsh J. H., Davis T. P., Brown M. R., Yamamura H. I. and Burks T. F. (1983) Characterization of the peptide and sensory neurotoxic effects of capsaicin in the guinea pig. J Neurosci **3**, 2064-2074.

Buj-Bello A., Pinon L. G. P. and Davies A. M. (1994) The Survival of NGF-Dependant but not BDNF-Dependant cranial sensory neurons is promoted by several different neurotrophins early in their development. Development **120**, 1573-1580.

Burden Gulley S. M. and Lemmon V. (1996) L1, N-cadherin, and laminin induce distinct distribution patterns of cytoskeletal elements in growth cones. Cell Motil Cytoskeleton **35**, 1-23.

Burgeson R. E., Chiquet M., Deutzmann R., Ekblom P., Engel J., Kleinman H., Martin G. R., Meneguzzi G., Paulsson M., Sanes J. and et al (1994) A new nomenclature for the laminins. Matrix Biol **14**, 209-211.

Cameron A. A., Leah J. D. and Snow P. J. (1988) The coexistence of neuropeptides in feline sensory neurons. Neurosci **27**, 969-979.

Carden M. J., Goldstein M. E., Bruce J., Cooper H. S. and Schlaepfer W. W. (1987) Studies of neurofilaments that accumulate in proximal axons of rats intoxicated with beta, beta'-iminodipropionitrile (IDPN). Neurochem Pathol **7**, 189-205.

Carroll S. L., Silos Santiago I., Frese S. E., Ruit K. G., Milbrandt J. and Snider W. D. (1992) Dorsal root ganglion neurons expressing trk are selectively sensitive to NGF deprivation in utero. Neuron **9**, 779-788.

Chao M. V. (1992a) Neurotrophin receptors: a window into neuronal differentiation. Neuron **9**, 583-593.

Chao M. V. (1992b) Growth factor signaling: where is the specificity? Cell **68**, 995-997.

Chao M. V., Battleman D. S. and Benedetti M. (1992) Receptors for nerve growth factor. Int Rev Cytol **137B**, 169-180.

Chao S., Benowitz L. I., Krainc D. and Irwin N. (1996) Use of a two-hybrid system to investigate molecular interactions of GAP-43. Molecular Brain Research **40**, 195-202.

Chapman E. R., Au D., Alexander K. A., Nicolson T. A. and Storm D. R. (1991) Characterization of the calmodulin binding domain of neuromodulin. Functional significance of serine 41 and phenylalanine 42. J Biol Chem **266**, 207-213.

Charnas L. R., Szaro B. G. and Gainer H. (1992) Identification and developmental expression of a novel low molecular weight neuronal intermediate filament protein expressed in Xenopus laevis. J Neurosci **12**, 3010-3024.

Cheng H. J., Nakamoto M., Bergemann A. D. and Flanagan J. G. (1995) Complementary gradients in expression and binding of ELF-1 and Mek4 in development of the topographic retinotectal projection map. Cell **82**, 371-381.

Chien C. L. and Liem R. K. (1994) Characterization of the mouse gene encoding the neuronal intermediate filament protein alpha-internexin. Gene **149**, 289-292.

Ching G. Y. and Liem R. K. (1993) Assembly of type IV neuronal intermediate filaments in nonneuronal cells in the absence of preexisting cytoplasmic intermediate filaments. J Cell Biol **122**, 1323-1335.

Ching Y. P., Averill S., Wilkin G. P., Wotherspoon G. and Priestley J. V. (1994) Serotonergic terminals express a growth associated protein (GAP-43) in the adult rat spinal cord. Neurosci Lett **167**, 67-72.

Chong M.-S., Fitzgerald M., Winter J., Hu-Tsai M., Emson P. C., Weise U. and Woolf C. J. (1992) GAP-43 mRNA in rat spinal cord and dorsal root ganglia neurons: developmental changes and re-expression following peripheral nerve injury. Eur J Neurosci **4**, 883-895.

Chong M.-S., Reynolds M. L., Irwin N., Coggeshall R. E., Emson P. C., Benowitz L. I. and Woolf C. J. (1994) GAP-43 expression in primary sensory neurons following central axotomy. J Neurosci **14**, 4375-4384.

Chung F., Wu L.-H., Vartanian M. A., Watling K., Guard S., Woodruff G. N. and Oxender D. L. (1994) The non-peptide tachykinin NK2 receptor antagonist SR 48968 interacts with human, but not rat, cloned tachykinin NK3 receptors. Biochem Biophys Res Comm **198**, 967-972.

Coggeshall R. E. (1980) Law of separation of function of the spinal roots. Physiol. Rev. **60**, 716-755.

Coggeshall R. E. (1992) A consideration of neural counting methods. TINS **15**, 9-114.

Coggeshall R. E., Jennings E. A. and Fitzgerald M. (1996) Evidence that large myelinated primary afferent fibers make synaptic contacts in lamina II of neonatal rats. Dev Brain Res **92**, 81-90.

Coggeshall R. E., Lekan H., Doubell T. P., Allchorne A. and Woolf C. J. (1997) A re-examination of adult primary sensory cell death after nerve lesions. Neurosci

Coggeshall R. E., Pover C. M. and Fitzgerald M. (1994) Dorsal root ganglion cell death and surviving cell numbers in relation to the development of sensory innervation in the hindlimb. Brain Res **82**, 193-212.

Coggeshall R. E., Reynolds M. L. and Woolf C. J. (1991) Distribution of the growth associated protein GAP-43 in the central processes of axotomized primary afferents in the adult rat spinal cord; presence of growth cone-like structures. Neurosci Lett **131**, 37-41.

Cohlberg J. A., Hajarian H., Tran T., Alipourjeddi P. and Noveen A. (1995) Neurofilament protein heterotetramers as assembly intermediates. J Biol Chem **270**, 9334-9339.

Colamarino S. A. and Tessier Lavigne M. (1995a) The axonal chemoattractant netrin-1 is also a chemorepellent for trochlear motor axons. Cell **81**, 621-629.

Colamarino S. A. and Tessier Lavigne M. (1995b) The role of the floor plate in axon guidance. Annu Rev Neurosci **18**, 497-529.

Collard J. F., Cote F. and Julien J. P. (1995) Defective axonal transport in a transgenic mouse model of amyotrophic lateral sclerosis. Nature **375**, 61-64.

Constantinou J., Reynolds M. L., Woolf C. J., Safieh-Garabedian B. and Fitzgerald M. (1994) Nerve Growth Factor Levels in Developing Rat Skin: Upregulation Following Skin Wounding. NeuroReport **5**, 2281-2284.

Cornbrooks C. J., Carey D. J., McDonald J. A., Timpl R. and Bunge R. P. (1983) In vivo and in vitro observations on laminin production by Schwann cells. Proc Natl Acad Sci U S A **80**, 3850-3854.

Couchman J. R., Austria M. R. and Woods A. (1990) Fibronectin-cell interactions. J Invest Dermatol **94**, 7S-14S.

Coucouvanis E. and Martin G. R. (1995) Signals for death and survival: a two-step mechanism for cavitation in the vertebrate embryo. Cell **83**, 279-287.

Crowley C., Spencer S. D., Nishimura M. C., Chen K. S., Pitts-Meek S., Armanini M. P., Ling L. H., McMahon S. B., Shelton D. L., Levinson A. D. and Phillips H. S. (1994) Mice Lacking Nerve Growth Factor Display Perinatal Loss of Sensory and Sympathetic Neurons Yet Develop Basal ForeBrain Cholinergic Neurons. Cell **76**, 1001-1011.

Cuello A. C., Del Fiacco M. and Paxinos G. (1978) The central and peripheral ends of the substance P-containing sensory neurones in the rat trigeminal system. Brain Res **152**, 499-500.

Culotti J. G. (1994) Axon guidance mechanisms in Caenorhabditis elegans. Curr Opin Genet Dev **4**, 587-595.

Culotti J. G. and Kolodkin A. L. (1996) Functions of netrins and semaphorins in axon guidance. Curr Opin Neurobiol **6**, 81-88.

Curtis R., Adryan K. M., Stark J. L., Park J. S., Compton D. L., Weskamp G., Huber L. J., Chao M. V., Jaenisch R., Lee K. F. and et alKFh (1995) Differential role of the low affinity neurotrophin receptor (p75) in retrograde axonal transport of the neurotrophins. Neuron **14**, 1201-1211.

Curtis R., Averill S., Priestley J. V. and Wilkin G. P. (1993a) The distribution of GAP-43 in normal rat spinal cord. J Neurocytol **22**, 39-50.

Curtis R., Green D., Lindsay R. M. and Wilkin G. P. (1993b) Up-regulation of GAP-43 and growth of axons in rat spinal cord after compression injury. J Neurocytol **22**, 51-64.

da Cunha A. and Vitkovic L. (1990) Regulation of immunoreactive GAP-43 expression in rat cortical macroglia is cell type specific. J Cell Biol **111**, 209-215.

Dahl D., Bignami A., Bich N. T. and Chi N. H. (1981) Immunohistochemical localization of the 150K neurofilament protein in the rat and the rabbit. J Comp Neurol **195**, 659-666.

Dahl D., Labkovsky B. and Bignami A. (1988) Neurofilament phosphorylation in axons and perikarya: immunofluorescence study of the rat spinal cord and dorsal root ganglia with monoclonal antibodies. J Comp Neurol **271**, 445-450.

Dalsgaard C. J. (1988) The sensory system. In Handbook of chemical neuroanatomy vol. 6. The peripheral nervous system. (Bjorklund, A, Hokfelt, T and Owman, C) Elsevier, Amsterdam.

Dalsgaard C. J., Rydh M. and Haegerstrand A. (1989) Cutaneous innervation in man visualized with protein gene product 9.5 (PGP 9.5) antibodies. Histochemistry **92**, 385-390.

Dani J. W., Armstrong D. M. and Benowitz L. I. (1991) Mapping the development of the rat brain by GAP-43 immunocytochemistry. Neuroscience **40**, 277-287.

Davies A. M. (1992) Cell death and the trophic requirements of developing sensory neurons. In Sensory neurons. Diversity, development and plasticity, (Scott, S.A.). 194-214. Oxford University Press, Oxford.

Davies A. M. and Lumsden A. (1990) Ontogeny of the somatosensory system: origins and early development of primary sensory neurons. Ann Rev Neurosci **13**, 61-73.

Davies A. M. and Lumsden A. G. (1986) Fasciculation in the early mouse trigeminal nerve is not ordered in relation to the emerging pattern of whisker follicles. J Comp Neurol **253**, 13-24.

Davies A. M., Lee K. and Jaenisch R. (1993) p75-Deficient Trigeminal Sensory neurons Have an Altered Response to NGF but not to Other Neurotrophins. Neuron **11**, 565-574.

Davies A. M., Minichiello L. and Klein R. (1995) Developmental changes in NT-3 signalling via trk A and trk B in embryonic neurons. EMBO J **14**, 4482-4489.

Davies A. M., Thoenen H. and Barde Y. A. (1986a) Different factors from the central nervous system and periphery regulate the survival of sensory neurones. Nature **319**, 497-499.

Davies A. M., Thoenen H. and Barde Y. A. (1986b) The response of chick sensory neurons to brain-derived neurotrophic factor. J Neurosci **6**, 1897-1904.

Davis B. M., Albers K. M., Seroogy K. B. and Katz D. M. (1994) Overexpression of nerve growth factor in transgenic mice induces novel sympathetic projections to primary sensory neurons. Journal of Comparative Neurology **349**, 464-474.

Davis B. M., Lewin G. R., Mendell L. M., Jones M. E. and Albers K. M. (1993) Altered expression of nerve growth factor in the skin of transgenic mice leads to profound changes in response to mechanical stimuli. Neurosci **56**, 789-795.

Davis B. M., Wang H. S., Albers K. M., Carlson S. L., Goodness T. P. and McKinnon D. (1996) Effects of NGF overexpression on anatomical and physiological properties of sympathetic postganglionic neurons. Brain Research **724**, 47-54.

Davis J. Q. and Bennett V. (1994) Ankyrin binding activity shared by the neurofascin/L1/NrCAM family of nervous system cell adhesion molecules. J Biol Chem **269**, 27163-27166.

Debus E., Flugge G., Weber K. and Osborn M. (1982) A monoclonal antibody specific for the 200 K polypeptide of the neurofilament triplet. EMBO J **1**, 41-45.

Dechant G., Biffo S., Okasawa H., Kolbeck R., Pottgiesser J. and Barde Y.-A. (1993) Expression and binding characteristics of the BDNF receptor chick trkB. Development **119** 545-558.

Deckworth T. L., Elliott J. L., Knudson C. M., Johnson E. M. J., Snider W. D. and Korsmeyer S. J. (1996) BAX is required for neuronal death after trophic factor deprivation and during development. Neuron **17**, 401-411.

Deller T., Martinez A., Nitsch R. and Frotscher M. (1996) A novel entorhinal projection to the rat dentate gyrus: direct innervation of proximal dendrites and cell bodies of granule cells and GABAergic neurons. J Neurosci **16**, 3322-3333.

Deloulme J. C., Janet T., Au D., Storm D. R., Sensenbrenner M. and Baudier J. (1990) Neuromodulin (GAP43): a neuronal protein kinase C substrate is also present in 0-2A glial cell lineage. Characterization of neuromodulin in secondary cultures of oligodendrocytes and comparison with the neuronal antigen. J Cell Biol **111**, 1559-1569.

Denis-Donini S., Chini B. and Vitadello M. (1993) Developmentally regulated expression of CGRP in the mouse olfactory pathway. Eur J Neurosci **5**, 648-656.

Dent E. W. and Meiri K. F. (1992) GAP-43 phosphorylation is dynamically regulated in individual growth cones. J Neurobiol **23**, 1037-1053.

Devor M. and Claman D. (1980) Mapping and plasticity of acid phosphatase afferents in the rat dorsal horn. Brain Res **190**, 17-28.

DiCicco-Bloom E., Friedman W. J. and Black I. B. (1993) NT-3 stimulates sympathetic neuroblast proliferation by promoting precursor survival. Neuron **11**, 1101-1111.

Djabali K., Portier M. M., Gros F., Blobel G. and Georgatos S. D. (1991) Network antibodies identify nuclear lamin B as a physiological attachment site for peripherin intermediate filaments. Cell **64**, 109-121.

Dodd J. and Jessell T. M. (1986) Cell surface glycoconjugates and carbohydrate-binding proteins: possible recognition signals in sensory neurone development. J Exp Biol **124**, 225-238.

Dodd J. and Schuchardt A. (1995) Axon guidance: a compelling case for repelling growth cones. Cell **81**, 471-474.

Dodd J., Solter D. and Jessell T. M. (1984) Monoclonal antibodies against carbohydrate differentiation antigens identify subsets of primary sensory neurones. Nature **311**, 469-472.

Dong D. L., Xu Z. S., Chevrier M. R., Cotter R. J., Cleveland D. W. and Hart G. W. (1993) Glycosylation of mammalian neurofilaments. Localization of multiple O-linked N-acetylglucosamine moieties on neurofilament polypeptides L and M. J Biol Chem **268**, 16679-16687.

Doughty S. E., Atkinson M. E. and Shehab S. A. (1991) A quantitative study of neuropeptide immunoreactive cell bodies of primary afferent sensory neurons following rat sciatic nerve peripheral axotomy. Regul Pept **35**, 59-72.

Drescher U., Kremoser C., Handwerker C., Loschinger J., Noda M. and Bonhoeffer F. (1995) In vitro guidance of retinal ganglion cell axons by RAGS, a 25 kDa tectal protein related to ligands for Eph receptor tyrosine kinases. Cell **82**, 359-370.

Duce I. R. and Keen P. (1977) The formation of free axonal sprouts from a dorsal root ganglion-nerve preparation maintained in organotypic culture, and the effects of demecolcine. Cell Tissue Res **180**, 111-121.

Duggan A. W., Hendry I. A., Morton C. R., Hutchison W. D. and Zhao Z. Q. (1988) Cutaneous stimuli releasing immunoreactive substance P in the dorsal horn of the cat. Brain Res **451**, 261-273.

Duprey P. and Paulin D. (1995) What can be learned from intermediate filament gene regulation in the mouse embryo. Int J Dev Biol **39**, 443-457.

Edelman G. M. and Crossin K. L. (1991) Cell adhesion molecules: implications for a molecular histology. Annu Rev Biochem **60**, 155-190.

Ehlers M. D., Kaplan D. R., Price D. L. and Koliatsos V. E. (1995) NGF-stimulated Retrograde Transport of trkA in the Mammalian Nervous System. J Cell Biol **130**, 149-156.

Engvall E., Davis G. E., Dickerson K., Ruoslahti E., Varon S. and Manthorpe M. (1986) Mapping of domains in human laminin using monoclonal antibodies: localization of the neurite-promoting site. J Cell Biol **103**, 2457-2465.

Ernfors P., Lee K. and Jaenisch R. (1994) Target derived and putative local actions of neurotrophins in the peripheral nervous system. Prog Brain Res **103**, 43-54.

Ernfors P., Merlio J. and Persson H. (1992) Cells Expressing mRNA for Neurotrophins and their Receptors During Embryonic Rat Development. Eur J Neurosci **4**, 1140-1158.

Ernfors P., Merlio M. P. and Persson H. (199) Developmentally regulated expression of HDNF/NT-3 mRNA in rat spinal cord motoneurons and expression of BDNF mRNA in embryonic dorsal root ganglion. Eur. J. Neurosci **3**, 953-961.

Escurat M., Djabali K., Gumpel M., Gros F. and Portier M. M. (1990) Differential expression of two neuronal intermediate-filament proteins, peripherin and the low-molecular-mass neurofilament protein (NF-L), during the development of the rat. J Neurosci **10**, 764-784.

Fan J. and Raper J. A. (1995) Localized collapsing cues can steer growth cones without inducing their full collapse. Neuron **14**, 263-274.

Farinas I., Jones K. R., Backus C., Wang W.-Y. and Reichardt L. F. (1994) Severe sensory and sympathetic deficits in mice lacking neurotrophin-3. Nature **369**, 658-661.

Ferri G. L., Sabani A., Abelli L., Polak J. M., Dahl D. and Portier M. M. (1990) Neuronal intermediate filaments in rat dorsal root ganglia: differential distribution of peripherin and neurofilament protein immunoreactivity and effect of capsaicin. Brain Res **515**, 331-335.

Fichard A., Verna J. M. and Saxod R. (1990) Effects of tunicamycin on the avoidance reaction of epidermis by sensory neurites in co-cultures. Int J Dev Neurosci **8**, 245-254.

Fields R. D. and Itoh K. (1996) Neural cell adhesion molecules in activity-dependent development and synaptic plasticity. TINS **19,** 473-475.

Fields R. D., Neale E. A. and Nelson P. G. (1990) Effects of patterned electrical activity on neurite outgrowth from mouse sensory neurons. J Neurosci **10**, 2950-2964.

Fitzgerald M. (1985a) The sprouting of saphenous nerve terminals in the spinal cord following early postnatal sciatic nerve section in the rat. J Comp Neurol **240**, 407-413.

Fitzgerald M. (1985b) The post-natal development of cutaneous afferent fibre input and receptive field organization in the rat dorsal horn. J Physiol Lond **364**, 1-18.

Fitzgerald M. (1987a) Cutaneous primary afferent properties in the hindlimb of the neonatal rat. J Physiol (Lond) **383**, 79-92.

Fitzgerald M. (1987b) Spontaneous and evoked activity of foetal primary afferents 'in vivo'. Nature **326**, 603-605.

Fitzgerald M. (1987c) The prenatal growth of fine diameter afferents into the rat spinal cord - a transganglionic study. J Comp Neurol **261**, 98-104.

Fitzgerald M. (1991) A physiological study of the prenatal development of cutaneous sensory inputs to dorsal horn cells in the rat. J Physiol Lond **432**, 473-482.

Fitzgerald M. and Fulton B. P. (1992) The physiological properties of developing sensory neurons. In Sensory Neurons. Diversity, Development, and Plasticity (Scott S. A.). 287-309. Oxford University Press, Oxford.

Fitzgerald M. and Shortland P. (1988) The effect of neonatal peripheral nerve section on the somadendritic growth of sensory projection cells in the rat spinal cord. Brain Res **470**, 129-136.

Fitzgerald M. and Swett J. E. (1983) The termination pattern of sciatic nerve afferents in the substantia gelatinosa of neonatal rats. Neurosci Lett **43**, 149-154.

Fitzgerald M. J. T. (1961) Developmental Changes in Epidermal Innervation. J. Anat. Lon **95**, 495-514.

Fitzgerald M., Butcher T. and Shortland P. (1994) Developmental changes in the laminar termination of A fibre cutaneous sensory afferents in the rat spinal cord dorsal horn. J Comp Neurol **348**, 225-233.

Fitzgerald M., Kwiat G. C., Middleton J. and Pini A. (1993) Ventral spinal cord inhibition of neurite outgrowth from embryonic rat dorsal root ganglia. Development **117**, 1377-1384.

Fitzgerald M., Reynolds M. L. and Benowitz L. I. (1991) GAP-43 expression in the developing rat lumbar spinal cord. Neuroscience **41**, 187-199.

Fitzgerald M., Wall P. D., Goedert M. and Emson P. C. (1985) Nerve growth factor counteracts the neurophysiological and neurochemical effects of chronic sciatic nerve section. Brain Res **332**, 131-141.

Fitzgerald M., Woolf C. J., Gibson S. J. and Mallaburn P. S. (1984) Alterations in the structure, function, and chemistry of C fibers following local application of vinblastine to the sciatic nerve of the rat. J Neurosci **4**, 430-441.

Fliegner K. H., Ching G. Y. and Liem R. K. (1990) The predicted amino acid sequence of alpha-internexin is that of a novel neuronal intermediate filament protein. EMBO J **9**, 749-755.

Fliegner K. H., Kaplan M. P., Wood T. L., Pintar J. E. and Liem R. K. (1994) Expression of the gene for the neuronal intermediate filament protein alpha-internexin coincides with the onset of neuronal differentiation in the developing rat nervous system. J Comp Neurol **342**, 161-173.

Fontaine J., Grivegnee A. R. and Robberecht P. (1986) Evidence against VIP as the inhibitory transmitter in non-adrenergic, non-cholinergic nerves supplying the longitudinal muscle of the mouse colon. Br J Pharmacol **89**, 599-602.

Friede R. L. and Samorajski T. (1970) Axon caliber related to neurofilaments and microtubules in sciatic nerve fibers of rats and mice. Anat Rec **167**, 379-387.

Fulton B. P. (1987) Postnatal changes in conduction velocity and soma action potential parameters of dorsal root ganglion neurons. Neurosci Lett **73**, 125-130.

Fundin B. (1997) The mystacial pad innervation. PhD Thesis **Uppsala University, Sweeden,**

Gabella G. (1984) Size of neurons and glial cells in the intramural ganglia of the hypertrophic intestine of the guinea-pig. J. Neurocytol **13**, 73-84.

Gabella G. and Uvelius B. (1993) Effect of decentralization or contralateral ganglionectomy on obstruction-induced hypertrophy of rat urinary bladder muscle and pelvic ganglion. J. Neurocytol **22**, 827-834.

Gabella G., Berggren T. and Uvelius B. (1992) Hypertrophy and reversal of hypertrophy in rat pelvic ganglion neurons. J. Neurocytol **21**, 649-662.

Gaese F., Kolbeck R. and Barde Y.-A. (1994) Sensory ganglia require neurotrophin-3 early in development. Development **120**, 1613-1619.

Gale N. W., Flenniken A., Compton D. C., Jenkins N., Copeland N. G., Gilbert D. J., Davis S., Wilkinson D. G. and Yancopoulos G. D. (1996) Elk-L3, a novel transmembrane ligand for the Eph family of receptor tyrosine kinases, expressed in embryonic floor plate, roof plate and hindbrain segments. Oncogene **13**, 1343-1352.

Gamse R. and Saria A. (1985) The spinal cord contains multiple factors causing plasma protein extravasation in the skin. Eur J Pharmacol **113**, 363-371.

Gardner E. E., Rueger D. C. and Dahl D. (1984) The relationship of bovine intermediate filament proteins. A comparative analysis of glial fibrillary acidic protein, desmin and the neurofilament 70 kDa protein. Biochim Biophys Acta **790**, 141-147.

Garrity P. A. and Zipursky S. L. (1995) Neuronal target recognition. Cell **83**, 177-185.

Georgatos S. D. and Blobel G. (1987) Lamin B constitutes an intermediate filament attachment site at the nuclear envelope. J Cell Biol **105**, 117-125.

Georgatos S. D., Weber K., Geisler N. and Blobel G. (1987) Binding of two desmin derivatives to the plasma membrane and the nuclear envelope of avian erythrocytes: evidence for a conserved site-specificity in intermediate filament-membrane interactions. Proc Natl Acad Sci U S A **84**, 6780-6784.

Gibbins I. L., Furness J. B. and Costa M. (1987a) Pathway-specific patterns of the co-existence of substance P, calcitonin gene-related peptide, cholecystokinin and dynorphin in neurons of the dorsal root ganglia of the guinea-pig. Cell Tissue Res **248**, 417-437.

Gibbins I. L., Wattchow D. and Coventry B. (1987b) Two immunohistochemically identified populations of calcitonin gene-related peptide (CGRP)-immunoreactive axons in human skin. Brain Res **414**, 143-148.

Gibson S. J., Polak J. M., Bloom S. R., Sabate I. M., Mulderry P. M., Ghatei M. A., McGregor G. P., Morrison J. F., Kelly J. S., Evans R. M. and et al (1984) Calcitonin gene-related peptide immunoreactivity in the spinal cord of man and of eight other species. J Neurosci **4**, 3101-3111.

Gibson S. J., Polak J. M., Giaid A., Hamid Q. A., Kar S., Jones P. M., Denny P., Legon S., Amara S. G., Craig R. K. and et al (1988) Calcitonin gene-related peptide messenger RNA is expressed in sensory neurones of the dorsal root ganglia and also in spinal motoneurones in man and rat. Neurosci Lett **91**, 283-288.

Glicksman M. A. and Willard M. (1985) Differential expression of the three neurofilament polypeptides. Ann N Y Acad Sci **455**, 479-491.

Glicksman M. A., Soppet D. and Willard M. B. (1987) Posttranslational modification of neurofilament polypeptides in rabbit retina. J Neurobiol **18**, 167-196.

Goedert M., Otten U., Hunt S. P., Bond A., Chapman D., Schlumpf M. and Lichtensteiger W. (1984) Biochemical and anatomical effects of antibodies against nerve growth factor on developing rat sensory ganglia. Proc Natl Acad Sci USA **81**, 1580-1584.

Goedert M., Stoeckel K. and Otten U. (1981) Biological Importance of the Retrograde Axonal Transport of Nerve Growth Factor in Sensory Neurons. Proc Natl Acad Sci USA **78**, (9):5895-5898.

Goldstein M. E., Grant P., House S. B., Henken D. B. and Gainer H. (1996) Developmental regulation of two distinct neuronal phenotypes in rat dorsal root ganglia. Neuroscience **71**, 243-258.

Goldstein M. E., House S. B. and Gainer H. (1991) NF-L and peripherin immunoreactivities define distinct classes of rat sensory ganglion cells. J Neurosci Res **30**, 92-104.

Goldstein M. E., Weiss S. R., Lazzarini R. A., Shneidman P. S., Lees J. F. and Schlaepfer W. W. (1988) mRNA levels of all three neurofilament proteins decline following nerve transection. Brain Res **427**, 287-291.

Gorham J. D., Baker H., Kegler D. and Ziff E. B. (1990) The expression of the neuronal intermediate filament protein peripherin in the rat embryo. Brain Res Dev Brain Res **57**, 235-248.

Gorin P. D. and Johnson E. M. (1979) Experimental autoimmune model of nerve growth factor deprivation: effects on developing peripheral sympathetic and sensory neurons. PNAS **76**, 5382-5386.

Gorin P. D. and Johnson E. M. (1980) Effects of long-term nerve growth factor deprivation on the nervous system of the adult rat: an experimental autoimmune approach. In *198* (ed pp. 27-42.

Goshima Y., Nakamura F., Strittmatter P. and Strittmatter S. M. (1995) Collapsin-induced growth cone collapse mediated by an intracellular protein related to UNC-33. Nature **376**, 509-514.

Goslin K. and Banker G. A. (1989) Experimental observations on the development of polarity by hippocanpal neurones in culture. J. Cell Biol. **188**, 1507-1516.

Goslin K., Schreyer D. J., Skene J. H. and Banker G. (1988) Development of neuronal polarity: GAP-43 distinguishes axonal from dendritic growth cones. Nature **336**, 672-674.

Greene L. A. (1989) A new neuronal intermediate filament protein. Trends Neurosci **12**, 228-230.

Gulbenkian S., Merighi A., Wharton J., Varndell I. M. and Polak J. M. (1986) Ultrastructural evidence for the coexistence of calcitonin gene-related peptide and substance P in secretory vesicles of peripheral nerves in the guinea pig. J Neurocytol **15**, 535-542.

Gulbenkian S., Wharton J. and Polak J. M. (1987) The visualization of cardiovascular innervation in the guinea-pig using an anti-serum to protein-gene-product 9.5. J Auton Nerv Syst **19**, 581-593.

Gumbiner B. M. (1996) Cell adhesion: the molecular basis of tissue architecture and morphogenesis. Cell **84**, 345-357.

Guthrie S. and Pini A. (1995) Chemorepulsion of developing motor axons by the floor plate. Neuron **14**, 1117-1130.

Habuchi H., Kimata K. and Suzuki S. (1986) Changes in proteoglycan composition during development of rat skin. The occurrence in fetal skin of a chondroitin sulfate proteoglycan with high turnover rate. J Biol Chem **261**, 1031-1040.

Hall A. K., Ai X., Hickman G. E., MacPhedran S. E., Nduaguba C. O. and Robertson C. P. (1997) The generation of neuronal heterogeneity in a rat sesnory ganglion. J. Neurosci **17**, 2775-2784.

Hamburger V. and Levi-Montalcini R. (1949) Proliferation, differentiation and degeneration in the spinal ganglia of the chick embryo under normal and experimental conditions. J Exp Zool **111**, 457-502.

Hammond D. L. and Ruda M. A. (1989) Developmental alterations in thermal nociceptive threshold and the distribution of immunoreactive calcitonin gene-related peptide and substance P after neonatal administration of capsaicin in the rat. Neurosci Lett **97**, 57-62.

Hammond D. L. and Ruda M. A. (1991) Developmental alterations in nociceptive threshold, immunoreactive calcitonin gene-related peptide and substance P, and fluoride-resistant acid phosphatase in neonatally capsaicin-treated rats. J Comp Neurol **312**, 436-450.

Han S., Blumenfeld O. O. and Seifter S. (1992) Specific identification of collagens and their fragments by clostridial and anti-collagenase antibody. Anal Biochem **201**, 336-342.

Hares K. A. and Foster G. A. (1991) Immunohistochemical analysis of the ontogeny of calcitonin gene-related peptide-like immunoreactivity in the rat central nervous system. J Chem Neuroanat **4**, 187-203.

Harris R., Sabatelli L. M. and Seeger M. A. (1996) Guidance cues at the Drosophila CNS midline: identification and characterization of two Drosophila Netrin/UNC-6 homologs. Neuron **17**, 217-228.

Hartschuh W., Weihe E., Buchler M., Helmstaedter V., Feurle G. E. and Forssmann W. G. (1979) Met enkephalin-like immunoreactivity in Merkel cells. Cell Tissue Res **201**, 343-348.

Hedgecock E. M., Culotti J. G. and Hall D. H. (1990) The unc-5, unc-6, and unc-40 genes guide circumferential migrations of pioneer axons and mesodermal cells on the epidermis in C. elegans. Neuron **4**, 61-85.

Henderson C. E. (1996) Programmed cell death in the developing nervous system. Neuron **17**, 579-585.

Henderson C. E., Camu W., Mettling C., Gouin A., Poulsen K., Karihaloo M., Rullamas J., Evans T., McMahon S. B., Armanini M. P., Berkemeier L., Phillips H. S. and Rosenthal A. (1993) Neurotrophins Promote Motor neuron Survival and are Present in Embryonic Limb Bud. Nature **363**, 266-270.

Hennings H. and Holbrook K. A. (1983c) Calcium regulation of cell-cell contact and differentiation of epidermal cells in culture. An ultrastructural study. Exp Cell Res **143**, 127-142.

Hennings H., Holbrook K. A. and Yuspa S. H. (1983a) Factors influencing calcium-induced terminal differentiation in cultured mouse epidermal cells. J Cell Physiol **116**, 265-281.

Hennings H., Holbrook K. A. and Yuspa S. H. (1983b) Potassium mediation of calcium-induced terminal differentiation of epidermal cells in culture. J Invest Dermatol **81**, 50-55.

Hens J. J., De Wit M., Boomsma F., Mercken M., Oestreicher A. B., Gispen W. H. and De Graan P. N. (1995) N-terminal-specific anti-B-50 (GAP-43) antibodies inhibit Ca(2+)-induced noradrenaline release, B-50 phosphorylation and dephosphorylation, and calmodulin binding. J Neurochem **64**, 1127-1136.

Heumann R., Korsching S., Scott J. and Thoenen H. (1984) Relationship between levels of nerve growth factor (NGF) and its messenger RNA in sympathetic ganglia and peripheral target tissues. EMBO J **3**, 3183-3189.

Himes B. T. and Tessler A. (1989) Death of some dorsal root ganglion neurons and plasticity of others following sciatic nerve section in adult and neonatal rats. J Comp Neurol **284**, 215-230.

Hirai H., Maru Y., Hagiwara K., Nishida J. and Takaku F. (1987) A novel putative tyrosine kinase receptor encoded by the eph gene. Science **238**, 1717-1720.

Hisanaga S. and Hirokawa N. (1988) Structure of the peripheral domains of neurofilaments revealed by low angle rotary shadowing. J Mol Biol **202**, 297-305.

Ho C. L., Chin S. S., Carnevale K. and Liem R. K. (1995a) Translation initiation and assembly of peripherin in cultured cells. Eur J Cell Biol **68**, 103-112.

Ho W. H., Armanini M. P., Nuijens A., Phillips H. S. and Osheroff P. L. (1995b) Sensory and motor neuron-derived factor. A novel heregulin variant highly expressed in sensory and motor neurons. J Biol Chem **270**, 14523-14532.

Hoffman P. N. and Lasek R. J. (1975) The slow component of axonal transport. Identification of major structural polypeptides of the axon and their generality among mammalian neurons. J Cell Biol **66**, 351-366.

Hoffman P. N. and Lasek R. J. (1980) Axonal transport of the cytoskeleton in regenerating motor neurons: constancy and change. Brain Res **202**, 317-333.

Hoffman P. N., Cleveland D. W., Griffin J. W., Landes P. W., Cowan N. J. and Price D. L. (1987) Neurofilament gene expression: a major determinant of axonal caliber. Proc Natl Acad Sci U S A **84**, 3472-3476.

Hoffman P. N., Griffin J. W. and Price D. L. (1984) Control of axonal caliber by neurofilament transport. J Cell Biol **99**, 705-714.

Hoffman P. N., Lasek R. J., Griffin J. W. and Price D. L. (1983) Slowing of the axonal transport of neurofilament proteins during development. J Neurosci **3**, 1694-1700.

Hoffman P. N., Thompson G. W., Griffin J. W. and Price D. L. (1985) Changes in neurofilament transport coincide temporally with alterations in the caliber of axons in regenerating motor fibers. J Cell Biol **101**, 1332-1340.

Hoheisel U., Mense S. and Scherotzke R. (1994) Calcitonin gene-related peptide-immunoreactivity in functionally identified primary afferent neurones in the rat. Anat Embryol Berl **189**, 41-49.

Hökfelt T., Elde R., Johansson O., Luft r., Nilsson G. and Arimura A. (1976) Immunohistochemical evidence for separate populations of somatostatin-containing and substance P-containing primary afferent neurons in the rat. Neuroscience **1**, 131-136.

Hökfelt T., Kellerth J. O., Nilsson G. and Pernow B. (1975a) Experimental immunohistochemical studies on the localization and distribution of substance P in cat primary sensory neurons. Brain Res **100**, 235-252.

Hökfelt T., Kellerth J. O., Nilsson G. and Pernow B. (1975b) Substance P: localization in the central nervous system and in some primary sensory neurons. Science **190**, 889-890.

Hökfelt T., Wiesenfeld Hallin Z., Villar M. and Melander T. (1987) Increase of galanin-like immunoreactivity in rat dorsal root ganglion cells after peripheral axotomy. Neurosci Lett **83**, 217-220.

Hokfelt T., Zhang X. and Wiesenfeld-Hallin Z. (1994) Messenger plasticity in primary sensory neurons following axotomy and its functional implications. Trends in Neurosciences **17**, 22-30.

Holford L. C., Case P. and Lawson S. N. (1994) Substance P, neurofilament, peripherin and SSEA4 immunocytochemistry of human dorsal root ganglion neurons obtained from post-mortem tissue: a quantitative morphometric analysis. J Neurocytol **23**, 577-589.

Hory-Lee R., Russell M., Lindsay R. M. and Frank E. (1993) Neurotrophin 3 supports the survival of developing muscle sensory neurons in culture. PNAS **90**, 2613-2617.

Hou X. E. and Dahlstrom A. (1995) Effects of decentralization on the levels of GAP-43 and p38 (synaptophysin) in sympathetic adrenergic neurons: a semi-quantitative study using immunofluorescence and confocal laser scanning microscopy. Brain Res **679**, 49-63.

Hsiao L. L., Engvall E., Peltonen J. and Uitto J. (1993) Expression of laminin isoforms by peripheral nerve-derived connective tissue cells in culture. Comparison with epitope distribution in normal human nerve and neural tumors in vivo. Lab Invest **68**, 100-108.

Hulsebosch C. E., Coggeshall R. E. and Chung K. (1986) Numbers of rat dorsal root axons and ganglion cells during postnatal development. Brain Res **391**, 105-113.

Hunt S. P. and Rossi J. (1985) Peptide- and non-peptide-containing unmyelinated primary afferents: the parallel processing of nociceptive information. Philos Trans R Soc Lond B Biol Sci **308**, 283-289.

Igarashi M., Strittmatter S. M., Vartanian T. and Fishman M. C. (1993) Mediation by G proteins of signals that cause collapse of growth cones. Science **259**, 77-79.

Iivanainen A., Vuolteenaho R., Sainio K., Eddy R., Shows T. B., Sariola H. and Tryggvason K. (1995) The human laminin beta 2 chain (S-laminin): structure, expression in fetal tissues and chromosomal assignment of the LAMB2 gene. Matrix Biol **14**, 489-497.

Ikenaka K., Nakahira K., Takayama C., Wada K., Hatanaka H. and Mikoshiba K. (1990) Nerve growth factor rapidly induces expression of the 68-kDa neurofilament gene by posttranscriptional modification in PC12h-R cells. J Biol Chem **265**, 19782-19785.

Inaishi Y., Kashihara Y., Sakaguchi M., Nawa H. and Kuno M. (1992) Cooperative regulation of calcitonin gene-related peptide levels in rat sensory neurons via their central and peripheral processes. J Neurosci **12**, 518-524.

Ip N. Y., Stitt T. N., Tapley P., Klein R., Glass D. J., Fandl J., Greene L. A., Barbacid M. and Yancopoulos G. D. (1993) Similarities and Differences in the Way Neurotrophins Interact with the Trk Receptors in Neuronal and Nonneuronal Cells. Neuron **10**, 137-149.

Ishii N., Wadsworth W. G., Stern B. D., Culotti J. G. and Hedgecock E. M. (1992) UNC-6, a laminin-related protein, guides cell and pioneer axon migrations in C. elegans. Neuron **9**, 873-881.

Itoh K., Stevens B., Schachner M. and Fields R. D. (1995) Regulated expression of the neural cell adhesion molecule L1 by specific patterns of neural impulses. Science **270**, 1369-1372.

Jacobson R. D., Virag I. and Skene J. H. (1986) A protein associated with axon growth, GAP-43, is widely distributed and developmentally regulated in rat CNS. J Neurosci **6**, 1843-1855.

Jahoda C. A. B., Mauger A. and Sengel P. (1987) Histochemical localisation of skin glycosaminoglycans. Roux's Arch. Dev. Biol. **196**, 303-315.

Jhaveri S., Erzurumlu R. S., Laywell E. D., Steindler D. A., Albers K. M., Davis K. and BMvis (1996) Excess nerve growth factor in the periphery does not obscure development of whisker-related patterns in the rodent brain. Journal of Comparative Neurology **374**, 41-5I.

Johnson E. M. J., Gorin P. D., Brandeis L. D. and Pearson J. (1980) Dorsal root ganglion neurones are destroyed by exposure in utero to maternal antibody to nerve growth factor. Science **210**, 916-918.

Jolles J., Zwiers H., van Dongen C. J., Schotman P., Wirtz K. W. and Gispen W. H. (1980) Modulation of brain polyphosphoinositide metabolism by ACTH-sensitive protein phosphorylation. Nature **286**, 623-625.

Jones K. R., Farinas I., Backus C. and Reichardt L. R. (1994) Targeted disruption of the BDNF gene perturbs brain and sensory neuron development but not motor neuron development. Cell **76**, 989-999.

Jones M. A. and Marfurt C. F. (1991) Calcitonin gene-related peptide and corneal innervation: a developmental study in the rat. J Comp Neurol **313**, 132-150.

Ju G., Hokfelt T., Brodin E., Fahrenkrug J., Fischer J. A., Frey P., Elde R. P. and Brown J. C. (1987) Primary sensory neurons of the rat showing calcitonin gene-related peptide immunoreactivity and their relation to substance P-, somatostatin-, galanin-, vasoactive intestinal polypeptide- and cholecystokinin-immunoreactive ganglion cells. Cell Tissue Res **247**, 417-431.

Julien J. P. and Mushynski W. E. (1983) The distribution of phosphorylation sites among identified proteolytic fragments of mammalian neurofilaments. J Biol Chem **258**, 4019-4025.

Julien J. P., Cote F., Beaudet L., Sidky M., Flavell D., Grosveld F. and Mushynski W. (1988) Sequence and structure of the mouse gene coding for the largest neurofilament subunit. Gene **68**, 307-314.

Kai-Kai M. A., Anderton B. H. and Keen P. (1986) A quantitative analysis of the interrelationships between subpopulations of rat sensory neurons containing arginine vasopressin or oxytocin and those containing substance P, fluoride-resistant acid phosphatase or neurofilament protein. Neuroscience **18**, 475-486.

Kakudo K., Hasegawa H., Komatsu N., Nakamura A., Itoh Y. and Watanabe K. (1988) Immuno-electron microscopic study of calcitonin gene-related peptide (CGRP) in axis cylinders of the vagus nerve. CGRP is present in both myelinated and unmyelinated fibers. Brain Res **440**, 153-158.

Kapfhammer J. P. and Raper J. A. (1987) Interactions between growth cones and neurites growing from different neural tissues in culture. J Neurosci **7**, 1595-1600.

Kaplan M. P., Chin S. S., Fliegner K. H. and Liem R. K. (1990) Alpha-internexin, a novel neuronal intermediate filament protein, precedes the low molecular weight neurofilament protein (NF-L) in the developing rat brain. J Neurosci **10**, 2735-2748.

Karanth S. S., Dhital S., Springall D. R. and Polak J. M. (1990) Reinnervation and neuropeptides in mouse skin flaps. J. Auton. Nerv. Syst. **31**, 127-134.

Karanth S. S., Springall D. R., Kuhn D. M., Levene M. M. and Polak J. M. (1991) An immunocytochemical study of cutaneous innervation and the distribution of neuropeptides and protein gene product 9.5 in man and commonly employed laboratory animals. Am J Anat **191**, 369-383.

Karlstrom R. O., Trowe T. and Bonhoeffer F. (1997) Genetic analysis of axon guidance and mapping in the zebrafish. TINS **20**, 3-8.

Keino Masu K., Masu M., Hinck L., Leonardo E. D., Chan S. S., Culotti J. G. and Tessier-Lavigne M. (1996) Deleted in Colorectal Cancer (DCC) encodes a netrin receptor. Cell **87**, 175-185.

Kelly B. M., Gillespie C. S., Sherman D. L. and Brophy P. J. (1992) Schwann cells of the myelin-forming phenotype express neurofilament protein NF-M. J Cell Biol **118**, 397-410.

Kennedy T. E. and Tessier-Lavigne M. (1995) Guidance and induction of branch formation in developing axons by target-derived diffusible factors. Current Opinion in Neurobiology **5**, 83-90.

Kennedy T. E., Serafini T., de la Torre J. R., and Tessier-Lavigne M. (1994) Netrins are diffusible chemotropic factors for commissural axons in the embryonic spinal cord. Cell **78**, 425-435.

Kent C. and Clarke P. J. (1991) The immunolocalisation of the neuroendocrine specific protein PGP9.5 during neurogenesis in the rat. Brain Res Dev Brain Res **58**, 147-150.

Keynes R. and Cook G. M. (1995) Axon guidance molecules. Cell **83**, 161-169.

Keynes R. and Cook G. M. (1996) Axons turn as netrins find their receptor. Neuron **17**, 1031-1034.

Kil S. H. and Bronner Fraser M. (1996) Expression of the avian alpha 7-integrin in developing nervous system and myotome. Int J Dev Neurosci **14**, 181-190.

Kirchmair R., Marksteiner J., Troger J., Mahata S. K., Mahata M., Donnerer J., Amann R., Fischer Colbrie R., Winkler H. and Saria A. (1994) Human and rat primary C-fibre afferents store and release secretoneurin, a novel neuropeptide. Eur J Neurosci **6**, 861-868.

Kitamura K. (1989) The structure and distribution of proteochrondroitin sulphate during the formation of chick embryo feather germs. Development **100**, 501-512.

Kitao Y., Robertson B., Kudo M. and Grant G. (1996) Neurogenesis of subpopulations of rat lumbar dorsal root ganglion neurons including neurons projecting to the dorsal column nuclei. J Comp Neurol **371**, 249-257.

Kitchener P. D., Wilson P. and Snow P. J. (1993) Selective labelling of primary sensory afferent terminals in lamina II of the dorsal horn by injection of Bandeiraea simplicifolia isolectin B4 into peripheral nerves. Neuroscience **54**, 545-551.

Klein R., Silos-Santiago I., Smeyne R. J., Lira S. A., Brambilla R., Bryant S., Zhang L., Snider W. D. and Barbacid M. (1994) Disruption of the neurotrophin-3 receptor gene trkC eliminates Ia muscle afferents and results in abnormal movements. Nature **368**, 249-251.

Klein R., Smeyne R. J., Wurst W., Long L. K., Auerbach B. A., Joyner A. L. and Barbacid M. (1993) Targeted disruption of the trkB neurotrophin receptor gene results in nervous system lesions and neonatal death. Cell **75**, 113-122.

Koerber H. R. and Brown P. B. (1980) Projections of two hindlimb cutaneous nerves to cat dorsal horn. J Neurophysiol **44**, 259-269.

Koerber H. R. and Mendell L. M. (1992) Functional heterogeneity of dorsal root ganglion cells. In Sensory Neurons. Diversity, Development, and Plasticity (Scott S. A.). 77-96. Oxford University Press, Oxford.

Kolodkin A. L., Matthes D. J. and Goodman C. S. (1993) The semaphorin genes encode a family of transmembrane and secreted growth cone guidance molecules. Cell **75**, 1389-1399.

Kolodkin A. L., Matthes D. J., O'Connor T. P., Patel N. H., Admon A., Bentley D. and Goodman C. S. (1992) Fasciclin IV: sequence, expression, and function during growth cone guidance in the grasshopper embryo. Neuron **9**, 831-845.

Konstantinidou A. D., Silos Santiago I., Flaris N. and Snider W. D. (1995) Development of the primary afferent projection in human spinal cord. J Comp Neurol **354**, 11-12.

Kruger L., Silverman J. D., Mantyh P. W., Sternini C. and Brecha N. C. (1989) Peripheral patterns of calcitonin-gene-related peptide general somatic sensory innervation: cutaneous and deep terminations. J Comp Neurol **280**, 291-302.

Kruse M. N., Bray L. A. and de Groat W. C. (1995) Influence of spinal cord injury on the morphology of bladder afferent and efferent neurons. J Auton Nerv Syst **54**, 215-224.

Kubota Y., Inagaki S., Shimada S., Girgis S., Zadi M., MacIntyre I., Tohyama M. and Kito S. (1988) Ontogeny of the calcitonin gene-related peptide in the nervous system of rat brain stem: an immunohistochemical analysis. Neuroscience **26**, 905-926.

Kucherer Ehret A., Pottgiesser J., Kreutzberg G. W., Thoenen H. and Edgar D. (1990) Developmental loss of laminin from the interstitial extracellular matrix correlates with decreased laminin gene expression. Development **110**, 1285-1293.

Kuraishi Y., Nanayama T., Ohno H., Fuji N., Otaka A., Yajima H. and Satoh M. (1989) Calcitonin gene-related peptide increases in the dorsal root ganglia of adjuvant arthritic rat. Peptides **10**, 447-452.

Lafrenie R. M. and Yamada K. M. (1996) Integrin-dependent signal transduction. J Cell Biochem **61**, 543-553.

Lamballe F., Klein R. and Barbacid M. (1991) TrkC, a new member of the trk family of tyrosine protein kinases, is a receptor for neurotrophin-3. Cell **66**, 969-979.

LaMotte C. C., Kapadia S. E. and Kocol C. E. (1989) Deafferentation-induced expansion of sciatic terminal field labelling in the adult rat dorsal horn following pronase injection of the sciatic nerve. J Comp Neurol **288**, 311-325.

Landmesser L., Dahm L., Tang J. C. and Rutishauser U. (1990) Polysialic acid as a regulator of intramuscular nerve branching during embryonic development. Neuron **4**, 655-667.

Landon F., Lemonnier M., Benarous R., Huc C., Fiszman M., Gros F. and Portier M. M. (1989) Multiple mRNAs encode peripherin, a neuronal intermediate filament protein. EMBO J **8**, 1719-1726.

Langford L. A. and Coggeshall R. E. (1979) Branching of sensory neurons in the dorsal root and evidence for the absence of dorsal root efferent fibres. J. Comp. Neurol **184**, 193-204.

Lasek R. J. (1986) Polymer sliding in axons. J Cell Sci Suppl **5**, 161-179.

Lasek R. J., Paggi P. and Katz M. J. (1992) Slow axonal transport mechanisms move neurofilaments relentlessly in mouse optic axons. J Cell Biol **117**, 607-616.

Lasek R. J., Paggi P. and Katz M. J. (1993) The maximum rate of neurofilament transport in axons: a view of molecular transport mechanisms continuously engaged. Brain Res **616**, 58-64.

Lawson S. N. (1979) The postnatal development of large light and small dark neurons in mouse dorsal root ganglia: a statistical analysis of cell numbers and size. J Neurocytol **8**, 275-294.

Lawson S. N. (1992) Morphological and Biochemical Cell types of Sensory Neurons. In Sensory Neurons. Diversity, Development, and Plasticity (Scott S. A.). 27-59. Oxford University Press, Oxford.

Lawson S. N. and Biscoe T. J. (1979) Development of mouse dorsal root ganglia: an autoradiographic and quantitative study. J Neurocytol **8**, 265-274.

Lawson S. N. and Waddell P. J. (1991) Soma neurofilament immunoreactivity is related to cell size and fibre conduction velocity in rat primary sensory neurons. J Physiol Lond **435**, 41-63.

Lawson S. N., Caddy K. W. and Biscoe T. J. (1974) Development of rat dorsal root ganglion neurones. Studies of cell birthdays and changes in mean cell diameter. Cell Tissue Res **153**, 399-413.

Lawson S. N., Harper A., Harper E. I., Garson J. A. and Anderton B. H. (1984) A monoclonal antibody against neurofilament protein specifically labels a subpopulation of rat sensory neurons. J Comp Neurol **228**, 163-272.

Le Greves P., Nyberg F., Terenius L. and Hokfelt T. (1985) Calcitonin gene-related peptide is a potent inhibitor of substance P degradation. Eur J Pharmacol **115**, 309-311.

Leah J. D., Cameron A. A. and Snow P. J. (1985) Neuropeptides in physiologically identified mammalian sensory neurones. Neurosci Lett **56**, 257-263.

Lefcort F., Clary D. O., Rusoff A. C. and Reichardt L. F. (1996) Inhibition of the NT-3 receptor TrkC, early in chick embryogenesis, results in severe reductions in multiple neuronal subpopulations in the dorsal root ganglia. J Neurosci **16**, 3704-3713.

Lendahl U., Zimmerman L. B. and McKay R. D. (1990) CNS stem cells express a new class of intermediate filament protein. Cell **60**, 585-595.

Lentz S. I., Miner J. H., Sanes J. R. and Snider W. D. (1997) Distribution of the ten known laminin chains in the pathways and targets of developing sensory axons. J. Comp. Neurol **378**, 547-561.

Leonard D. G., Gorham J. D., Cole P., Greene L. A. and Ziff E. B. (1988) A nerve growth factor-regulated messenger RNA encodes a new intermediate filament protein. J Cell Biol **106**, 181-193.

Leonard D. G., Ziff E. B. and Greene L. A. (1987) Identification and characterization of mRNAs regulated by nerve growth factor in PC12 cells. Mol Cell Biol **7**, 3156-3167.

Leskawa K. C. and Hogan E. L. (1985) Quantitation of the in vivo neuroblastoma response to exogenous, purified gangliosides. J. Neurosci. Res. **13**, 539-550.

Levine J. D., Fields H. L. and Bausbaum A. I. (1993) Peptides and the primary afferent nociceptor. J Neurosci **13**, 2273-2286.

Lewin G. R. and Mendell L. M. (1994) Regulation of Cutaneous C-Fiber Heat Nociceptors by Nerve Growth Factor in the Developing Rat. J Neurophysiol **71**, 941-949.

Lewin G. R., Lisney S. J. W. and Mendell L. M. (1992) Neonatal anti-NGF treatment reduces the A-delta-fiber and C-fiber evoked vasodilator responses in rat skin - evidence that nociceptor afferents mediate antidromic vasodilatation. Eur J Neurosci **4**, 1213-1218.

Lieberman A. R. (1976) Sensory Ganglia. In The Peripheral Nerve (Landon D. M.). 188-278. Chapman and Hall, London.

Liem R. K., Yen S. H., Salomon G. D. and Shelanski M. L. (1978) Intermediate filaments in nervous tissues. J Cell Biol **79**, 637-645.

Liesi P., Dahl D. and Vaheri A. (1984) Neurons cultured from developing rat brain attach and spread preferentially to laminin. J Neurosci Res **11**, 241-251.

Lin W. and Szaro B. G. (1995) Neurofilaments help maintain normal morphologies and support elongation of neurites in Xenopus laevis cultured embryonic spinal cord neurons. J Neurosci **15**, 8331-8344.

Linda H., Piehl F., Dagerlind A., Verge V. M., Arvidsson U., Cullheim S., Risling M., Ulfhake B. and Hokfelt T. (1992) Expression of GAP-43 mRNA in the adult mammalian spinal cord under normal conditions and after different types of lesions, with special reference to motoneurons. Exp Brain Res **91**, 284-295.

Lindenbaum M. H., Carbonetto S., Grosveld F., Flavell D. and Mushynski W. E. (1988) Transcriptional and post-transcriptional effects of nerve growth factor on expression of the three neurofilament subunits in PC-12 cells. J Biol Chem **263**, 5662-5667.

Lindsay R. M., Lockett C., Sternberg J. and Winter J. (1989) Neuropeptide expression in cultures of adult sensory neurons: modulation of substance P and calcitonin gene-related peptide levels by nerve growth factor. Neuroscience **33**, 53-65.

Lindsay R. M., Wiegand S. J., Altar C. A. and DiStefano P. S. (1994) Neurotrophic factors: from molecule to man. Trends Neurosci **17**, 182-190.

Liu Y. C. and Storm D. R. (1989) Dephosphorylation of neuromodulin by calcineurin. J Biol Chem **264**, 12800-12804.

LoPresti P. and Scott S. A. (1994) Target Specificity and Size of Avian Sensory neurons Supported in vitro by Nerve Growth Factor, Brain-Derived Neurotrophic Factor, and Neurotrophin-4. J Neurobiol **25**, 1613-1624.

Lumsden A. G. and Davies A. M. (1983) Earliest sensory nerve fibres are guided to peripheral targets by attractants other than nerve growth factor. Nature **306**, 786-788.

Lumsden A. G. and Davies A. M. (1986) Chemotropic effect of specific target epithelium in the developing mammalian nervous system. Nature **323**, 538-539.

Luo Y., Raible D. and Raper J. A. (1993) Collapsin: a protein in brain that induces the collapse and paralysis of neuronal growth cones. Cell **75**, 217-227.

Luo Y., Shepherd I., Li J., Renzi M. J., Chang S. and Raper J. A. (1995) A family of molecules related to collapsin in the embryonic chick nervous system. Neuron **14**, 1131-1140.

Malinda K. M. and Kleinman H. K. (1996) The laminins. Int J Biochem Cell Biol **28**, 957-959.

Manek S. G., Terenghi C., Shurey C., Nishikawa H., Green C. J. and Polak J. M. (1993) Neovascularisation precedes neural changes in the rat groin skin flap following denervation: an immunohistochemical study. Br J Plast Surg **46**, 48-55.

Mansour H., Bignami A., Labkovsky B. and Dahl D. (1989) Neurofilament phosphorylation in neuronal perikarya following axotomy: a study of rat spinal cord with ventral and dorsal root transection. J Comp Neurol **283**, 481-485.

Manthorpe M., Engvall E., Ruoslahti E., Longo F. M., Davis G. E. and Varon S. (1983) Laminin promotes neuritic regeneration from cultured peripheral and central neurons. J Cell Biol **97**, 1882-1890.

Marksteiner J., Saria A. and Hinterhuber H. (1994) Distribution of secretoneurin-like immunoreactivity in comparison with that of substance P in the human brain stem. J Chem Neuroanat **7**, 253-270.

Marti E., Gibson S. J., Polak J. M., Facer P., Springall D. R., Van Aswegen G., Aitchison M. and Koltzenburg M. (1987) Ontogeny of peptide- and amine-containing neurones in motor, sensory, and autonomic regions of rat and human spinal cord, dorsal root ganglia, and rat skin. J Comp Neurol **266**, 332-359.

Martin P., Khan A. and Lewis J. (1989) Cutaneous nerves of the embryonic chick wing do not develop in regions denuded of ectoderm. Development **106**, 335-346.

Masu Y., Nakayama K., Tamaki H., Harada Y., Kuno M. and Nakanishi S. (1987) cDNA cloning of bovine substance-K receptor through oocyte expression system. Nature **329**, 836-838.

Mata M. and Fink D. J. (1988) Calmodulin distribution in peripheral nerve: an EM immunocytochemical study. Brain Res **475**, 297-304.

Matteoli M., Balbi S., Sala C., Chini B., Cimino M., Vitadello M. and Fumagalli G. (1990) Developmentally regulated expression of calcitonin gene-related peptide at mammalian neuromuscular junction. J Mol Neurosci **2**, 175-184.

Matthes D. J., Sink H., Kolodkin A. L. and Goodman C. S. (1995) Semaphorin II can function as a selective inhibitor of specific synaptic arborizations. Cell **81**, 631-639.

McCarthy P. W. and Lawson S. N. (1989) Cell type and conduction velocity of rat primary sensory neurons with substance P-like immunoreactivity. Neuroscience **28**, 745-753.

McCarthy P. W. and Lawson S. N. (1990) Cell type and conduction velocity of rat primary sensory neurons with calcitonin gene related peptide like immunoreactivity. Neuroscience **34**, 623-632.

McCarthy P. W., Prabhakar E. and Lawson S. N. (1995) Evidence to support the peripheral branching of primary afferent C-fibres in the rat: an in vitro intracellular electrophysiological study. Brain Res **704**, 79-84.

McGarvey M. L., Baron Van Evercooren A., Kleinman H. K. and Dubois Dalcq M. (1984) Synthesis and effects of basement membrane components in cultured rat Schwann cells. Dev Biol **105**, 18-28.

McGuire C. B., Snipes G. J. and Norden J. J. (1988) Light-microscopic immunolocalization of the growth- and plasticity-associated protein GAP-43 in the developing rat brain. Brain Res **469**, 277-291.

McMahon S. B., Armanini M. P., Ling L. H. and Phillips H. S. (1994) Expression and Coexpression of Trk Receptors in Subpopulations of Adult Primary Sensory Neurons Projecting to Identified Peripheral Targets. Neuron **12**, 1161-1171.

McNeill D. L., Chung K., Carlton S. M. and Coggeshall R. E. (1988b) Calcitonin gene-related peptide immunostained axons provide evidence for fine primary afferent fibers in the dorsal and dorsolateral funiculi of the rat spinal cord. J Comp Neurol **272**, 303-308.

McNeill D. L., Coggeshall R. E. and Carlton S. M. (1988a) A light and electron microscopic study of calcitonin gene-related peptide in the spinal cord of the rat. Exp Neurol **99**, 699-708.

McQuarrie I. G., Brady S. T. and Lasek R. J. (1989) Retardation in the slow axonal transport of cytoskeletal elements during maturation and aging. Neurobiol Aging **10**, 359-365.

Meakin S. O. and Shooter E. M. (1992) The Nerve Growth Factor Family of Receptors. Trends Neurosci **15**, (9):323-331.

Meiri K. F. and Gordon Weeks P. R. (1990) GAP-43 in growth cones is associated with areas of membrane that are tightly bound to substrate and is a component of a membrane skeleton subcellular fraction. J Neurosci **10**, 256-266.

Meiri K. F., Pfenniger H. H. and Willard M. B. (1986) Growth-associated protein, GAP 43, a polypeptide that is induced when neurons extend axons, is a component of growth cones and corresponds to pp46, a major polypeptide of a subcellular fraction enriched in growth cones. PNAS **83**, 3337-3541.

Meiri K. F., Willard M. and Johnson M. I. (1988) Distribution and phosphorylation of the growth-associated protein GAP-43 in regenerating sympathetic neurons in culture. J Neurosci **8**, 2571-2581.

Mendell L. M. (1996) Neurotrophins and sensory neurons: role in development, maintenance and injury. A thematic summary. Phil Trans Royal Soc B **351**, 463-467.

Meredith J. E. J. and Schwartz M. A. (1997) Integrins, adhesion and apoptosis. **7**, 146-150.

Merighi A., Polak J. M., Gibson S. J., Gulbenkian S., Valentino K. L. and Peirone S. M. (1988) Ultrastructural studies on calcitonin gene-related peptide-, tachykinins- and somatostatin-immunoreactive neurones in rat dorsal root ganglia: evidence for the colocalization of different peptides in single secretory granules. Cell Tissue Res **254**, 101-109.

Messersmith E. K., Leonardo E. D., Shatz C. J., Tessier Lavigne M., Goodman C. S. and Kolodkin A. L. (1995) Semaphorin III can function as a selective chemorepellent to pattern sensory projections in the spinal cord. Neuron **14**, 949-959.

Miletic V. and Tan H. (1988) Iontophoretic application of calcitonin gene-related peptide produces a slow and prolonged excitation of neurons in the cat lumbar dorsal horn. Brain Res **446**, 169-172.

Millard C. L. and Woolf C. J. (1988) Sensory innervation of the hairs of the rat hindlimb: a light microscopic analysis. J Comp Neurol **277**, 183-194.

Milosevic A., Kanazir S. and Zecevic N. (1995) Immunocytochemical localization of growth-associated protein GAP-43 in early human development. Brain Res Dev Brain Res **84**, 282-286.

Miner J. H., Lewis R. M. and Sanes J. R. (1995) Molecular cloning of a novel laminin chain, alpha 5, and widespread expression in adult mouse tissues. J Biol Chem **270**, 28523-28526.

Mirnics K. and Koerber H. R. (1995a) Prenatal development of rat primary afferent fibers: I. Peripheral projections. J Comp Neurol **355**, 589-600.

Mirnics K. and Koerber H. R. (1995b) Prenatal development of rat primary afferent fibers: II. Central projections. J Comp Neurol **355**, 601-614.

Mitchell K. J., Doyle J. L., Serafini T., Kennedy T. E., Tessier Lavigne M., Goodman C. S. and Dickson B. J. (1996) Genetic analysis of Netrin genes in Drosophila: Netrins guide CNS commissural axons and peripheral motor axons. Neuron **17**, 203-215.

Molander C. and Grant G. (1985) Cutaneous projections from the rat hindlimb foot to the substantia gelatinosa of the spinal cord studied by transganglionic transport of WGA-HRP conjugate. J Comp Neurol **237**, 476-484.

Molliver D. C. and Snider W. D. (1995) TrkA is downregulated during postnatal development by a subset of dorsal root ganglion cells. Soc Neuroscience Abstr **21**: 515.2.

Molliver D. C., Radeke M. J., Feinstein S. C. and Snider W. D. (1995) Presence or absence of TrkA protein distinguishes subsets of small sensory neurons with unique cytochemical characteristics and dorsal horn projections. J Comp Neurol **361**, 404-416.

Monteiro M. J., Hoffman P. N., Gearhart J. D. and Cleveland D. W. (1990) Expression of NF-L in both neuronal and nonneuronal cells of transgenic mice: increased neurofilament density in axons without affecting caliber. J Cell Biol **111**, 1543-1557.

Morris H. R., Panico M., Etienne T., Tippins J., Girgis S. I. and MacIntyre I. (1984) Isolation and characterization of human calcitonin gene-related peptide. Nature **308**, 746-748.

Morton A. J. and Buss T. N. (1992) Accelerated differentiation in response to retinoic acid after retrovirally mediated gene transfer of Gap-43 into mouse neuroblastoma cells. Eur J Neurosci **4**, 910-916.

Moss D. J., Fernyhough P., Chapman K., Baizer L., Bray D. and Allsopp T. (1990) Chicken growth-associated protein GAP-43 is tightly bound to the actin-rich neuronal membrane skeleton. J Neurochem **54**, 729-736.

Mu X., Silos-Santiago I., Carroll S. L. and Snider W. D. (1993) Neurotrophin receptor genes are expressed in distinct patterns in developing dorsal root ganglia. J Neurosci **13**, 4029-4041.

Mulderry P. K., Nicholl C. G., Ghatei M. A., Springall D. R., Polak J. M. and Bloom S. R. (1984) Distribution and possible dual role of CGRP-containing nerves in the skin of the rat. In *9* (ed pp. 341.

Muma N. A., Hoffman P. N., Slunt H. H., Applegate M. D., Lieberburg I. and Price D. L. (1990) Alterations in levels of mRNAs coding for neurofilament protein subunits during regeneration. Exp Neurol **107**, 230-235.

Nacimiento W., Mautes A., Topper R., Oestreicher A. B., Gispen W. H., Nacimiento A. C., Noth J. and Kreutzberg G. W. (1993) B-50 (GAP-43) in the spinal cord caudal to hemisection: Indication for lack of intraspinal sprouting in dorsal root axons. J Neurosci Res **35**, 603-617.

Navarro X., Verdu E., Wendelschafer-Crabb G. and Kennedy W. R. (1995) Innervation of cutaneous structures in the mouse hindpaw: A confocal microscopy immunocytochemical study. J. Neurosci. Res **41**, 111-120.

Navarro X., Verdu E., Wendelschafer-Crabb G. and Kennedy W. R. (1997) Immunohistochemical study of skin reinnervation by regenerative axons. J. Comp. Neurol **380**, 164-174.

Nelson R. W., Bates P. A. and Rutishauser U. (1995) Protein determinants for specific polysialylation of the neural cell adhesion molecule. J Biol Chem **270**, 17171-17179.

Neumann S., Doubell T. P., Leslie T. A. and Woolf C. J. (1996) Inflammatory pain hypersensitivity mediated by phenotypic switch in myelinated primary sensory neurones. Nature **384**, 360-364.

Ni L. and Jonakait G. M. (1988) Development of substance P-containing neurons in the central nervous system in mice: an immunocytochemical study. J Comp Neurol **275**, 493-510.

Nieto M. A. (1996) Molecular biology of axon guidance. Neuron **17**, 1039-1048.

Nitsos I., Sexton P. M. and Rees S. (1994) The ontogeny of [125I]rat-alpha-CGRP binding sites in the spinal cord of sheep: a prenatal and postnatal study. Neuroscience **62**, 257-264.

Nixon R. A. and Logvinenko K. B. (1986) Multiple fates of newly synthesized neurofilament proteins: evidence for a stationary neurofilament network distributed nonuniformly along axons of retinal ganglion cell neurons. J Cell Biol **102**, 647-659.

Nixon R. A. and Sihag R. K. (1991) Neurofilament phosphorylation: a new look at regulation and function. Trends Neurosci **14**, 501-506.

Noguchi K., Morita Y., Kiyama H., Ono K. and Tohyama M. (1988) A noxious stimulus induces the preprotachykinin-A gene expression in the rat dorsal root ganglion: a quantitative study using in situ hybridization histochemistry. Mol Brain Res **4**, 31-35.

Noguchi K., Senba E., Morita Y., Sato M. and Tohyama M. (1989) Prepro-VIP and preprotachykinin mRNAs in the rat dorsal root ganglion cells following peripheral axotomy. Brain Res Mol Brain Res **6**, 327-330.

Nose A., Mahajan V. B. and Goodman C. S. (1992) Connectin: a homophilic cell adhesion molecule expressed on a subset of muscles and the motoneurons that innervate them in Drosphila. Cell **70**, 553-567.

Nose A., Takeichi M. and Goodman C. S. (1994) Ectopic expression of connectin reveals a repulsive function during growth cone guidance and synapse formation. Neuron **13**, 525-539.

Nothias F., Tessler A. and Murray M. (1993) Restoration of substance P and calcitonin gene-related peptide in dorsal root ganglia and dorsal horn after neonatal sciatic nerve lesion. J Comp Neurol **334**, 370-384.

Novotny G. E. and Gommert Novotny E. (1988) Intraepidermal nerves in human digital skin. Cell Tissue Res **254**, 111-117.

O'Brien C., Woolf C. J., Fitzgerald M., Lindsay R. M. and Molander C. (1989) Differences in the chemical expression of rat primary afferent neurons which innervate skin, muscle or joint. Neuroscience **32**, 493-502.

Oakley R. A. and Tosney K. W. (1991) Peanut agglutinin and chondroitin-6-sulfate are molecular markers for tissues that act as barriers to axon advance in the avian embryo. Dev Biol **147**, 187-206.

Oakley R. A., Garner A. S., Large T. H. and Frank E. (1995) Muscle sensory neurons require neurotrophin-3 from peripheral tissues during the period of normal cell death. Development **121**, 1341-1350.

Oblinger M. M. (1987) Characterization of posttranslational processing of the mammalian high-molecular-weight neurofilament protein in vivo. J Neurosci **7**, 2510-2521.

Oblinger M. M. and Lasek R. J. (1988) Axotomy-induced alterations in the synthesis and transport of neurofilaments and microtubules in dorsal root ganglion cells. J Neurosci **8**, 1747-1758.

Oblinger M. M., Szumlas R. A., Wong J. and Liuzzi F. J. (1989a) Changes in cytoskeletal gene expression affect the composition of regenerating axonal sprouts elaborated by dorsal root ganglion neurons in vivo. J Neurosci **9**, 2645-2653.

Oblinger M. M., Wong J. and Parysek L. M. (1989b) Axotomy-induced changes in the expression of a type III neuronal intermediate filament gene. J Neurosci **9**, 3766-3775.

Oppenheim R. W. (1989) The neurotrophic theory and naturally occurring motoneuron death. Trends Neurosci **12**, 252-255.

Otten U., Goedert M., Mayer N. and Lembeck F. (1980) Requirement of nerve growth factor for development of substance P-containing sensory neurones. Nature **287**, 158-159.

Ozaki S, and Snider, W. D. (1997) Initial trajectories of sensory neurons toward laminar targets in the developing mouse spinal cord. J. Comp. Neurol **380**, 215-229.

Pachter J. S. and Liem R. K. (1984) The differential appearance of neurofilament triplet polypeptides in the developing rat optic nerve. Dev Biol **103**, 200-210.

Parysek L. M. and Goldman R. D. (1987) Characterization of intermediate filaments in PC12 cells. J Neurosci **7**, 781-791.

Parysek L. M. and Goldman R. D. (1988) Distribution of a novel 57 kDa intermediate filament (IF) protein in the nervous system. J Neurosci **8**, 555-563.

Parysek L. M., McReynolds M. A., Goldman R. D. and Ley C. A. (1991) Some neural intermediate filaments contain both peripherin and the neurofilament proteins. J Neurosci Res **30**, 80-91.

Payne J. (1993) The development of cutaneous sensory innervation in the rat. PhD Thesis **University College London,**

Payne J., Middleton J. and Fitzgerald M. (1991) The pattern and timing of cutaneous hair follicle innervation in the rat pup and human fetus. Brain Res Dev Brain Res **61**, 173-182.

Perris R. (1997) The extracellular matrix in neural crest-cell migration. TINS **20**, 23-31.

Perry M. J. and Lawson S. N. (1993) Neurofilaments in rat and cat spinal cord; a comparative immunocytochemical study of phosphorylated and non-phosphorylated subunits. Cell Tissue Res **272**, 249-256.

Perry M. J., Lawson S. N. and Robertson J. (1991) Neurofilament immunoreactivity in populations of rat primary afferent neurons: a quantitative study of phosphorylated and non-phosphorylated subunits. J Neurocytol **20**, 746-758.

Phillips H. S. and Armanini M. P. (1996) Expression of the trk family of neurotrophin receptors in developing and adult dorsal root ganglion neurons. Phil Trans Royal Soc Lond B **29**, 413-416.

Piehl F., Arvidsson U., Hokfelt T. and Cullheim S. (1993) Calcitonin gene-related peptide-like immunoreactivity in motoneuron pools innervating different hind limb muscles in the rat. Exp Brain Res **96**, 291-303.

Pindzola R. R., Doller C. and Silver J. (1993) Putative inhibitory extracellular matrix molecules at the dorsal root entry zone of the spinal cord during development and after root and sciatic nerve lesions. Dev Biol **156**, 34-48.

Placzek M., Tessier Lavigne M., Yamada T., Dodd J. and Jessell T. M. (1990) Guidance of developing axons by diffusible chemoattractants. Cold Spring Harb Symp Quant Biol **55**, 279-289.

Plenderleith M. B. and Snow P. J. (1993) The plant lectin Bandeiraea simplicifolia I-B4 identifies a subpopulation of small diameter primary sensory neurones which innervate the skin in the rat. Neurosci Lett **159**, 17-20.

Plenderleith M. B., Haller C. J. and Snow P. J. (1990) Peptide coexistence in axon terminals within the superficial dorsal horn of the rat spinal cord. Synapse **6**, 344-350.

Plenderleith M. B., Wright L. L. and Snow P. J. (1992) Expression of lectin binding in the superficial dorsal horn of the rat spinal cord during pre- and postnatal development. Brain Res Dev Brain Res **68**, 103-109.

Portier M. M., Brachet P., Croizat B. and Gros F. (1983a) Regulation of peripherin in mouse neuroblastoma and rat PC 12 pheochromocytoma cell lines. Dev Neurosci **6**, 215-226.

Portier M. M., Croizat B. and Gros F. (1982) A sequence of changes in cytoskeletal components during neuroblastoma differentiation. FEBS Lett **146**, 283-288.

Portier M. M., Croizat B., de Nechaud B., Gumpel M. and Gros F. (1983b). C R Seances Acad Sci III **297**, 57-61.

Portier M. M., de Nechaud B. and Gros F. (1983c) Peripherin, a new member of the intermediate filament protein family. Dev Neurosci **6**, 335-344.

Portier M. M., Escurat M., Landon F., Djabali K. and Bousquet O. (1993) Peripherin and neurofilaments: expression and role during neural development. C R Acad Sci III **316**, 1124-1140.

Portier M.-M., Brachet P., Croizat B. and Gros F. (1984a) Regulation of peripherin in mouse neuroblastoma and rat PC12 pheochromocytoma cell lines. Dev. Neurosci **6**, 215-226.

Portier M.-M., DeNechaud B. and Gros F. (1984b) Peripherin, a new member of the intermediate filament protein family. Dev. Neurosci **6**, 335-344.

Pover C. M., Orr M. H. and Coggeshall R. E. (1993) A method for producing unbiased histograms of neuronal profile sizes. J. Neurosci. Methods **49**, 123-131.

Price J. (1985) An immunohistochemical and quantitative examination of dorsal root ganglion neuronal subpopulations. J Neurosci **5**, 2051-2059.

Purves D. (1988) Body and brain, a trophic theory of neural conections. Harvard University Press, Cammbridge.

Puschel A. W., Adams R. H. and Betz H. (1995) Murine semaphorin D/collapsin is a member of a diverse gene family and creates domains inhibitory for axonal extension. Neuron **14**, 941-948.

Puschel A. W., Adams R. H. and Betz H. (1996) The sensory innervation of the mouse spinal cord may be patterned by differential expression of and differential responsiveness to semaphorins. Mol Cell Neurosci **7**, 419-431.

Quitschke W. and Schechter N. (1984) 58,000 dalton intermediate filament proteins of neuronal and nonneuronal origin in the goldfish visual pathway. J Neurochem **42**, 569-576.

Raff M. C. (1992) Social controls on cell survival and cell death. Nature **356**, 397-400.

Rambourg A., Clermont Y. and Beaudet A. (1983) Ultrastructural features of six types of neurons in rat dorsal root ganglia. J Neurocytol **12**, 47-66.

Ramon y. C. S. (1909) Histologie du systeme nerveux de l'homme et des vertebres. Institute Cajal, Madrid

Ranvier L. (1875) Des tubes nerveux en T et de leurs relation avec les cellules ganglionnaires. CR Acad. Sci. (Paris) **81**, 1274-1276.

Redmond L., Xie H., Ziskind-Conhaim L. and Hockfield S. (1997) Cues Intrinsic to the spinal cord determine the pattern and timing of primary afferent growth. Dev. Biol **182**, 205-218.

Reichardt L. F. and Tomaselli K. J. (1991) Extracellular matrix molecules and their receptors: functions in neural development. Annu Rev Neurosci **14**, 531-570.

Rethelyi M., Metz C. B. and Lund P. K. (1989) Distribution of neurons expressing calcitonin gene-related peptide mRNAs in the brain stem, spinal cord and dorsal root ganglia of rat and guinea-pig. Neuroscience **29**, 225-239.

Reynolds M. L. and Fitzgerald M. (1992) Neonatal sciatic nerve section results in thiamine monophosphate but not substance P or calcitonin gene-related peptide depletion from the terminal field in the dorsal horn of the rat: the role of collateral sprouting. Neuroscience **51**, 191-202.

Reynolds M. L. and Fitzgerald M. (1995) Long-term sensory hyperinnervation following neonatal skin wounds. J Comp Neurol **358**, 487-498.

Reynolds M. L., Fitzgerald M. and Benowitz L. I. (1991) GAP-43 expression in developing cutaneous and muscle nerves in the rat hindlimb. Neuroscience **41**, 201-211.

Reynolds M. L., Ward A., Graham C. E., Coggeshall R. and Fitzgerald M. (1997) Decreased skin sensory innervation in transgenic mice overexpressing insulin-like growth factor-II - *in press*

Rice F. L. (1993) Structure, vascularization, and innervation of the mystacial pad of the rat as revealed by the lectin Griffonia simplicifolia. J Comp Neurol **337**, 386-399.

Rimm D. L., Koslov E. R., Kebriaei P., Cianci C. D. and Morrow J. S. (1995) Alpha 1(E)-catenin is an actin-binding and -bundling protein mediating the attachment of F-actin to the membrane adhesion complex. Proc Natl Acad Sci U S A **92**, 8813-8817.

Ritter A. M., Lewin G. R. and Mendell L. (1991) Regulation of Myelinated Nociceptor Function by Nerve Growth Factor in Neonatal and Adult Rats. Brain Res Bull **30**, 245-249.

Rivero-Melian C. (1993) Simultaneous demonstration of central projections of different peripheral nerves by anti-choleragenoid immunoglobulin markers. Neurorep **4**, 743-746.

Robertson B. and Grant G. (1989) Immunocytochemical evidence for the localization of the GM1 ganglioside in carbonic anhydrase-containing and RT97-immunoreactive rat primary sensory neurons. J Neurocytol **18**, 77-86.

Robertson B., Lindh B. and Aldskogius H. (1992) WGA-HRP and choleragenoid-HRP as anterogradely transported tracers in vagal visceral afferents and binding of WGA and choleragenoid to nodose ganglion neurons in rodents. Brain Res **590**, 207-212.

Robertson B., Perry M. J. and Lawson S. N. (1991) Populations of rat spinal primary afferent neurons with choleragenoid binding compared with those labelled by markers for neurofilament and carbohydrate groups: a quantitative immunocytochemical study. J Neurocytol **20**, 387-395.

Rogers S. L., Letourneau P. C., Palm S. L., McCarthy J. and Furcht L. T. (1983) Neurite extension by peripheral and c entral nervous system neurons in response to substratum-bound fibronectin and laminin. Dev. Biol **98**, 212-220.

Rosenthal A., Goeddel D. V., Nguyen T., Lewis M., Shis A., Larannee G. R., Nikolics K. and Winslow J. W. (1990) Primary structure and biological activity of a novel human neurotrophic factor. Neuron **4**, 767-773.

Ruda M. A., Bennett G. J. and Dubner R. (1986) Neurochemistry and neural circuitry in the dorsal horn. Prog Brain Res **66**, 219-268.

Ruit K. G., Elliott J. L., Osbourne P. A., Yan Q. and Snider W. D. (1992) Selective dependence of mammalian dorsal root ganglion neurons on nerve growth factor during embryonic development. Neuron **8**, 573-587.

Sann H., McCarthy P. W., Mader M. and Schemann M. (1995) Choline acetyltransferase-like immunoreactivity in small diameter neurones of the rat dorsal root ganglion. Neurosci Lett **198**, 17-20.

Santamaria L. G., Terenghi G., Curtis J., de Blaquiere G. E., Pereira J. H., Turk J. L. and Polak J. M. (1994) Recovery of peptide-containing nerves assessed by quantitative immunohistochemistry. Int. J. Lepr **62**, 64-74.

Sargent P. B. (1989) What distinguishes axons from dendrites? Neurons know more than we do. TINS **12**, 203-205.

Schecterson L. C. and Bothwell M. (1992) Novel Roles for Neurotrophins Are Suggested by BDNF and NT-3 mRNA Expression in Developing Neurons. Neuron **9**, 449-463.

Schlaepfer W. W. and Bruce J. (1990) Simultaneous up-regulation of neurofilament proteins during the postnatal development of the rat nervous system. J Neurosci Res **25**, 39-49.

Schlaepfer W. W. and Freeman L. A. (1978) Neurofilament proteins of rat peripheral nerve and spinal cord. J Cell Biol **78**, 653-662.

Schmidt R. E., Spencer S. A., Coleman B. D. and Roth K. A. (1991) Immunohistochemical localization of GAP-43 in rat and human sympathetic nervous system-effects of aging and diabetes. Brain Res **552**, 190-197.

Schornig M., Heumann R. and Rohrer H. (1993) Synthesis of nerve growth-factor messenger-RNA in cultures of developing mouse whisker pad, a peripheral target tissue of sensory trigeminal neurons. J Cell Biol **120**, 1471-1479.

Schreyer D. J. and Skene J. H. (1991) Fate of GAP-43 in ascending spinal axons of DRG neurons after peripheral nerve injury: delayed accumulation and correlation with regenerative potential. J Neurosci **11**, 3738-3751.

Schwartz M., Sivron T., Eitan S., Hirschberg D. L., Lotan M. and Elman Faber A. (1994) Cytokines and cytokine-related substances regulating glial cell response to injury of the central nervous system. Prog Brain Res **103**, 331-341.

Scott S. A. (1982) The development of the segmental pattern of skinsensory innervation in embryonic chick hind limb. J. Physiol **330,** 203-220.

Scott S. A. (1986) Skin sensory innervation patterns in embryonic chick hindlimb following dorsal root ganglion reversals. J. Neurobiol **17**, 649-668.

Scott S. A. (1987) The development of skin sensory innervation patterns. TINS **10**, 468-473.

Scott S. A. (1992) The development of peripheral sensory innervation patterns. In Sensory Neurons. Diversity, Development, and Plasticity (Scott S. A.). 242-264. Oxford University Press, Oxford.

Sendtner M., Stockli D. A. and Thoenen H. (1992) Synthesis and localization of ciliary neurotrophic factor in the sciatic nerve of the adult rat after lesion and during regeneration. J Cell Biol **118**, 139-148.

Serafini T., Colamarino S. A., Leonardo E. D., Wang H., Beddington R., Skarnes W. C. and Tessier Lavigne M. (1996) Netrin-1 is required for commissural axon guidance in the developing vertebrate nervous system. Cell **87**, 1001-1014.

Serafini T., Kennedy T. E., Galko M. J., Mirzayan C., Jessell T. M. and Tessier Lavigne M. (1994) The netrins define a family of axon outgrowth-promoting proteins homologous to C. elegans UNC-6. Cell **78**, 409-424.

Sharma K., Korade Z. and Frank E. (1994) Development of specific muscle and cutaneous sensory projections in cultured segments of spinal cord. Development **120,** 1315-1223.

Sharma K., Luo Y., Raper J. and Frank E. (1996) Collapsin-1 delays the growth of senosory afferents into the dorsal spinal cord. Soc. Neurosci Abstr **22**: 585.6.

Sharp G. A., Shaw G. and Weber K. (1982) Immunoelectronmicroscopial localization of the three neurofilament triplet proteins along neurofilaments of cultured dorsal root ganglion neurons. Exp. Cell Res. **137**, 403-413.

Sharpe C. R. (1988) Developmental expression of a neurofilament-M and two vimentin-like genes in Xenopus laevis. Development **103**, 269-277.

Sharpe C. R., Pluck A. and Gurdon J. B. (1989) XIF3, a Xenopus peripherin gene, requires an inductive signal for enhanced expression in anterior neural tissue. Development **107**, 701-714.

Shaw G. and Weber K. (1982) Differential expression of neurofilament triplet proteins in brain development. Nature **298**, 277-279.

Shaw G., Osborn M. and Weber K. (1981) An immunofluorescence microscopical study of the neurofilament triplet proteins, vimentin and glial fibrillary acidic protein within the adult rat brain. Eur J Cell Biol **26**, 68-82.

Sheppard A. M., Onken M. D., Rosen G. D., Noakes P. G. and Dean D. C. (1994) Expanding roles for alpha 4 integrin and its ligands in development. Cell Adhes Commun **2**, 27-43.

Shirasaki R., Tamada A., Katsumata R. and Murakami F. (1995) Guidance of cerebellofugal axons in the rat embryo: directed growth toward the floor plate and subsequent elongation along the longitudinal axis. Neuron **14**, 961-972.

Shortland P., Woolf C. J. and Fitzgerald M. (1989) Morphology and somatotopic organization of the central terminals of hindlimb hair follicle afferents in the rat lumbar spinal cord. J Comp Neurol **289**, 416-433.

Sieber-Blum M., Ito K., Richardson M. K., Langtimm C. J. and Duff R. S. (1993) Distribution of pluripotent neural crest cells in the embryo and the role of brain-derived neurotrophic factor in the commitment to the primary sensory neuron lineage. J Neurobiol **24**, 173-184.

Sihag R. K. and Nixon R. A. (1990) Phosphorylation of the amino-terminal head domain of the middle molecular mass 145-kDa subunit of neurofilaments. Evidence for regulation by second messenger-dependent protein kinases. J Biol Chem **265**, 4166-4171.

Silverman J. D. and Kruger L. (1988a) Lectin and neuropeptide labeling of separate populations of dorsal root ganglion neurons and associated "nociceptor" thin axons in rat testis and cornea whole-mount preparations. Somatosens Res **5**, 259-267.

Silverman J. D. and Kruger L. (1988b) Acid phosphatase as a selective marker for a class of small sensory ganglion cells in several mammals: spinal cord distribution, histochemical properties, and relation to fluoride-resistant acid phosphatase (FRAP) of rodents. Somatosens Res **5**, 219-246.

Silverman J. D. and Kruger L. (1989) Calcitonin-gene-related-peptide-immunoreactive innervation of the rat head with emphasis on specialized sensory structures. J Comp Neurol **280**, 303-330.

Silverman J. D. and Kruger L. (1990) Selective neuronal glycoconjugate expression in sensory and autonomic ganglia: relation of lectin reactivity to eptid and enzyme markers. J Neuro Cytol **19**, 789-801.

Skene J. H. P. (1989) Axonal growth associated proteins. Ann Rev Neurosci **12**, 127-156.

Skene J. H., Jacobson R. D., Snipes G. J., McGuire C. B., Norden J. J. and Freeman J. A. (1986) A protein induced during nerve growth (GAP-43) is a major component of growth-cone membranes. Science **233**, 783-786.

Skofitsch G. and Jacobowitz D. M. (1985) Autoradiographic distribution of 125I calcitonin gene-related peptide binding sites in the rat central nervous system. Peptides **6**, 975-986.

Smeyne R. J., Klein R., Schnapp A., Long S. K., Bryant S., Lewin A., Lira S. A. and Barbacid M. (1994) Severe sensory and sympathetic neuropathies in mice carrying a disrupted Trk/NGF receptor gene. Nature **386**, 246-249.

Smith C. L. (1983) The development and postnatal organization of primary afferent projections to the rat thoracic spinal cord. J Comp Neurol **220**, 29-43.

Snider W. D. (1994) Functions of the Neurotrophins during Nervous System Development: What the Knockouts Are Teaching Us. Cell **77**, 627-638.

Snider W. D. and Silos-Santiago I. (1996) Dorsal root ganglion neurons require functional neurotrophin receptors for survival during development. Phil. Trans. Royal. Soc. B **351**, 395-403.

Snider W. D., Zhang L., Yusoof S., Gorukanti N. and Tserung C. (1992) Interactions between dorsal root axons and their target motor neurons in developing mammalian spinal cord. J Neurosci **12**, 3494-3508.

Snipes G. J., Chan S. Y., McGuire C. B., Costello B. R., Norden J. J., Freeman J. A. and Routtenberg A. (1987) Evidence for the coidentification of GAP-43, a growth-associated protein, and F1, a plasticity-associated protein. J Neurosci **7**, 4066-4075.

Snow D. M. and Letourneau P. C. (1992) Neurite outgrowth on a step gradient of chondroitin sulfate proteoglycan (CS-PG). J Neurobiol **23**, 322-336.

Snow D. M., Lemmon V., Carrino D. A., Caplan A. I. and Silver J. (1990a) Sulfated proteoglycans in astroglial barriers inhibit neurite outgrowth in vitro. Exp Neurol **109**, 111-130.

Snow D. M., Steindler D. A. and Silver J. (1990b) Molecular and cellular characterization of the glial roof plate of the spinal cord and optic tectum: a possible role for a proteoglycan in the development of an axon barrier. Dev Biol **138**, 359-376.

Song W. K., Wang W., Foster R. F., Bielser D. A. and Kaufman S. J. (1992) H36-alpha 7 is a novel integrin alpha chain that is developmentally regulated during skeletal myogenesis. J Cell Biol **117**, 643-657.

Stahl B., von Boxberg Y., Muller B., Walter J., Schwarz U. and Bonhoeffer F. (1990) Directional cues for retinal axons. Cold Spring Harb Symp Quant Biol **55**, 351-357.

Stankovic N., Johansson O. and Hildebrand C. (1996) Occurrence of epidermal nerve endings in glabrous and hairy skin of the rat foot after sciatic nerve regeneration. Cell Tissue Res **284**, 161-166.

Steers W. D., Kolbeck S., Creedon D. and Tuttle J. B. (1991) Nerve growth factor in the urinary bladder of the adult regulates neuronal form and function. J. Clin Invest **88,** 1709-1715.

Sternini C., Su D., Arakawa J., De G. R., Rickman D. W., Davis B. M., Albers K. M. and Brecha N. C. (1996) Cellular localization of pan-trk immunoreactivity and trk(C) mRNA in the enteric nervous system. Journal of Comparative Neurology **368**, 597-607.

Stewart H. J., Jessen K. R., Curtis R. and Mirsky R. (1992) Schwann cells, neurons and GAP-43. Perspect Dev Neurobiol **1**, 45-52.

Strack A. M., Sawyer W. B., Marubio L. M. and Loewy A. D. (1988) Spinal origin of sympathetic preganglionic neurons in the rat. Brain Res **455**, 187-191.

Suburo A. M., Wood J. N., Latchman D. S. and Polak J. M. (1992) Transient expression of neuropeptide Y and its C-flanking peptide immunoreactivities in the spinal cord and ganglia of human embryos and fetuses. Neuroscience **46**, 571-584.

Sugiura Y., Lee C. L. and Perl E. R. (1986) Central projections of identified, unmyelinated (C) afferent fibers innervating mammalian skin. Science **234**, 358-361.

Swett J. E. and Woolf C. J. (1985) Somatotopic organization of primary afferent terminals in the superficial dorsal horn of the rat spinal cord. J Comp Neurol **231**, 66-71.

Tainio H., Vaalasti A. and Rechardt L. (1987) The distribution of substance P-, CGRP-, galanin- and ANP-like immunoreactive nerves in human sweat glands. Histochem J **19**, 375-380.

Tamada A., Shirasaki R. and Murakami F. (1995) Floor plate chemoattracts crossed axons and chemorepels uncrossed axons in the vertebrate brain. Neuron **14**, 1083-1093.

Tanaka E. and Sabry J. (1995) Making the connection: cytoskeletal rearrangements during growth cone guidance. Cell **83**, 171-176.

Tandrup T. (1995) Are the neurons in the dorsal root ganglion pseudounipolar? A comparison of the numbers of neurons and number of myelinated and unmyelinated fibres in the dorsal root. J. Comp. Neurol **357**, 341-347.

Tapscott S. J., Bennett G. S., Toyama Y., Kleinbart F. and Holtzer H. (1981) Intermediate filament proteins in the developing chick spinal cord. Dev Biol **86**, 40-54.

Tennenbaum T., Li L., Belanger A. J., De Luca L. M. and Yuspa S. H. (1996) Selective changes in laminin adhesion and alpha 6 beta 4 integrin regulation are associated with the initial steps in keratinocyte maturation. Cell Growth Differ **7**, 615-628.

Terenghi G., Riveros Moreno V., Hudson L. D., Ibrahim N. B. and Polak J. M. (1993) Immunohistochemistry of nitric oxide synthase demonstrates immunoreactive neurons in spinal cord and dorsal root ganglia of man and rat. J Neurol Sci **118**, 34-37.

Tessarollo L., Tsoulfas P., Martin-Zanca D., Gilbert D. J., Jenkins N. A., Copeland N. G. and Parada L. F. (1993) TrkC, a receptor for neurotrophin-3, is widely expressed in the developing nervous system and non-neuronal tissues. Development **118**, 463-475.

Tessier-Lavigne M., Placzek M., Lumsden A. G., Dodd J. and Jessell T. M. (1988) Chemotropic guidance of developing axons in the mammalian central nervous system. Nature **336**, 775-778.

Tetzlaff W., Alexander S. W., Miller F. D. and Bisby M. A. (1991) Response of facial and rubrospinal neurons to axotomy: changes in mRNA expression for cytoskeletal proteins and GAP-43. J Neurosci **11**, 2528-2544.

Tetzlaff W., Zwiers H., Lederis K., Cassar L. and Bisby M. A. (1989) Axonal transport and localization of B-50/GAP-43-like immunoreactivity in regenerating sciatic and facial nerves of the rat. J Neurosci **9**, 1303-1313.

Thorey I. and Seifert W. (1989) Developmentally regulated epitopes on a neurofilament protein visualized by monoclonal antibodies. Brain Res Dev Brain Res **49**, 229-241.

Timpl R. and Brown J. C. (1994) The laminins. Matrix Biol **14**, 275-281.

Tomaselli K. J., Doherty P., Emmett C. J., Damsky C. H., Walsh F. S. and Reichardt L. F. (1993) Expression of beta 1 integrins in sensory neurons of the dorsal root ganglion and their functions in neurite outgrowth on two laminin isoforms. J Neurosci **13**, 4880-4888.

Tosney K. W. and Landmesser L. T. (1985a) Specificity of early motoneuron growth cone outgrowth in the chick embryo. J Neurosci **5**, 2336-2344.

Tosney K. W. and Landmesser L. T. (1985b) Development of the major pathways for neurite outgrowth in the chick hindlimb. Dev Biol **109**, 193-214.

Tosney K. W. and Landmesser L. T. (1985c) Growth cone morphology and trajectory in the lumbosacral region of the chick embryo. J Neurosci **5**, 2345-2358.

Tosney K. W. and Oakley R. A. (1990) The perinotochordal mesenchyme acts as a barrier to axon advance in the chick embryo: implications for a general mechanism of axonal guidance. Exp Neurol **109**, 75-89.

Traub R. J., Iadarola M. J. and Ruda M. A. (1989) Effect of multiple dorsal rhizotomies on calcitonin gene-related peptide-like immunoreactivity in the lumbosacral dorsal spinal cord of the cat: a radioimmunoassay analysis. Peptides **10**, 979-983.

Troy C. M., Brown K., Greene L. A. and Shelanski M. L. (1990a) Ontogeny of the neuronal intermediate filament protein, peripherin, in the mouse embryo. Neuroscience **36**, 217-237.

Troy C. M., Muma N. A., Greene L. A., Price D. L. and Shelanski M. L. (1990b) Regulation of peripherin and neurofilament expression in regenerating rat motorneurons. Brain Res **529**, 232-238.

Tuchscherer M. M. and Seybold V. S. (1985) Immunohistochemical studies of substance P, cholecystokinin-octapeptide and somatostatin in dorsal root ganglia of the rat. Neuroscience **14**, 593-605.

Urschel B. A., Brown P. N. and Hulsebosch C. E. (1991) Differential effects on sensory nerve processes and behavioural alterations in the rat after treatment with antribodies to nerve growth factor. Exp. Neurol **114**, 44-52.

Van der Zee C. E. E. M., Fawcett J., Staibz J., Racine R. and Diamond J. (1991) Anti-NGF treatment blocks the collateral sprouting of cholinergic fibres in the hippocampus. Soc Neurosci Abstr **17**, 1312-5261.

Van der Zee C. E., Nielander H. B., Vos J. P., Lopes da Silva S., Verhaagen J., Oestreicher A. B., Schrama L. H., Schotman P. and Gispen W. H. (1989) Expression of growth-associated protein B-50 (GAP43) in dorsal root ganglia and sciatic nerve during regenerative sprouting. J Neurosci **9**, 3505-3512.

Vedder H., Affolter H. U. and Otten U. (1993) Nerve growth-factor (NGF) regulates tachykinin gene-expression and biosynthesis in rat sensory neurons during early postnatal-development. Neuropep **24**, 351-357.

Vega J. A., Vazquez E., Naves F. J., Del Valle M. E., Calzada B. and Represa J. J. (1994) Immunohistochemical localization of the high-affinity NGF receptor (gp 140-trkA) in the adult human dorsal root and sympathetic ganglia and in the nerves and sensory corpuscles supplying digital skin. The Anatomical record **240**, 579-588.

Venstrom K. and Reichardt L. (1995) Beta 8 integrins mediate interactions of chick sensory neurons with laminin-1, collagen IV, and fibronectin. Mol Biol Cell **6**, 419-431.

Verge V. M., Merlio J. P., Grondin J., Ernfors P., Persson H., Riopelle R. J., Hokfelt T. and Richardson P. M. (1992) Colocalization of NGF binding sites, trk mRNA, and low-affinity NGF receptor mRNA in primary sensory neurons: responses to injury and infusion of NGF. J Neurosci **12**, 4011-4022.

Verge V. M., Richardson P. M., Wiesenfeld Hallin Z. and Hokfelt T. (1995) Differential influence of nerve growth factor on neuropeptide expression in vivo: a novel role in peptide suppression in adult sensory neurons. J Neurosci **15**, 2081-2096.

Verkade P., Oestreicher A. B., Verkleij A. J. and Gispen W. H. (1995) The increase in B-50/GAP-43 in regenerating rat sciatic nerve occurs predominantly in unmyelinated axon shafts: a quantitative ultrastructural study. J Comp Neurol **356**, 433-443.

Verkade P., Verkleij A. J., Annaert W. G., Gispen W. H. and Oestreicher A. B. (1996b) Ultrastructural localization of B-50/growth-associated protein-43 to anterogradely transported synaptophysin-positive and calcitonin gene-related peptide-negative vesicles in the regenerating rat sciatic nerve. Neuroscience **71**, 489-505.

Verkade P., Verkleij A. J., Gispen W. H. and Oestreicher A. B. (1996a) Ultrastructural evidence for the lack of co-transport of B-50/GAP-43 and calmodulin in myelinated axons of the regenerating rat sciatic nerve. J Neurocytol **25**, 583-595.

Verna J. M. (1985) In vitro analysis of interactions between sensory neurons and skin: evidence for selective innervation of dermis and epidermis. J Embryol Exp Morphol **86**, 53-70.

Verna J. M., Fichard A. and Saxod R. (1989) Influence of glycosaminoglycans on neurite morphology and outgrowth patterns in vitro. Int J Dev Neurosci **7**, 389-399.

Verna J. M., Usson Y. and Saxod R. (1986) Differential growth of sensory neurons in vitro in presence of dermis and epidermis. A quantitative time-lapse analysis. Cell Differ **18**, 183-188.

Villar M. J., Wiesenfeld Hallin Z., Xu X. J., Theodorsson E., Emson P. C. and Hokfelt T. (1991) Further studies on galanin-, substance P-, and CGRP-like immunoreactivities in primary sensory neurons and spinal cord: effects of dorsal rhizotomies and sciatic nerve lesions. Exp Neurol **112**, 29-39.

Vitkovic L., Steisslinger H. W., Aloyo V. J. and Mersel M. (1988) The 43-kDa neuronal growth-associated protein (GAP-43) is present in plasma membranes of rat astrocytes. Proc Natl Acad Sci U S A **85**, 8296-8300.

von Bartheld C. S., Byers M. R., Williams R. and Bothwell M. (1996a) Anterograde transport of neurotrophins and axodendritic transfer in the developing visual system. Nature **379**, 830-833.

von Bartheld C. S., Williams R., Lefcort F., Clary D. O., Reichardt L. F. and Bothwell M. (1996b) Retrograde transport of neurotophins from the eye to the brain in chick embryos: roles of the p75NTR and trkB receptors. J Neurosci **16**, 2995-3008.

Wadsworth W. G., Bhatt H. and Hedgecock E. M. (1996) Neuroglia and pioneer neurons express UNC-6 to provide global and local netrin cues for guiding migrations in C. elegans. Neuron **16**, 35-46.

Wall P. D. (1987) The central consequences of the application of capsaicin to one peripheral nerve in adult rat. Acta Physiol Hung **69**, 2750-2286.

Wall P. D. and Fitzgerald M. (1982) If substance P fails to fulfil the criteria as a neurotransmitter in somatosensory afferents, what might be its function? Ciba Found Symp **91**, 249-266.

Wang H., Rivero Melian C., Robertson B. and Grant G. (1994) Transganglionic transport and binding of the isolectin B4 from Griffonia simplicifolia I in rat primary sensory neurons. Neuroscience **62**, 539-551.

Wang L., Hilliges M., Jernberg T., Wiegleb Edstrom D. and Johansson O. (1990) Protein gene product 9.5-immunoreactive nerve fibres and cells in human skin. Cell Tissue Res **261**, 25-33.

Watson D. F., Hoffman P. N., Fittro K. P. and Griffin J. W. (1989) Neurofilament and tubulin transport slows along the course of mature motor axons. Brain Res **477**, 225-232.

Weaver C. D., Yoshida C. K., de Curtis I. and Reichardt L. F. (1995) Expression and in vitro function of beta 1-integrin laminin receptors in the developing avian ciliary ganglion. J Neurosci **15**, 5275-5285.

Wessels W. J. T., Feirabend H. K. P. and Marani E. (1990) Evidence for a rostrocaudal organization in dorsal root ganglia during development as demonstrated by intra-uterine WGA-HRP injections into the hindlimb of rat fetuses. Dev Brain Res **54**, 273-281.

Weston J. A. (1970) The migration and differentiation of neural crest cells. Adv Morphog **8**, 41-114.

White F. A., Silos-Santiago I., Moliver D. C., Nishimura M., Phillips H., Barbacid M. and Snider W. D. (1996) Synchronous onset of NGF and trkA survival dependence in developing dorsal root ganglia. J. Neurosci **16**, 4662-4672.

Wilkenson K. D., Lee K., Deshpande S., Duerkson-Hughes P., Boss J. M. and Pohl J. (1989) The neurons specific protein PGP 9.5 is a ubiquitin carboxyl-terminal hydroxylase. Science **246,** 670-673.

Willard M. and Simon C. (1983) Modulations of neurofilament axonal transport during the development of rabbit retinal ganglion cells. Cell **35**, 551-559.

Williams L. R., Azzam N. A., Zalewski A. A. and Azzam R. N. (1993) Regenerating axons are not required to induce the formation of a Schwann cell cable in a silicone chamber. Exp Neurol **120**, 49-59.

Willis W. D. and Coggeshall R. E. (1991) Sensory mechanisms of the spinal cord. Plenum Press, New York.

Wong J. and Oblinger M. M. (1987) Changes in neurofilament gene expression occur after axotomy of dorsal root ganglion neurons: an in situ hybridization study. Metab Brain Dis **2**, 291-303.

Wong J. and Oblinger M. M. (1991) NGF rescues substance P expression but not neurofilament or tubulin gene expression in axotomized sensory neurons. J Neurosci **11**, 543-552.

Wong P. C., Marszalek J., Crawford T. O., Xu Z., Hsieh S. T., Griffin J. W. and Cleveland D. W. (1995) Increasing neurofilament subunit NF-M expression reduces axonal NF-H, inhibits radial growth, and results in neurofilamentous accumulation in motor neurons. J Cell Biol **130**, 1413-1422.

Woolf C. J. (1987) Central terminations of cutaneous mechanoreceptive afferents in the rat lumbar spinal cord. J Comp Neurol **261**, 105-119.

Woolf C. J. (1990) The contribution of both the peripheral and central nervous systems to the pain that follows peripheral nerve injury. Springer Verlag, Heidelberg **51-58**,

Woolf C. J. (1996) Phenotypic modification of primary sensory neurons: the role of nerve growth factor in the production of persistent pain. Phil Trans Royal Soc B **351,** 441-449.

Woolf C. J. and Fitzgerald M. (1986) The somatotopic organization of cutaneous afferent terminals and dorsal horn neuronal receptive fields in the superficial and deep laminae of the rat lumbar spinal cord. J Comp Neurol **251**, 517-531.

Woolf C. J., Reynolds M. L., Chong M. S., Emson P., Irwin N. and Benowitz L. I. (1992b) Denervation of the motor endplate results in the rapid expression by terminal Schwann cells of the growth-associated protein GAP-43. J Neurosci **12**, 3999-4010.

Woolf C. J., Shortland P. and Coggeshall R. E. (1992a) Peripheral nerve injury triggers central sprouting of myelinated afferents. Nature **355**, 75-78.

Wright D. E. and Snider W. D. (1995) Neurotrophin receptor mRNA expression defines distinct populations of neurons in rat dorsal root ganglia. J Comp Neurol **351**, 329-338.

Wright D. E., White F. A., Gerfen R. W., Silos Santiago I. and Snider W. D. (1995) The guidance molecule semaphorin III is expressed in regions of spinal cord and periphery avoided by growing sensory axons. J Comp Neurol **361**, 321-333.

Wright E. M., Vogel K. S. and Davies A. M. (1992) Neurotrophic Factors Promote the Maturation of Developing Sensory Neurons before They Become Dependent on the These Factors for Survival. Neuron **9**, 139-150.

Xu Z., Marszalek J. R., Lee M. K., Wong P. C., Folmer J., Crawford T. O., Hsieh S. T., Griffin J. W. and Cleveland D. W. (1996) Subunit composition of neurofilaments specifies axonal diameter. J Cell Biol **133**, 1061-1069.

Yokota Y., Sasai Y., Tanaka K., Fujiwara T., Tsuchida K., Shigemoto R., Kakizuka A., Ohkubo H. and Nakanishi S. (1989) Molecular characterization of a functional cDNA for rat substance P receptor. J Biol Chem **264**, 17649-17652.

Zhang L., Schmidt R. E., Yan Q. and Snider W. D. (1994) NGF and NT-3 have differing effects on the growth of dorsal root axons in developing mammalian spinal cord. J Neurosci **14**, 5187-5201.

Zhou L., Lentz S. I., White F. A., Wright D. E. and Snider W. D. (1996) Cloning and expression of two novel murine semaphorin family members. Soc Neurosci Abstr **22**:585.10.

Zimmerman L., Parr B., Lendahl U., Cunningham M., McKay R., Gavin B., Mann J., Vassileva G. and McMahon A. (1994) Independent regulatory elements in the nestin gene direct transgene expression to neural stem cells or muscle precursors. Neuron **12**, 11-24.

Ziskind-Conhaim L. (1990) NMDA receptors mediate poly- and monosynaptic potentials in motoneurons of rat embryos. J. Neurosci **10**, 125-135.

Zuber M. X., Goodman D. W., Karns L. R. and Fishman M. C. (1989) The neuronal growth-associated protein GAP-43 induces filopodia in non-neuronal cells. Science **244**, 1193-1195.

APPENDIX I

Labelling of Oligonucleotide Probes

Thaw 35-S dATP (1200 CI/mmol, Dupont/NEN NEG-034H) on ice for 30 mins and aliquot into 3 microlitre aliquots. Store unused aliquots at -70^{0}C avoiding repeated freeze-thaw cycles.

On ice combine:

3µl	35S-dATP
10µl	5x tailing buffer (provided with enzyme)
4 pmol	oligonucleotide
5µl	terminal deoxynucleotide transferase (Promega cat. no. M1872)

Mix and microcentrifuge after making up to 50 µl with ultrapure water. Incubate at 37^{0}C for 1-2 hrs. Separate probe from unincorporated nucleotide using a Sepharose G50 NICK column (Pharmacia) as directed by manufacturer. Collect 400 µl sample containing oligonucleotide in a tube containing 5 µl of 1M DTT, freeze and lyophilise. Add 2 mls hybridisation buffer to dried probe to yield a 2nM solution.

Hybridisation Buffer

2X Denhardt's solution
4x SSC
50% deionised formamide
10% dextran sulfate
100 µg/ml sheared salmon sperm DNA
100 µg/ml poly A
20 µg/ml yeast tRNA
20mM DTT
0.1% SDS (optional)

Hybridisation Protocol

Fix slides in freshly prepared 4% paraformaldehyde for 5 mins. Wash in PBS twice for 5 mins, followed by 0.1M triethanolamine and 0.25M acetic anhydride in PBS/saline for 10 mins. Wash in PBS for 5 mins, then dehydrate through alcohols (70, 90, 100%) for 2 mins each. Treat with chloroform for 5 mins, 100% ethanol for 2 mins and 95% ethanol for 2 mins then air dry slides.

Heat probe in hybridisation buffer at 60^0C for 5 mins and cool on ice. Apply hybridisation solution, coverslip and incubate at 37^0C overnight in a humidified chamber (4% SSC plus 50% foramide).

Post Hybridisation

Remove coverslips in 2x SSC plus 2-mercaptoethanol (1ml/250ml) at room temperature. Wash twice for 15 mins each in 1x SSC at 50^0C followed by one 15 min wash in 0.2x SSC at 50^0C and finally two 1 hr washes in 1x SSC at room temp.

Dehydrate through alcohols (70, 95, 100%) for 15 secs each. Dry and appose to Hyperfilm (Beta-Max) for 6 weeks. Develop with Kodak GBX developer and fixer, 4 mins each. Coat slides in liquid nuclear emulsion (Ilford).

APPENDIX II

RIBOPROBE PREPARATION

In Vitro Transcription

ISH was carried out using digoxygenin-labelled riboprobes. Promega T vector containing the CGRP insert were amplified via small scale DNA preparations. The DNA was linearised with an Nco1 (antisense) and Nde1 (sense), phenol-chloroform extracted and ethanol-precipitated overnight at -20°C. Yield was estimated from a 0.7% TBE agarose gel (normally approximately 50µg DNA per miniprep) and the following reaction was set up:

1µg linearised template

2µl transcription buffer

2µl digoxygenin labelling mix

2µl RNA polymerase (either SP6, T7 or T3)

Made up to 20µl with RNAse free H_20

The transcription mix was then left at 37°C. After 2 hours the reaction was stopped with 1.5µl 0.2M EDTA and 2.5µl 4M LiCl, 75µl 100% ethanol were added. RNA was left to precipitate at -20°C for 2 hours, then spun at 13000rpm, 4°C for 15 minutes. The pellet was washed with 70% ethanol, vacuum dried for 60 seconds and redissolved in 100µl RNAse-free H_20. To check that the probe was the correct size, 10µl probe was run on a 1.5% denaturing (formaldehyde) agarose gel and blotted overnight onto nylon membrane (Boehringer Mannheim). Serial dilutions of probe were dot-blotted onto nylon membrane in order to estimate relative concentrations of sense and antisense probes. For both the northern and the dot blot, RNA was UV crosslinked onto the

membrane and washed once in buffer B1 (15 mins), once in buffer B2 (30 mins), once in buffer B2 with anti-digoxygenin alkaline phosphatase-conjugated fab fragments (1 hour), twice in buffer B3 (5 mins) and colour reaction product was visualised in buffer B4. The reaction was stopped in TE (15 mins - 1 hour). Probes were then aliquoted and stored at -70°C until needed.

Buffers

B1: 0.1M tris pH 7.5, 0.15M NaCl

B2: 5g blocking reagent (Boehringer Mannheim) and 2.5g BSA in 500ml B1. Heat to 60°C then aliquot into 25 ml universals and store at -20°C.

B3: 0.1M tris pH 9.5, 0.1M NaCl, 0.05M $MgCl_2$

B4: 75µg/ml NBT (Boehringer Mannheim), 50µg/ml BCIP, 0.24mg/ml levamisole (Sigma) in buffer B3.